Methods in Molecular Biology 2667

Springer Protocols

Rebecca A. Drummond *Editor*

Antifungal Immunity

Methods and Protocols

Humana Press

METHODS IN MOLECULAR BIOLOGY

Series Editor
John M. Walker
School of Life and Medical Sciences
University of Hertfordshire
Hatfield, Hertfordshire, UK

For further volumes:
http://www.springer.com/series/7651

For over 35 years, biological scientists have come to rely on the research protocols and methodologies in the critically acclaimed *Methods in Molecular Biology* series. The series was the first to introduce the step-by-step protocols approach that has become the standard in all biomedical protocol publishing. Each protocol is provided in readily-reproducible step-by step fashion, opening with an introductory overview, a list of the materials and reagents needed to complete the experiment, and followed by a detailed procedure that is supported with a helpful notes section offering tips and tricks of the trade as well as troubleshooting advice. These hallmark features were introduced by series editor Dr. John Walker and constitute the key ingredient in each and every volume of the *Methods in Molecular Biology* series. Tested and trusted, comprehensive and reliable, all protocols from the series are indexed in PubMed.

Antifungal Immunity

Methods and Protocols

Edited by

Rebecca A. Drummond

Institute of Immunology & Immunotherapy, College of Medical and Dental Sciences, University of Birmingham, Birmingham, UK; Institute of Microbiology & Infection, School of Biosciences, University of Birmingham, Birmingham, UK

Humana Press

Editor
Rebecca A. Drummond
Institute of Immunology & Immunotherapy
College of Medical and Dental Sciences
University of Birmingham
Birmingham, UK

Institute of Microbiology & Infection
School of Biosciences
University of Birmingham
Birmingham, UK

ISSN 1064-3745 ISSN 1940-6029 (electronic)
Methods in Molecular Biology
ISBN 978-1-0716-3198-0 ISBN 978-1-0716-3199-7 (eBook)
https://doi.org/10.1007/978-1-0716-3199-7

This Humana imprint is published by the registered company Springer Science+Business Media, LLC, part of Springer Nature.
The registered company address is: 1 New York Plaza, New York, NY 10004, U.S.A.

Preface

The incidence of invasive fungal infections in humans has steadily increased over the last few decades, resulting in nearly one million deaths each year. In addition to causing mortality, fungi are becoming increasingly appreciated to modulate and influence our immune system, by either residing as gut commensals or shaping the pulmonary immune response following inhalation from the environment. Despite the impact of fungi and fungal infections on human health, our understanding of antifungal immunity has lagged behind that of other types of infections. This is partly due to a lack of expertise, with a relatively small number of laboratories focusing on anti-fungal immunity. This book aims to help recruit new investigators to the field by providing them with the protocols needed to set up clinically relevant animal models of fungal infection (in mice, insects and fish), as well as methods for developing the latest cutting-edge techniques for analysing in vivo immunology and fungal morphology/biology.

Even within the medical mycology field, some fungal diseases remain particularly understudied. These include phaeohyphomycosis, coccidioidomycosis, mucormycosis and pneumocystis pneumonia. Each of these infections have been difficult to model in animals, and therefore the use of mice to study these infections have been limited to a small number of research groups. To help address this and improve uptake of these infection models, this book has particularly focused on gathering protocols from the experts who developed and routinely use mouse models of these understudied fungal diseases. Many of the protocols feature specific insights into what adverse effects can be expected and recommended techniques and assays to study the immunological response during infection.

Fungal infections have a global impact with a particularly high concentration of cases in parts of Africa, Asia and South America. It therefore felt important that the authorship of this book adequately represented the different continents and reflected the great diversity of the medical mycology and fungal immunology research communities. I am proud that we have achieved a 50% gender balance in the contributing authors and have chapters submitted by scientists based across the world including within the UK, South Africa, USA, Brazil, Germany, Belgium, Colombia and Japan. This demonstrates the collaborative and collegiate nature of the scientists working in our field and I am grateful to call them my colleagues, who have helped put together a fantastic resource for our community.

Rebecca A. Drummond

Contents

Contributors

Amalia N. Awala • *Division of Cell Biology, Faculty of Health Sciences, Department of Human Biology, University of Cape Town, Cape Town, South Africa; Faculty of Health Sciences, Neuroscience Institute, University of Cape Town, Groote Schuur Hospital, Cape Town, South Africa; Division of Physiological Sciences, Faculty of Health Sciences, Department of Human Biology, University of Cape Town, Cape Town, South Africa; CMM AFRICA Medical Mycology Research Unit, Institute of Infectious Disease and Molecular Medicine, Faculty of Health Sciences, University of Cape Town, Cape Town, South Africa*

Anamelia L. Bocca • *Department of Cell Biology, Institute of Biological Sciences, University of Brasilia, Brasilia, DF, Brazil*

Christine D. Butkiewicz • *Valley Fever Center for Excellence, University of Arizona, Tucson, AZ, USA*

Z. P. Chalakova • *University of Sheffield, Firth Court, Western Bank, UK*

Rachael Dangarembizi • *Faculty of Health Sciences, Neuroscience Institute, University of Cape Town, Groote Schuur Hospital, Cape Town, South Africa; Division of Physiological Sciences, Faculty of Health Sciences, Department of Human Biology, University of Cape Town, Cape Town, South Africa; CMM AFRICA Medical Mycology Research Unit, Institute of Infectious Disease and Molecular Medicine, Faculty of Health Sciences, University of Cape Town, Cape Town, South Africa*

Rebecca A. Drummond • *Institute of Immunology & Immunotherapy, College of Medical and Dental Sciences, University of Birmingham, Birmingham, UK; Institute of Microbiology & Infection, School of Biosciences, University of Birmingham, Birmingham, UK*

Man Shun Fu • *Institute of Immunology & Immunotherapy, College of Medical and Dental Sciences, University of Birmingham, Birmingham, UK*

Kristie Goughenour • *Department of Veterans Affairs Health System, Research Service, Ann Arbor VA Healthcare System, Ann Arbor, MI, USA; Division of Pulmonary and Critical Care Medicine, Department of Internal Medicine, University of Michigan Health System, Ann Arbor, MI, USA*

Sofia Hain • *Institute of Immunology and Immunotherapy, University of Birmingham, Birmingham, UK*

Emily Ruth Higgitt • *Faculty of Health Sciences, Neuroscience Institute, University of Cape Town, Groote Schuur Hospital, Cape Town, South Africa; Division of Physiological Sciences, Faculty of Health Sciences, Department of Human Biology, University of Cape Town, Cape Town, South Africa; CMM AFRICA Medical Mycology Research Unit, Institute of Infectious Disease and Molecular Medicine, Faculty of Health Sciences, University of Cape Town, Cape Town, South Africa*

J. Claire Hoving • *AFRICA CMM Medical Mycology Research Unit, Institute of Infectious Disease and Molecular Medicine (IDM), Cape Town, South Africa; Department of Pathology, Faculty of Health Sciences, University of Cape Town, Cape Town, South Africa; MRC Centre for Medical Mycology, University of Exeter, Exeter, UK*

Ilse D. Jacobsen • *Research Group Microbial Immunology, Leibniz Institute for Natural Product Research and Infection Biology-Hans Knöll Institute (HKI), Jena, Germany; Institute of Microbiology, Faculty of Biological Sciences, Friedrich Schiller University Jena, Jena, Germany*

S. A. Johnston • *University of Sheffield, Firth Court, Western Bank, UK*

Christopher R. Jones • *School of Chemical Engineering, University of Birmingham, Birmingham, UK*

Maahir Kauchali • *Faculty of Health Sciences, Neuroscience Institute, University of Cape Town, Groote Schuur Hospital, Cape Town, South Africa; Division of Physiological Sciences, Faculty of Health Sciences, Department of Human Biology, University of Cape Town, Cape Town, South Africa; CMM AFRICA Medical Mycology Research Unit, Institute of Infectious Disease and Molecular Medicine, Faculty of Health Sciences, University of Cape Town, Cape Town, South Africa*

Kazuyoshi Kawakami • *Department of Medical Microbiology, Mycology and Immunology, Tohoku University Graduate School of Medicine, Sendai, Miyagi, Japan; Department of Intelligent Network for Infection Control, Tohoku University Graduate School of Medicine, Sendai, Miyagi, Japan*

Jay K. Kolls • *Centre for Translational Research in Infection and Inflammation, Tulane School of Medicine, New Orleans, LA, USA*

Anja de Lange • *Division of Cell Biology, Faculty of Health Sciences, Department of Human Biology, University of Cape Town, Cape Town, South Africa; Faculty of Health Sciences, Neuroscience Institute, University of Cape Town, Groote Schuur Hospital, Cape Town, South Africa; Division of Physiological Sciences, Faculty of Health Sciences, Department of Human Biology, University of Cape Town, Cape Town, South Africa; CMM AFRICA Medical Mycology Research Unit, Institute of Infectious Disease and Molecular Medicine, Faculty of Health Sciences, University of Cape Town, Cape Town, South Africa*

Ruoyu Li • *Department of Dermatology and Venereology, Peking University First Hospital, Beijing, China; Research Center for Medical Mycology, Peking University, Beijing, China; Beijing Key Laboratory of Molecular Diagnosis on Dermatoses, Beijing, China; National Clinical Research Center for Skin and Immune Diseases, Beijing, China*

Tshepiso Mbangiwa • *CMM AFRICA Medical Mycology Research Unit, Institute of Infectious Disease and Molecular Medicine, Faculty of Health Sciences, University of Cape Town, Cape Town, South Africa; Division of Immunology, Faculty of Health Sciences, Department of Pathology, University of Cape Town, Cape Town, South Africa*

Ferris T. Munyonho • *Centre for Translational Research in Infection and Inflammation, Tulane School of Medicine, New Orleans, LA, USA*

Michal A. Olszewski • *Department of Veterans Affairs Health System, Research Service, Ann Arbor VA Healthcare System, Ann Arbor, MI, USA; Division of Pulmonary and Critical Care Medicine, Department of Internal Medicine, University of Michigan Health System, Ann Arbor, MI, USA*

Joseph V. Raimondo • *Division of Cell Biology, Faculty of Health Sciences, Department of Human Biology, University of Cape Town, Cape Town, South Africa; Faculty of Health Sciences, Neuroscience Institute, University of Cape Town, Groote Schuur Hospital, Cape Town, South Africa*

Adriana Marcela Celis Ramírez • *Grupo de Investigación Celular y Molecular de Microorganismos Patógenos (CeMoP), Departamento de Ciencias Biológicas, Universidad de los Andes, Bogotá, Colombia*

Agustin Resendiz-Sharpe • *KU Leuven, Department of Imaging and Pathology, Biomedical MRI / MoSAIC, Leuven, Belgium*

Ko Sato • *Department of Medical Microbiology, Mycology and Immunology, Tohoku University Graduate School of Medicine, Sendai, Miyagi, Japan; Department of Intelligent Network for Infection Control, Tohoku University Graduate School of Medicine, Sendai, Miyagi, Japan*

Lisa F. Shubitz • *Valley Fever Center for Excellence, University of Arizona, Tucson, AZ, USA*

Isaque Medeiros Siqueira • *Instituto Brasileiro do Meio Ambiente e dos Recursos Naturais Renováveis, IBAMA, Brasília, DF, Brazil*

Maritza Torres • *Grupo de Investigación Celular y Molecular de Microorganismos Patógenos (CeMoP), Departamento de Ciencias Biológicas, Universidad de los Andes, Bogotá, Colombia*

Hien T. Trinh • *Valley Fever Center for Excellence, University of Arizona, Tucson, AZ, USA*

Hung-Ji Tsai • *Institute of Microbiology and Infection, School of Biosciences, University of Birmingham, Birmingham, UK*

W. Rex Underwood • *Department of Veterans Affairs Health System, Research Service, Ann Arbor VA Healthcare System, Ann Arbor, MI, USA; Division of Pulmonary and Critical Care Medicine, Department of Internal Medicine, University of Michigan Health System, Ann Arbor, MI, USA*

Eliane Vanhoffelen • *KU Leuven, Department of Imaging and Pathology, Biomedical MRI / MoSAIC, Leuven, Belgium*

Simon Vautier • *The Binding Site Group Limited, Birmingham, UK*

Greetje Vande Velde • *KU Leuven, Department of Imaging and Pathology, Biomedical MRI / MoSAIC, Leuven, Belgium*

Jintao Xu • *Department of Veterans Affairs Health System, Research Service, Ann Arbor VA Healthcare System, Ann Arbor, MI, USA; Division of Pulmonary and Critical Care Medicine, Department of Internal Medicine, University of Michigan Health System, Ann Arbor, MI, USA*

Yi Zhang • *Department of Dermatology and Venereology, Peking University First Hospital, Beijing, China; Research Center for Medical Mycology, Peking University, Beijing, China; Beijing Key Laboratory of Molecular Diagnosis on Dermatoses, Beijing, China; National Clinical Research Center for Skin and Immune Diseases, Beijing, China*

Zhenyu Jason Zhang • *School of Chemical Engineering, University of Birmingham, Birmingham, UK*

Chapter 1

Quantifying the Mechanical Properties of Yeast *Candida albicans* Using Atomic Force Microscopy-based Force Spectroscopy

Christopher R. Jones, Zhenyu Jason Zhang, and Hung-Ji Tsai

Abstract

Fungi can adapt to a wide range of environmental stresses in the wild and host milieu by employing their plastic genome and great diversity in morphology. Among different adaptive strategies, mechanical stimuli, such as changes in osmotic pressure, surface remodeling, hyphal formation, and cell divisions, could guide the physical cues into physiological responses through a complex signaling network. While fungal pathogens require a pressure-driven force to expand and penetrate host tissues, quantitatively studying the biophysical properties at the host–fungal interface is critical to understand the development of fungal diseases. Microscopy-based techniques have enabled researchers to monitor the dynamic mechanics on fungal cell surface in responses to the host stress and antifungal drugs. Here, we describe a label-free, high-resolution method based on atomic force microscopy, with a step-by-step protocol to measure the physical properties in human fungal pathogen *Candida albicans*.

Key words Fungal infections, Hyphal formation, Surface stiffness, Turgor pressure, Atomic force microscopy, Young's modulus

1 Introduction

Fungal pathogens can change their cell surface composition and morphology to respond to environmental stimuli and to facilitate their virulence [1–4]. Throughout the process of cell division and hyphal expansion, a hydrostatic pressure (turgor), generated by an accumulation of solutes, including amino acids and polyols which change intracellular osmolarity, serves as a key driver for tissue invasion and colonization [5, 6]. Understanding the underlying mechanism and where its related physical properties act on can offer as invaluable insight into the development of fungal diseases. As such, a quantitative measurement with a nanoscopic resolution for the pressure-driven force is critical to connect the biophysical cues and physiological responses in fungi.

Rebecca A. Drummond (ed.), *Antifungal Immunity: Methods and Protocols*, Methods in Molecular Biology, vol. 2667,
https://doi.org/10.1007/978-1-0716-3199-7_1,

Microorganism cell wall provides a physical barrier to resist both internal force (turgor) [6, 7] and external perturbations (e.g., macrophage engulfment) [8], and its composition can constantly change in response to the cell physiological state [3]. For example, upon heat stress, the abundance of chitin changes with a twofold increase of surface stiffness [9]. At the host–fungal interface, innate immune cells can recognize fungal cell wall components such as β-glucan and initiate phagocytosis for fungal killing [8, 10]. During such process, polymorphic fungal pathogens, such as *Candida albicans*, can form lengthy hyphae, where β-glucan is masked by mannan to attenuate phagosome maturation [11], and also extend their cell body to escape from phagocytic engulfment [12, 13]. This complex morphogenetic program is not only governed by stress-induced signaling pathways but also a series of mechanical cues to achieve infections by overcoming host immunity [11, 14–17]. In parallel, macrophages can counteract the physical challenges by folding hyphae and further damaging hyphal structure while re-exposing β-glucan to promote immune recognition [18]. This two-way host–fungal response highlights the important role of physical properties in fungal pathogenesis. Furthermore, to colonize host tissue or implanted abiotic surface, a sufficient adhesive force, resulting from either adhesins (e.g., Als proteins [19]) or carbohydrate moiety, is essential for the aforementioned pathogenic process [20, 21]. Additionally, fungal cell wall is a major target for current antifungal treatments, and antifungal drugs, including fluconazole and caspofungin, can alter fungal surface mechanics differently [22, 23]. These surface physical properties are critical parameters for antifungal efficacy while developing strategies in fungal clearance and the measurements of antifungal drug efficacy.

Techniques employing different fluorescence probes and soft substrates are used to measure cell surface stiffness as a proxy of turgor changes and to monitor its dynamics in response to environment [24–26]. Over the past two decades, atomic force microscopy (AFM) has been used extensively to investigate the mechanical and topographical characteristics of living microorganisms without additional labeling or sophisticated sample preparation procedures [27–30]. A unique advantage of this technique is to acquire nanoscopic spatial resolution under physiological condition in response to stress applied. As the method in evaluating mechanical properties in *C. albicans* is proven versatile in mycology, here we describe the measurements of cell surface stiffness and turgor pressure in *C. albicans* with step-by-step instructions.

2 Materials

2.1 Fungal Strain, Medium, and Solutions

1. *Candida albicans* SC5314 (wild-type).
2. YPD medium (liquid and solid): 1% bacto yeast extract, 2% bacto peptone, 2% dextrose, and 1.5% bacto agar (solid media only).
3. Poly-L-Lysine (0.1% w/v).
4. PBS: Phosphate buffer saline.

2.2 Consumables

1. Parafilm.
2. Petri-dishes.
3. PAP pen (Hydrophobic barrier pen).
4. Poly-L-Lysine Adhesive Microscope Slides (*see* **Note 1**).

2.3 Microscope Specifications

1. A range of commercially available atomic force microscopes (AFM) are suitable for studying the mechanical properties of cells by force spectroscopy. The representative data shown here was acquired using the following:
   (a) FlexAFM (Nanosurf AG, Switzerland).
   (b) Mounted on an IX73 (Olympus, Japan) inverted microscope.
2. Measurements were carried out in an air-conditioned laboratory at 21 °C.
3. An AFM cantilever with appropriate tip geometry, stiffness, and coating material should be chosen.
   (a) For the present work, PPP-CONTR (Nanosensors, Switzerland) cantilevers with a nominal spring constant of 0.2 N m^{-1} and tip radius of 7 nm were used.
   (b) Further details on cantilever selection can be found in **Notes 2–4**.
4. All calibrations and measurements were carried out using Nanosurf C3000 software (Nanosurf AG, Switzerland).

3 Methods

3.1 Yeast Growth and Preparation

1. Inoculate 2 mL of YPD with a single yeast colony from a newly streaked plate and grow overnight at 30 °C.
2. For imaging cells on a glass slide, draw a circle by PAP pen to form a hydrophobic barrier for inoculating yeast cells in the next day. Alternatively, place a ring-shape parafilm on the glass slide and heat the glass-slide on a preheated block for 10 s to melt the parafilm and form a barrier.

3. If the glass slide is not precoated, deposit 100 μL of 0.1% (w/v) poly-L-lysine (PLL) on a glass slide to cover the area and leave the slide in a petri-dish (air-dry) for the experiment next day.
4. Dilute the overnight culture in 5 mL of fresh YPD at an OD600 of 0.2 and grow at 30 °C for at least one doubling time (>90 min but less than 3 doublings).
5. Remove the remaining poly-L-lysine solution on the glass slide and wash it by PBS once, following another wash using YPD medium (or medium suitable for the experiment).
6. Dilute the yeast culture for >100 times in YPD medium and spot 50,100 μL of the diluted culture within the ring area on the glass slide. Keep the slide statically in the room temperature for 30 min.
7. Remove the medium gently and wash the area with YPD medium for (at least) twice to remove suspended cells. Add 50–100 μL of YPD medium to keep cells in a constant condition and ready for microscopy.

3.2 AFM Setup and Calibration

1. The procedure for many of the setup steps listed below will be specific to each instrument and should be carried out following the manufacturer's instructions. In this protocol, a schematic diagram of the experimental setup is shown in Fig. 1.
2. Load the selected AFM cantilever into the cantilever holder and attach this to the AFM scan head. When handling probes with a

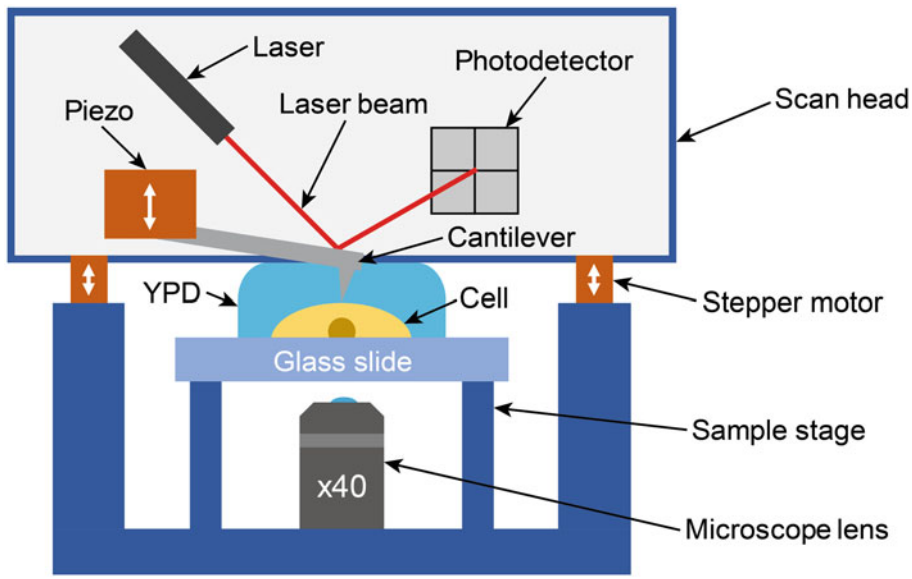

Fig. 1 Schematic representation of an Atomic Force Microscope (AFM) instrument mounted on an inverted microscope with glass slide with affixed yeast cell on sample stage

sharp tip, it is recommended to use an electrostatic discharge (ESD) wrist strap and mat to prevent static discharge.

3. Adjust the height and position of the AFM scan head and inverted microscope optics so that the end of the cantilever beam is focused in the field of view.
4. Position the laser beam onto the back of the cantilever, centered laterally, and near the tip end, then center the reflection of the laser on the photodetector.
5. Set up the AFM software in contact mode.
6. Place a clean glass microscope slide on the sample stage of the inverted microscope and pipette a 0.2 mL drop of YPD (or a solution used to keep cells under their natural state; e.g., PBS) onto the center of the slide.
7. Place the AFM scan head on the stage and lower the cantilever until it is submerged in the droplet. It may help to pipette a small droplet onto the cantilever holder before lowering towards the droplet, to prevent an air bubble being trapped at the interface.
8. Calibrate the cantilever spring constant. Most AFMs have the ability to carry out this calibration using the thermal tuning method [31]. Where this is not available, it is recommended to purchase precalibrated probes, as the true value can vary significantly from the nominal value.
9. Approach the cantilever to the surface and calibrate its deflection sensitivity using the glass substrate.
10. Withdraw the cantilever from the surface and remove the glass slide from the stage.

3.3 Force Spectroscopy Measurements

1. Set up the AFM software for force spectroscopy, selecting the appropriate mode to stop at a maximum force rather than a fixed distance.
2. Input the required parameters (example values are provided below).
   (a) Maximum force: 1 nN.
   (b) Modulation time: 1 s.
   (c) Distance range: 5 μm.
   (d) Data points: 1024.
   (e) Grid size: 6 × 6 points.
3. To ensure results are reproducible, it is advised to carry our force spectroscopy measurements close to the cell center. Measurements near the edge of the cell may lead to an increased probability of variation due to the surface gradient of the cell. Either a single measurement at the cell center or a grid of

measurements over the cell surface may be used. Using a grid allows investigation of localized behavior over the cell area.

4. Place the poly-L-lysine (PLL) coated glass slide with immobilized yeast cells on the microscope sample stage with a droplet of YPD (based on experimental needs) coating the surface.
5. Lower the cantilever into the droplet.
6. Focus the microscope on the cells.
7. Slowly bring the cantilever towards the surface, stopping when the beam starts to come into focus indicating it is close to the cell surface.
8. Move the sample so the cantilever tip is above the center of a cell and approach the cantilever to the surface.
9. Start the force spectroscopy measurements.
10. Once the process has been completed, withdraw the cantilever from the cell surface, move the tip to above another cell, and carry out repeat measurements.

3.4 Data Preprocessing

Data analysis can be carried out using a range of commercial or open-source software packages, or using custom written analysis codes in programming languages such as MATLAB or Python [32]. The example data here was analyzed using a home developed "nanoforce" (v0.3.21) package implemented in Python (v 3.8.1), available from https://pypi.org/project/nanoforce/. The steps used are similar for each platform and are summarized below.

1. Export raw data from the AFM software and import it into a desired analysis package.
2. The output signal from the photodetector measures cantilever deflection as a voltage signal that should be converted to force data using the spring constant and deflection sensitivity calibrated as described in Subheading 3.2. Some AFM software may apply this conversion automatically.
3. The mean value of a selected range of the noncontact portion of the force distance curve is calculated and subtracted from the force data to align the baseline region to 0 nN (as shown in Fig. 2b). For some datasets, it may be necessary to instead calculate a linear fit of the noncontact portion and subtract this from the force data, to account for any tilting of the baseline.
4. The contact point at which the tip reaches the sample surface is identified and subtracted from the distance data, so the contact point is at 0 nm (as shown in Fig. 2b).
5. Distance data is recorded by the piezoelectric positioner used to control the cantilever height. Due to the physical bending of the cantilever, this may not be able to represent the absolute tip

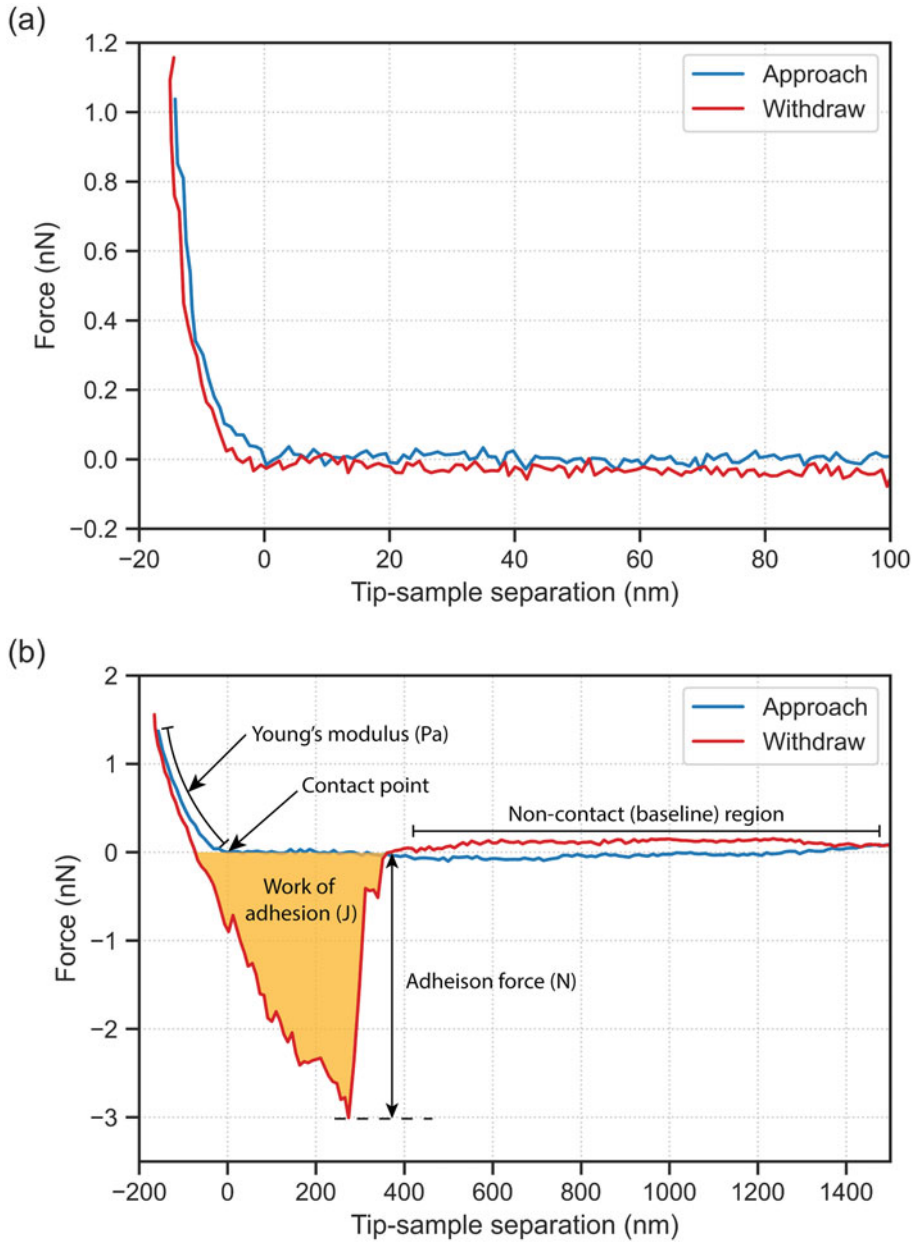

Fig. 2 Representative AFM force–distance curves for (**a**) PLL substrate used to immobilize cells, used to exclude measurements where cantilever did not contact cell surface, and (**b**) cell surface with key parameters annotated

position when in contact with a surface. The true tip position could be calculated from the piezo position, cantilever deflection, and deflection sensitivity.

6. Figure 2a presents a force–distance curve acquired on the PLL substrate as benchmark. This was recorded to distinguish between the cell surface and substrate.
7. Figure 2b shows a force–distance curve measured on the surface of a cell identified by the optical microscopy.
8. Figure 2a, b shows distinctively different characteristics: in the approaching component of the force curve (blue lines), a much deeper indentation can be observed on the cell than the PLL substrate, and there is a considerable hysteresis on the cell surface when withdrawing the cantilever.
9. A range of information can be quantified from an AFM force–distance curve, including the following which are labeled in Fig. 2b:
   (a) Adhesion force (N)—maximum force recorded on the withdraw curve when separating the AFM tip from the surface.
   (b) Work of adhesion (J)—area between the baseline and the withdraw curve when separating the AFM tip from the surface.
   (c) Young's modulus (Pa)—calculated from the slope of the approach curve in the indentation region.

3.5 Contact Mechanics Analysis

1. A range of contact models reported in the literature can be used to calculate Young's modulus from a force–distance curve. An appropriate model should be selected depending on the geometries of the surface (i.e., the cell) and the indenter (i.e., the AFM tip) [33].
2. The cell can be assumed a flat surface if its size dimension is much greater than that of the indenter.
3. For a spherical indenter on a flat surface (Fig. 3a), the force–distance curve can be fitted to the Hertz model (Eq. 1) [34].

$$F = \frac{4}{3} E^* R^{0.5} \delta^{1.5} \tag{1}$$

where F is force (N), R is tip radius (m), δ is indentation depth (m), and E^* is reduced modulus (Pa), which is given by Eq. (2).

$$\frac{1}{E^*} = \frac{1 - \nu_i^2}{E_i} - \frac{1 - \nu_s^2}{E_s} \tag{2}$$

where E is Young's modulus (Pa) and ν is Poisson ratio, with subscript i representing the indenter (AFM cantilever) and s the

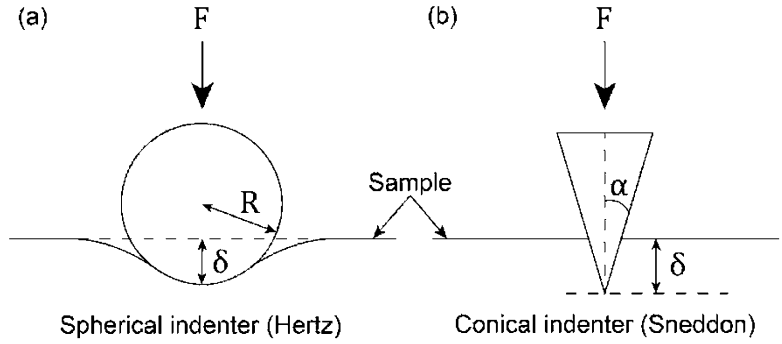

Fig. 3 Schematic representation diagrams of the indentation of a flat sample by (**a**) a spherical indenter and (**b**) a conical indenter with the relevant parameters required to fit force–distance data shown for the Hertz and Sneddon models, respectively

sample. Assuming a rigid indenter (i.e., Eq. 3) with a Young's modulus much greater than that of the sample, simplifies to Eq. (4).

$$\frac{1-\nu_i^2}{E_i} \gg \frac{1-\nu_s^2}{E_s} \tag{3}$$

$$F = \frac{4}{3}\frac{E_s}{1-\nu_s^2} R^{0.5}\delta^{1.5} \tag{4}$$

4. For a conical indenter on a flat surface (Fig. 3b), the force–distance curve can be fitted to the Sneddon model (Eq. 5) [35].

$$F = \frac{2}{\pi}\frac{E_s}{1-\nu_s^2} \tan(\alpha)\delta^2 \tag{5}$$

where α is the half angle of the indenter.

5. Hertz (Eq. 4) and Sneddon (Eq. 5) model fits of the approaching force–distance curve (Fig. 2b) are shown in Fig. 4a alongside the raw data points.
6. Data can be fitted to each model by taking a linear fit of the force versus distance terms (i.e., F vs. $\delta^{1.5}$ for the Hertz model and F vs. δ^2 for the Sneddon model), using an ordinary least squared linear regression model.
7. The gradient of the calculated linear fit can be substituted into the equation for the appropriate model, along with the Poisson ratio and tip radius or tip half-angle, to calculate the Young's modulus of the sample.
8. The Sneddon model fitting in Fig. 4a is a much better representation of the raw data than the Hertz model fitting. This is expected as the AFM cantilever used to record this data has

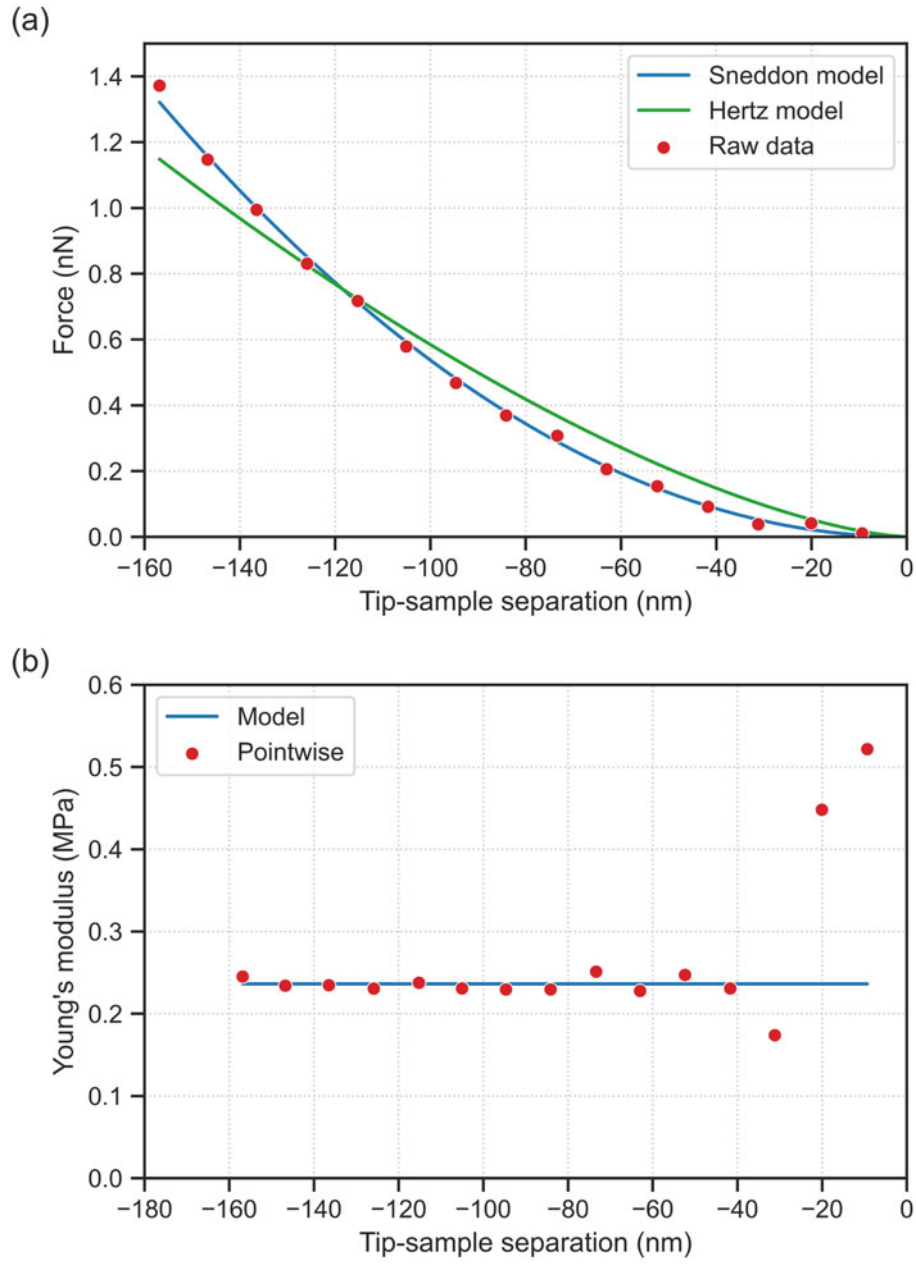

Fig. 4 (**a**) Raw force–distance data for indentation portion of AFM measurements, along with Sneddon model and Hertz model fits of this data, and (**b**) comparison of Young's modulus calculated by the Sneddon model using the fit shown in (**a**), along with a pointwise calculation for each raw data point

primarily conical shape, excluding a small spherical region at the tip with a radius of less than 7 nm.

9. Figure 4b shows a pointwise analysis of the Young's modulus at each raw datapoint, along with the value predicted by the

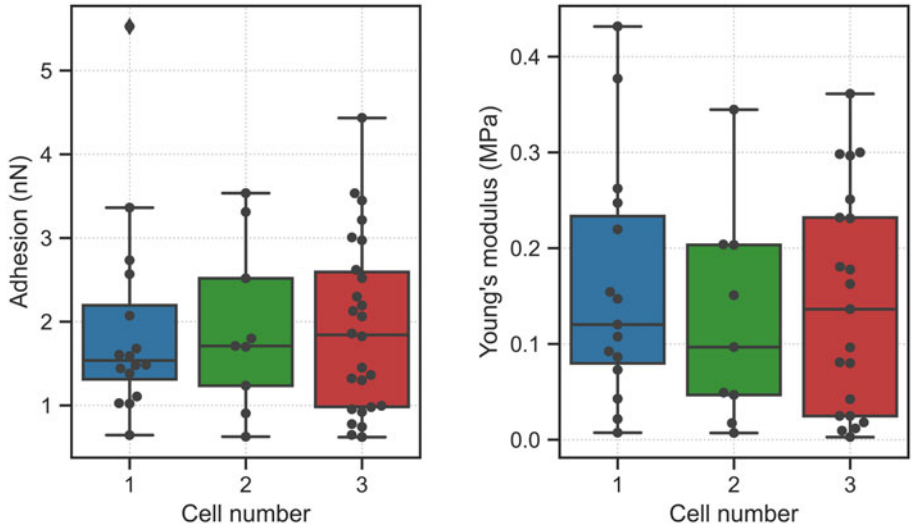

Fig. 5 Box plots showing the variation of adhesion force and Young's modulus for three representative cells

Sneddon model fitting shown in Fig. 4a. The model proves an accurate representation of the raw data points at indentation depths of greater than 40 nm.

10. The divergence from the model at low indentation depths is likely caused by the small spherical region at the tip of the cantilever. Once the indentation depth is much greater than this tip radius, the cantilever can be assumed cylindrical, for which the Sneddon model fits well.
11. Literature investigating the adhesion and Young's modulus of yeast cells has observed variation in measured values across the cell surface [22, 36].
12. Figure 5 shows the variation of values measured over the surface of three representative cells.

4 Notes

1. Yeast cell immobilization using an adhesive (e.g., poly-L-lysine and concanavalin A) is recommended, because yeast cell may move away while the cantilever makes contact. Cell entrapment using microfabricated chambers/microwells may alter the mechanical properties in their natural state since the space confinement could apply an artificial force to the cell.
2. A cantilever should be chosen with a spring constant that allows large cantilever deflection to improve the resolution of the force–distance curve while being stiff enough to allow sufficient indentation into the cell and ensure the cantilever

detaches from the cell surface during the withdraw curve. Typically, a spring constant between 0.01 and 0.6 N/m is appropriate for cell studies [32].

3. Cantilever tip geometry is an important consideration for studying the nanomechanical properties of cells. In general, a spherical tip with a 2.5–10 μm radius is most appropriate for soft and fragile cellular structures, while a conical tip may be used for stiffer features. The sharp tip of a conical indenter enables determination of more localized surface properties, while a spherical tip gives information related to the whole-cell behavior [35].
4. When aligning the AFM tip with the cell surface by optical microscopy, it may be advantageous to use a cantilever with the tip aligned with the end of the cantilever beam for ease of alignment, such as OPUS 3XC-NA (Mikromasch, USA) or ARROW-CONTR (NanoWorld, Switzerland).

Acknowledgement

The work is supported by the Royal Society Research Grant RGS \R2\202400 to H-J. T.; Engineering and Physical Science Research Council Grants EP/V029762/1 to Z.J.Z. and EP/R511845/1 to C.R.J.

References

1. Li Z, Nielsen K (2017) Morphology changes in human fungal pathogens upon interaction with the host. J Fungi (Basel) 3. https://doi.org/10.3390/jof3040066
2. Sudbery PE (2011) Growth of Candida albicans hyphae. Nat Rev Microbiol 9:737–748
3. Gow NAR, Latge J-P, Munro CA (2017) The fungal cell wall: structure, biosynthesis, and function. Microbiol Spectr 5. https://doi.org/10.1128/microbiolspec.FUNK-0035-2016
4. Chai LYA, Netea MG, Vonk AG, Kullberg B-J (2009) Fungal strategies for overcoming host innate immune response. Med Mycol 47:227–236
5. Lew RR (2011) How does a hypha grow? The biophysics of pressurized growth in fungi. Nat Rev Microbiol 9:509–518
6. Hohmann S (2002) Osmotic stress signaling and osmoadaptation in yeasts. Microbiol Mol Biol Rev 66:300–372
7. Wood JM (1999) Osmosensing by bacteria: signals and membrane-based sensors. Microbiol Mol Biol Rev 63:230–262
8. Erwig LP, Gow NAR (2016) Interactions of fungal pathogens with phagocytes. Nat Rev Microbiol 14:163–176
9. Pillet F, Lemonier S, Schiavone M et al (2014) Uncovering by atomic force microscopy of an original circular structure at the yeast cell surface in response to heat shock. BMC Biol 12:6
10. Hopke A, Brown AJP, Hall RA, Wheeler RT (2018) Dynamic fungal cell wall architecture in stress adaptation and immune evasion. Trends Microbiol 26:284–295
11. Bain JM, Louw J, Lewis LE et al (2014) Candida albicans hypha formation and mannan masking of β-glucan inhibit macrophage phagosome maturation. MBio 5:e01874
12. Bain JM, Lewis LE, Okai B et al (2012) Non-lytic expulsion/exocytosis of Candida albicans from macrophages. Fungal Genet Biol 49:677–678
13. Lewis LE, Bain JM, Lowes C et al (2012) Stage specific assessment of Candida albicans phagocytosis by macrophages identifies cell wall composition and morphogenesis as key determinants. PLoS Pathog 8:e1002578

14. Lenardon MD, Munro CA, Gow NAR (2010) Chitin synthesis and fungal pathogenesis. Curr Opin Microbiol 13:416–423
15. Brand A (2012) Hyphal growth in human fungal pathogens and its role in virulence. Int J Microbiol 2012:517529
16. Crampin H, Finley K, Gerami-Nejad M et al (2005) Candida albicans hyphae have a Spitzenkörper that is distinct from the polarisome found in yeast and pseudohyphae. J Cell Sci 118:2935–2947
17. O'Meara TR, Duah K, Guo CX et al (2018) High-throughput screening identifies genes required for candida albicans induction of macrophage pyroptosis. MBio 9. https://doi.org/10.1128/mBio.01581-18
18. Bain JM, Alonso MF, Childers DS et al (2021) Immune cells fold and damage fungal hyphae. Proc Natl Acad Sci USA 118. https://doi.org/10.1073/pnas.2020484118
19. Hoyer LL (2001) The ALS gene family of Candida albicans. Trends Microbiol 9:176–180
20. Gow NAR, Hube B (2012) Importance of the Candida albicans cell wall during commensalism and infection. Curr Opin Microbiol 15:406–412
21. Gulati M, Nobile CJ (2016) Candida albicans biofilms: development, regulation, and molecular mechanisms. Microbes Infect 18:310–321
22. Çolak A, Ikeh MAC, Nobile CJ, Baykara MZ (2020) In situ imaging of candida albicans hyphal growth via atomic force microscopy. mSphere 5. https://doi.org/10.1128/mSphere.00946-20
23. El-Kirat-Chatel S, Beaussart A, Alsteens D et al (2013) Nanoscale analysis of caspofungin-induced cell surface remodelling in Candida albicans. Nanoscale 5:1105–1115
24. Ryder LS, Lopez SG, Michels L et al (2022) Direct measurement of appressorium turgor using a molecular mechanosensor in the rice blast fungus Magnaporthe oryzae. bioRxiv 2022.08.30.505899
25. Ravishankar JP, Davis CM, Davis DJ et al (2001) Mechanics of solid tissue invasion by the mammalian pathogen Pythium insidiosum. Fungal Genet Biol 34:167–175
26. Howard RJ, Ferrari MA, Roach DH, Money NP (1991) Penetration of hard substrates by a fungus employing enormous turgor pressures. Proc Natl Acad Sci USA 88:11281–11284
27. Zhang Z, Pen Y, Edyvean RG et al (2010) Adhesive and conformational behaviour of mycolic acid monolayers. Biochim Biophys Acta 1798:1829–1839
28. El-Kirat-Chatel S, Dufrêne YF (2016) Nanoscale adhesion forces between the fungal pathogen Candida albicans and macrophages. Nanoscale Horiz 1:69–74
29. Valotteau C, Prystopiuk V, Cormack BP, Dufrêne YF (2019) Atomic force microscopy demonstrates that candida glabrata uses three epa proteins to mediate adhesion to abiotic surfaces. mSphere 4. https://doi.org/10.1128/mSphere.00277-19
30. Dufrêne YF, Viljoen A, Mignolet J, Mathelié-Guinlet M (2021) AFM in cellular and molecular microbiology. Cell Microbiol 23:e13324
31. Hutter JL, Bechhoefer J (1993) Calibration of atomic-force microscope tips. Rev Sci Instrum 64:1868–1873
32. Gavara N (2017) A beginner's guide to atomic force microscopy probing for cell mechanics. Microsc Res Tech 80:75–84
33. Han R, Chen J (2021) A modified Sneddon model for the contact between conical indenters and spherical samples. J Mater Res 36:1762–1771
34. Johnson KL (1985) Contact mechanics. Cambridge University Press
35. Chen J (2014) Nanobiomechanics of living cells: a review. Interface Focus 4:20130055
36. Formosa C, Schiavone M, Martin-Yken H et al (2013) Nanoscale effects of caspofungin against two yeast species, Saccharomyces cerevisiae and Candida albicans. Antimicrob Agents Chemother 57:3498–3506

Chapter 2

Standardization of *Galleria mellonella* as an Infection Model for *Malassezia furfur* and *Malassezia pachydermatis*

Maritza Torres and Adriana Marcela Celis Ramírez

Abstract

Galleria mellonella larva has been widely exploited as an infection model for bacteria and fungi. Our laboratory uses this insect as a model for fungal infection caused by the genus *Malassezia*, in particular, systemic infections caused by *Malassezia furfur* and *Malassezia pachydermatis,* which are poorly understood. Here, we describe the *G. mellonella* larva inoculation process with *M. furfur* and *M. pachydermatis* and the posterior assessment of the establishment and dissemination of the infection in the larvae. This assessment was done through the evaluation of larval survival, melanization, fungal burden, hemocytes populations, and histological changes. This methodology allows for the identification of virulence patterns between *Malassezia* species and the impact of inoculum concentration and temperature.

Key words Alternative animal model, *Galleria mellonella* larva, *Malassezia furfur*, *Malassezia pachydermatis*, Systemic infection modeling, Fungemia

1 Introduction

Galleria mellonella larva was implemented as a model for bacterial infection in 1968. Since then, there have been an increasing number of publications in which this model has been used to evaluate both the pathogens virulence from different approaches and the host response and antimicrobial activity [1]. This model has gained attention for various reasons. First, the development of the 3Rs principle in which studies that use animal models for laboratory experimentation require investigators to consider Replacement (alternative animal models, in vitro technologies), Reduction (reduce numbers needed in experimental groups), and Refinement (better animal models and welfare) approaches [2]. The use of alternative models such as *G. mellonella* larvae will contribute to the partial replacement due to their current status as nonsentient animals, which implies that they do not require ethical approval for experimentation [3]. Second, the larvae are small and reproduce

Rebecca A. Drummond (ed.), *Antifungal Immunity: Methods and Protocols*, Methods in Molecular Biology, vol. 2667,
https://doi.org/10.1007/978-1-0716-3199-7_2,

fast, which makes it easy to maintain and handle in laboratory conditions and also reduces space [3]. This, in turn, lowers the costs associated with animal maintenance and experimentation. Third, the larvae can be incubated at 37 °C, which is the human corporal temperature [1]. Moreover, the immune system shows some homology with the human innate immune system, both in the cellular and humoral innate immune response [1]. This allows for preliminary high throughput approaches to the understanding of host–pathogen interactions.

Galleria mellonella larva has been implemented as an infection model for yeasts like *Candida albicans* [4, 5], among others. Studies that used this model have shown that the results obtained correlate with the results of virulence evaluation in mammal models [4]. The *G. mellonella* larvae have allowed for the study of the virulence trend of mutants' libraries and different isolates of fungi [6]. For the above reasons, this model is attractive as an infection model for the genus *Malassezia*. The yeasts belonging to this genus are found as part of the mycobiota of humans and animals, but their impact on human health is not fully understood. For example, under specific conditions, these yeasts can cause skin and systemic disease or exacerbate skin disorders [7]. Indeed two species, *Malassezia furfur* and *Malassezia pachydermatis,* have been associated with fungemia in neonates and immunosuppressed patients [8]. Reports of these cases of fungemia are growing, and it has been shown that its prevalence is higher than it was believed before [8, 9]. For this reason, there is a need to study this host–microbe interaction in systemic infections since the majority of studies have focused on superficial infections [10], and the *G. mellonella* larva could be a suitable model for making the first approach to the understanding of this interaction.

In this protocol, *G. mellonella* larvae were implemented and standardized as infection models for *M. furfur* CBS 1878 and *M. pachydermatis* CBS 1879. The results demonstrated that *G. mellonella* larvae is a suitable model for the two species of *Malassezia*. This was shown through the evaluation of larval survival, melanization, fungal burden, hemocytes populations, and histological changes. Also, it was found than the larval mortality and the dissemination of these yeasts in the host depended on the inoculum concentration, the temperature, and the species.

2 Materials

2.1 Larvae Preparation

1. Fifteen *Galleria mellonella* larvae per treatment. These larvae must be used between the fifth and sixth instar with a weight ranging from 200 mg to 300 mg without any mark(s) or spot (s) on the larval surface (*see* **Note 1**).

2. Three sterilized 500 mL beakers.
3. Sterilized paper towel.
4. 0.1% sodium hypochlorite solution.
5. Reusable coffee filter bag with plastic handle.
6. Fourteen standard size Petri dishes (90 mM × 15 mM).

2.2 Larval Inoculation and Survival and Melanization Evaluation

1. A 48-to-72-h *Malassezia furfur* or *Malassezia pachydermatis* culture on modified Dixon agar (36 g.L^{-1} Mycosel agar, 20 g L^{-1} Oxgall, 36 g L^{-1} malt extract, 2 mL L^{-1} glycerol, 2 mL L^{-1} oleic acid, and 10 mL L^{-1} Tween 40) at 33 °C (*see* **Note 2**).
2. A 0.5% Tween 80 solution.
3. Triple folded woven gauze cut into a 3 × 3 cm square.
4. 1 mL Veo insulin syringe with the BD Ultra-Fine 6 mM needle.
5. A plastic inoculation loop.
6. Two 5 mL glass test tubes with a screw cap.
7. Eight 2.0 mL volume microcentrifuge tubes.
8. A Neubauer chamber.
9. Set of pipettes volume 0.5–10 μL, 10–100 μL, 100–1000 μL.
10. Tips for pipettes 10 μL, 100 μL, 1000 μL.
11. Plastic Thimble.
12. Sterilized toothpicks.
13. Fourteen standard size Petri dishes (90 mM × 15 mM) per day of evaluation.

2.3 Fungal Burden Evaluation

The following list of materials is to test the *Malassezia* infection in *G. mellonella* at one temperature, 33 °C or 37 °C. If you evaluate the interaction at both temperatures, you must duplicate the amounts of each material and posterior procedures.

1. Set of pipettes volume 0.5–10 μL, 10–100 μL, 100–1000 μL.
2. Tips for pipettes 10 μL, 100 μL, 1000 μL.
3. Forty-five 2.0 mL volume microcentrifuge tubes.
4. Pestles for microcentrifuge tubes (*see* **Note 3**).
5. A 0.5% Tween 80 solution [Sigma Aldrich, USA].
6. 5 mM glass plating beads.
7. Forty-five standard size Petri dishes (90 mM × 15 mM) with 20 mL of modified Dixon agar containing the specified reagent in Subheading 2.2, **item 1**.

2.4 Hemocytes Population Evaluation

1. Larvae.
2. Scalpel.
3. Cool container.
4. Ice.
5. Microscope slides.
6. Staining rack.
7. Wright stain reagent.

2.5 Histological Procedure

1. Fourteen 2.0 mL volume microcentrifuge tubes.
2. 1 mL Veo insulin syringes with the BD Ultra-Fine 6 mM needle [Becton Dickinson, USA].
3. Cold PBS 1× pH 7.4: dilute 10 mL of PBS 10× [Gibco™, Thermo Scientific, USA] in 90 mL of sterilized distilled water, then adjust, if necessary, the pH to 7.4 with 0.1 N HCL or 0.1 N NaOH as required.
4. 4% paraformaldehyde (PFA) solution in PBS: To prepare 100 mL of this solution, pour 80 mL of PBS 1× in a beaker and heat it while stirring, avoid boiling this PBS 1×. Add 4 g of paraformaldehyde powder [Sigma Aldrich, USA] to the heated PBS 1×, and continue stirring while adding two to three drops of 1 N NaOH (*see* **Note 4**), this will help to dissolve the paraformaldehyde powder. Once the paraformaldehyde is dissolved, cool the solution, filter it with a Whatman filter, adjust the volume of the PFA to 100 mL, and adjust the pH to 7.4. Store at 4 °C in darkness (*see* **Note 5**).
5. Sterilized distilled water.
6. 10% potassium hydroxide (10% KOH).
7. 33% acetic acid: dilute 33 mL of acetic acid (glacial) 100% [Sigma Aldrich, USA] in 67 mL of sterilized distilled water.
8. 70%, 80%, 90%, and 100% ethanol.
9. Scalpel.
10. Microscope slides.
11. Microscope cover glasses.
12. Calcofluor white stain [Sigma Aldrich, USA].
13. Histoplast PE paraffin [Thermo Scientific, USA].
14. Rotary microtome.
15. Hematoxylin-eosin stain kit.

3 Methods

3.1 Larvae Preparation

1. Once *G. mellonella* larvae have arrived from the larvae provider, they need to be dried and stored in darkness from 24 h to 72 h at 33 °C before using them for experimentation (*see* **Note 6**).
2. After this incubation period, select larvae with a weight ranging from 200 mg to 300 mg without any mark(s) or spot(s) on the larval surface. Place the selected larvae into the standard Petri dishes in groups of 15 larvae per treatment until they are ready to be washed. There are a total of seven treatments. First, the batch control treatment that contains larvae that are not washed. Second, the wash control treatment that has larvae that are washed but are not inoculated with the vehicle of the *Malassezia* sp. Inoculum (*see* **Note 7**). Third, the inoculum control treatment that contains larvae inoculated with the 0.5% Tween 80 solution. Finally, the remaining four larvae treatment groups are inoculated with different inoculum concentrations of *Malassezia* sp. Each of these treatment groups must be duplicated to use one group of larvae to evaluate larval survival and melanization, while the other group is used to evaluate fungal burden and histological and hemocyte population changes in each treatment group (Table 1).
3. To set the larval washing station, place the three 500 mL beakers and fill the first one with 0.1% sodium hypochlorite and the second and third beaker with sterile distilled water (*see* **Note 8**).
4. Once the larval washing station is set, repeatedly immerse and remove each of the corresponding groups of larvae for 30 s in the beaker that contains the 0.1% sodium hypochlorite [11].
5. Then, rinse the larvae with sterile distilled water, dipping them in and out for 30 s in the second beaker and 10 s in the third beaker.
6. After washing and rinsing the larvae, use the sterile paper towel to dry the larvae and place them into new sterilized standard size Petri dishes organizing them into the seven different treatments and duplicates (*see* **Note 9**) (Fig. 1).

3.2 Larval Inoculation and Survival and Melanization Evaluation

Follow the next steps to prepare the *M furfur* or *M. pachydermatis* inoculum.

1. Take a 5 mL glass test tube with a screw cap and fill it with 5 mL of 0.5% Tween 80 solution.
2. Then, use the plastic inoculation loop to take half of the *M. furfur* or *M. pachydermatis* lawn of the 48-to-72-h culture on modified Dixon agar incubated at 33 °C.

Table 1
Experimental larval groups distribution

Purpose	Treatments and procedures						
To evaluate larval survival and melanization	**Batch control**	**Wash control**	**Inoculum control**	**$1.5*10^6$ CFU/mL**	**$1.5*10^7$ CFU/mL**	**$1.5*10^8$ CFU/mL**	**$1.5*10^9$ CFU/mL**
	15 larvae Do not wash	15 larvae Wash	15 larvae Wash	15 larvae Wash	15 larvae Wash	15 larvae Wash	15 larvae Wash
		Do not inoculate	Inoculate with 0.1% tween 80 solution	Inoculate with the *Malassezia* sp. inoculum concentration $1.5*10^6$ CFU/mL T6	Inoculate with the *Malassezia* sp. inoculum concentration $1.5*10^7$ CFU/mL T7	Inoculate with the *Malassezia* sp. inoculum concentration $1.5*10^8$ CFU/mL T8	Inoculate with the *Malassezia* sp. inoculum concentration $1.5*10^9$ CFU/mL T9
	Daily larval cleaning and evaluation of larval survival and melanization						
To evaluate fungal burden, and histological and hemocytes population changes	**Batch control**	**Wash control**	**Inoculum control**	**$1.5*10^6$ CFU/mL**	**$1.5*10^7$ CFU/mL**	**$1.5*10^8$ CFU/mL**	**$1.5*10^9$ CFU/mL**
	15 larvae Do not wash	15 larvae Wash	5 larvae Wash	15 larvae Wash	15 larvae Wash	15 larvae Wash	15 larvae Wash
		Do not inoculate	Inoculate with 0.1% tween 80 solution	Inoculate with the *Malassezia* sp. inoculum concentration $1.5*10^6$ CFU/mL T6	Inoculate with the *Malassezia* sp. inoculum concentration $1.5*10^7$ CFU/mL T7	Inoculate with the *Malassezia* sp. inoculum concentration $1.5*10^8$ CFU/mL T8	Inoculate with the *Malassezia* sp. inoculum concentration $1.5*10^9$ CFU/mL T9
	At the day the 50% mortality is reached, three larvae are grounded to evaluate fungal burden, the hemolymph of two larvae is extracted to evaluate changes in hemocytes population, and two larvae per treatment are stored in 4% PFA for histology.						

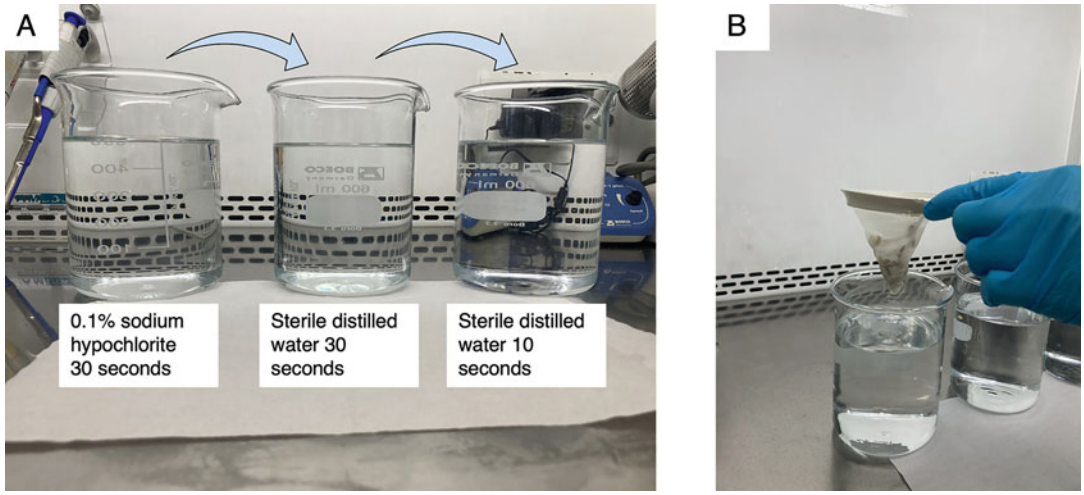

Fig. 1 Wash station. (**a**) Diagram of the position, sequence, and content of each of the beakers in the wash station. Also, the time of washing and rinsing in each of the beakers. (**b**) The reusable coffee filter bag with the group of larvae must be repeatedly immersed and removed during the washing process in each beaker

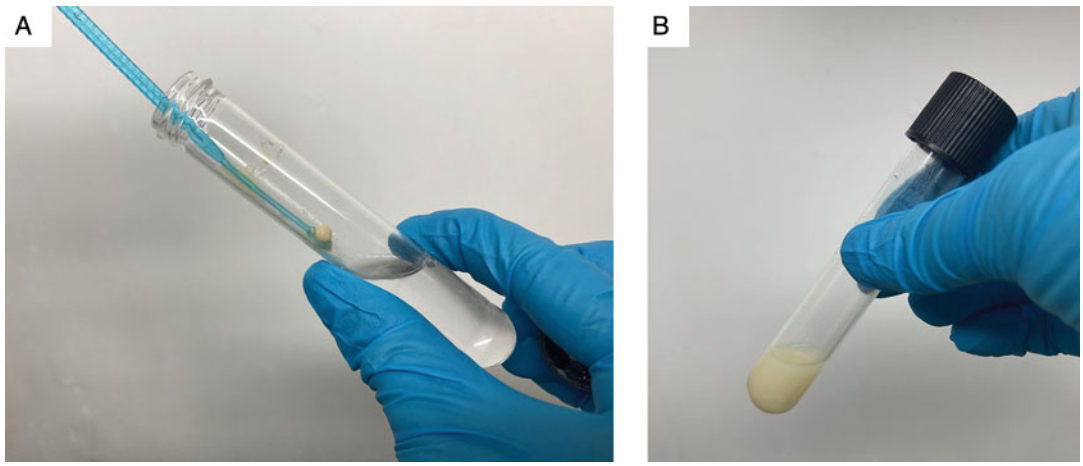

Fig. 2 Inoculum preparation. (**a**) The entire yeast inoculum loop against the sides of the inclined test tube to mix the 0.1% Tween 80 solution with the yeast and suspend them homogeneously. (**b**) The final appearance of the yeast suspension

3. Each time you take a part of the yeast lawn, incline the glass test tube with 0.5% Tween 80 solution 30° to slowly mix the yeast lawn contained in the inoculation loop and the 0.5% Tween 80 solution against the sides of the tube. This must be done until you obtain a whitish highly concentrated yeast suspension (Fig. 2).
4. After producing the yeast suspension described above, mix it for 5 min using a vortex mixer and filter it with the triple folded gauze into a new glass test tube. This new tube will become the original inoculum (*see* **Note 10**).

5. Use the Neubauer chamber to determine the original inoculum concentration and from this original inoculum adjust the *M. furfur* or *M. pachydermatis* inoculum to $1.5*10^6$ CFU/mL, $1.5*10^7$ CFU/mL, $1.5*10^8$ CFU/mL, and $1.5*10^9$ CFU/mL with 0.5% Tween 80.
6. Take the Petri dishes that contain each of the larval groups of the following duplicated treatments: (1) inoculum control treatment, (2) $1.5*10^6$ CFU/mL treatment, (3) $1.5*10^7$ CFU/mL treatment, (4) $1.5*10^8$ CFU/mL treatment, and (5) $1.5*10^9$ CFU/mL treatment for inoculation.
7. The first group of larvae that must be inoculated is the inoculum control treatment group. This group is inoculated with 20 μL of a 0.5% Tween 80 solution. Then, the remaining groups' larvae belonging to the different *Malassezia* inoculum-concentration treatments are inoculated. This inoculation must be done in order from the lowest concentration to the highest concentration.
8. To inoculate the larvae, place a thimble on the index finger, lay a larva on the thimble, and hold the larva with the middle finger and the thumb exposing the larval prolegs [12]. Introduce the insulin syringe needle into the last left proleg at a 35° angle and slowly release a volume of 20 μL of 0.5% Tween 80 solution or the different inoculum inside the larval hemocoel, according to the treatment (Fig. 3).
9. Once the larvae are inoculated, take the Petri dish with the different groups of larvae to incubate at 37 °C or 33 °C, according to the case (*see* **Note 11**).
10. Remove the silk produced by the larvae in each Petri dish on a daily basis. To do this, use sterilized toothpicks to eliminate the silk. In the cases where the cocoon is formed, puncture it in one of the extremes of the structure and pull it off. Once the silk is removed, the larvae can be moved to new clean and sterilized Petri dishes (*see* **Note 12**).
11. Assess larval survival by using the toothpicks to touch larvae and evaluate the response to mechanical stimulus. Report as dead those larvae that do not respond to this stimulus after more than 30 min.
12. Then, evaluate larval melanization through melanization scores according to a modified health index scoring system. In this modified health index scoring system, a score of 4 means no melanized larva; a score of 3 means beige larvae with less than three spots; a score of 2 means beige larvae with more than three spots; a score of 1 means brown larva with more than three spots; and a score of 0 means full melanized larva [13, 14] (Fig. 4).

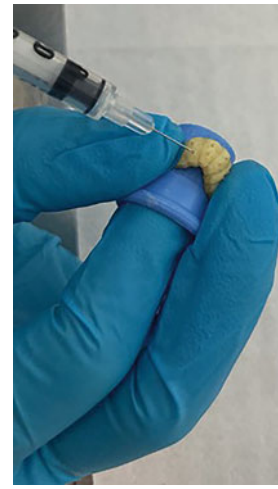

Fig. 3 Larval microinjection. With the help of a thimble to protect from puncturing the glove, the larva is laid out, and the proleg is exposed. The tip of the needle is introduced into the last left proleg at a 35° angle

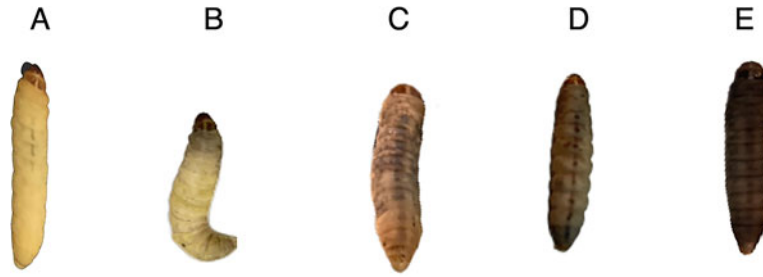

Fig. 4 Larval melanization scores. (**a**) Score 4: no melanized larva. (**b**) Score 3: beige larvae with less than three spots; (**c**) Score 2: beige larvae with more than three spots. (**d**) Score 1: brown larva with more than three spots. (**e**) Score 0: full melanized larva

13. A daily photographic record must be kept.
14. Analyze the resulting data from the larval survival constructing survival curves with the Kaplan and Meier method and compare them with the Log-Rank (Mantel-Cox) test. For the melanization assessment, conduct a 2-way ANOVA test (*see* **Note 13**) (Fig. 5).

3.3 Fungal Burden Evaluation

The fungal burden is evaluated when larval mortality reaches 50%, denoting the mean lethal time to 50% mortality (LT50). The fungal burden evaluation must be carried out by triplicate in each replicate.

1. Before processing the larvae for fungal burden evaluation, prechill three larvae per treatment at 4 °C for 10 min to anesthetize them.

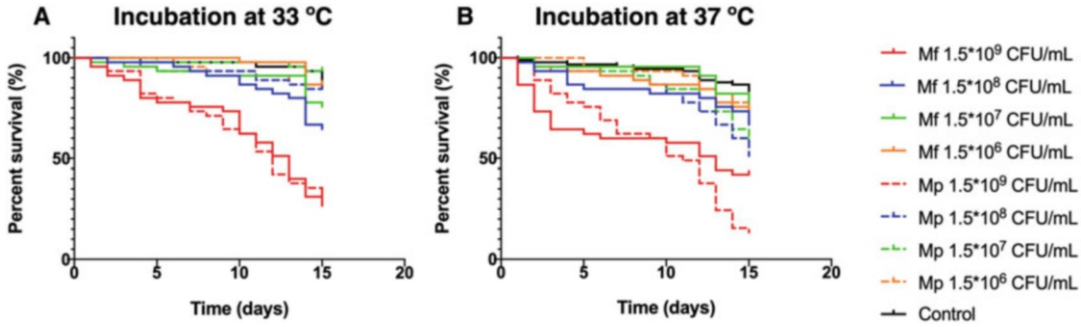

Fig. 5 *G. mellonella* larval survival curves. Larvae inoculated with the four different inoculum concentrations of *M. furfur* and *M. pachydermatis* and incubated at (**a**) 33 °C and (**b**) 37. (**a**) At 33 °C, it shows a significant negative effect on larval survival (p-value < 0.0001) of larvae inoculated with $1.5*10^9$ CFU/mL. (**b**) At 37 °C, you can observe the bimodal pattern of the survival curve of larvae inoculated with highest inoculum concentration of *M. furfur*, differing from the survival curve of larvae inoculated with *M. pachydermatis* (p-value $= 0.0528$). Continuous line, survival curve of larvae inoculated with *M. furfur*; discontinuous line, survival curve of larvae inoculated with *M. pachydermatis*; *Mf M furfur*, *Mp M. pachydermatis*

2. Inside a laminar flow cabinet, label the forty-five 2 mL microcentrifuge tubes and Petri dishes according to the different treatments and each of the larvae processed (3 larvae per treatment). Since the batch control, wash control, and the inoculum control were not inoculated with *Malassezia* spp., it is not necessary to make serial dilutions from the processed larvae. However, for the larvae that were inoculated with any of the four concentrations of these yeasts, serial dilutions until 10^3 will need to be made.
3. Add 1000 μL of the 0.5% Tween 80 solution to each of the tubes where larvae will be grounded.
4. Add 900 μL of the 0.5% Tween 80 solution to the tubes where the original inoculum obtained from the homogenized larva will be serially diluted.
5. Before grounding the larvae, take the larvae from the prechill treatment, introduce them into a microcentrifuge tube with 70% ethanol, and dry each larva with a sterilized paper towel.
6. To ground the larvae, introduce them to each of the corresponding labeled treatment tubes. Then, using the pestle for microcentrifuge tube [15], homogenize the larval tissue for 5 min and mix it using a vortex mixer for 1 min.
7. Do the serial dilutions for the treatments where larvae were inoculated with the different inoculum concentrations of *Malassezia* sp.
8. After all the tubes contain the corresponding dilution of uninfected and infected *G. mellonella* larvae tissue of each treatment, plate 100 μL on the surface of the modified Dixon agar and use the glass plating beads to spread the yeasts over the Petri dish homogeneously.

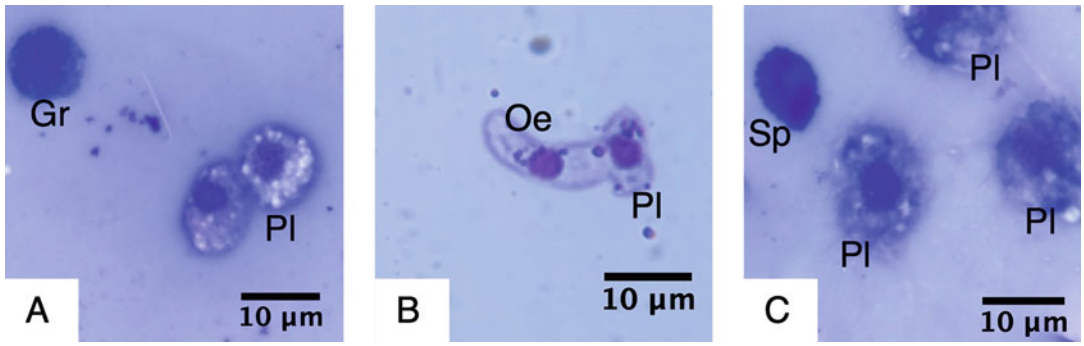

Fig. 6 Hemocyte of *G. mellonella* under light microscope (1000×). (**a**) Plasmocyte (Pl) and Granulocyte (Gr). (**b**) Oenocytoid (Oe) and Plasmocyte (Pl). (**c**) Spherulocyte (Sp) [14]

9. Finally, incubate at 33 °C and revise daily for the appearance of new colony-forming units until they stop growing.

3.4 Hemocytes Population Evaluation

As in the case of fungal burden, the hemocytes evaluation must be done when the LT50 has been reached.

1. Take two larvae per treatment from the groups of larvae inoculated for fungal burden and hemocytes evaluation. Then, place the larvae into the cool container with ice for a period of 5 min (*see* **Note 14**).
2. Once the larvae have stopped moving, take each of them and pierce the last segment of each larva, allowing one drop of the hemolymph to fall on a microscope slide.
3. Then, use another microscope slide to produce a hemolymph smear.
4. Stain the hemolymph smear with the Wright stain.
5. Observe each slide under a light microscope and count 200 hemocyte cells discriminating by the cell populations (plasmocytes, granulocytes, spherulocytes, oenocytoids, and prohemocytes) (Fig. 6). From this, determine the percentages of each the hemocytes populations.

3.5 Histological Procedure

1. To prepare the larvae for histological staining, take two larvae per treatment and put each of them into a 2 mL microcentrifuge tube. Then, through the last left proleg, microinject 50–100 µL of 4% PFA in PBS as a tissue fixative. Also, add approximately 500 µL of 4% PFA in PBS to the microcentrifuge tube (*see* **Note 15**). Store at 4 °C for 10 days previous to paraffin embedding (*see* **Note 16**).
2. Before starting the paraffin embedding, larvae tissue must be dehydrated in four increasing ethanol concentrations (70%, 80%, 90%, and 100% ethanol). The larvae must remain for 1 hour in each ethanol concentration [12].

3. Once the larvae have been dehydrated, start the paraffin embedding process using the histoplast PE paraffin. Then, section the paraffin blocks every 5 μM and stain the resulting sections with hematoxylin-eosin.
4. To observe the larval nodules formation in the entire larvae and their location, cut a prefixed larvae in 4% PFA in two halves vertically with a scalpel (*see* **Note 17**). Then, observe each larva half under a stereoscope and identify the location of each of the larval nodules.
5. To observe and confirm the establishment of the infection by either of the two species of *Malassezia*, dissect the black nodule structures with two insulin syringes and place them on the top of a microscope slide. Then, add one drop of Calcofluor white followed by one drop of 10% KOH. Keep in darkness for 30 min prior to microscopic observation. Cover the sample with a cover glass and take it under a laser scanning confocal microscope ($\lambda_{Ex} = 355$ and $\lambda_{Em\ max} = 433$) (*see* **Note 18**).

4 Notes

1. Some larvae display a darker color on the surface, but these darker larvae can be used if they do not present any spot(s) or mark(s) on the cuticle surface.
2. To keep the reproducibility of the assays, the *Malassezia* sp. culture must not be more than 72 h old since after this time period it has shown a virulence decrease.
3. If you do not have a pestle for microcentrifuge tubes, a 1000 μL piper tip can be used to ground the larvae.
4. After adding the 1 N NaOH, be patient and wait until the paraformaldehyde dissolves in the PBS. You must wait at least 30 s before adding one more drop of 1 N NaOH, if necessary. The solution is ready when it becomes clear.
5. The 4% PFA in PBS needs to be kept in darkness at 4 °C for a period no longer than 1 month, so it is important to calculate and prepare the necessary amount of 4% PFA needed for your experiment.
6. If the larvae are not properly rested after the trip from the provider to your institution, they will not be suitable for the assay since more than 50% of unrested larvae will die in the first 24 h even in the control treatments. When storing larvae, introduce a piece of sterilized paper towel to eliminate humidity associated with larval transpiration. This humidity could affect larval fitness.

7. The vehicle of the *Malassezia* sp. inoculum is the 0.5% Tween 80 solution. This solution permits the disaggregation of *Malassezia* yeast aggregates that are formed owing to the outer lipid layer.
8. Warm the water used in each beaker at the washing station to 37 °C. If the water is cold or at room temperature, the larvae are negatively affected with darkishness and loss of movement.
9. After washing the larvae, they show a reduced movement due to the lowering of their temperature and metabolism. For this reason, until the inoculation process begins, incubate the larvae at 33 °C, so they reactive their metabolism. It is crucial to avoid leaving the larvae outside the incubator for extended periods.
10. The 5-min mix with the vortex mixer is essential to avoid the presence of the aggregate; otherwise, a significant number of yeasts are lost when the yeast suspension is filtered through the gauze.
11. Seal the Petri dishes with tape. That is important since the larvae tend to lift the dish's lid to escape.
12. It is necessary to clean the larvae every day because the larvae produce silk constantly, and as time passes, the cocoons become harder to eliminate. Also, eliminating the cocoons prevents the larval transition to pupae.
13. As was expected, we found differences between the two species related to their niche, the temperature in which they are usually found, and their low virulence. For instance, in all treatments, significant changes (p-value < 0.0001) in larval survival were observed in larvae inoculated with the highest inoculum concentration ($1.5*10^9$ CFU/mL). In fact, the larval survival of larvae inoculated with the three remaining inoculum concentrations *of M. furfur* demonstrated an insignificant difference when compared to the control group. In contrast, larvae inoculated with *M. pachydermatis* and incubated at 37 °C show lower levels of larval survival. In this case, the larvae inoculated with the inoculum concentrations $1.5*10^8$ CFU/mL and $1.5*10^7$ CFU/mL showed a significant decrease in their larval survival (p-value < 0.5), but with lower effect. Besides, as a result of incubating the inoculated larvae at 33 °C (the human superficial skin temperature, where *Malassezia* is usually found) and 37 °C (the internal human body temperature), we found differences between the virulence patterns of *M. furfur* and *M. pachydermatis* (Fig. 4). As can be observed in Fig. 4a, the survival curve of larvae inoculated with the highest inoculum concentration of *M. furfur* and *M. pachydermatis* and incubated at 33 °C showed similar behavior, reaching 50% of mortality between day 12 and 13. Contrasting with this result, the larval survival curve of larvae

inoculated with a concentration of $1.5*10^9$ CFU/mL of *M. furfur* and *M. pachydermatis* and incubated at 37 °C showed a different survival pattern. In the case of larvae inoculated *with M. furfur*, a bimodal larval survival pattern that encompassed a fast increase in the larval mortality during the first 5 days was observed. Then, a pause in the larval mortality occurred between day 6 to 10, and finally, larval mortality restarted until day 15 with 57% of mortality. On the other hand, larvae inoculated with *M. pachydermatis* conserved a larval mortality pattern similar to that of larvae incubated at 33 °C, but with a higher percentage of larva death at day 15 (87%)**.** Similarly, in the histological assessment, we observed greater tissue invasion, while the fungal burden evaluation led to a higher recovery of yeast from larvae inoculated with *M. pachydermatis* than from those inoculated with *M. furfur*. This was mainly in larvae incubated at 37 °C.

14. The ice bath will help to anesthetize the larvae since the temperature of these organisms depends on an external heat source. When the temperature drops, the larvae are immobilized. The time needed to reach this state can vary, and sometimes you will need more than 5 min. Touch the larvae, if they do not respond to the mechanical stimulus, they are ready for the process.
15. It is important to fully immerse the larvae in the 4% PFA in PBS. Add as much of this solution that is needed to completely submerge the larvae.
16. After the 10 days of the fixative process, the larvae can be put in 70% ethanol prior to paraffin embedding. However, larval sectioning can be challenging due to the thickness of the cuticula, which makes it difficult to obtain a complete intact section. In this case, it is recommended to immerse the larvae in 10% KOH for 24 h, after this, wash the larvae with sterile distilled water for 6 hours and store them at 4 °C. Then, remove the sterile distilled water, add 33% acetic acid, and store it at 4 °C for 24 h. Finally, wash with sterile distilled water and store them at 4 °C for 6 h [16]. If possible, initiate the paraffin embedding process immediately, otherwise immerse larvae in 70% ethanol and store at 4 °C. This cuticle softening is recommended for systemic infection modeling.
17. While dissecting and observing larvae under the stereoscope, keep the tissue hydrated by adding cold PBS 1× pH 7.4. This will facilitate the dissection of larvae and will also prevent the tissue from damage. This will lead to having a good estimative of the nodules' location in the whole larval body plane.
18. If there is no access to a laser scanning confocal microscope, you can use a fluorescence microscope. In this case, observe the samples under UV light.

Acknowledgments

We thank the Faculty of Sciences for financial support grant No. INV-2018-31-1252, the department of biological science, the Vice-Presidency of Research and Creation, the AnimalCore and the department of languages and culture, Universidad de los Andes.

References

1. Dinh H, Semenec L, Kumar SS et al (2021) Microbiology's next top model: *Galleria* in the molecular age. Pathog Dis 79(2):1–11. https://doi.org/10.1093/femspd/ftab006
2. Hubrecht RC, Carter E (2019) The 3Rs and humane experimental technique: implementing change. Animals 9:754. https://doi.org/10.3390/ani9100754
3. Piatek M, Sheehan G, Kavanagh K (2020) Utilising *Galleria mellonella* larvae for studying in vivo activity of conventional and novel antimicrobial agents. Pathog Dis 78:1–13. https://doi.org/10.1093/femspd/ftaa059
4. Amorim-Vaz S, Delarze E, Ischer F et al (2015) Examining the virulence of *Candida albicans* transcription factor mutants using *Galleria mellonella* and mouse infection models. Front Microbiol 6:1–14. https://doi.org/10.3389/fmicb.2015.00367
5. García-Carnero LC, Clavijo-Giraldo DM, Gómez-Gaviria M et al (2020) Early virulence predictors during the *Candida* species–*Galleria mellonella* interaction. J Fungi 6:152. https://doi.org/10.3390/jof6030152
6. Trevijano-Contador N, Zaragoza O (2019) Immune response of *Galleria mellonella* against human fungal pathogens. J Fungi 5:3. https://doi.org/10.3390/jof5010003
7. Sparber F, Ruchti F, LeibundGut-Landmann S (2020) Host immunity to *Malassezia* in health and disease. Front Cell Infect Microbiol 10:198. https://doi.org/10.3389/fcimb.2020.00198
8. Rhimi W, Theelen B, Boekhout T et al (2020) *Malassezia* spp. yeasts of emerging concern in fungemia. Front Cell Infect Microbiol 10:370. https://doi.org/10.3389/fcimb.2020.00370
9. Iatta R, Cafarchia C, Cuna T et al (2014) Bloodstream infections by *Malassezia* and *Candida* species in critical care patients. Med Mycol 52:264–269. https://doi.org/10.1093/mmy/myt004
10. Torres M, de Cock H, Celis Ramírez AM (2020) In vitro or in vivo models, the next frontier for unraveling interactions between *Malassezia* spp. and hosts. How much do we know? J Fungi 6:155. https://doi.org/10.3390/jof6030155
11. Stephens JM (1962) Bactericidal activity of the blood of actively immunized wax moth larvae. Can J Microbiol 8:491–499. https://doi.org/10.1139/m62-064
12. Firacative C, Khan A, Duan S et al (2020) Rearing and maintenance of *Galleria mellonella* and its application to study fungal virulence. J Fungi 6:130. https://doi.org/10.3390/jof6030130
13. Kay S, Edwards J, Brown J et al (2019) *Galleria mellonella* infection model identifies both high and low lethality of *Clostridium perfringens* toxigenic strains and their response to antimicrobials. Front Microbiol 10:1281. https://doi.org/10.3389/fmicb.2019.01281
14. Torres M, Pinzón EN, Rey FM et al (2020) *Galleria mellonella* as a novelty in vivo model of host-pathogen interaction for *Malassezia furfur* CBS 1878 and *Malassezia pachydermatis* CBS 1879. Front Cell Infect Microbiol 10:199. https://doi.org/10.3389/fcimb.2020.00199
15. Fallon J, Kelly J, Kavanagh K (2012) *Galleria mellonella* as a model for fungal pathogenicity testing. In: Brand A, MacCallum D (eds) Host-fungus interactions. Methods in molecular biology (methods and protocols), vol 845. Humana, Totowa. https://doi.org/10.1007/978-1-61779-539-8_33
16. Barbosa P, Berry DL, Kary CS (2014) Problems of sclerotized chitin: softening insect cuticle. In: Barbosa P, Berry DL, Kary CS (eds) Insect histology. Wiley, London

Chapter 3

Mouse Organotypic Brain Slice Cultures: A Novel Model for Studying Neuroimmune Responses to Cryptococcal Brain Infections

Amalia N. Awala, Maahir Kauchali, Anja de Lange, Emily Ruth Higgitt, Tshepiso Mbangiwa, Joseph V. Raimondo, and Rachael Dangarembizi

Abstract

Cryptococcal meningitis affects millions of people worldwide and is especially prevalent in regions with a high burden of HIV/AIDS. The study of the pathophysiology of this often fatal disease has been significantly hindered by the lack of reliable experimental models, especially at the level of the brain, which is the main organ of injury. Here we outline our novel protocol for the use of hippocampal organotypic brain slice cultures (HOCs) to study the host–fungal interactions during cryptococcal infections of the brain. HOCs are a powerful platform for investigating neuroimmune interactions as they allow for the preservation of all innate neuroglial cells including microglia, astrocytes, and neurons, all of which maintain their three-dimensional architecture and functional connectivity. We made HOCs from neonatal mice and infected these with a fluorescent strain of *Cryptococcus neoformans* for 24 h. Using immunofluorescent staining, we confirmed the presence and morphology of microglia, astrocytes, and neurons in HOCs prior to infection. Using fluorescent and light microscopy, we also confirmed that *Cryptococcus neoformans* encapsulates and buds in vitro, as it would in a host. Finally, we demonstrate that infection of HOCs with *Cryptococcus neoformans* results in close association of the fungal cells with host microglial cells. Our results demonstrate the utility of HOCs as a model to study the pathophysiology and host neuroimmune responses in neurocryptococcosis, which may assist in improving our collective understanding of the pathogenesis of this disease.

Key words Brain slice cultures, Cryptococcal meningitis, Neuroinfections, Neuroimmune responses, Microglia

1 Introduction

The ubiquitous and encapsulated fungus *Cryptococcus neoformans* is the primary causative agent of cryptococcal meningitis (CM), the

Supplementary Information The online version contains supplementary material available at https://doi.org/10.1007/978-1-0716-3199-7_3.

Rebecca A. Drummond (ed.), *Antifungal Immunity: Methods and Protocols*, Methods in Molecular Biology, vol. 2667,
https://doi.org/10.1007/978-1-0716-3199-7_3,

leading cause of adult meningitis and mortality in people living with human immunodeficiency virus (HIV). CM is an often fatal infection of the brain that disproportionately affects people living in poor urban and rural parts of the developing world [1, 2]. Despite the unacceptably high mortality rates associated with CM, the development of effective drugs to treat this disease has been hindered by a lack of understanding of its pathogenesis especially at the level of the brain, which is the main organ of injury. The limited research and data availability are exacerbated by the lack of reliable experimental models of CM. Here we propose the use of hippocampal organotypic brain slice cultures (HOCs) as a model to study the pathogenesis of CM.

HOCs present a powerful platform for studying the innate immune responses to infection at the cellular and molecular level [3–8]. The main advantage of this brain model system for studying innate immune responses to infection is its excellent representation of the various resident immune cells of the brain. Additionally, the structural and functional connections between all glial cells and neurons remain intact. As such, HOCs could serve as a powerful model for studying cryptococcal infections of the brain.

We have therefore developed a protocol, detailed below, for the infection of HOCs with a fluorescent strain of *Cryptococcus neoformans*. Using fluorescent immunostaining techniques, we demonstrate the presence and morphology of all principal neuroglial cells in HOCs prior to infection and then proceed to demonstrate that cryptococcal cells infect the HOCs and are closely associated with microglial cells. This serves to confirm the utility of the HOC model in studying the pathophysiology of neurocryptococcosis.

2 Materials

2.1 Cryptococcus neoformans *Culture*

1. Sterile petri dishes.
2. Plate spreaders.
3. T75 cell culture flask.
4. Sterile 15 mL falcon tubes.
5. Neubauer hemocytometer.
6. Light microscope.
7. Yeast extract Peptone Dextrose (YPD) agar: To make 1 L of YPD agar, dissolve 15 g agar, 20 g bacteriological peptone, 20 g glucose, and 10 g yeast extract in 1 L of distilled water. Autoclave the solution at 121 °C for 2 h before use.

8. YPD broth: To make 1 L of YPD broth, dissolve 20 g bacteriological peptone, 20 g glucose, and 10 g yeast extract in 1 L of distilled water. Autoclave the solution at 121 °C for 2 h before use.
9. Phosphate-buffered saline (1×) (PBS).

2.2 Organotypic Culturing

1. Six-well plates.
2. Millipore inserts.

2.2.1 Culture Trays

3. Growth medium (GM): To make 500 mL of growth medium add 115 mL of Earle's balanced salt solution (EBSS), 250 mL of minimum essential medium (MEM), 3.25 g of D-glucose, 125 mL of horse serum, and 10 mL of B-27 supplement to a measuring cylinder (*see* **Note 1**). Cover the measuring cylinder with parafilm, shake/invert, and filter sterilize the solution. Aliquot into 50 mL falcon tubes and store at 4 °C. pH should be between 7.2 and 7.4 and osmolarity should be 320 ± 10 mOsm/L [9].

2.2.2 Decapitation and Brain Removal

1. Dissection medium (DM): To make 500 mL of dissection medium, add 500 mL of EBSS, 3.05 g of 4-(2-hydroxyethyl)-1-piperazineethanesulfonic acid (HEPES), 3.30 g of glucose, and 100 μL of saturated sodium hydroxide (NaOH) (or 2.5 mL of 1 M NaOH) to a measuring cylinder. Shake the mixture well and filter sterilize. Aliquot into 50 mL falcon tubes and store at −20 °C [9] (*see* **Note 2**).
2. One chrome platinum double-edged razor blade (for tissue chopper).
3. Sterile 50 mL falcon tubes.
4. Ethanol (70%).
5. Decapitation instruments.
   (i) Small metal bar (for internal cervical dislocation).
   (ii) Decapitation scissors (large enough to easily decapitate mouse pups).
   (iii) Fine point splinter forceps (for holding the head in place).
   (iv) Small, curved-blade scissors (for cutting the scalp skin).
   (v) Two splinter forceps (for removing scalp skin and skull pieces).
   (vi) Mini dissecting scissors (to cut through the skull).
6. Hippocampal dissection instruments.
   (i) Curved forceps (for holding the brain).
   (ii) Scalpel no. 11 (with a sterile, straight-edged, pointed-tip, blade).

(iii) Micro spatula (straight flat strip on one side and rounded angled flat strip on the other end).

7. Paper towels.
8. Filter paper.
9. Disposal container for mouse carcass.
10. Pasteur pipettes.
11. Petri dishes (35 mM).
12. Petri dish (60 mM).
13. Lamp for extra light on hippocampal dissection zone.
14. McIlwain Tissue chopper (set to 350 μM).
15. Ice-cold metal slab.
16. Postnatal day 7 mouse (P7).
17. Two plastic chopping discs.
18. Two 250 mL beakers.
19. Light microscope.

2.3 Hippocampal Brain Slice Infection and Sample Collection

1. Growth medium.
2. Eppendorf tubes.
3. Prepared *C. neoformans* inoculum.

2.3.1 Stimulation

2.3.2 Sample Collection

1. Eppendorf tubes.
2. Petri dishes.
3. Scalpel.
4. Forceps.
5. Ethanol (70%).
6. PBS (1×).

2.4 Immunohistochemistry

1. One 24-well Plate.
2. PBS (1×).
3. Paraformaldehyde (4%) (PFA).
4. Wash buffer: 0.3% Triton-X in 1 X PBS.
5. Blocking buffer: 5% bovine serum albumin (BSA), 1% Triton-X in 1 X PBS.
6. Primary antibodies.
   (i) Anti-IBA1 (microglial marker).
   (ii) Anti-S100β (astrocyte marker).
   (iii) Anti-NeuN (neuronal marker).
7. Secondary Antibodies.

(i) Donkey Anti-Rabbit Alexa Fluor 647.
(ii) Hoechst nuclear marker.

8. Mowiol (aqueous mounting medium).
9. Kim-wipes.
10. Microscope slides (75 mM × 25 mM).
11. Cover slips (24 mM × 50 mM).
12. Small paint brushes for mounting.

3 Methods

3.1 Organotypic Culturing

This procedure entails the removal of the brain of a postnatal day 7 mouse, dissecting out the hippocampus and sectioning it into 350 μM slices. These slices are plated on Millipore membrane inserts with access to growth medium and kept in culture for 6 days; thereafter, they can be treated and used for various analyses (Fig. 1).

3.1.1 Plate Preparation (Complete in a Biological Safety Cabinet)

1. Use a steripette to fill each well of the 6-well plate with 1.2 mL of growth medium.
2. Use sterile forceps to place a Millipore insert in each of the wells individually.
3. Label the plate and thereafter spray it down externally with 70% ethanol before placing it in a 37 °C incubator.

3.1.2 Organotypic Culture Set-Up

1. Sterilize all working areas with 70% ethanol and sterilize all dissection instruments with a cold sterilant prior to use. Thereafter place the instruments in a beaker half-filled with 70% ethanol.
2. Cut out a circle of filter paper, and line the bottom of a medium (60 mM) petri dish then place under the UV light for at least 5 min.
3. Place one 50 mL falcon tube of dissection medium (DM) in the heating bath to thaw but only thaw it to a slush/ice-cold consistency and keep on ice throughout the culture procedure.
4. Place the plastic sheet on the counter in one area and create the decapitation zone.
5. Lay out some paper towels (folded at least 3 times) for the decapitation for each pup (this serves to absorb blood from decapitation and can then be thrown away and replaced to create a blood-free area for the decapitation of the subsequent mouse).
6. Lay out decapitation instruments on a folded paper towel next to the decapitation zone.

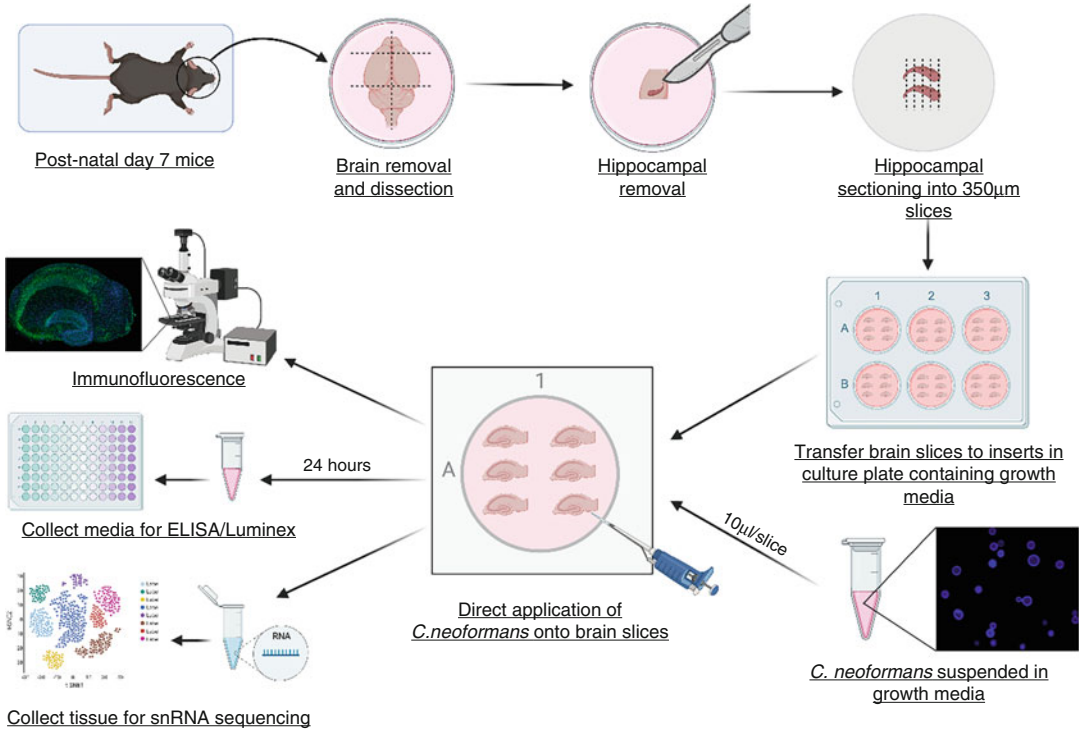

Fig. 1 An illustration of the workflow for organotypic culture of mouse hippocampal brain slices and subsequent infection with *C. neoformans*. 1: A postnatal day 7 mouse is decapitated, and the brain is removed. 2. Excess anterior and posterior portions of the brain are removed, and the brain is separated into its two hemispheres, using a scalpel. 3: Brain is further dissected, and the hippocampus is gently removed. 4: Using a McIlwain tissue chopper, the hippocampus is sectioned into 350 µM-thick slices. 5: Once appropriate slices are selected, they are transferred onto Millipore membrane inserts in a 6-well plate containing growth medium and allowed to recover in the incubator, with regular medium replacement, for a 6-day period. 6: After 6 days in culture, *C. neoformans* cells, suspended in growth medium, are applied directly to brain slices. 7. After 24 h of exposure to *C. neoformans*, the brain slices and growth medium are collected for subsequent analysis using immunofluorescent staining, enzyme-linked immunosorbent assays (ELISA), multiplex assays, or even single-nucleus RNA sequencing. Figure created with BioRender.com

7. Attach a sterile, chrome platinum double-edged razor blade to the McIlwain tissue chopper. Ensure the tissue chopper is set to 350 µM and medium speed (approx. 2 Hz).
8. Lay the plastic chopping discs next to the tissue chopper on a folded paper towel and flash sterilize them 70% ethanol.
9. Wrap a flat ice-cold metal slab in tissue paper and drench in ethanol, place on top of ice in a polystyrene lid/dish filled with ice; this will be the hippocampus removal zone.
10. Turn on the light source and direct light over the hippocampal removal zone.

11. Fill a small (35 mM) petri dish with 6 mL of DM using a Pasteur pipette and place on ice in the hippocampal removal zone.
12. Using a Pasteur pipette add some DM to the now sterile medium petri dish (60 mM) containing the filter paper disc (add enough DM to fill the bottom half of the petri dish to a depth of 2–3 mm). Place the closed petri dish on the cold metal slab in the hippocampal removal zone.

3.1.3 Extracting the Brain

1. Put on two pairs of gloves, spray hands (gloves) with 70% ethanol.
2. In the decapitation zone, place some paper towel on the plastic sheet to soak up any blood.
3. Place the mouse pup on the paper towel. Swiftly push the metal bar down just behind the mouse's skull in order to internally decapitate the mouse.
4. Use the decapitation scissors to cut off the head and discard the carcass in a disposal container.
5. Spray the head thoroughly with 70% ethanol.
6. Push the fine point splinter forceps down through the nose of the mouse to hold the head in place and cut the scalp skin along the sagittal axis of the skull with the curved-blade scissors, being careful not to cut through the bone.
7. Use splinter forceps to peel away the scalp skin and expose the skull. Next, using the mini dissecting scissors, carefully cut the skull along the midline in the sagittal plane (between the brain hemispheres). Use only the tip of the scissors to cut through the skull, cutting as shallow as possible to avoid any damage to the brain tissue.
8. Using the same mini dissecting scissors, cut the skull from the posterior end to the eye socket, at a level below the brain, on both sides.
9. Insert one blade of mini dissection scissors into one eye socket and push it through to the eye socket on the opposite side of the head. Cut the skull after having done so (*see* **Note 3**).
10. Remove both halves of the loosened skull cap by gently gripping one half of the loosened skull cap with a fine point splinter forceps and peeling it away from the brain, starting at the nose bridge and pulling laterally and backwards.
11. Once the skull cap has been removed, gently tip the brain out of the skull into the awaiting small petri dish (35 mM) filled with 6 mL of DM.
12. Dispose of the remainder of the head in the disposal container.
13. Remove the first pair of gloves, so that you remain with one pair disinfecting generously with 70% alcohol.

3.1.4 Hippocampal Removal

1. In the small petri dish containing the brain, use the curved forceps to gently grip both temporal sides of the brain and use the scalpel to cut off a small anterior portion (olfactory bulbs and about 0.5 mM more) as well as a small posterior portion (cerebellum), as shown in Fig. 1.
2. Still using the curved forceps, gently grip the brain on the anterior and posterior aspects and separate the two hemispheres by making a cut along the sagittal plane using a scalpel (Fig. 1).
3. Using the curved forceps, gently transfer both of the hemispheres to the medium petri dish containing the filter paper disc and which has been half-filled with DM. Ensure that the hemispheres are resting on the corpus callosum side (medial aspect).
4. Using the flat end of the microspatula, tip the hemisphere onto the flat anterior surface and keep it upright by gently supporting/gripping the hemisphere with the curved forceps halfway up on the dorsal/ventral surfaces. You will notice a faint fissure midway through the posterior surface (which is now facing upward).
5. Carefully insert the tip of the flat end of the spatula into the fissure and gently pull the medial tissue away from the tissue on the cortical side (*see* **Note 4**). Try to minimize contact with the cortical side of the fissure with the spatula, as this is where the hippocampus is located. The medial tissue can now be discarded. The remaining tissue should be placed cortex-side down.
6. The hippocampus should now be visible toward the posterior end of the brain nestled under the cortex. It can be identified by curved lines that are a slightly darker pink to the surrounding brain tissue (*see* Fig. 1. For a graphical representation of the shape and location of the hippocampus).
7. Place the angled end of the spatula at one end of the hippocampus and gently lift it, then move the spatula underneath the hippocampus, along the length, to loosen it from the surrounding tissue. Next, carefully flip the hippocampus over, towards the posterior aspect of the brain. It should now only be connected to the rest of the brain tissue by a fine layer of tissue along one edge.
8. Use the angled end of the spatula to gently pull the hippocampus away from the rest of the tissue and sever the remaining connected tissue by pressing the spatula down along the edge where it is still attached. Try to leave as little excess tissue attached to the hippocampus as possible.
9. Repeat with the second hemisphere.

10. Place both hippocampi on a white disk for chopping by gently lifting each hippocampus onto the curved end of the spatula, medial side up, and then inverting the spatula in order to lay the hippocampus out onto the chopping disk. Ensure that the two hippocampi are parallel to each other (see illustration in Fig. 1) (*see* **Note 5**).

3.1.5 Slicing and Plating of the Hippocampal Slices

1. Place the chopping disk with the hippocampi on the stage of the McIlwain tissue chopper. Ensure that the hippocampi are perpendicular to the blade.
2. Using the 350 μm slice width setting, engage the tissue chopper, slicing at medium speed.
3. Once the tissue is chopped, remove the chopping disc and hold it over an empty 50 mL falcon tube. Use a Pasteur pipette filled with cold DM to spray the tissue off of the chopping disc and into the 50 mL falcon tube.
4. Shake/swirl the falcon tube to separate the slices.
5. Pour the DM containing the suspended slices from the 50 mL falcon tube into a small 35 mm petri dish and place under a light microscope (*see* **Note 6**).
6. Observe slices under low magnification (10×) and using a Pasteur pipette, select the slices with well-preserved morphology (*see* **Note 7**).
7. Once you have selected the appropriate slices, transfer them to the biosafety cabinet. Remove one of the prepared plates from the incubator and carefully transfer the slices, one at a time, onto the membranes of the Millipore insert within the 6-well plate (Fig.1).
8. Using a sterile Pasteur pipette, remove any excess DM solution surrounding the slices.
9. Close the 6-well plate, spray with a fine mist of alcohol, and return to the incubator for 6 days to allow the tissue to recover. GM should be changed every second day and should be replaced with 1.2 mL of fresh GM. Incubator conditions should be 37 °C with 5% CO_2 levels, see Fig. 2 for an example of what a healthy organotypic hippocampal slice and the various cell markers look like.

*3.2 Culturing (*Cryptococcus neoformans*)*

1. Take a loopful of *C. neoformans* and spread on a YPD Agar plate. Leave to grow in a closed petri dish at room temperature and in the presence of light for 48 h.
2. After 48 h, take a loopful of the *C. neoformans* colony grown on YPD agar and inoculate 10 mL of YPD broth in a T75 flask.
3. Incubate at 30 °C with shaking at 110 rcf for 22 h in the presence of light.

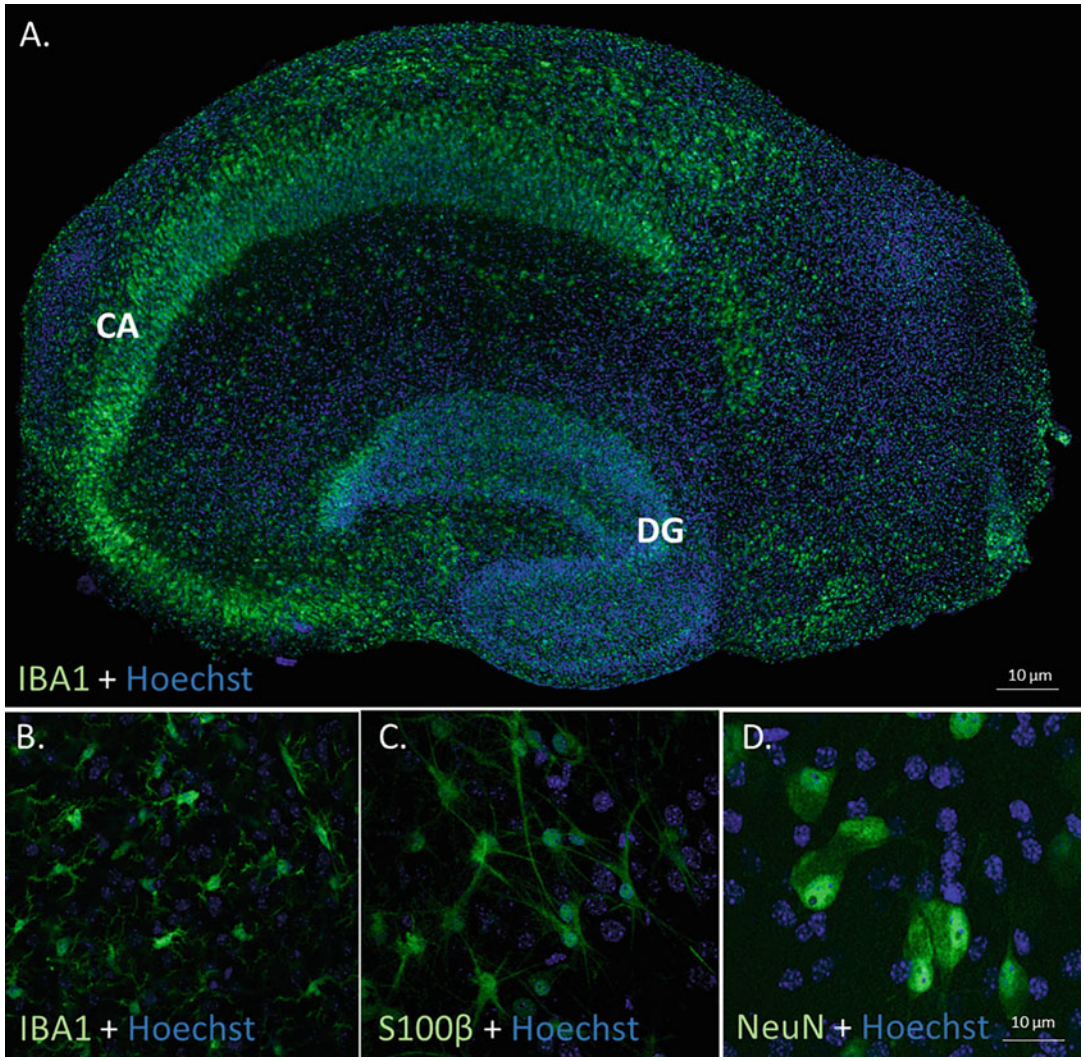

Fig. 2 Hippocampal organotypic brain slices (made from postnatal day 7 mice and imaged after 6 days in culture) display preserved architecture and retain microglial, astrocyte, and neuronal populations. (**a**) A low magnification (20X) confocal tile scan showing the preserved architecture of an organotypic hippocampal brain slice. Microglial cells are visualized in green (IBA1) and cell nuclei are visualized in blue (Hoechst). Both the cornu ammonis (CA) region and in the dentate gyrus (DG) are clearly visible. (**b**–**d**) Microglial, astrocytic, and neuronal cell populations and morphology are preserved. High magnification (63X) images of microglia (IBA1) (**b**), astrocytes (S100β) (**c**), and neurons (NeuN) (**d**), all co-stained with a nuclear cell marker (Hoechst), display preserved presence and morphology of resident brain cells

4. Thereafter, centrifuge the 10 mL of *C. neoformans* culture at 2438 rcf for 5 min at 27 °C.
5. Remove the supernatant and wash the pellet with 10 mL of 1× PBS.
6. Repeat the wash (**step 4**–**5**) three times.

7. Count the number of cells using a Neubauer hemocytometer as follows.
   (i) Dilute a hundredfold by adding 10 μL of the cell culture in 990 μL of 1× PBS.
   (ii) Aliquot 10 μL of the hundredfold dilution to the hemocytometer.
   (iii) Using a light microscope, count the number of cells in the four outer-most squares and calculate the average. Multiply the average number of cells by 10^4 and the dilution factor (10^2) to get the initial concentration of cells in the culture (Ci).
   (iv) Use this initial concentration (Ci), the final concentration (Cf) and the final volume (Vf) to calculate the initial volume (Vi) of the cells to add in 1.2 mL of growth medium.

$$Ci = (\text{average no.of cells counted in iii}) \times 10^4 \times 10^2$$

$$CiVi = CfVf$$

Ci = number of cells in the cell culture (cells/ml).

Vi = unknown volume of cell culture required (ml).

Cf = number of cells required for infection (cells/ml).

Vf = volume of inoculum required for infection (ml).

3.3 Infection of Organotypic Brain Slices with C. neoformans

3.3.1 Direct Stimulation of Brain Tissue with Whole-Cell C. neoformans

1. Immediately after preparation, centrifuge the *C. neoformans* inoculum at 2438 rcf for 5 min at 27 °C.
2. Carefully discard the supernatant without disrupting the pellet. Tip: A small volume of supernatant can be left in the tube to ensure no cells are accidentally discarded.
3. Resuspend the pellet in 375 μL of GM (warmed to 37 °C).
4. Remove the organotypic brain culture plates from the incubator and replace the medium from all the wells with fresh GM.
5. Infection with *C. neoformans*:
   (i) Carefully drop 10 μL of the *C. neoformans* inoculum (prepared in **step 3**) onto each brain slice in the allocated wells (*see* **Note 8**).
   (ii) An inoculum of 375 μL is enough to infect 37 brain slices.
6. Treat controls with 1.2 mL of fresh growth medium (warmed to 37 °C).
7. Upon completion, return the organotypic culture plates to the incubator for 24 h.
8. Discard all unused inoculum and used materials appropriately to prevent contamination.

3.3.2 Sample Collection

1. Twenty-four hours postinfection, remove the plates from the incubator and collect the growth medium from each well:
   (i) For each well, place 400 µL of growth medium into three 1.5 mL Eppendorf tubes for analysis of releasable factors, for example, cytokine or chemokine analysis by enzyme-linked immunosorbent assays (ELISAs) or multiplex assays.
2. Collect the brain tissue by carefully cutting out the membrane of the Millipore insert using a scalpel and forceps, which have been flash disinfected with 70% ethanol.
3. Cut along the outer border of the insert without disrupting the brain tissue.
4. Place the membranes directly into separate, labeled, petri dishes containing PBS, in preparation for immunofluorescence staining.

3.4 Immunofluorescence Staining

3.4.1 Fixation, Blocking, and Primary Antibody Incubation (Day 1)

1. Drain the PBS off the slices and transfer them into a 24-well plate with 300 µL per well of PBS (transfer one slice per well).
2. Replace the PBS with 300 µL of 4% PFA and fix for 20 min on ice. PFA is toxic and should be handled with gloves. After use, waste PFA should be disposed of into a designated waste container.
3. Drain the PFA and wash the slices three times with 300 µL of wash buffer for 10 min at room temperature (RT).
4. Replace wash solution with 300 µL of blocking buffer and block the slices at RT for 4 h.
5. Prepare your primary antibody solutions in blocking buffer to the following concentrations.
   (i) Anti-IBA1–1:500.
   (ii) Anti-S100β – 1:500.
   (iii) Anti-NeuN – 1:500.
6. Remove the blocking buffer and incubate the brain slices with 300 µL of primary antibodies for 16 h at 4 °C.

3.4.2 Secondary Antibody Incubation, Nuclear Staining, and Mounting (Day 2)

1. Wash the slices three times in 300 µL of wash buffer for 10 min at RT.
2. Prepare secondary antibody solutions in blocking buffer to the following concentrations:
   (i) Donkey Anti-Rabbit Alexa Fluor 647-1:500.
3. Incubate the slices with 300 µL of secondary antibodies in the dark for 5 h at RT.
4. Wash the slices three times with 300 µL of wash solution for 10 min at RT.

5. Prepare the Hoechst nuclear marker solution to a final concentration of 1:5000 in blocking buffer. Stain nuclei using 300 μL of Hoechst solution per slice for 10 min at RT.
6. Wash the slices in PBS for 10 min at RT.
7. Carefully mount the slices onto microscope slides using a small paint brush and add 40 μL of Mowiol (aqueous mounting medium) then coverslip. Wipe off excess Mowiol using a Kim-wipe and dry your slides overnight in a dark dry place before imaging with a confocal microscope, see Fig. 3 for expected results.

4 Notes

1. When making growth medium, defrost and heat the horse serum in a water bath or bead bath. Then add the D-glucose directly to the warm horse serum, as it will easily dissolve in the warm solution, while it does not dissolve easily in colder solutions. This solution can then be added to the other elements of the growth medium.
2. We utilize Stericup® Filter Units for filter sterilization of growth medium and dissection medium. Dissection medium can be filtered directly after the growth medium using the same filter unit.
3. After making all the prescribed cuts of the mouse's skull, you should end up with the entire skull cap being separated from the rest of the skull, making it easy to peel off to expose the brain.
4. When separating the medial tissue from the cortical tissue during brain dissection, it is important to gently pull the medial tissue away from the tissue on the cortical side, as opposed to just pushing down with the flat end of the mini spatula. This is because, by prying the tissue away, you uncover the hippocampus on the cortical aspect, while if you just push the flat end of the micro spatula down into the posterior fissure, you will end up with some excess tissue covering the hippocampus, making it difficult to identify and remove.
5. After laying the hippocampi onto the chopping disc, use the tip of the spatula to draw away any excess moisture surrounding the hippocampi. This will help to ensure that the hippocampi do not get stuck to the blade of the tissue chopper during chopping.
6. After pouring the suspended slices into a small petri dish, carefully check the 50 ml centrifuge tube, as some slices may get stuck to the sides of the tube and be left behind. Use a Pasteur pipette with a small volume of dissection medium to retrieve any remaining slices from the centrifuge tube.

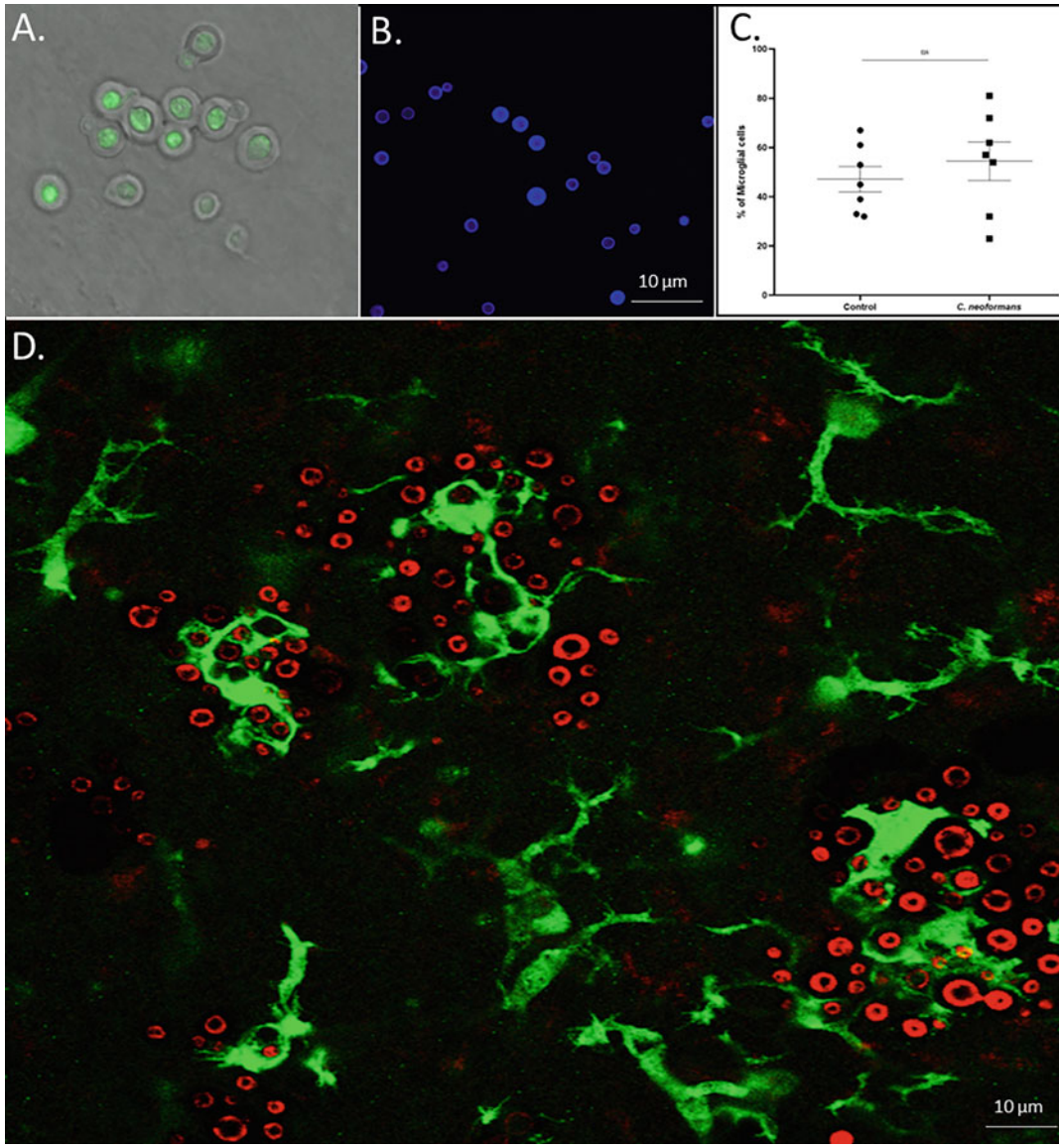

Fig. 3 Cryptococcal infection of organotypic hippocampal slices with a fluorescent H99 strain of *C. neoformans*. (**a**) *C. neoformans* encapsulates and divides when grown in the ex vivo organotypic culture conditions as it would in the host. (**b**) Calcofluor white stain of *C. neoformans*. (**c**) Microglial cell composition of organotypic hippocampal slices infected with *C. neoformans* vs controls. (**d**) High magnification (63×) image shows that *C. neoformans* cells (red) are phagocytosed by microglial cells (green) in an organotypic hippocampal slice

7. Hippocampal brain slices have a very characteristic morphology. The most common reason for excluding slices at the selection stage is that the outer aspect of the dentate gyrus is damaged and is pulling away from the rest of the slice. This may occur due to imperfect hippocampal removal, or if slices are

swirled/shaken too vigorously in the slice separation step. If slices are intact but the morphology is "blurry," it is likely that they were not chopped in the correct plane (i.e., perpendicular the length of the hippocampus).

8. Using the direct stimulation method as described, a total of 3.2×10^9 CFU of *C. neoformans* will be added to each brain slice.

References

1. Bicanic T, Harrison TS (2004) Cryptococcal meningitis. Br Med Bull 72:99–118. https://doi.org/10.1093/BMB/LDH043
2. Williamson PR et al (2016) Cryptococcal meningitis: epidemiology, immunology, diagnosis and therapy. Nat Rev Neurol 13(1):13–24. https://doi.org/10.1038/nrneurol.2016.167
3. Montpied P et al (2003) Caffeic acid phenethyl ester (CAPE) prevents inflammatory stress in organotypic hippocampal slice cultures. Mol Brain Res 115(2):111–120. https://doi.org/10.1016/S0169-328X(03)00178-5
4. Hailer NP, Vogt C, Korf HW, Dehghani F (2005) Interleukin-1β exacerbates and interleukin-1 receptor antagonist attenuates neuronal injury and microglial activation after excitotoxic damage in organotypic hippocampal slice cultures. Eur J Neurosci 21(9):2347–2360. https://doi.org/10.1111/J.1460-9568.2005.04067.X
5. Chong SA et al (2018) Intrinsic inflammation is a potential anti-epileptogenic target in the organotypic hippocampal slice model. Neurotherapeutics 15(2):470–488. https://doi.org/10.1007/S13311-018-0607-6/FIGURES/7
6. Bernardino L et al (2008) Inflammatory events in hippocampal slice cultures prime neuronal susceptibility to excitotoxic injury: a crucial role of P2X7 receptor-mediated IL-1β release. J Neurochem 106(1):271–280. https://doi.org/10.1111/J.1471-4159.2008.05387.X
7. Papageorgiou IE et al (2016) TLR4-activated microglia require IFN-γ to induce severe neuronal dysfunction and death in situ. Proc Natl Acad Sci 113(1):212–217. https://doi.org/10.1073/pnas.1513853113
8. Huuskonen J, Suuronen T, Miettinen R, van Groen T, Salminen A (2005) A refined in vitro model to study inflammatory responses in organotypic membrane culture of postnatal rat hippocampal slices. J Neuroinflammation 2. https://doi.org/10.1186/1742-2094-2-25
9. de Simoni A, Yu LMY (2006) Preparation of organotypic hippocampal slice cultures: interface method. Nat Protoc 1(3):1439–1445. https://doi.org/10.1038/nprot.2006.228

Chapter 4

Zebrafish Larvae as an Experimental Model of Cryptococcal Meningitis

Z. P. Chalakova and S. A. Johnston

Abstract

This chapter provides guidance for introducing *Cryptococcus neoformans* into the zebrafish larvae model system to establish a CNS infection phenotype that mimics cryptococcal meningitis as seen in humans. The method outlines techniques for visualizing different stages of pathology development, from initial to severe infection profiles. The chapter provides tips for real time visualization of the interactions between the pathogen and different aspects of the CNS anatomy and immune system.

Key words *Cryptococcus neoformans*, Cryptococcal meningitis, Fungal meningitis, Host–pathogen interactions, Zebrafish, Live imaging, Time lapse microscopy

1 Introduction

Cryptococcal meningitis (CM) is an opportunistic fungal infection of the central nervous system (CNS) caused by members of the genus *Cryptococcus*. Annual cases of CM were last estimated to be 223,100 globally, and despite the presence of antifungal pharmaceuticals, AIDS-related CM mortality is very high with CM accounting for 15% of all AIDS-related deaths worldwide [1].

At the point of diagnosis of CM, symptoms are already severe, and the pathology is in its late stage of development [2, 3]. Therefore, human clinical studies rarely provide information about early processes that lead to severe pathology, which masks potential targets for treatment. MRI imaging is the best tool we have for observation of CNS pathology in living patients, but MRI imaging has a lot of limitations in resolution, and it does not allow for visualization of smaller scale interactions on the levels of capillary vessels and immune cell behavior in the CNS [4].

Experimental research in CM aims to shine light on the gaps in our understanding of pathology as seen in humans. Murine models have been a powerful tool for examining immune responses to

Rebecca A. Drummond (ed.), *Antifungal Immunity: Methods and Protocols*, Methods in Molecular Biology, vol. 2667,
https://doi.org/10.1007/978-1-0716-3199-7_4,

cryptococcal infection, and the model is seen to recapitulate the pathology characteristics in patients [5]. Nonetheless, mouse models (and other mammalian animal models) are limited as they do not allow for observation of host pathogen interactions in real time in vivo. Nonmammalian models like *Caenorhabditis elegans* and *Drosophila melanogaster* are highly tractable for live imaging, but they do not provide the opportunity to mimic complex multicellular immune interactions, and critically, anatomical and physiological aspects of CNS pathology as seen in humans.

The zebrafish (*Danio rerio*) is a powerful vertebrate model that has strong parallels with mammalian genetics and anatomy. The simplicity of the system in comparison to murine models makes it easier to focus on individual pathological mechanisms. The zebrafish infection system is now well established for experimentally examining host pathogen interactions in cryptococcosis [6–10]. Fluorescent transgenic zebrafish lines are a state-of-the-art model for high resolution in vivo visualization of small cranial vasculature, brain parenchyma, and CNS innate immune cell types [11–13]. Due to their transparency, zebrafish allows for noninvasive visualization of CNS pathology development in real time.

In this method chapter, we outline procedures that enable the utilization of the zebrafish infection system to study host pathogen interactions of *C. neoformans* in the CNS in real time. Major procedures in the method include preparing cryptococcal culture for microinjection, introducing pathogens into the bloodstream or brain ventricles of zebrafish larvae, procedures on immobilizing zebrafish for imaging, and tips on high content imaging of living infected larvae. In this chapter, we outline variations of the main method, each more suitable for studying a particular aspect of the pathophysiology of CM (*see* **Note 21**).

2 Materials

Solutions should be prepared using distilled water. Solutions should be stored according to instructions given below.

2.1 Preparing Streaking Plate and Pathogen Culture

1. *Cryptococcus neoformans* var. grubii KN99 (*see* **Note 1**).

   Strains (select according to fluorescent reporters in chosen transgenic):

   (a) KN99 GFP [11].

   (b) KN99 mCherry [11].

2. Yeast peptone dextrose (YPD) broth: 20 g/L Bacteriological peptone, 20 g/L Glucose, 10 g/L Yeast extract. Suspend 50 g in 1 L of distilled water. Autoclave for 15 min at 121 °C.

3. 90 mM Petri Dishes for making YPD agar plates.

4. YPD agar plates: YPD broth solution with 2% Oxoid Agar Bacteriological (Agar No. 1). Autoclave for 15 min at 121 °C before pouring (*see* **Note 2**).
5. Incubator set at 28 °C with a Blood tube rotator.
6. Inoculation loops.
7. 1% Virkon solution or other suitable sterilizing solution active against *Cryptococcus*.
8. 70% Industrial methylated spirit (IMS or denatured ethanol): used for disinfection of working space.
9. Simport tubes with clip on caps.
10. Laminar flow hood or other suitable safe lab site for handling fungal pathogens.
11. Filtered tips.
12. Phosphate buffered Saline (PBS): In tablet form**.** One tablet dissolved in 200 mL of deionized water to yield 0.01 M phosphate buffer, 0.0027 M potassium chloride and 0.137 M sodium chloride, pH 7.4, at 25 °C.
13. 6000 g Benchtop centrifuge.
14. 10% Polyvinylpyrrolidone (PVP), 0.5% Phenol Red in PBS (*see* **Note 3**): Autoclaved before use.
15. Hemocytometer.

2.2 Zebrafish Husbandry, Sorting, and Dechorinating

1. Lines:
   (a) *Tg(kdrl:mCherry)*^{S916} – *mCherry* marker of endothelial vascular cells [21]**.**
   (b) *Tg(kdrl:mCherry)*^{is5}*; TgBAC(cldn5a:EGFP)*^{vam2} – GFP *claudin5a* tight junction protein marker expressed on the zebrafish choroid plexus ependymal cells; *mCherry* marker of endothelial vascular cells [12]**.**
   (c) *Tg(mpeg:mCherry-CAAX)*^{sh378} – *mCherry* reporter of macrophages and macroglia. Origin – Johnston lab [8]**.**
2. Breeding trap for marbling or any standard zebrafish husbandry material for obtaining embryos [14]**.**
3. 90 mM Petri Dishes for transport and collection of embryos.
4. Plastic tea strainer for collecting embryos from adult fish tank.
5. Fire-polished wide-bore Pasteur pipet: Used to transfer larvae between containers.
6. E3 with methylene blue: 10× stock of E3 (NaCl 5 mM, KCl 170 μM, CaCl2 330 μM, MgSO4 330 μM). Dilute to 1× and add methylene blue (0.000025%). Store at 28 °C.
7. Dissecting stereomicroscope: For observing and manipulating embryos.

8. 1% Virkon solution: Used to cull zebrafish embryos that will not be raised.
9. Dumont #5 forceps: Used for removing the chorion around larvae.

2.3 Zebrafish Injection with C. neoformans, Plating Inoculum and Mounting

1. Injecting equipment set up (Fig. 1):
   (a) Pneumatic Pico Pump (PV 830P): for creating pump pressure for injecting.
   (b) Micromanipulator (Sutter Instrument, MM-33): for adjusting the needle position.
   (c) Dissecting stereomicroscope: For observing and manipulating embryos.
2. Tricaine methanesulfonate (MS222): 0.168 mg/mL solution in E3.
3. Gel loading pipette tips.
4. Graticule slide 100 × 0.05 = 5 mM scale (Fig. 2b).
5. Microneedle: Injection needles are needed for injecting pathogens into the bloodstream or brain ventricles of the larvae. Injection needles are prepared by pulling glass capillaries 1.0 mM OD glass capillary (World Precision Instruments) using a pipette puller. Pipette pullers all have different heating elements; therefore, trial and error are needed to find the settings for your puller that produce needles as shown in Fig. 2a.
6. E3 agarose injection plates: 2% Agarose (Molecular Biology Grade Agarose) solution in E3 with methylene blue.
7. Cell spreader.
8. Heat block/Digital dry bath at 38 °C: keeping LMPA from solidifying.
9. Low melting point agarose (LMPA) mounting solution: Transparent mounting solution used to immobilize live zebrafish embryos during imaging. In a 15 mL falcon, add 9.6 mL of E3, 420 μL tricaine (4%), and 0.1 g LMPA powder (1%) to make 1% LMPA mounting solution (*see* **Note 21**).
10. Corning® high content imaging plate; 96 well: High resolution imaging is not possible using plastic well plates due to the thickness of the material. Acquire glass bottom imaging plates specific for high resolution imaging.
11. Glass mounting capillaries with a micro plunger (provided by Zeiss for Light sheet microscopy): volume 20 μL, internal diameter 0.8 mM, Pk 100, color code black.
12. Imaging equipment.
    (a) *Nikon custom widefield*: A custom-build widefield microscope, Nikon Ti-E with a CFI Plan Apochromat λ 10×, N.

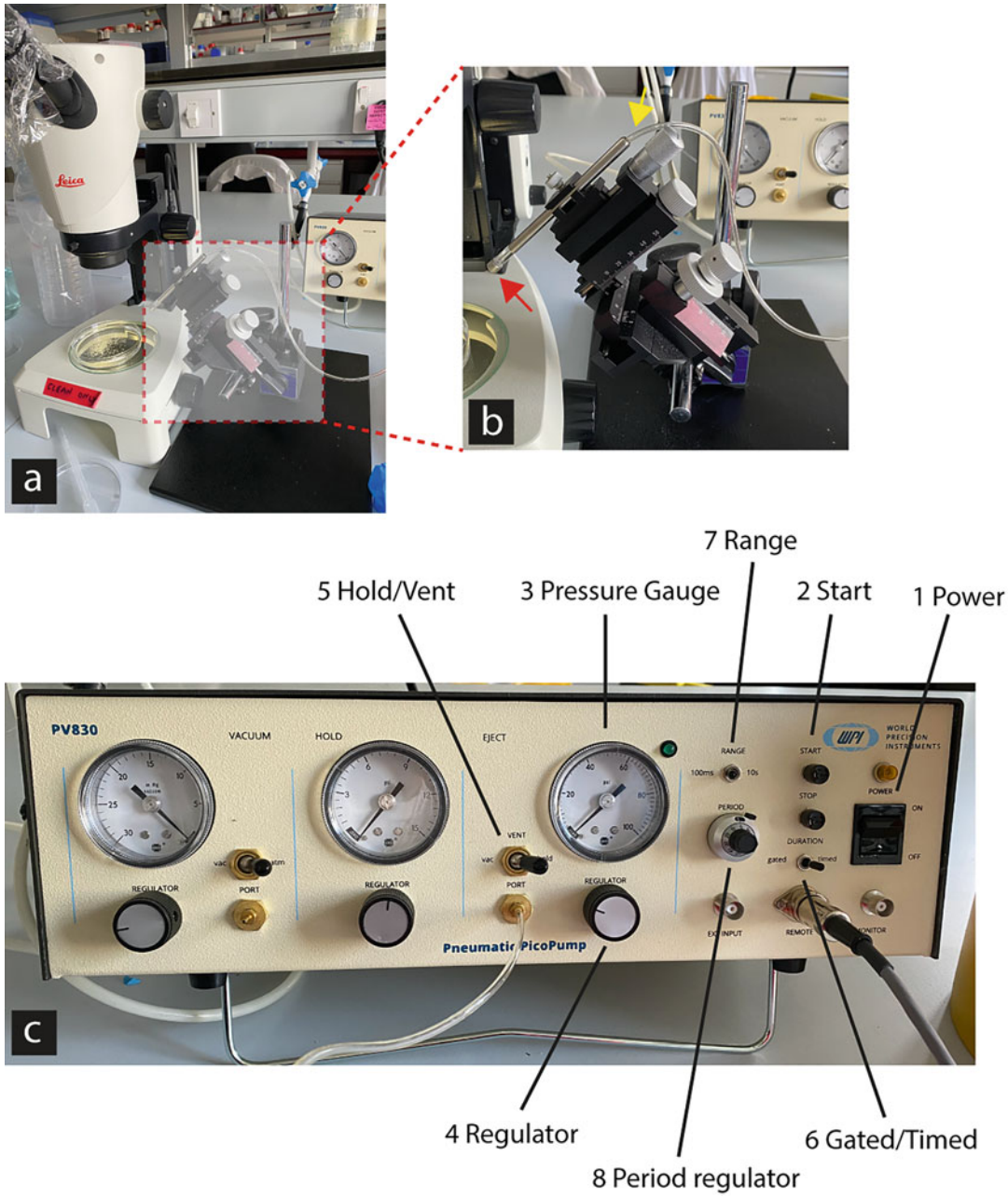

Fig. 1 Injecting equipment set up: panel (**a**) shows a dissecting stereomicroscope with a micromanipulator (**b**) next to it and a Pico Pump (**c**) behind. In panel (**b**) the red arrowhead points to a microneedle gets inserted, the yellow arrowhead points to the tube connecting the Pico Pump and the micromanipulator. The silver nodules on the micromanipulator control the position of the needle in 3D space. In panel (**c**) we can see the controls of a Pico Pump clearly. Labels are pointing to controls adjusted during the injection procedure in the method

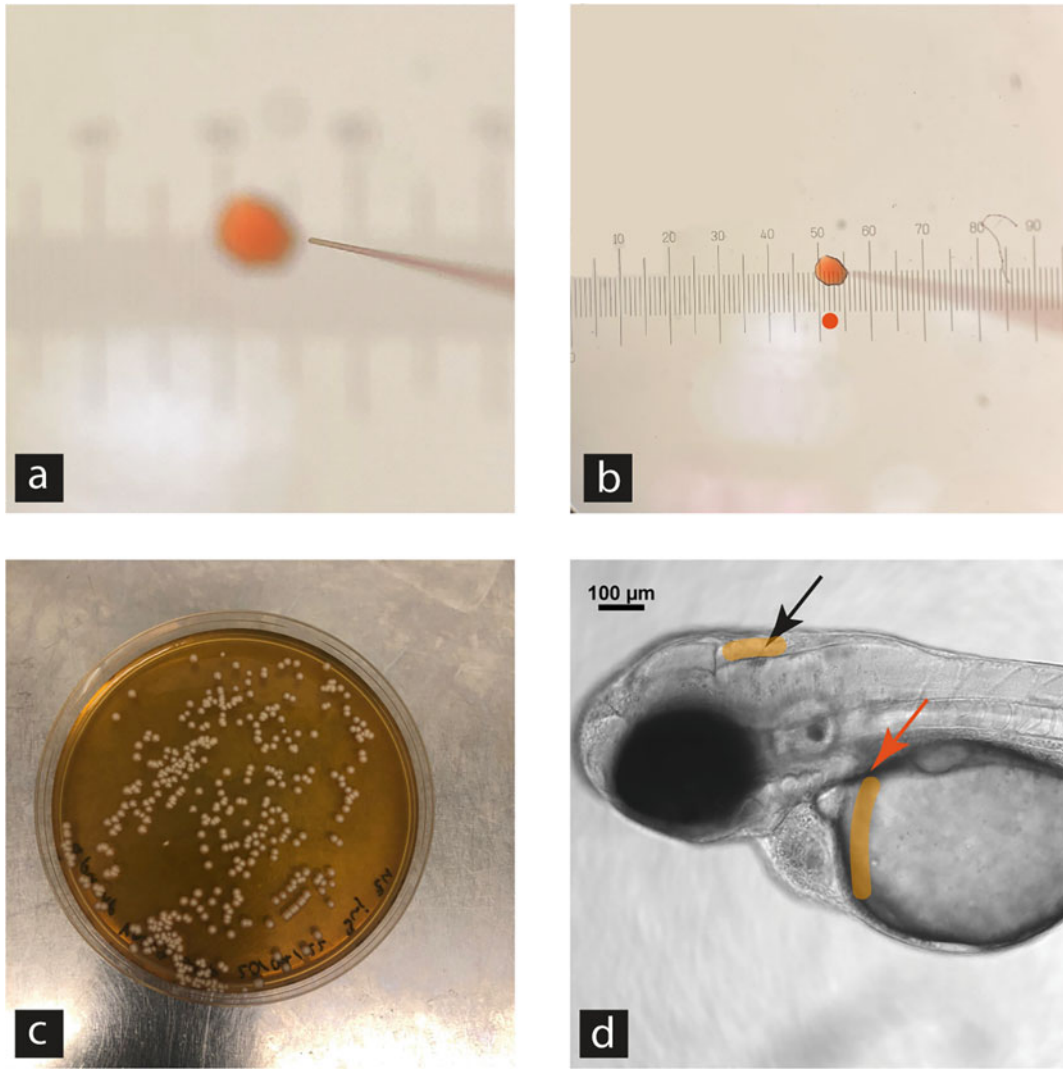

Fig. 2 Injecting and plating inoculum: Panel (**a**) shows an example of a needle for injection. The needle is above a droplet spread on a 5 mM graticule. The needle is broken and the size of the needle tip and shape are optimised for injecting 1 and 2 dpf larvae. Panel (**b**) shows the inoculum coming out of the needle from one pump, and the graticule in focus. An orange circle indicates what the inoculum looks like in droplet form as it floats in the mineral oil above the scale. The size of the droplet is approximately 0.12 mM in diameter (2 nL). Panel (**c**) shows a plated 2 nL of 700 cfu/nL inoculum that came out of an injection needle. The plate was incubated at 28 °C for 48 h. The colonies on this plate are ~400. In our method we inject 4 nL of 700 cfu/nL inoculum per larva to account for discrepancies between concentration estimation in a haemocytometer count and concentration in a micro needle droplet. Panel (**d**) shows sites of injecting on a 2 dpf larva. The orange arrow points to the duct of Cuvier, a site of injection for bloodstream infection. The black arrow points to the hindbrain ventricle, a site of injection for CSF infection. It is important to note that hindbrain ventricle injections are typically done in 30 hpf larvae. The orange areas on the fish are where the inoculum will travel immediately after injection into respective injection sites

A.0.45 objective lens, a custom built 500 μM Piezo Zstage (Mad City Labs, Madison, WI, USA) and using Intensilight fluorescent illumination with ET/sputtered series fluorescent filters 49,002 and 49,008 (Chroma, Bellow Falls, VT, USA). NIS software for acquisition.

(b) *Zeiss Z1 Lightsheet Microscope*: Lightsheet.Z1. Laser lines: 405, 445, 488, 514, 561, 638 nM. Plan-Apochromat 20×/1.0 Corr nd = 1.38 objective and a scientific complementary metal-oxide semiconductor (sCMOS) detection unit. ZEN black software for acquisition.

13. Data analysis software: ImageJ, System software.

3 Methods

3.1 Zebrafish Microinjections with C. neoformans

3.1.1 Making a Streaking Plate

Streak an YPD agar plate with the desired *C. neoformans* strain from suitable frozen stocks (e.g., Microbank beads) and incubate at 28 °C for 48 h. Check plate for good and uniform growth. If growth is poor or some areas show differences in color or morphology reisolate from frozen stocks, otherwise restreak onto a second YPD agar plate being careful to take a sweep across the plate. Incubate restreaked plate at 28 °C for 48 h and dispose of original plate. Restreaked plate should be sealed with parafilm and can be stored at 4 °C for up to 1 month. For experimental cultures, an inoculation loop sweep is taken from stock plate and used to inoculate 2 mL of YPD broth as 24 h cultures which are used to prepare zebrafish infection inoculum (*see* Subheading 3.1.4).

3.1.2 Day 1: Zebrafish Husbandry and Marbling

1. Adult zebrafish should be kept in aquarium facilities that meet ethical and local legal requirements. They should be maintained on a 14- to 10-h light and dark cycle at 28 °C.
2. Zebrafish embryos can be generated by "marbling" (or other suitable breeding trap) or by pair mating. "Marble" a selected tank after 6 h prior to dark period to allow adult fish to adjust to their new environment prior to light cycle transitioning into dark.

3.1.3 Day 2: Obtaining Embryos and Sorting

1. Obtain embryos from breeding trap within 4 h following light cycle initiation. If pair mated zebrafish are divided prior to mating, then dividers should be removed as soon as possible after light cycle initiation and embryos collected within 4 h following light cycle initiation. To collect the embryos, pour the contents of the bottom container of the breeding trap through a tea strainer. Using a wash bottle filled with E3 medium, rinse the eggs from the tea strainer into a 90 mM petri dish.

2. Under a stereo dissecting microscope, observe the petri dish with collected eggs. Developmentally stage zebrafish embryos. Depending on the time of sorting, the embryos selected should be around 4 h postfertilization (hpf), mostly in their high or oblong stage of development. Select healthy embryos that have been fertilized at 8 am the same day (*see* **Note 4**).
3. Transfer selected embryos into a 90 mM petri dish approximately ¾ full with E3 methylene blue media (*see* **Note 4**). Maximum number of embryos per dish is 80 (*see* **Note 4**).
4. Discard embryos that were not selected in 1% Virkon solution or other suitable disinfectant.
5. Store embryos in a 28 °C incubator with a 14- to 10-h light and dark cycle.
6. 8–10 h postfertilization, observe embryos under a light microscope. Discard all dead or damaged embryos in 1% Virkon solution (*see* **Note 4**).

3.1.4 Day 3: Dechorinating and Preparing Pathogen Culture

1. Dechorinating: At 30hpf (*see* **Note 5**) using two sets of Dumont #5 forceps (it is critical for the forceps to be sharp), remove the chorion around the larvae. This can be done by using both forceps, one to hold the embryo in one place and the other to pinch and pull. Dechorinating can also be done using one forceps by pocking a small hole in the chorion as the forceps ends are touching and then releasing the forceps to open the chorion. It is essential to keep the larvae in the same plate in which they were dechorinated (*see* **Note 5**).
2. Preparing zebrafish infection inoculum: From a *C. neoformans* KN99 GFP streaking plate, take a sweep using an inoculation loop and use it to inoculate 2 mL YPD broth. Rotate horizontally at 20 rpm at 28 °C for 16–24 h.
3. At the end of the working day, check plates with larvae to again remove dead or damaged specimens.

3.1.5 Day 4: Preparing Injection Inoculum

1. Put E3 agarose plate and 3 YPD agar plates stored at 4–28 °C incubator to warm up (*see* **Note 6**).
2. *Cryptococcus neoformans* inoculum preparation.
3. Wash cryptococcus culture with PBS: collect KN99 GFP overnight culture; add 1 mL of culture to a 1.5 mL microcentrifuge tube; pellet 1 mL culture at 6000 g, RT for 1 min; remove supernatant and resuspend pellet in 1 mL of PBS.
4. Second PBS wash: Pellet 1 mL resuspended pellet (**Step 3**) at 6000 g, RT for 1 min; remove supernatant and resuspend pellet in 1 mL of PBS; use this as washed culture suspension.
5. Make a 20× dilution of washed culture suspension: take 5 μL from 1 mL washed culture suspension and dilute with 95 μL of

fresh PBS. Add 10 μL of diluted culture to a hemocytometer slide under a coverslip.

6. Count 20× dilution: Count colony forming units (cfu) (*see* **Note 7**) using an upright light microscope. Calculate the number of cfu in the diluted and therefore 1 mL washed culture suspension according to the hemocytometer manufacturer's instructions.
7. Resuspend washed culture suspension in 10% PVP phenol red PBS: Pellet 1 mL culture at 6000 g, RT for 1 min; Remove supernatant; Resuspend culture in 10% PVP in phenol red PBS to achieve a desired cfu/nL. For our experiments we use 1000 cfu/nL or 700 cfu/nL (*see* **Note 7**).
8. Clean all areas that have come into contact with pathogens with 70% IMS or other suitable disinfectant. Suspend all contaminated consumables into 1% Virkon solution or other suitable disinfectant.

3.1.6 Day 4: Setting Up Needle and Anesthetizing Fish

1. Setting up Pneumatic Pico Pump (Fig. 1c).
   (a) Open air supply to Pneumatic Pico pump.
   (b) Switch on pump (1 Power).
   (c) Check for air (2 Start).
   (d) Check pressure (3 Pressure gauge)—should be approx. 40 psi for injecting 1000 cfu—alter using the regulator (4).
   (e) Select "Vent" (5 Hold/Vent).
   (f) Select "Timed" (6 Gated/Timed).
   (g) Select 100 ms (7 Range).
2. Anesthetize a plate of zebrafish larvae (~50hpf) in a 0.168 mg/mL Tricaine in E3. Larvae are ready to be manipulated once no evidence of motility (e.g., no startle reflex) is observed.
3. Add 5–8 μL of *C. neoformans* inoculum into a microneedle using a gel loading tip (*see* **Note 8**).
4. Unscrew the end of the micromanipulator needle holder, attach the needle, and tighten.
5. Under dissecting stereo microscope, place a graticule slide onto an upturned petri dish, add a drop of mineral oil, and focus on the scale bar.
6. Bring the needle tip into view and break the tip at an angle using Dumont #5 forceps resulting in a beveled point (*see* **Note 9**) (Fig. 2a).
7. Using the micromanipulator move the tip of the needle so that it enters the oil on the slide and depress the foot peddle once (you will need to withdraw the needle quickly to prevent reuptake of droplet unless microinjector has balanced pressure capability).

8. Measure the size of the droplet produced—3 small divisions on the illustrated graticule for 2 nL inoculation volume with each foot pedal depression (Fig. 2b*; see* **Note 9**).

3.1.7 Day 4: Injecting Zebrafish Larvae

(Duct of Cuvier, bloodstream infection, *see* **Notes on method variation;** Fig. 2d)

1. Prepare a fresh plate (**collection plate**) with clear E3 (no methylene blue) for containing injected fish (*see* **Note 3**).
2. Take a prewarmed E3 agarose plate (injection plate) from the incubator.
3. Dip a gloved finger into the E3 medium containing anesthetized fish to be injected and wet the surface of the E3 agarose.
4. Take a Pasteur pipette. With a circular motion, swirl the E3 and tricaine media in the Petri dish filled with anesthetized larvae; this allows larvae to collect in the middle of the plate.
5. Pipette 15 larvae with using Pasteur pipette.
6. Pipette the larvae onto tilted injection plate letting them slide from the top down, this way the tails will orient in one direction.
7. Remove excess E3 until larvae are not floating but sit submerged on injection plate.
8. Place the infection plate under dissecting stereo microscope and bring the left most larva into focus.
9. With the naked eye, adjust the micromanipulator apparatus so the needle is above the fish in focus.
10. Under the microscope, focus on the needle and adjust the micromanipulator to hover the needle above the duct of Cuvier (Fig. 2d).
11. With one swift motion, inject the needle into the duct of Cuvier, depress the foot pedal twice (2 pumps), and pull out the needle. If the injection is successful, you will see a red liquid going over the yolk and into the heart (Fig. 2d, *see* **Note 10**).
12. Repeat for all fish on the plate.
13. Take 3 mL of clear E3 from collection plate.
14. Tilt the injection plate and pipette clear E3 from top to bottom over the collection plate. The injected larvae will collect in the bottom corner of the injection plate and spill into the collection plate. Keep pipetting clear E3 until all larvae are in the collection plate.
15. Repeat the injection and collection process until you reach the desired number of infected larvae, leaving a desired number of fish for control groups (*see* **Note 11**).

16. Once a desired number of larvae are injected, a collection container with infected fish needs to be returned into the incubator for 2 h for the fish to recover. Separate containers with control fish in clear E3 should also be left in the incubator for 2 h.

3.1.8 Day 4: Plating Inoculum

Plating the injection inoculum is a secondary method of estimating how many cfu are being injected into the zebrafish larvae (*see* **Note 12**). Once the desired number of larvae is injected, plate some of the inoculum using the same injection needle and inoculum used to inject larvae.

1. Prepare a cell spreader next to the injector scope.
2. Collect a warmed YPD agar plate from the incubator.
3. Fill a pipette with 20 μL of PBS.
4. With one hand hold the pipette under the injector scope, with the other, adjust the micromanipulator to get the needle in front of the opening of the pipette tip. Pipette lightly so a droplet holds on the tip of the pipette tip. Lower the needle into the droplet and inject 1 pump (2 nL) into the droplet. Suck the droplet back into the pipette tip so it mixes in. Pipette the 20 μL in the center of the YPD agar plate. Spread the liquid evenly around the plate and place the lid on.
5. Repeat with another plate.
6. Perform 2 repeats with 2 pumps (4 nL) of inoculum.
7. Incubate inoculated YPD agar plates at 28 °C.
8. Check if colonies are visible after 24 h, 48 h, and 72 h.
9. Once visible (Fig. 2c), count the number of colony forming units on each plate. Take the mean number between replicate plates and adjust depending on injection volume.
10. Clearing up working area: Dispose of all contaminated materials into suitable waste streams and clean equipment with disinfectant such as 1% Virkon.

3.2 Mounting for Widefield Fluorescence Microscopy

1. Preheat block to 38 °C.
2. Low melting point agarose (LMPA) mounting solution prep.
   (a) Prepare low melting point agarose mounting solution at desired percentage (*see* **Note 21**).
   (b) Heat with low temperature until solution reaches boiling point. Repeat several times until the powder is dissolved and the solution is clear and homogeneous. Aliquot 500 μL of clear solution per microcentrifuge tube and keep it in a 38 °C heat block prevents setting before use. You will need approx. 100 μL/larvae to mount. Prepare the desired amount of LMPA accordingly.

3. Collect plates with recovered injected and control larvae. Anesthetize plates. Distribute larvae in a high content imaging 96-well plate, with one larva per well and enough clear tricaine E3 to just cover larva. Keep the 2 groups of fish (control and injected) in separate rows and handle each group with its own pipettes to avoid cross contamination. Always keep the rows around the edges of the plate empty, short working distance (e.g., most high magnification) lenses do not allow focusing on the edges of the plate.
4. Pipette 100 μL LMPA per well for 5 larvae. Return LMPA to heat block to prevent it solidifying.
5. Use a gel loading tip to position larvae in LMPA to the bottom of their wells.
6. Use the tip to manipulate the orientation of the larvae (lateral side or dorsal side downward) (*see* **Note 21**). Do this until the LMPA solidifies.
7. Repeat **steps 4, 5**, and **6** until all larvae are mounted.
8. If doing time lapse imaging allow for the anesthesia of the larvae to subside after mounting for at least 20 min to stabilize heart rate.

3.3 Screening and Mounting for Light Sheet Microscopy (see Note 13)

3.3.1 Screening

1. Collect plates with recovered injected and control larvae. Anesthetize plates. Distribute larvae in a high content imaging 96 well plate, with one larva per well and enough clear tricaine E3 to just cover larvae. Keep the 2 groups of fish (control and injected) in separate rows and handle each group with its own pipettes to avoid cross contamination. Always keep the rows around the edges of the plate empty, short working distance (e.g., most high magnification) lenses do not allow focusing on the edges of the plate.
2. Using a gel loading tip carefully manipulate fish to go to the bottom of their wells and on their side (lateral view) (*see* **Note 14**).
3. Carefully transport plate to widefield fluorescence microscope.
4. Place the 96-well plate in a widefield microscope sample holder.
5. Locate and image each larva with appropriate settings to identify desired reporter fluorescence and dissemination into the CNS (examples of infection burden in CNS Fig. 3).
6. Add 50–100 μL E3 to wells to prevent them from drying out before mounting.

3.3.2 Mounting

1. Preheat block to 38 °C.
2. Put 500 μL aliquots of 2% LMPA in heat block.
3. In one of the marked wells of the 96-well plate, add 1 μL of tricaine and mix E3.

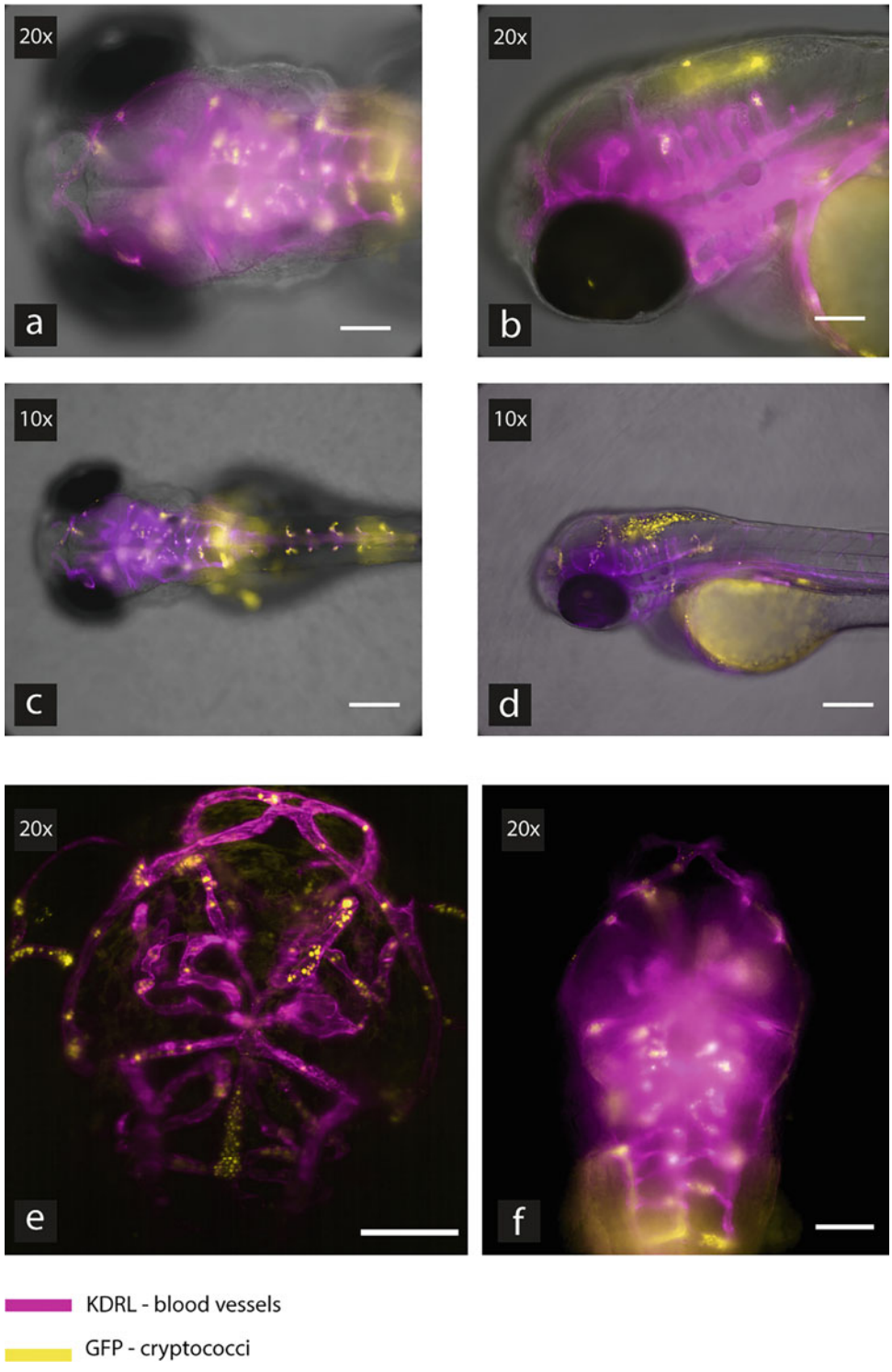

Fig. 3 Different mounting orientation and microscopy: All larvae shown on this figure are 2dpf in development and imaged in real time. Panel (**a**) and (**c**) show dorsal mounting in 20× (**a**) and 10× (**c**) magnification. Similarly, panel (**b**) and (**d**) shoe lateral mounting in different magnifications. The images in (**a**–**d**) are taken with a fluorescent widefield microscope. Panel (**e**) and (**f**) show the difference in the spatial resolution between blood vessels that light sheet imaging can provide (**e**) as opposed to widefield fluorescence imaging (**f**). Scales on 20× images are 100 μM and on 10× images are 200 μM

4. Pick an embryo from the marked well along with the tricaine E3 in a Pasteur pipette.
5. Pipette onto suitable flat surface, for example, lid of a Petri dish squeeze so the medium remains as a droplet around the larva.
6. Collect media around the larva until it is just covered. Pipette 200 μL 2% LMPA on top of the fish.
7. Using glass capillary tube pipette larva headfirst.
8. Slowly rotate the capillary tube so the fish mounts straight in the tube.
9. Place the capillary in the light sheet imaging chamber for imaging.
10. If doing time lapse imaging allow for the anesthesia of the larvae to subside after mounting for at least 20 minutes to stabilize heart rate.

3.4 Imaging

3.4.1 Widefield Set-Up Variations

1. General set up (the same in all imaging): Humidified temperature controlled at 28 °C.
2. Real-time imaging (focus on acute change in blood vessels size and shape; *see* **Note 15** and **16**): Suggested 20× and 40× objective lens with 0.7–1.1NA. Wavelength for 555 nM for mCherry (KDRL reporter line; *See Materials*). Exposure between 20 and 300 ms for mCherry reporter. Capture 1fps for mCherry channel.
3. High speed imaging (*see* **Note 15** and **17**): Suggested Lenses 20× and 40× objective lens with 0.7–1.1NA. Wavelength for 555 nM for dsRed (gata1 reporter line; *See Materials*), 470 nM for GFP (reporter in KN99 GFP strain or silicon beads; *see Materials*). Exposure max 20 ms. Achieve using increased gain and/or illumination. Capture at least 30fps for chosen reporter (*see* **Note 17**).
4. 24 h time lapse imaging (focus on dissemination progression; *see* **Note 18**): Consider using lower magnification lens, if possible, to reduce problems related to photo toxicity Wavelength for 555 nm for mCherry (KDRL reporter line; *see Materials*), 470 nM for GFP (reporter in KN99 GFP strain; *see Materials*). Reduce exposure where possible but longer exposure is preferred to increased illumination. Capture 1 frame every 5 min.
5. One time point Z stack imaging (focus on pathogen distribution; *see* **Note 19**): The acquisition time for a whole group of fish should be as short as possible, set up a list of coordinates from each larva in a group and allow for automated acquisition (*see* **Note 19**). Consider using lower magnification lens, if possible, to reduce problems related to photo toxicity Wavelength for 555 nM for mCherry (KDRL reporter line; *see* **Materials**), 470 nM for GFP (reporter in KN99 GFP strain;

see **Materials**). Laser power and exposure can be varied depending on what produces the best quality images, but the settings need to be the same for each channel across all larvae images for measurements. Suggested Z stack interval 3 μM (the size of smaller cryptococcal cells).

*3.4.2 Light Sheet Set-Up Variations (*see ***Note 20****)*

1. General set-up and 1 time point Z stack imaging: Image acquisition chamber incubation at 28 °C. Lasers should be set up for dual side illumination with online fusion, turn on lasers 488 nM (for GFP) and 561 nM (for mCherry). LBF 405/488/561 filter set, and beans split with SBS LP 560 or LP 580 mirror. Two tracks and sequential imaging to be used for imaging of two reporters (e.g., one track for GFP and another for mCherry). Lens to be at 0.7× zoom, 16-bit image depth, 1920 × 1920px (approximately 0.33 × 0.33 μM) image size and minimum z-stack interval (approximately 0.5 μM). Exposure automatically adjusted.
2. Real-time lapse imaging: adjust illumination to be one side illumination and keep to a single track to reduce acquisition time. Manipulate the exposure to allow for 1fps capture time.

3.5 Processing Data

We suggest using automated Otsu thresholding in ImageJ.

1. Real-time data: Select frames of interest to represent events observed and analyze and extract from a time lapse file using ImageJ.
2. Slow motion imaging: For particle tracking software use the free Track Mate plugin in ImageJ.
3. 24 h time lapse imaging: Can be challenging with ImageJ due to Java memory usage implementation. In this case, software from acquisition system might be preferable.
4. Light sheet Z stack processing: Utilize ImageJ plugins for tubular, volume and branching analysis of vascular bed architecture.

4 Notes

1. We chose *C. neoformans* var. grubii KN99 strain as it is known to exhibit represent human type virulence in animal models [15].

   General handling of pathogen:

   (a) Long-term storage cultures for use in experimental procedures are kept in Microbank (Pro-lab Diagnostics, UK) stock vials at −80 °C. See *Methods* for information on handling the pathogen.

(b) *Cryptococcus neoformans* var. grubii is a Hazard 2 class pathogen and it should be handled in a Containment Level 2 infection facility.

(c) Consumables and containers that have come into contact with the pathogen should be disposed of in sealed containers or inactivated with 1% Virkon solution for 30 minutes or other suitable disinfectant. Inactivated or sealed waste should be disposed of in an appropriate waste stream.

(d) All pathogens that need to be transported between rooms (e.g., from tissue culture to microscopy rooms) should be in a sealed container such as a securely closed microcentrifuge tube or well-plate. Distance of travel between rooms should be reduced as much as possible.

(e) Zebrafish larvae and fungi are both grown at 28 °C. This is the temperature of the natural environment of zebrafish; the fungi are grown in the same temperature to condition the pathogen to favor the host's environment.

2. To prevent bacterial contaminants from growing on YPD agar plates, plates should be poured in sterile conditions (in a laminar flow hood or under a Bunsen burner flame). An additional precaution can be taken by adding antibiotics (e.g., penicillin and gentamicin) to YPD agar before pouring.

3. Cryptococcal cultures are to be re-suspended in PVP in phenol red, where PVP is a polymer which prevents needle blockage in cryptococcal injection and Phenol Red is an inert dye that allows us to see if the inoculum has been successfully injected.

4. Sorting and husbandry tips:

(a) Discard unfertilized eggs.

(b) The health of zebrafish embryos can be determined by the lack of dark spots in their tissue. Darker tissue usually indicates dying cells.

(c) All zebrafish embryos used in experiments should be in the same stage of development to avoid any variability in physiology that can create data outliers and skew results.

(d) Methylene blue is an antimicrobial agent that prevents unwanted growth of pathogens in the growth environment. However, it has been seen that overuse of E3 methylene blue can cause autofluorescence in imaging and can activate autophagy in host and pathogen cells. When preparing methylene blue E3, the solution should be pale blue in color (approx. 0.000025% methylene blue). After infecting larvae with *C. neoformans,* keep them in E3 without methylene blue.

(e) Increased numbers of embryos (over 80) in a single petri dish can create an environment with low nutrient and oxygen availability, which would lead to developmental and health issues that are not due to the infection procedure [14].

(f) The presence of dead embryos in the environment of growth is bad husbandry practice [14] and factors released from the decay of tissue can be damaging to living embryos.

5. Zebrafish larvae under 24 hpf are fragile and easily damaged. In our work, we have found that dechorinating around 30 hpf produces the best results (less to no damage). We have also seen that 1dpf larvae can adhere to plastic consumables. Adherence also seems to occur more frequently when larvae are transferred to a fresh plate. To avoid damage from sticking to a Pasteur pipette or a new Petri dish, larvae are left in the same Petri dish they have been dechorinated in for at least 2–5 h recovery period prior to injecting. If the method is varied for injections to be done in 1 dpf larvae, dechorination can be done earlier in the day to allow for the larvae to recover in time prior to injecting.
6. E3 agarose injection plates are warmed up to the body temperature of zebrafish larvae, to allow less stress and damage to occur during the injection procedures.
7. The cfu/nl suggested in the methods (1000 or 700) works best in bloodstream larvae infection; it is the amount of cfu required to see dissemination into the cranial vasculature at the desired imaging time points. For infection of brain ventricles, we suggest 200 cfu/nL. That prevents excessive growth and allows for better resolution between cryptococci during imaging. Brain ventricles injections are also done at 1dpf developmental stage of larvae. If that is a more desired procedure, vary the method accordingly.
8. Extreme care should be taken when handling injection needles containing pathogens. Needles should be loaded, used, and disposed of in the same location, under no circumstances should they be transported. To protect from needle stick injury, a fingerguard can be worn on the hand that is handling the needle. Should injury still occur encourage bleeding, thoroughly wash the area with water and seek medical attention.
9. When breaking the injection needle, the aim is to get the tip as small as possible so it allows for less damage to occur when injecting the larvae. The needle tip needs to be also big enough to let inoculum escape when 40 psi pump pressure is applied. However, cryptococci are very prone to clumping, especially when injecting 700–1000 cfu/nL. This means the needle tip

needs to be broken with a relatively bigger opening and that the pump period regulator (Fig. 1c, *see* **Note 8**) needs to be on the higher end values ~2.5–3. The period regulator on the Pico Pump alters the length of period in which air is pushed into the needle—it should be somewhere between 1 and 3.

10. To avoid any differences in infection burden across larvae, aim to inject all larvae with the same needle. Unfortunately, that is sometimes not possible as injection needles (especially with high cfu content) tend to clog at their tip. Once the needle is clogged, it needs to be discarded, a new needle and volume of inoculum is used, which may cause variation in needle tip size and cfu injected. Tips on avoiding needle clogging or unclogging the needle:
    (a) Prior to pipetting inoculum, each time vortex 3 times for 10 s. This is done to prevent clumps of the pathogen forming and clogging the injection needle. This also favors a more even distribution of cfu across the volume of the inoculum.
    (b) If the needle clogs, you can try injecting several times into the E3 agar.
    (c) Try breaking the needle slightly larger, but not too big to avoid bleeding following injection.
    (d) Try diluting inoculum further, reducing the droplet size and pumping more than 2 times when injecting. Count what comes out of the needle and estimate how many pumps are necessary for 700–1000 cfu. Make sure you maintain the same pump number across all injections and plate the inoculum afterwards to get a quantification of how many cfu have been injected.
11. Two different control groups can be used. One group of fish that have been treated the same way as injected cohort (dechorinated, anesthetized the same number of times). This group allows to account for differences in physiology due to tricaine treatment or dechorinating. Another group can be an injection procedure control; this cohort can be injected with 2 nL of just 10% PVP phenol red, to account for any physiological changes that might occur due to the injection procedure.
12. When preparing the *C. neoformans* inoculum, the cfu concentration is determined by a hemocytometer count. That cfu estimate, however, does not account for several factors during the injecting procedure. Cryptococci are not completely homogeneously distributed in the inoculum, when transporting it via pipetting a different amount of cfu would be picked up each time, despite it being in the same volume of inoculum. The cryptococci in the inoculum would also replicate during

the time of the injection procedure. Also, the inoculum distributes unevenly into the injection needle, which would yield different concentrations at the tip of the needle as opposed to the top (due to the 80° angle of the needle when injecting). The closest and most accurate estimation of infection burden at the time of injection is by counting what comes out of the injection needle. The method of plating the inoculum that comes out of the needle seems the most representative of the infection burden we see during imaging. The hemocytometer count is still done to get a rough estimate of how much dilution the culture needs before injecting.

13. Many light sheet microscopes only allow imaging of one sample at a time. Mounting and processing each specimen takes up to 1 h. Therefore, it is important that samples are carefully screened on another microscope prior to imaging with the light sheet microscope.
14. When screening fish to image in the light sheet, they cannot be mounted. Taking as much media out of the 96 wells as possible will keep the fish from floating away from the bottom of the wells. If adjustments are made, the larvae can also keep lying on their side without much disruption of their orientation to ease the process of screening. It is easier to examine overall infection burden and health of each larva if they are in a lateral orientation, instead of dorsal or ventral for example.
15. An important advantage of this method is that it provides options for observation of host pathogen interactions in different time scales: slow-motion, real-time, 24 h time frame, and one time-point.
16. Real-time imaging is attempting to take a time lapse where the whole process of acquisition takes place within maximum 1 s (illuminating sample, opening and closing camera shutter, collecting information from camera matrix). Time lapses cannot be of two reporters because acquisition time cannot be within 1 s, that is, imaging GFP reporter and mCherry at the same time is not possible in real-time imaging. Real-time imaging is usually done for a short time range (2–10 min) to decrease file size and make data processing less cumbersome. In our work, we use real-time imaging to observe acute changes in vascular size and shape in infection. We have found important patterns which are imperceivable in longer intervals of acquisition (imaging that is not representative of real time changes).
17. High speed imaging is reducing acquisition time even further than real time imaging. We can reduce acquisition time further from 1fps to 30fps. The biggest factor changed in this type of imaging is reducing the field of view significantly and so shortening the time necessary for information transfer between camera and computer.

18. Longer time-lapses do not necessarily require short exposure and data collection times. Adjusting the acquisition settings is done in favor of clearer, higher quality images. Intervals of capturing should be a minimum of 5 min (or longer) to prevent data loss in large files and make data processing less cumbersome. In our work, we use 24 h time lapses for exploratory purposes or to show dissemination progression over time.
19. Single time point Z stacks are used to show in detail cryptococcal yeast distribution across tissues at a particular point in the infection progression. Can be used to show infection burden and distribution, for example, with or without treatment with pharmaceuticals of interest. When collecting information for several groups, it is important that the time of imaging between groups (or single fish) is as short as possible. This is because between 2 infected groups a larger time interval will allow for the infection to progress and 1 group might be more infected than the other because of procedural issues not actual differences. Also, a larger time interval between imaging an infected and control groups, for example, can show differences due to imaging in different developmental stages.
20. Light sheet imaging can be used to get higher resolution real-time or single point imaging. You should choose light sheet microscopy if, for example,
    (a) In real time: you want to observe changes in interconnected vascular structures in a smaller illumination plane.
    (b) In a single time, point: you want to observe the spatial distribution of infection in 3D or the morphology of the vascular bed in infection.
21. *Notes on method variation.*

    For observing dissemination in the parenchyma, blood vessel morphology and damage

    (a) *Developmental stage of zebrafish: 2dpf.* Dissemination root in human patients with cryptococcal meningitis is from lung infection to blood circulation to CNS. To mimic the pathology as seen in humans, replicate the infection root from blood vessels to brain tissue/parenchyma.
    (b) 2dpf as opposed to 1dps is a good point for introducing a systemic infection into the larvae. The lumen formation and onset of circulation in zebrafish larvae start around 24hpf [16]. Heartbeat is essential for intra-cerebral vessels development at 32hpf [17]. At 48hpf, the primary vasculogenesis is complete and CNS vessel networks well established [18, 19]. The 2dpf infection point allows for a long enough period of infection development before 5 days postfertilization, after which it becomes much more unethical to use the animal model for infection work.

(c) *Choice of infection route: Duct of Cuvier*. This is a common infection route when attempting to achieve a bloodstream infection. We prefer this injection site to the Caudal vein as it is larger, has a higher velocity of flow, and appears to allow for better distribution of pathogens across the whole larva. This is important especially when attempting to achieve CNS dissemination.

(d) *Choice of cfu content in inoculum: 700–1000 cfu***;** it is enough to disseminate into the CNS, smaller infection burden rarely produces CNS dissemination within 24 h of infection, and severe infection profile after 2 days.

(e) *Choice of time point of imaging:*

1. For a severe infection profile: 2 days postinfection.
2. For tracking infection progression: between 4 h and 24 h postinfection.

(f) *Choice of LMPA concentration*: The percentage of LMPA can be varied depending on the imaging technique used or the time that the larvae are to be kept immobilized. The higher the percentage, the quicker the solution will solidify and the less stretch it will provide for an organism to grow within it. In the imaging acquisition, a single larva lasts more than 1 h, choose a low percentage (0.3–0.5%). For light-sheet imaging, fast solidifying is the most important to get the orientation of the larvae right, choose high percentage (1–2%).

(g) *Choice of mounting orientation and imaging:* Dependent on what is imaged.

For dissemination into the parenchyma and ventricles, it is good to visualize with a widefield fluorescent microscope in a lateral view (Fig. 3b, d). The widefield allows for image collection from a larger cohort in comparison to the light sheet.

For blood vessel morphology and dynamics have data both in dorsal and lateral orientation of the larvae. Light sheet microscopy and dorsal orientation will provide a better resolution when attempting to represent the vascular bed in 3D at a single time point (Fig. 3e, f).

*For 24 h time lapse imaging***,** use the widefield microscope to avoid large data files. Real-time time lapses can be done in the Light Sheet as well and widefield fluorescence like systems.

For observing flow of infected CSF in vivo

(a) *Developmental stage of zebrafish: 1dpf*. Injections into the CNS after 40 hpf becomes harder to achieve and is more likely to cause damage. The tissue around the brain ventricles is more

difficult penetrate as bone cell progenitors are already localizing and adopting fate, although ossification occurs later [20].

(b) *Choice of infection route: Hindbrain ventricle*. Allows to immediately monitor CNS infection. Dissemination from bloodstream infection is a relatively rare event.

(c) *Choice of cfu content in inoculum: 100 cfu*.

(d) *Choice of time point of imaging: 2 h after injection*.

(e) *Choice of LMPA concentration: 0.3–0.5%*.

(f) *Choice of mounting orientation and imaging: lateral orientation and widefield imaging*. There are several types of flow within the ventricular system; it is easier to see them in a lateral orientation of the larvae. In this case, it is more efficient to select a 2D imaging model and observe a simplified version of the system overall. Widefield microscopy is a good tool to do exactly that.

References

1. Rajasingham R, Smith RM, Park BJ et al (2017) Global burden of disease of HIV-associated cryptococcal meningitis: an updated analysis. Lancet Infect Dis 17:873–881
2. Lee SC, Dickson DW, Casadevall A et al (1996) Pathology of cryptococcal meningoencephalitis: analysis of 27 patients with pathogenetic implications. Hum Pathol 27:839–847
3. Jarvis JN, Bicanic T, Loyse A et al (2014) Determinants of mortality in a combined cohort of 501 patients with HIV-associated Cryptococcal meningitis: implications for improving outcomes. Clin Infect Dis 58:736–745
4. Van Reeth E, Tham IWK, Tan CH et al (2012) Super-resolution in magnetic resonance imaging: a review. Concepts Magn Reson 40A:306–325
5. Mukaremera L, McDonald TR, Nielsen JN et al (2019) The mouse inhalation model of Cryptococcus neoformans infection recapitulates strain virulence in humans and shows that closely related strains can possess differential virulence. Infect Immun 87(5)
6. Tenor JL, Oehlers SH, Yang JL et al (2015) Live imaging of host-parasite interactions in a zebrafish infection model reveals Cryptococcal determinants of virulence and central nervous system invasion. MBio 6(5):e01425–e01415
7. Davis JM, Huang M, Botts MR et al (2016) A zebrafish model of Cryptococcal infection reveals roles for macrophages, endothelial cells, and neutrophils in the establishment and control of sustained Fungemia. Infect Immun 84(10):3047–3062
8. Bojarczuk A, Miller KA, Hotham R et al (2016) Cryptococcus neoformans intracellular proliferation and capsule size determines early macrophage control of infection. Sci Rep 18(6):21489
9. Evans RJ, Pline K, Loynes CA et al (2019) 15-keto-prostaglandin E2 activates host peroxisome proliferator-activated receptor gamma (PPAR-γ) to promote Cryptococcus neoformans growth during infection. PLoS Pathog 15(3):e1007597
10. Singulani JL, Oliveira LT, Ramos MD et al (2021) The antimicrobial peptide MK58911-NH2 acts on planktonic, biofilm, and Intramacrophage cells of Cryptococcus neoformans. Antimicrob Agents Chemother
11. Gibson JF, Bojarczuk A, Evans RJ et al (2017) Dissemination of Cryptococcus neoformans via localised proliferation and blockage of blood vessels. PLoS Pathog
12. van Leeuwen LM, Evans RJ, Jim KK et al (2018) A transgenic zebrafish model for the in vivo study of the blood and choroid plexus brain barriers using claudin 5. Biol Open 7(2): bio030494
13. Hamilton N, Rutherford HA, Petts JJ et al (2020) The failure of microglia to digest developmental apoptotic cells contributes to the pathology of RNASET2-deficient leukoencephalopathy. Glia 2020(68):1531–1545

14. Nüsslein-Volhard C, Dahm R (2002) Zebrafish: a practical approach. Oxford University Press
15. Morrow CA, Lee IR, Chow EW et al (2012) A unique chromosomal rearrangement in the Cryptococcus neoformans var. grubii type strain enhances key phenotypes associated with virulence. MBio 3:e00310–e00311
16. Fouquet B, Weinstein BM, Serluca FC et al (1997) Vessel patterning in the embryo of the zebrafish: guidance by notochord. Dev Biol 183(1):37–48
17. Kugler E, Snodgrass R, Bowley G et al (2021) The effect of absent blood flow on the zebrafish cerebral and trunk vasculature. Vasc Biol 3(1)
18. Isogai S, Lawson ND, Torrealday S et al (2003) Angiogenic network formation in the developing vertebrate trunk. Development 130(21): 5281–5290
19. Quiñonez-Silvero C, Hübner K, Herzog W et al (2020) Development of the brain vasculature and the blood-brain barrier in zebrafish. Dev Biol 457(2):181–190
20. Mork L, Crump G (2015) Zebrafish craniofacial development. A window into early patterning. Curr Top Dev Biol 115:235–269
21. Krueger J, Liu D, Scholz K et al (2011) Flt1 acts as a negative regulator of tip cell formation and branching morphogenesis in the zebrafish embryo. Development 138(10):2111–2120

Chapter 5

Immunological Analysis of Cryptococcal Meningoencephalitis in a Murine Model

Jintao Xu, Kristie Goughenour, W. Rex Underwood, and Michal A. Olszewski

Abstract

Cryptococcal meningoencephalitis (CM), caused by the fungal pathogen *Cryptococcus neoformans* species complex, can lead to high mortality or severe neurological sequelae in survivors that are associated with excessive inflammation in the central nervous system (CNS), especially in those who develop immune reconstitution inflammatory syndrome (IRIS) or postinfectious immune response syndrome (PIIRS). While the means to establish a cause-and-effect relationship of a specific pathogenic immune pathway during CM by human studies are limited, mouse models allow dissection of the potential mechanistic links within the CNS immunological network. In particular, these models are useful for separating pathways contributing predominantly to immunopathology from those important for fungal clearance. In this protocol, we described methods to induce a robust, physiologically relevant murine model of *C. neoformans* CNS infection that reproduces multiple aspects of human cryptococcal disease immunopathology and subsequent detailed immunological analysis. Combined with tools including gene knockout mice, antibody blockade, cell adoptive transfer, as well as high throughput techniques such as single-cell RNA sequencing, studies using this model will provide new insights regarding the cellular and molecular processes that elucidate the pathogenesis of cryptococcal CNS diseases in order to develop more effective therapeutic strategies.

Key words Cryptococcal meningoencephalitis, Mice model, Neuroinflammation

1 Introduction

The opportunistic fungal pathogen *Cryptococcus neoformans* causes substantial morbidity and mortality worldwide [1], with most cases of symptomatic illness or death resulting from fungal dissemination to the central nervous system (CNS) and subsequent meningoencephalitis. Cryptococcal meningoencephalitis (CM) is not only characterized by high mortality rates, but it also frequently results in long-lasting severe neurological damage, such as memory loss, vision deficiencies, hearing and speech impairments, and motor deficits [2, 3] in patients who survive. These incredibly poor clinical

Rebecca A. Drummond (ed.), *Antifungal Immunity: Methods and Protocols*, Methods in Molecular Biology, vol. 2667,
https://doi.org/10.1007/978-1-0716-3199-7_5,

outcomes for cryptococcal meningitis are reflective of the severe lack of therapeutic options for the treatment of CNS-disseminated cryptococcosis. In order to develop novel more effective therapeutic strategies, there is an urgent need to study the cellular and molecular processes that elucidate the pathogenesis of cryptococcal CNS diseases.

Prior studies have established a central role for host immune responses, especially T-cell-mediated immunity in microbiological control and limiting of cryptococcal diseases [4, 5]. However, accumulating evidence supports that immune inflammatory factors, including T-cells, can significantly contribute to CNS pathology in at least certain subsets of patients with complicated CNS disease [6, 7]. Cryptococcus-infected HIV+ patients initiating antiretroviral therapy often develop immune reconstitution inflammatory syndrome (IRIS) upon restoration of T-cell counts accompanied with severe neurological sequela and morbidity despite fungal eradication [8, 9]. A similar phenomenon occurs among non-HIV patients with severe cryptococcal CNS disease in the setting of microbiological control, termed postinfectious immune response syndrome (PIIRS) [10]. Studies confirm that cryptococcal IRIS and PIIRS share many characteristic immunological features, including elevated CD4+ T-cell counts in cerebrospinal fluid (CSF) and their IFN-γ production, suggesting that the host immune responses necessary for fungal clearance at the same time contribute to clinical disease [10].

While it is challenging to establish a cause-and-effect relationship of a specific mechanism of disease in human studies, mouse models allow for the dissection of mechanistic links and causative relationships to be determined. Thus, a mouse model of cryptococcal meningoencephalitis within the CNS is necessary to determine the exact immunological network involved in the suggested immunopathology identified in human studies. Several models of cryptococcal CNS infection have been previously described; however, these models induce rapid complete mortality by 4–14 days postinfection, prior to the development of a measurable adaptive T-cell response, and thus have not focused on the role of CNS inflammation in pathogenesis of cryptococcal CNS disease [11–13]. In this protocol, we described the induction of a robust *C. neoformans* CNS infection model in immunocompetent mice that reproduces key aspects of human cryptococcal disease pathology and thus is suitable for detailed immunological analysis and translation to human infections [7]. Using this model of disseminated CNS infection, we have demonstrated that Th1-biased CD4+ T-cells in the CNS are a primary cause of detrimental pathology, characterized not only by early mortality and loss of body weight, but also neuronal cell death in the brain [14]. In addition to T-cells, we further showed that CCR2 signaling promotes brain infiltration of inflammatory monocytes which contribute to neuropathology and

dysregulated gene expression involved in neurotransmission, connectivity, and neuronal cell structure during cryptococcal meningoencephalitis, suggesting that CCR2-dependent inflammatory monocytes work hand-in-hand with CD4+ T cells to drive disease pathology during cryptococcal meningoencephalitis [15]. These studies provide new insights regarding clinical outcomes observed in IRIS and PIIRS patients and support the development of therapeutic strategies that limit selected aspects of inflammation to prevent CNS damage in a subset of patients with CNS cryptococcosis accompanied by inflammatory brain damage.

2 Materials

2.1 Cryptococcus neoformansCryptococcus neoformans (C. neoformans) Culture

1. Sterile culture flask.
2. Sterile Sabouraud Dextrose Broth.
3. Incubator; capable of shaking at 160 rpm at 37 °C.

2.2 Retro-Orbital Injections in Mice

1. Sterile PBS.
2. 1 mL syringe.
3. 30½G needle.
4. Isoflurane.

2.3 Organ Collection

1. 10 mL syringe prefilled with cooled PBS and kept on ice.
2. Whirl-Bags prefilled with sterile Milli-Q water (under the hood) and kept on ice throughout the procedure.
3. Surgical spatula.

2.4 CFU Assay

1. 96-well plate.
2. Sterile water.
3. Sterile Sabouraud Dextrose Agar plates.

2.5 Brain Leukocyte Isolation

1. Complete media: RPMI Medium 1640 (1×, sterile) supplemented with 10% fetal bovine serum (FBS), 25 mM GlutaMAX, 1 U/mL penicillin-streptomycin, 0.1 mM nonessential amino acids, 1 mM sodium pyruvate, and 55 nM beta-mercaptoethanol. Make in the hood and store at 4 °C.
2. Digest Media: complete media supplemented 100 U/mL DNAse I and 50 μg/mL collagenase A. Each mouse requires 5 mL of digest media made fresh immediately prior to organ harvest. Sterile filter the digest media directly into the C tubes (see below).
3. PBS sterile (10× and 1×).

4. gentleMACS™ C Tubes from Miltenyi Biotec (one per brain).
5. Percoll.
6. GentleMACs Dissociator (Miltenyi).
7. Sterile scissors.
8. Trypan blue and haemocytometer.

2.6 Flow Cytometry Analysis Extracellular and Intracellular*

1. Flow Buffer: 1× PBS, 5 % (v/v) FBS, 2 mM EDTA, 2 mM sodium azide (NaN3).

   NaN3 is added as a preservative. Use the buffer without NaN3 if you want to do functional assays.
2. 0.1 mg/mL PMA stock solution *.
3. 1 mM Ionomycin stock solution *.
4. 5.0 mg/mL Brefeldin A stock solution *.
5. 2.0 mM Monensin stock solution *.
6. LIVE/DEAD fixable dead cell stain kit.
7. 20% paraformaldehyde.
8. Foxp3/Transcription Factor Staining Buffer Set (eBioscience)*.
9. 96-well V bottom plate.
10. Unconjugated anti-CD16/32.
11. Fluorophore conjugated antibodies.
12. Multicolor flow cytometer.
13. FlowJo software (TreeStar).

3 Methods

3.1 Cryptococcus neoformans Culture

Initiation of *C. neoformans* culture should be performed within a BSL2 hood to avoid culture contamination and ensure laboratory safety.

1. Remove cryptococcal strain stock from −80 °C freezer and thaw.
2. Using a serological pipet, transfer 20 mL of sterile Sabouraud Dextrose Broth into a sterile 125 mL culture flask.
3. Once defrosted, transfer 20 μL of the cryptococcal strain into the culture flask.
4. Culture at on a shaker at 160 RPM at 37 °C for 72–96 h.

3.2 Mice Infection (see Note 1)

Mouse infection procedures should optimally be performed within a BSL2 hood to minimize the risk of contamination. There are three stages to the mouse infection: preparing the cryptococcus inoculum, intravenous injection, and mouse monitoring.

3.2.1 Wash, Count, and Adjustment of C. neoformans Culture

1. In the BSL2 hood, transfer 1 mL of *C. neoformans* culture to a 15 mL conical tube filled with 9 mL sterile PBS.
2. Centrifuge tube for 2 min at 400 g at 4 °C. Discard supernatant into liquid biohazard disposal. Add 10 mL of fresh sterile PBS to the pellet, vortex thoroughly to re-suspend the pellet.
3. Centrifuge tube again for two minutes at 400 g at 4 °C. Discard supernatant into liquid biohazard disposal and re-suspend to 5 mL in PBS.
4. Count cells in 0.4% trypan blue and hemacytometer stain under microscope, dilute as needed to obtain countable cell numbers in microscope field; count and calculate cell concentrations.
5. Adjust cell concentration to match the desired inoculum for the infection.

3.2.2 Mouse Intravenous Injection (see **Note 1**)

1. Fill a 1 mL syringe with the cryptococcus inoculum (ensure that tube has been mixed well before filling) and attach a 30½ G needle to the syringe.
2. We recommend short-term inhaled anesthesia (e.g., Isoflurane in an anesthesia jar) to fully immobilize mice for the short period of time (~2 min) for the procedure.
3. Pinch both of the mouse's ears together to pull back the skin of its head, allowing for its eyeballs to be slightly protruded. Carefully insert the needle into the anterior corner of the eye (lacrimal caruncle). Slowly push the needle behind the eye at approximately a 45° angle until the needle tip gently touches the orbital bone. Expel the desired inoculum from the syringe. Ensure that the liquid is not leaking from the eye, otherwise the needle will need to be repositioned (*see* **Note 1**).
4. Remove the needle from the eye and place the mouse into the prepared fresh cage. The mouse should recover to full activity within 2 min.

3.2.3 Mice Monitoring Postinfection

1. After mice have been infected, weigh each mouse to obtain a baseline weight to evaluate disease progression.
2. Check the infection site daily for the week following infection to ensure that there is no external infection from the entry site.
3. Mice can be weighed and evaluated behavior every other day (*see* Subheading 3.3).
4. Once a mouse approaches 20% of the baseline weight, or if the animal displays other endpoints determined by institutional ethics committee, the mouse should be humanely euthanized using approved procedures.

3.3 Murine Coma and Behavioral Scale (MCBS) Adapted for Cryptococcal Meningoencephalitis

This test was adapted from Carroll et al. [16] to quantify the neurological damage seen in *Cryptococcal* meningoencephalitis in mice. Several behaviors and mice responses to stimuli are assessed on a numeric scale from healthy scoring 3 to no response/clearly severely impaired scoring 0. This experiment can be done on any mouse and in combination with any desired experimental condition. It is noninvasive and only requires clean tweezers and commonly used mouse cages containing a lid and a wire cage. If your animal facility uses another set-up to house mice, a medium square container can replace the lid and the grab test can be performed on the rim of the container provided it is thin enough for the mice paws to hold. Please *see* **Note 2** on performing blinded experiments to avoid bias.

1. Remove lid and wire cover from mouse cage.
2. Place a single mouse in the upside-down lid and replace the wire on the cage.
3. Evaluate the mouse for:
   (a) Gait – how the mouse walks around the lid.
      i. 3: normal, 2: stiff, 1: ataxic, 0: none.
   (b) Balance – can the mouse rise up on the walls of the cage.
      i. 3: full body lift on wall in less than 3 attempts, 2: one back leg only, 1: front legs only, 0: no lift.
   (c) Exploration – how actively is the mouse moving round the cage.
      i. 3: visits 4 corners in less than 15 s. 2: visits 4 corners in less than 90 s. 1: visits 2–3 corners. 0: none.
   (d) Body position – when still how does the mouse stand.
      i. 3: full body extension, 2: mild hump, 1: hunched, 0: on side.
   (e) Coat condition.
      i. 3: normal, 2: dusty/piloerection, 1: mildly ruffled, 0: severely ruffled.
4. Using a pair of tweezers, gently touch the mouse as follows to evaluate its ability to respond to stimuli:
   (a) Head/neck touch.
      i. 3: both sides twitch in response to first touch attempt, 2: both sides twitch in response to first less than three attempts, 1: only one side twitches in response, 0: no response.
   (b) Body touch (aim for sides of the stomach).
      i. 3: both sides twitch in response to first touch attempt, 2: both sides twitch in response to first less than three

attempts, 1: only one side twitches in response, 0: no response.

(c) Ear touch.

i. 3: both sides twitch in response to first touch attempt, 2: both sides twitch in response to first less than three attempts, 1: only one side twitches in response, 0: no response.

5. Place the mouse on top of the wire cage cover. Using the tweezers, gently touch the mouse as follows to evaluate its ability to respond to stimuli:

(a) Touch next to the corner of the mouse eye to test for a blink response.

i. 3: both sides twitch in response to first touch attempt, 2: both sides twitch in response to first less than three attempts, 1: only one side twitches in response, 0: no response.

(b) Ear touch.

i. 3: both sides twitch in response to first touch attempt, 2: both sides twitch in response to first less than three attempts, 1: only one side twitches in response, 0: no response.

6. Grasping the mouse by the tail, allow the mouse to try and grab the wire bars of the cage cover to test its grasp.

(a) 3: grabs and pulls/walks, 2: abnormal/one handed grab, 1: weak grasp/attempted movement but no true grasp, 0: no attempt to grab.

7. Replace the mouse in the cage and repeat until all mice have been scored

8. Record scores for all mice, see Table 1 as an example of expected results.

3.4 Collect Organs

All surgical instruments should be sterile. While this protocol encompasses the collection of the brains, other organs such as spleens, lungs and kidneys can also be harvested [17].

3.4.1 Perfusion

1. Humanely euthanize animals using procedures approved in the animal license and institutional ethics committee.
2. Place the mouse in supine position on a bodyboard and pin down all four extremities using needles to maintain a tight, immobile body position. Spray the body with 70% ethanol to sterilize.
3. Using forceps, pinch the skin slightly inferior to the transverse plane and make an incision using surgical scissors. Cut the skin laterally until the majority of the abdomen has been exposed,

Table 1
Murine coma and behavioral scale (MCBS) score chart with example outcomes found in uninfected (Mouse 1) and severely affected (Mouse 2) animals

MCBS Parameter	3 Points	2 Points	1 Point	0 Point	Mouse 1	Mouse 2
Gait	Normal	Stiff	Ataxic	None	3	1
Balance	Full body lift ≤ 3 attempts	One back leg lifted ≤ 3 attempts	Front legs only ≤ 3 attempts	None	3	1
Exploration	4 corners ≤ 15 s	4 corners ≤ 90 s	2–3 corners ≤ 90 s	None	3	2
Body Position	Full extension	Mild hunch	Hunched	Tilted or On side	3	1
Coat Condition	Normal	Dusty, slight piloerection	Mildly ruffled	Ruffled	3	1
Neck Touch	Both sides 1 attempt	Both sides ≤ 3 attempts	One side ≤ 3 attempts	No response	3	3
Body Touch	Both sides 1 attempt	Both sides ≤ 3 attempts	One side ≤ 3 attempts	No response	3	3
Pinna Touch	Both sides 1 attempt	Both sides ≤ 3 attempts	One side ≤ 3 attempts	No response	3	3
Toe Touch	Both sides 1 attempt	Both sides ≤ 3 attempts	One side ≤ 3 attempts	No response	3	3
Blink Reflex	Both eyes 1 attempt	Both eyes ≤ 3 attempts	One eye ≤ 3 attempts	None	3	3
Grasp Strength	Strong pull, walks	Mild pull, abnormal	Weak grasp	None	3	1
Total score	–	–	–	–	33	22

then move up until reaching the rib cage on both sides. Peel away the skin first, followed by the peritoneal sac.

4. After the entire abdomen has been exposed, gently move the liver to reveal the diaphragm. Use scissors to gently pierce a hole through the diaphragm, thus deflating the lungs. The rib cage can now be cut and peeled up.
5. Gently push the intestines and other organs aside from the center of the mouse until the iliac artery is visible. Cut this artery to collect blood if needed.
6. Expose the heart, insert a 25⅝ G needle attached to a 10 mL syringe filled with cold PBS. The needle should be placed into the left ventricle of the heart, and the entire 10 mL of PBS pushed through the circulatory system slowly (*see* **Note 3**). Be sure to apply gauze at the site of the cut caudal vein to absorb any extra PBS. The organs are now perfused and ready for collection.

3.4.2 Brain Collection Procedure

1. After perfusion, unpin the mouse from the bodyboard and place it into a supine position.
2. Spray the entire head of the mouse with 70% ethanol. Use forceps to pinch the skin on the top of the head directly between the ears and make an incision. Peel the skin away anteriorly, exposing the entirety of the skull.
3. Using a set of forceps, hold the head through grasping the eye-sockets to prevent movement. Pull the head up and cut the spine at the base of the skull. Insert the scissors into the hole at the back of the skull (foramen magnum) and cut at a 45° angle towards the occipital lobe, until the midpoint is reached. Repeat for the opposite side. Make small, controlled incisions to avoid damaging the brain tissue. Using a pair of forceps, gently lift the skull away from the brain.
4. With a surgical spatula, gently push the brain away from the skull, encircling the entire brain to disconnect any tissue from the walls of the bone.
5. From the bottom of the brain, lift using the surgical spatula to remove it from the skull and place it into the organ bag.

3.5 Colony Forming Unit (CFU) Plating Procedure

Following collection, organs are now ready to be homogenized and plated onto SDA plates to measure the fungal burden. For organs with high fungal load (> 100 CFU), serial dilution and plating should be performed. However, if the fungal burden is expected to be very low, the entire organ should be plated for accuracy. This procedure is designed for a quick brain CFU analysis and thus not compatible with leukocyte isolation and subsequent flow cytometry analysis. If both CFU results and leukocyte analysis are needed, please follow procedure Subheading 3.6.

1. Transfer brains into "whirl bags" prefilled with 2 mL sterile ddH_2O. Brains can be homogenized by using a cylindrical instrument and repetitively "scraping" the bag into the corners, forcing the contents against each other against the friction. This should be performed until the contents of the bags are a uniform mixture.
2. Remove 200 μL of the homogenate from the bag into the top well of a 96-well plate. The bag should be saved for repeat dilutions or for whole organ plating.
3. Add 90 μL sterile Milli-Q to all other wells in the column, and perform descending dilutions, 10 μL at a time.
4. Using a multichannel pipet, plate all eight wells onto an SDA plate. Do so twice per organ for redundancy. Allow to dry in hood then remove after 20 min. Incubate on the benchtop for 48 h before counting.

3.6 Brain Leukocyte Isolation

To examine the immune response to cryptococcal meningitis, the brain must be gently digested for high quality cell isolation (*see* **Note 4**). Once cells are isolated and counted, further analysis such as flow cytometry, culture, or RNA extraction can be performed.

1. Prior to harvest, gentleMACS™ C tubes should be filled with 5 mL digest media and prewarmed to 37 °C.
2. Euthanize and harvest the brain from infected mice as in Subheading 3.4.
3. Mince brains to a smooth paste with sterile scissors on the side of the C tube. Slide the brain paste into the C-tube.
4. Insert C tubes into the GentleMacs Dissociator and homogenize using the [m_brain_01.01] manufacturer's program on the device.
5. Incubate on a rocker at 37 °C within an incubator for 15 min.
6. Homogenize using GentleMacs Dissociator selecting manufacturer's program [m_brain_02.01].
7. Incubate C tubes at 37 °C for 10 min.
8. Homogenize using m_brain_03.01 on the GentleMacs Dissociator.
9. Incubate C tubes at 37 °C for 10 min.
10. Centrifuge for 1 min at 200 g to pellet all the digested material.
11. Resuspend the pellet by mixing via pipetting with a P1000 pipette.
12. If analyzing RNA or CFU, remove 100 μL of resuspension for CFU, and 200 μL for RNA (*see* **Note 5**).
13. Centrifuge C tubes for 10 min at 400 g. Decant the supernatant into bleach waste.

14. Resuspend the pellet in 10 mL RPMI media by pipetting up and down.
15. Filter the suspension through a 70 μM cell strainer. Wash with 5 mL RPMI media.
16. Centrifuge the C tubes for 10 min at 400 g at RT on high brake setting.
17. Percoll solutions: Prepare Isotonic Percoll by combining 1-part 10× sterile PBS with 9 parts Percoll. Prepare 70% Percoll by combining 7 parts isotonic Percoll with 3 parts 1× sterile PBS. Prepare 30% Percoll by combining 3 parts isotonic Percoll with 7 parts complete media. Fill one 15 mL conical tube with 5 mL of 70% Percoll per mouse.
18. Resuspend the pellet in 5 mL of 30% Percoll by pipetting up and down.
19. Using a serological pipette on a slow setting, draw the 30% Percoll cell suspension up and layer it over the 70% Percoll in the 15 mL conical tube.
20. Layer 2 mL of PBS over the 30% Percoll cell suspension.
21. Centrifuge the 15 mL conical vial for 30 min at 1100 g at RT on the NO BREAK setting on the centrifuge.
22. Prepare 15 mL conical tubes filled with 10 mL sterile PBS.
23. Once centrifuged, the Percoll gradient will generate a clear bottom layer (70% Percoll) and a pink top layer (30% Percoll). Myelin debris will sometimes be seen as "floating islands" at the very top. The leucocytes will be a cloudy ring at the interface of the pink and clear bottom layer. Aspirate the myelin and collect the leukocytes at the indicated interface using a sterile disposable transfer. Pipet the cells into the 15 mL conical vials prepared in **step 21**.
24. Centrifuge for 10 min at 400 g. Decant the supernatant.
25. Resuspend the pellet in 10 mL sterile PBS. Centrifuge for 10 min at 400 g.
26. Resuspend cells in PBS for downstream applications.

3.7 Flow Cytometry Analysis of Brain Immune Isolates

Leukocytes enriched from the brain, including resident microglia and infiltrated immune cells, can be analyzed by flow cytometry to quantify their numbers and phenotypes. For cytokines and chemokines detection, such as IFN-γ, TNF-α, IL17A, and IL-4, a combination of PMA (a phorbol ester, a protein kinase C activator) and Ionomycin (a calcium ionophore) can be used to stimulate cells *in vitro* with the presence of protein transport inhibitors Monensin or Brefeldin A Solution during the final hours of the stimulation protocol.

3.7.1 In vitro Stimulation of Brain Immune Cells for Intracellular Flow Cytometry (Optional)

This part of the protocol involves the stimulation of cells to detect intracellular cytokines or chemokines. You can skip this step and go to Subheading 3.6, **step 2** if you are only analyzing surface markers of immune cells.

1. Prepare plate layout and add 1 million freshly isolated immune cells (*see* **Note 4**) suspended in 200 μL complete medium to wells of 96-well plate.
2. Add 25 μL 10× 500 ng/mL PMA and 10 μg/mL ionomycin in complete media to wells and incubate at 37 °C for 2 h.
3. Add 25 μL 10× 50 μg/mL Brefeldin A and 20 nM Monensin mix in complete media. Incubate at 37 °C for 4 h.
4. After incubation, centrifuge at 400 g for 5 min at 4 °C. Flick off supernatant.

3.7.2 Surface Staining of Brain Immune Cells for Flow Cytometry in 96-Well Plates

Once the cells have been stimulated, they can now be stained with antibodies against surface protein markers of interest. Use this part of protocol to perform surface staining on freshly isolated cells.

1. Prepare plate layout and Ab staining templates, keeping in mind you will need to add wells for isotype and compensation controls.
2. Add 1 million freshly isolated immune cells into wells of 96 well V-bottom plate or use stimulated cells from **step 4** of Subheading 3.6, **step 1**. Keep cells on ice for the entire protocol.
3. Centrifuge the plate at 400 g for 5 min at 4 °C. Flick off supernatant.
4. Stain with LIVE/DEAD fixable dye: First, mix 0.25 μL LIVE/DEAD fixable dead cell stain per sample in 100 μL PBS. Next, add Live/Dead dye solution to cells and incubate in dark for 30 min. Finally, wash samples by adding 100 μL PBS and centrifuging at 400 g for 5 min at 4 °C.
5. Perform Fc Block: First, mix 2 μL Fc Block (we recommend TruStain FX, anti-CD16/32) per sample in 50 μL Flow Buffer. Then, add to cells and incubate on ice for 15 min, protected from light.
6. Perform extracellular antibody staining: First, add 50 μL of antibody cocktails directly to Fc blocked samples. Incubate in the dark for 30 min. Next, add 200 μL Flow Buffer to cells to wash. Centrifuging at 400 g for 5 min, Flick off supernatant. Repeat wash for additional 2 times.
7. Fix cells (Optional): Add 200 μL of 2% buffered paraformaldehyde, making sure pellets are well suspended with no clumps. Incubate in dark for at least 15 min. Then centrifuge at 400 g for 5 min, flick off supernatant. Re-suspend cells in Flow Buffer.

3.7.3 Staining for Intracellular Proteins

Once the cells have been stained with antibodies against surface markers, you can further stain cells with antibodies against intracellular cytokines such as IFN-γ, TNF-α, IL17A, and IL-4 if cells are stimulated, or transcriptional factors like Tbet for Th1 cells and Foxp3 for Treg cells. Staining for intracellular proteins is important to analyze cell status and their potential functions.

1. Resuspend cells from **step 6** of Subheading 3.6, **step 2** in 100 μL 2% buffered formaldehyde. Incubate at room temperature for 30 min in dark (protected from light). For transcriptional factors such as FoxP3 and Tbet detection, use Fixation/Permeabilization solution from Foxp3/Transcriptional Factor Staining Buffer Set.
2. Add 100 μL 1× Perm Buffer from Foxp3/Transcriptional Factor Staining Buffer Set. Centrifuge at 400 g for 5 min, flick off supernatant.
3. Wash with 200 μL Perm Buffer.
4. Stain cells with intracellular antibody mix in 100 μL Perm Buffer. Incubate at room temperature for at least 30 min in dark.
5. Wash with Perm Buffer for three times.
6. Wash with 200 μL PBS.
7. Resuspend in 100 μL 2% formaldehyde for 15 min. [Can skip if analyzing immediately]
8. Add 100 μL Flow Buffer. Centrifuge at 400 g for 5 min, flick off supernatant.
9. Resuspend in 200 μL Flow Buffer and run on the cytometer or store in dark at 4 °C for a short period of time (*see* **Note 6**).

4 Notes

1. Retro-orbital injection: A novice operator should receive enough training for retro-orbital injections. We recommend novice operators to practice on terminally anesthetized mice before using this technique in live mice. To avoid vascular overload, the injection volume should not exceed 200 μL and the injection should be given slowly. Once the injection is done, withdraw the needle slowly and smoothly. There should be little or no bleeding. Another commonly used equivalent infection route is the tail vein injection and this has been used by other groups [18, 19]; however, we believe that the tail injection works slightly less consistently and may result in higher variability if part of the volume is injected outside of the vein.

2. Avoid bias for MCBS scores: To avoid bias, a blinded experiment is recommended where the experimenter does not know which treatment is given to mice (control versus experimental). While mice can be assessed for the MCBS at any time, an initial baseline assessment immediately before infection and then weekly postinfection will give a good overview of the neurological changes in mice in this *C. neoformans* meningoencephalitis model.
3. Transcardial perfusion: Incomplete removal of blood circulating immune cells will result in a biased view on the actual amount and phenotypes of the immune cells accumulating in the fungal infected brain. From experience, the usage of needles for left ventricle puncture with a flow rate of less than 10 mL/min should perfuse the systemic circulation nicely. Brain tissue should be a pale to white color, which indicates a good perfusion.
4. Isolate immune cells from brain: High quality isolation of cells per brain hemisphere allows reproducible multiparameter flow cytometry analysis and other applications. Efficient dissociation of brain tissue that comprises mechanical fragmentation as well as enzymatic digestion is essential for high quality and yield of immune cells. Mincing the tissue thoroughly is critical to provide improved effectiveness of proteases. When homogenizing the tissues and suspending cells, avoid excessive pressure and speed for viability. The separation protocol produces reliable results with about 0.1–0.2 million total cells from uninfected brains and 0.5–3 million total cells from infected mice depending on the stage of infections.
5. Additional samples for immunological analysis from brain digestion: Total brain homogenate or total brain RNA can also be obtained for quantification of cytokine levels in the brain and determination of gene expression to get a complete image of the neurological damage in inflammation. For the RNA sample preparation, brain tissues should be dispersed in TRIzol immediately. Samples can be stored at −80 °C.
6. Flow cytometry analysis: Long-term cell storage in formaldehyde is not recommended. After fixation, wash and resuspend cells in flow buffer. For fixed samples, perform the analysis as soon as possible. If you cannot run your samples immediately, store the cells in the dark at 4 °C. We recommend performing the analysis within 48 hrs if you use tandem fluorophores such as PE-Cy7, APC-Cy7, PerCp-Cy5.5.

Acknowledgement

This work was supported by the Veterans Administration Merit Review Awards to M.A.O. (1I01BX000656), VA RCS Award to M.A.O. (1IK6BX003615). National Institutes of Health postdoctoral fellowship T32 grant through the Division of Pulmonary and Critical Care Medicine, Department of Internal Medicine, University of Michigan (5T32HL007749-27) to K.D.G., and American Lung Association Catalyst Award CA-827199 to J.X.

Bibliography

1. Rajasingham R, Smith RM, Park BJ, Jarvis JN, Govender NP, Chiller TM et al (2017) Global burden of disease of HIV-associated cryptococcal meningitis: an updated analysis. Lancet Infect Dis 17(8):873–881
2. Lionakis MS, Levitz SM (2018) Host control of fungal infections: lessons from basic studies and human cohorts. Annu Rev Immunol 36: 157–191
3. Ecevit IZ, Clancy CJ, Schmalfuss IM, Nguyen MH (2006) The poor prognosis of central nervous system cryptococcosis among nonimmunosuppressed patients: a call for better disease recognition and evaluation of adjuncts to antifungal therapy. Clin Infect Dis 42(10): 1443–1447
4. Olszewski MA, Zhang Y, Huffnagle GB (2010) Mechanisms of cryptococcal virulence and persistence. Future Microbiol 5(8): 1269–1288
5. Rohatgi S, Pirofski L-a (2015) Host immunity to Cryptococcus neoformans. Future Microbiol 10(4):565–581
6. Jarvis JN, Bicanic T, Loyse A, Namarika D, Jackson A, Nussbaum JC et al (2014) Determinants of mortality in a combined cohort of 501 patients with HIV-associated Cryptococcal meningitis: implications for improving outcomes. Clin Infect Dis 58(5):736–745
7. Neal LM, Xing E, Xu J, Kolbe JL, Osterholzer JJ, Segal BM et al (2017) CD4+ T cells orchestrate lethal immune pathology despite fungal clearance during Cryptococcus neoformans meningoencephalitis. MBio 8(6):e01415–e01417
8. Shelburne SA III, Darcourt J, White AC Jr, Greenberg SB, Hamill RJ, Atmar RL et al (2005) The role of immune reconstitution inflammatory syndrome in AIDS-related Cryptococcus neoformans disease in the era of highly active antiretroviral therapy. Clin Infect Dis 40(7):1049–1052
9. Wiesner DL, Boulware DR (2011) Cryptococcus-related immune reconstitution inflammatory syndrome (IRIS): pathogenesis and its clinical implications. Curr Fung Infect Rep 5(4):252–261
10. Panackal AA, Wuest SC, Lin Y-C, Wu T, Zhang N, Kosa P et al (2015) Paradoxical immune responses in non-HIV cryptococcal meningitis. PLoS Pathog 11(5):e1004884
11. Uicker WC, McCracken JP, Buchanan KL (2006) Role of CD4+ T cells in a protective immune response against Cryptococcus neoformans in the central nervous system. Sabouraudia 44(1):1–11
12. Uicker WC, Doyle HA, McCracken JP, Langlois M, Buchanan KL (2005) Cytokine and chemokine expression in the central nervous system associated with protective cell-mediated immunity against Cryptococcus neoformans. Med Mycol 43(1):27–38
13. Buchanan KL, Doyle HA (2000) Requirement for CD4+ T lymphocytes in host resistance against Cryptococcus neoformans in the central nervous system of immunized mice. Infect Immun 68(2):456–462
14. Xu J, Neal LM, Ganguly A, Kolbe JL, Hargarten JC, Elsegeiny W et al (2020) Chemokine receptor CXCR3 is required for lethal brain pathology but not pathogen clearance during cryptococcal meningoencephalitis. Sci Adv 6(25):eaba2502
15. Xu J, Ganguly A, Zhao J, Ivey M, Lopez R, Osterholzer JJ et al (2021) CCR2 signaling promotes brain infiltration of inflammatory monocytes and contributes to neuropathology during cryptococcal meningoencephalitis. MBio 12(4):e01076–e01021
16. Carroll RW, Wainwright MS, Kim K-Y, Kidambi T, Gomez ND, Taylor T et al (2010) A rapid murine coma and behavior scale for quantitative assessment of murine cerebral malaria. PLoS One 5(10):e13124

17. Goughenour KD, Zhao J, Xu J, Zhao ZP, Ganguly A, Freeman CM et al (2021) Murine inducible nitric oxide synthase expression is essential for antifungal defenses in kidneys during disseminated cryptococcus deneoformans infection. J Immunol 207(8):2096–2106
18. Chrétien F, Lortholary O, Kansau I, Neuville S, Gray F, Dromer F (2002) Pathogenesis of cerebral Cryptococcus neoformans infection after fungemia. J Infect Dis 186(4): 522–530
19. Sun D, Zhang M, Sun P, Liu G, Strickland AB, Chen Y, Fu Y, Yosri M, Shi M (2020) VCAM1/VLA4 interaction mediates Ly6Clow monocyte recruitment to the brain in a TNFR signaling dependent manner during fungal infection. PLoS Pathog 16(2):e1008361

Chapter 6

Mouse Model of Latent Cryptococcal Infection and Reactivation

Ko Sato and Kazuyoshi Kawakami

Abstract

Abstract *Cryptococcus neoformans* is an opportunistic fungal pathogen that frequently causes fatal meningoencephalitis in patients with impaired immune responses. This fungus, an intracellularly growing microbe, evades host immunity, leading to a latent infection (latent *C. neoformans* infection: LCNI), and cryptococcal disease is developed by its reactivation when host immunity is suppressed. Elucidation of the pathophysiology of LCNI is difficult due to the lack of mouse models. Here we show the established methods for LCNI and reactivation.

Key words *Cryptococcus neoformans*, Latent infection, Reactivation, Mouse model

1 Introduction

Cryptococcus neoformans, a yeast-type fungal pathogen with thick capsules, infects the lungs by airborne transmission and causes life-threatening meningoencephalitis in patients with impaired cell-mediated immunity such as acquired immunodeficiency syndrome [1]. The cellular immune mechanism plays a central role in eradicating *C. neoformans*, which is critically regulated by Th1–Th2 immune balance [1–4]. The Th1-mediated immune response supports host defense by inducing the production of nitric oxide (NO), which enhances macrophages' ability to kill *C. neoformans*, and by promoting the formation of granulomas at infection sites, which prevents the spread of this fungal pathogen to the surrounding lung tissues and to the central nervous system (CNS) [3–7]. The Th2 immune response, in contrast, disturbs host defense by suppressing macrophages' killing of this fungus and granuloma formation [3–5, 8]. The precise role of the Th17-mediated host defense to cryptococcal infection remains controversial [9–14].

Rebecca A. Drummond (ed.), *Antifungal Immunity: Methods and Protocols*, Methods in Molecular Biology, vol. 2667,
https://doi.org/10.1007/978-1-0716-3199-7_6,

This fungus resists being killed by macrophages through (1) melanin synthesis, (2) capsular polysaccharide, (3) vomocytosis, and (4) titan cell formation, which enables its intracellular growth within these cells [15–22]. In this way, *C. neoformans* can evade host immunity and cause the development of a latent infection and its reactivation when the host becomes immunocompromised. Indeed, some clinical cases have suggested reactivation after latent cryptococcal infection [23–25]. Although analysis using a mouse model is one of the most effective tools for elucidating the host defense mechanism of cryptococcal infection, most studies use a mouse model of primary infection, not of latent infection and reactivation [5, 7–14, 22, 26–31]. In most primary infection models, mice die from out of control cryptococcal infection within a few months after infection. Therefore, in order to establish a latent *C. neoformans* infection (LCNI) mouse model, it is necessary to use rat or mouse strains such as CBA/J and CnT-II that are resistant to cryptococcal infection or to use attenuated cryptococcal strains such as Δgcs1, UgCl223, or UgCl552 [14, 16, 32–34].

The criteria for defining LCNI in a mouse model are not standardized. Normile et al. defined LCNI in a mouse model as follows: (1) the fungal cells are present in the lung tissue after infection, (2) the host develops adaptive immunity against yeast cells and contains it by granuloma, and (3) the host is able to control the infection during an immunocompetent state [35]. In addition, Ding et al. developed the following set of criteria to define latency in a persistent *C. neoformans* infection model: (1) stable fungal counts in the lungs throughout the entirety of the infection, (2) generation of pulmonary granulomas and no alveolar inflammation in the surrounding lung parenchyma, (3) no clinical signs of disease throughout the entirety of infection (i.e., animals behave and appear healthy), (4) no weight loss attributable to disease, (5) serum CrAg (GXM) LFA negative, and (6) no mortality associated with disease [34]. In this chapter, we show these established methods of LCNI and reactivation mouse models [33, 34].

2 Materials

2.1 LCNI Mouse Model Using Δ gcs1 Strain

1. Microorganism: A mutant strain of H99 (*C. neoformans* var. grubii, serotype A) lacking glucosylceramide synthase, designated Δ*gcs1* (*see* **Note 1**). Maintain a stock in 10% glycerol or 10% skim milk at −80 °C.
2. Fungal culture medium: yeast nitrogenous base (YNB) medium containing 2% glucose, pH 7.2 (*see* **Note 2**).
3. Physiological saline.
4. Mouse strain: CBA/J or C57BL/6 female or male mice aged 3–4 weeks (*see* **Note 3**).

5. Anesthetics: ketamine/xylazine mixture (*see* **Note 4**). Ketamine and xylazine are diluted with saline to 95 mg and 5 mg per kilogram of mouse body weight, respectively.

2.2 LCNI Mouse Model Using UgCl223 or UgCl552 Strains

1. Microorganism: Clinically isolated UgCl223 or UgCl552 strain (*C. neoformans* var. grubii, serotype A) (*see* **Note 1**). Maintain a stock in 10% glycerol or 10% skim milk at −80 °C.
2. Fungal culture medium: yeast peptone dextrose (YPD) broth (*see* **Note 2**).
3. Sterile 1× phosphate-buffered saline (PBS).
4. Mouse strain: C57BL/6 or A/J female or male mice aged 6–8 weeks (*see* **Note 3**).
5. Anesthetics: Pentobarbital is diluted with saline to 70 mg per kilogram of mouse body weight (*see* **Note 4**).

2.3 Cryptococcal Reactivation Mouse Model Using Δ gcs1 Strain

1. FTY720 (fingolimod; Cayman Chemical, MI, USA) (*see* **Note 5**): A stock solution is made by dissolving in organic solvents such as ethanol, DMSO, and dimethyl formamide, which should be purged with an inert gas. The solubility in these solvents is approximately 20 mg/mL. A stock solution is stored at −80 °C.

2.4 Cryptococcal Reactivation Mouse Model Using UgCl223 or UgCl552 Strains

1. Mouse strain: $CD4^{DTR}$ female or male mice aged 6–8 weeks [36] (*see* **Note 6**).
2. Diphtheria toxin.

2.5 Burden Analysis

Tissue burden analysis is performed by the general colony forming unit (CFU) counting method.

1. 1× PBS or distilled water.
2. YNB or YPD agar plate (*see* **Note 2**).
3. Stomacher 80 (Seward, United Kingdom) (*see* **Note 7**).

2.6 Histological Analysis

Tissue slides are prepared by standard methods and observed after hematoxylin and eosin (HE) staining (*see* **Note 8**). The required reagents are briefly described below.

1. 1× PBS.
2. 10% natural buffered formalin. The volume should exceed a 10:1 ratio of fixative to tissue.
3. Ethanol.
4. Xylene (or chloroform).
5. Paraffin.

6. Automatic tissue processor.
7. Microtome.
8. Hematoxylin.
9. Eosin.

3 Methods

3.1 Preparation of the Fungus

1. Grow 10^4 to 10^7 cells/mL *C. neoformans* Δ*gcs1*, UgCl223, or UgCl552 in 10 mL fungal culture medium for 16–18 h at 30 °C with or without 225 rpm before experiments (*see* **Notes 1** and **2**).
2. Collect and wash the yeast cells three times in physiological saline or sterile 1× PBS under centrifugal conditions at 1600–1800 × g for 5 min at 4 °C.
3. After the final wash, count the yeast cells on a hemocytometer after proper dilution and resuspend them at 2.5×10^6 cells/mL for Δ*gcs1* and 2×10^3 cells/mL for UgCl223 and UgCl552 in physiological saline or sterile 1× PBS.

3.2 Infection Procedure

1. Anesthetize the mice with an intraperitoneal injection of 60 Ml ketamine/xylazine mixture containing 95 mg ketamine and 5 mg xylazine per kilogram of body weight, respectively, or 70 mg pentobarbital per kilogram of body weight (*see* **Notes 3** and **4**). Ensure that the mice are fully anesthetized. (i.e., no longer respond to a toe pinch).
2. Infect the mice intranasally with 5×10^5 cells/20 μL of *C. neoformans* Δ*gcs1* or 1×10^2 cells in 50 μL of *C. neoformans* UgCl223 or UgCl552 (*see* **Note 9**). The method of infection is described in detail in Chapters 11 and 14. Briefly, the mouse ismanually held by gripping the neck skin using the thumb and forefinger, and the tail between the little finger and the palm. The mouse is held in a supine position with the head elevated. The end of the micropipette is placed at or in the external nares, and then the solution is poured in slowly.

3.3 Monitoring and Confirmation of LCNI

1. Feed and water the mice ad libitum and monitor them twice a day for discomfort and signs of disease. Endpoint criteria are defined as moribund appearance, significant weight loss (>20% of the vehicle-treated control), and/or obvious decrease in body temperature (<31 °C).
2. A few months after infection, check if the mice meet the criteria to define LCNI in the mouse model by the method described in Subheadings 3.3.1 and 3.3.2. Latent infection may also be confirmed using the serum cryptococcal antigen test (*see* **Note 10**).

3.3.1 Analysis of Fungal Burden

Tissue burden analysis is performed by the general CFU counting method.

1. Euthanize the mice at the appropriate time point. If you want to avoid blood contamination, perform blood removal or perfusion. Blood perfusion is performed by injecting 3 mL of cold physiological saline into the right ventricle (*see* **Note 11**).
2. Collect the organs in the appropriate amount of cold sterile 1× PBS or distilled water (e.g., 2–10 mL for the lungs and 1–2 mL for the brains). Option: By measuring the weight of collected organ, the fungal burden corrected by the tissue weight can be calculated. The calculated value per gram organ is useful for comparing fungal burden between tissues.
3. Homogenize the tissues using Stomacher 80 for 2 min at high speed (*see* **Note 7**). Option: By storing the supernatant of homogenate at −80 °C, it can be used for other analysis such as cytokine measurement.
4. Dilute the homogenized sample at multiple tenfolds with distilled water (dilution of approximately 10^1–10^6) and inoculate at 100 μL onto YPD agar plates (*see* **Note 2**). Determine the dilution ratio with reference to the Expected results section.
5. Culture the inoculated plates for 48–72 h at 30 °C.
6. Identify and count the plates containing 30–250 colonies.
7. Calculate the total number of CFUs per organ by adjusting for the final volume of the homogenate and the associated dilution factor.

3.3.2 Histological Analysis

Since HE-stained tissue slides are prepared by a general method, the preparation method is briefly described here.

1. Euthanize the mice at the appropriate time point.
2. Remove and thoroughly wash the lungs with 1× PBS.
3. Fixation: fix the lungs in 10 mL of 10% natural buffered formalin for 6–72 h as soon as possible after removal of the tissues. After fixation, gross the tissue if necessary.
4. Tissue processing: dehydrate, clear, and infiltrate the tissues with paraffin. These processes are almost always automated by an automatic tissue processor as follows:
   - 4.1. Dehydration: This is usually done with a series of alcohols, 70% to 95% to 100%. Sometimes the first step is a mixture of formalin and alcohol.
   - 4.2. Clearing: Remove the dehydrant with xylene that will be miscible with the paraffin.
   - 4.3. Infiltration with paraffin: Infiltrate the tissues with paraffin.

5. Embedding: Make the block of paraffin by pouring molten paraffin over the processed tissues.
6. Sectioning: Cut the embedded tissue into 3–10 μM sections using a microtome and place the sections on a slide.
7. Deparaffinizing: Deparaffinize the tissue slides by running them through xylenes to alcohols to water.
8. Stain the tissue slides by HE staining (*see* **Note 8**).
9. Observe the tissue slides under a light microscope.

3.4 Reactivation of LCNI

1. Treat the mice with a daily gavage administration of 1 mg FTY720 per kilogram of body weight during the LCNI phase (*see* **Note 10**). If you need vehicle-treated control mice, administer deionized water alone.

3.4.1 Cryptococcal Reactivation Mouse Model Using Δgcs1 Strain

3.4.2 Cryptococcal Reactivation Mouse Model Using UgCl223 or UgCl552 Strains

1. Treat the $CD4^{DTR}$ mice with an initial intraperitoneal injection of 1 μg diphtheria toxin and an additional 200 ng/100 mL diphtheria toxin every 4 days during the LCNI phase (*see* **Note 10**).

3.5 Expected Results

The criteria to define LCNI in the mouse model are as follows:

1. Stable fungal counts in the lungs. For the LCNI mouse model, confirm that the fungus can be detected in the lungs and the infection is controlled. For the cryptococcal reactivation mouse model, confirm that the fungal burden is increasing compared with control mice.
2. Generation of pulmonary granulomas and no alveolar inflammation in the surrounding lung parenchyma. For the LCNI mouse model, confirm that the granuloma containing the fungus can be detected in the lungs (Fig. 1A). Granulomas are mainly formed by fungal cells surrounded by macrophages, fibroblasts, and lymphocytes (Fig. 1a, c). Occasionally, multinucleated giant cells and phagocytosed fungi are observed in granulomas (Fig. 1b). If you want to observe these cells in more detail, other staining is effective (*see* **Note 8**). For the cryptococcal reactivation mouse model, confirm that granuloma disintegration can be detected. The mouse model using FTY720 showed a reversal in the layers of granuloma structure, as macrophages were found in a thick layer outside of the fibrotic ring of fibroblasts [33].
3. No clinical signs, no weight loss, and no mortality associated with disease.
4. With or without extrapulmonary dissemination.
5. Option: serum cryptococcal antigen negative.

Table 1 shows the summary of established LCNI mouse models.

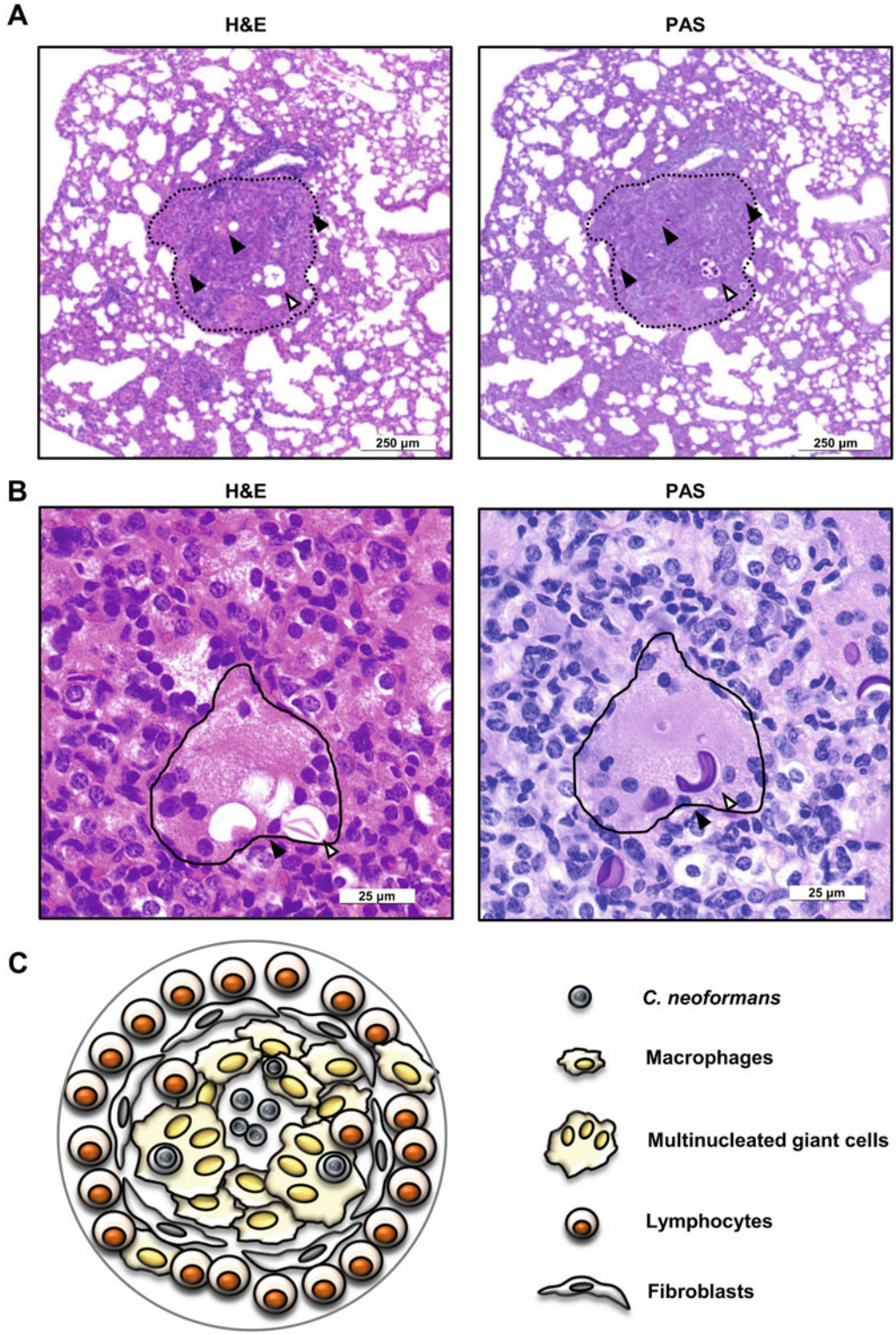

Fig. 1 Pulmonary histological findings after infection with *C. neoformans*. CnT-II mice were infected intratracheally with *C. neoformans* B3501 strain. Lung sections were stained with HE or PAS and observed under a light microscope. Original magnifications: ×40 (**a**) and ×400 (**b**). Black and white arrows show multinucleated giant cells and yeast cells, respectively. Dashed and solid line denotes the border of the granuloma and multinucleated giant cells, respectively. (**c**) Morphological image of granuloma against cryptococcal infection

Table 1
Established conditions and expected results for each LCNI mouse model

C. neoformans strain	Δgcs1	UgCl223	UgCl552	B3501
Mouse strain	CBA/J or C57BL/6	C57BL/6 or A/J	C57BL/6 or A/J	CnT-II
Number of infected fungi (cells/mouse)	5×10^5	1×10^2	1×10^2	1×10^6
Anesthetics	Ketamine/ xylazine	Pentobarbital	Pentobarbital	Midazolam/ Medetomidine/ Pentobarbital
Route of infection	i.n.	i.n.	i.n.	i.t.
Stable fungal count in the lung	Yes	Yes	Yes	Yes
Lung CFUs (CFUs/mouse)	$10^2 \sim 10^7$ (80 dpi)	$10^5 \sim 10^6$ (70 dpi)	$10^5 \sim 10^6$ (70 dpi)	$10^2 \sim 10^3$ (90 dpi)
Pulmonary granuloma	Yes	Yes	Yes	Yes
Predominantly normal lung parenchyma	Yes	Yes	Yes	Yes
Clinical signs	No	No	No	No
Weight loss	No	No	No	No
Mortality associated with disease	No	No	No	No
Survival period	>90 days	>70 days	>90 days	>90 days
Extrapulmonary dissemination	Yes	Yes	Yes	No
Serum cryptococcal antigen	ND	Low	ND	ND
Reactivation of LCNI	Yes	Yes	ND	ND
Mouse model	FTY720 treatment	$CD4^{DTR}$ mice	–	–
Lung CFU (CFU/mouse)	$10^6 \sim 10^8$	$10^7 \sim 10^9$	–	–
References	[33]	[34]	[34]	Unpublished data

i.n. intranasal, *i.t.* intratracheal, *dpi* days post infection, *ND* not done

4 Notes

1. In this chapter, we describe the published LCNI mouse models using *C. neoformans* Δ*gcs1*, UgCl223, and UgCl552 strains [33, 34]. These strains could be replaced with other suitable attenuated *C. neoformans* strains. If using a new strain, initial robust testing against the criteria to define LCNI might be necessary. Δ*gcs1* can grow at a neutral/alkaline pH in the

presence of atmospheric CO2 concentration, but not in the presence of 5% CO_2 [38].

2. Fungal culture medium could be replaced with another suitable medium such as Sabouraud dextrose agar or potato dextrose agar. If the medium is changed, the culture time might change.
3. The methods using CBA/J, A/J, and C57BL/6 mice are published as established LCNI mouse models. These mice could be replaced with other suitable mouse strains, although adaptations might be necessary.
4. Anesthetics could be replaced with another suitable anesthetic such as 0.3 mg/kg midazolam, 0.02 mg/kg medetomidine hydrochloride, or 15 mg/kg pentobarbital [30]. Avoid using kappa opioid receptor agonists such as butorphanol due to their anti-inflammatory effects [38].
5. An established cryptococcal reactivation mouse model by the administration of reagents has only been reported for FTY720. Risk factors for clinical cryptococcal infections are primarily acquired immune deficiency syndrome, diabetes mellitus, hematologic disease, collagen disease, and corticosteroid administration [39]. FTY720 could be replaced with another suitable compound such as steroid, which suppresses the immune response, or streptozotocin, which induces diabetes mellitus, although adaptations might be necessary.
6. CD8 off-target depletion was previously noted in $CD4^{DTR}$ mice. In addition to the method using $CD4^{DTR}$ mice, there is also a method using anti-CD4 monoclonal antibody as a method for depleting $CD4^+$ T cells [34]. However, only partial depletion might be achieved for $CD4^+$ T cells in the lungs.
7. Stomacher 80 could be replaced with another suitable homogenizer. If you do not have a homogenizer, you can use a stainless-steel mesh to tease the tissue.
8. In addition to HE staining, period acid–Schiff (PAS), mucicarmine, Verhoeff–Van Gieson (VVG), Elastica Masson (EM) staining, and immunostaining are suitable for histological analysis of this model. PAS and mucicarmine staining can stain the polysaccharides of the yeast cells, making it easier to observe the fungus. VVG and EM staining can stain the collagen and elastin deposited fibroblasts to observe the border of granulomas.
9. Intranasal (i.n.) infection could be replaced with intratracheal (i.t.) infection. i.n. infection is an easy way for the inoculum to be applied to the nares of the mouse and respired through the nasal passage into the lungs. However, the majority of the inoculum remains within the nasal passages or is removed through the gastrointestinal tract [40]. In

addition, this route of infection often results in high rates of infections of CNS in mice [40]. In contrast, although it is slightly complicated, i.t. infection has the advantages of being able to introduce a known quantity of sample directly into the lungs and to avoid potential CNS infection.

10. The latex agglutination test and lateral flow assay (LFA) are usually used for detection of serum cryptococcal antigen. Serodirect Cryptococcus (Eiken, Tokyo, Japan), Pastorex Crypto Plus (Bio-Rad, Marne-la-Coquette, France), and CrAg LFA (IMMY, Norman, OK, USA) are available on a commercial basis.
11. The procedure for blood perfusion is as follows: 1) open the mouse chest and expose the heart and lung. Take care not to injure the lung. 2) Perfuse the lung to remove blood by puncturing the right ventricle of the heart with a 26G needle connected to a 10 ml syringe contained 3 ml of cold physiological saline. Slowly inject the saline until the lung tissue becomes white.
12. FTY720 is also effective when administered to mice with drinking water containing FTY720. In this case, allow the mice to drink ad libitum fresh water with 10.5 μg/mL FTY720 daily.

Acknowledgments

This work was supported in part by a Grant-in-Aid for Scientific Research (B) (18H02851 and 21H02965) and Early-Career Scientists (19 K17920 and 21 K16314) from the Ministry of Education, Culture, Sports, Science and Technology of Japan; by the Strategic International Collaborative Research Program (SICORP), AMED (JP19jm0210073, JP20jm0210073, JP21jm0210073 and JP22jm0210073); and by the MSD Life Science Foundation, Public Interest Incorporated Foundation (ID-014).

References

1. Perfect JR, Casadevall A (2002) Cryptococcosis. Infect Dis Clin North Am 16:837–874, v–vi
2. Lim TS, Murphy JW (1980) Transfer of immunity to cryptococcosis by T-enriched splenic lymphocytes from *Cryptococcus neoformans*-sensitized mice. Infect Immun 30:5–11
3. Koguchi Y, Kawakami K (2002) Cryptococcal infection and Th1-Th2 cytokine balance. Int Rev Immunol 21:423–428
4. Sato K, Kawakami K (2017) Recognition of *Cryptococcus neoformans* by pattern recognition receptors and its role in host defense to this infection. Med Mycol J 58:J83–J90

5. Arora S, Olszewski MA, Tsang TM et al (2011) Effect of cytokine interplay on macrophage polarization during chronic pulmonary infection with *Cryptococcus neoformans*. Infect Immun 79:1915–1926
6. Tohyama M, Kawakami K, Futenma M et al (1996) Enhancing effect of oxygen radical scavengers on murine macrophage anticryptococcal activity through production of nitric oxide. Clin Exp Immunol 103:436–441
7. Hardison SE, Ravi S, Wozniak KL et al (2010) Pulmonary infection with an interferon-gamma-producing *Cryptococcus neoformans* strain results in classical macrophage activation and protection. Am J Pathol 176:774–785
8. Müller U, Stenzel W, Köhler G et al (2007) IL-13 induces disease-promoting type 2 cytokines, alternatively activated macrophages and allergic inflammation during pulmonary infection of mice with *Cryptococcus neoformans*. J Immunol 179:5367–5377
9. Zhang Y, Wang F, Tompkins KC et al (2009) Robust Th1 and Th17 immunity supports pulmonary clearance but cannot prevent systemic dissemination of highly virulent *Cryptococcus neoformans* H99. Am J Pathol 175:2489–2500
10. Murdock BJ, Huffnagle GB, Olszewski MA et al (2014) Interleukin-17A enhances host defense against cryptococcal lung infection through effects mediated by leukocyte recruitment, activation, and gamma interferon production. Infect Immun 82:937–948
11. Szymczak WA, Sellers RS, Pirofski L (2012) IL-23 dampens the allergic response to *Cryptococcus neoformans* through IL-17-independent and -dependent mechanisms. Am J Pathol 180: 1547–1559
12. Hardison SE, Wozniak KL, Kolls JK et al (2010) Interleukin-17 is not required for classical macrophage activation in a pulmonary mouse model of *Cryptococcus neoformans* infection. Infect Immun 78:5341–5351
13. Wozniak KL, Hole CR, Yano J et al (2014) Characterization of IL-22 and antimicrobial peptide production in mice protected against pulmonary *Cryptococcus neoformans* infection. Microbiology 160:1440–1452
14. Sato K, Yamamoto H, Nomura T et al (2020) Production of IL-17A at innate immune phase leads to decreased Th1 immune response and attenuated host defense against infection with *Cryptococcus deneoformans*. J Immunol 205: 686–698
15. Feldmesser M, Tucker S, Casadevall A (2001) Intracellular parasitism of macrophages by *Cryptococcus neoformans*. Trends Microbiol 9: 273–278
16. Goldman DL, Lee SC, Mednick AJ et al (2000) Persistent *Cryptococcus neoformans* pulmonary infection in the rat is associated with intracellular parasitism, decreased inducible nitric oxide synthase expression, and altered antibody responsiveness to cryptococcal polysaccharide. Infect Immun 68:832–838
17. Tucker SC, Casadevall A (2002) Replication of *Cryptococcus neoformans* in macrophages is accompanied by phagosomal permeabilization and accumulation of vesicles containing polysaccharide in the cytoplasm. Proc Natl Acad Sci USA 99:3165–3170
18. Levitz SM, Nong SH, Seetoo KF et al (1999) *Cryptococcus neoformans* resides in an acidic phagolysosome of human macrophages. Infect Immun 67:885–890
19. Zaragoza O, Chrisman CJ, Castelli MV et al (2008) Capsule enlargement in *Cryptococcus neoformans* confers resistance to oxidative stress suggesting a mechanism for intracellular survival. Cell Microbiol 10:2043–2057
20. Vecchiarelli A, Pericolini E, Gabrielli E et al (2013) Elucidating the immunological function of the *Cryptococcus neoformans* capsule. Future Microbiol 8:1107–1116
21. Alvarez M, Casadevall A (2006) Phagosome extrusion and host-cell survival after *Cryptococcus neoformans* phagocytosis by macrophages. Curr Biol 16:2161–2165
22. Okagaki LH, Nielsen K (2012) Titan cells confer protection from phagocytosis in *Cryptococcus neoformans* infections. Eukaryot Cell 11: 820–826
23. Goldman DL, Khine H, Abadi J et al (2001) Serologic evidence for *Cryptococcus neoformans* infection in early childhood. Pediatrics 107: E66
24. Saha DC, Goldman DL, Shao X et al (2007) Serologic evidence for reactivation of cryptococcosis in solid-organ transplant recipients. Clin Vaccine Immunol 14:1550–1554
25. Garcia-Hermoso D, Janbon G, Dromer F (1999) Epidemiological evidence for dormant *Cryptococcus neoformans* infection. J Clin Microbiol 37:3204–3209
26. Yamamoto H, Nakamura Y, Sato K et al (2014) Defect of CARD9 leads to impaired accumulation of gamma interferon-producing memory phenotype T cells in lungs and increased susceptibility to pulmonary infection with *Cryptococcus neoformans*. Infect Immun 82:1606–1615
27. Nakamura Y, Sato K, Yamamoto H et al (2015) Dectin-2 deficiency promotes Th2 response and mucin production in the lungs after

pulmonary infection with *Cryptococcus neoformans*. Infect Immun 83:671–681

28. Sato K, Yamamoto H, Nomura T et al (2015) *Cryptococcus neoformans* infection in mice lacking type I interferon signaling leads to increased fungal clearance and IL-4-dependent mucin production in the lungs. PLoS One 10: e0138291
29. Sato Y, Sato K, Yamamoto H et al (2020) Limited role of Mincle in the host defense against infection with *Cryptococcus deneoformans*. Infect Immun 88:e00400–e00420
30. Sato K, Matsumoto I, Suzuki K et al (2021) Deficiency of lung-specific claudin-18 leads to aggravated infection with *Cryptococcus deneoformans* through dysregulation of the microenvironment in lungs. Sci Rep 11:21110
31. Kitai Y, Sato K, Tanno D et al (2021) Role of Dectin-2 in the phagocytosis of *Cryptococcus neoformans* by dendritic cells. Infect Immun 89:e00330–e00321
32. Lindell DM, Ballinger MN, McDonald RA et al (2006) Immunologic homeostasis during infection: coexistence of strong pulmonary cell-mediated immunity to secondary *Cryptococcus neoformans* infection while the primary infection still persists at low levels in the lungs. J Immunol 177:4652–4661
33. Bryan AM, You JK, McQuiston T et al (2020) FTY720 reactivates cryptococcal granulomas in mice through S1P receptor 3 on macrophages. J Clin Invest 130:4546–4560
34. Ding M, Smith KD, Wiesner DL et al (2022) Use of clinical isolates to establish criteria for a mouse model of latent *Cryptococcus neoformans* infection. Front Cell Infect Microbiol 11: 804059
35. Normile TG, Bryan AM, Del Poeta M (2020) Animal models of *Cryptococcus neoformans* in identifying immune parameters associated with primary infection and reactivation of latent infection. Front Immunol 11:2197
36. Buch T, Heppner FL, Tertilt C et al (2005) A Cre-inducible diphtheria toxin receptor mediates cell lineage ablation after toxin administration. Nat Methods 2:419–426
37. Rittershaus CP, Kechichian BT, Allegood CJ et al (2006) Glucosylceramide synthase is an essential regulator of pathogenicity of Cryptococcus neoformans. J Clin Invest 116:1651–1659
38. Luan G, Pan F, Bu L et al (2021) Butorphanol promotes macrophage phenotypic transition to inhibit inflammatory lung injury via κ receptors. Front Immunol 12:692286
39. Kohno S, Kakeya H, Izumikawa K et al (2015) Clinical features of pulmonary cryptococcosis in non-HIV patients in Japan. J Infect Chemother 21:23–30
40. Revelli AD, Boylan AJ, Gherardini CF (2012) A non-invasive intratracheal inoculation method for the study of pulmonary melioidosis. Front Cell Infect Microbiol 2:164

Chapter 7

Adoptive Transfer of *Cryptococcus neoformans*-Specific CD4 T-Cells to Study Anti-fungal Lymphocyte Responses In Vivo

Man Shun Fu, Kazuyoshi Kawakami, and Rebecca A. Drummond

Abstract

CD4 T-cells are important for long-term control and clearance of several fungal infections in humans, particularly those caused by *Cryptococcus* species. Understanding the mechanisms underlying protective T-cell immunity against fungal infection is critical for developing mechanistic insights into the pathogenesis of the disease. Here, we describe a protocol that enables analysis of fungal-specific CD4 T-cell responses in vivo, using adoptive transfer of fungal-specific T-cell receptor (TCR) transgenic CD4 T-cells. While the protocol here uses a TCR transgenic model reactive to peptide deriving from *Cryptococcus neoformans*, this method could be adapted to other fungal infection experimental settings.

Key words Adoptive transfer, TCR transgenic T-cell, CD4 T-cell, *Cryptococcus neoformans*

1 Introduction

Invasive fungal infections are systemic, life-threatening infections with excessive morbidity and mortality in immunocompromised patients and responsible for around 1.5 million deaths each year [1]. Although the first line of defense against fungal infection is innate immunity, the coordination between innate and adaptive immune systems is required to successfully eliminate the fungal pathogens and promote long-lived immunological memory [2]. Protective antifungal adaptive immunity involves CD4 T-cells that generate IFNγ and/or IL-17 to give best protection from invasive fungal infection because these cytokines promote effective killing by innate effector cells. However, adaptive immunity against fungi is only partially understood. In particular, most studies to date have focused on global T-cell responses and have not analyzed the fungal-specific population due to a lack of appropriate tools within the medical mycology field.

Rebecca A. Drummond (ed.), *Antifungal Immunity: Methods and Protocols*, Methods in Molecular Biology, vol. 2667,
https://doi.org/10.1007/978-1-0716-3199-7_7,

In this protocol, we describe the use of T-cell receptor (TCR) transgenic T-cells that specifically react to cryptococcal antigen to describe how adoptive transfer of antigen-specific T-cells can be applied to study the antifungal T-cell response [3]. Adoptive transfer is a method where T-cells of interest from a transgenic donor animal are injected into study animals (recipient) to increase the frequency of antigen-specific T-cells and track their function and/or behavior during infection or antigen challenge. T-cell receptor (TCR)-transgenic T-cells uniformly express a TCR specific for a known antigen. Adoptive transfer of TCR-transgenic T-cells is a powerful system for monitoring the response and fate of antigen-specific T-cells in vivo including their proliferation, activation, differentiation, and cytokine production. One of the benefits of doing the adoptive transfer is the possibility to study the impact of recipient genetic background on T-cell responses by adoptive transfer into mice with specific gene deficiency.

Recent research by the Kawakami group led to the generation of a TCR transgenic mouse (CnT. II) that is reactive to *C. neoformans* chitin deactylase 2 (Cda2), the major antigen-stimulating anti-cryptococcal CD4 T-cell responses [3]. By using CnT. II mice, the group showed that IL-17 is able to suppress protective Th1 differentiation of *C. neoformans*-specific CD4 T-cells in the lung. Other fungal-specific TCR transgenic mice have been generated to enable in vivo study of fungal-specific CD4 T-cell activation and differentiation. For example, the Pamer group generated *Aspergillus*-specific CD4 TCR transgenic mice and used these to demonstrate that activation of *A. fumigatus*-specific T-cells is dependent on MyD88- and TLR-meditated signaling during respiratory *Aspergillus* infection [4]. *Candida*-specific TCR transgenic mice have been used to investigate the roles of different subsets of dendritic cells on antigen presentation and Th17 priming in the infected oral mucosa [5]. If TCR transgenic models specific for particular fungal antigens are unavailable, TCR transgenic T-cells against model antigens can be used with engineered fungi which express these antigens. For example, *C. albicans* strain Calb-Ag expresses ovalbumin and I-Eα peptides, which have enabled the use of transgenic OT. I/II and TEα TCR transgenic adoptive transfer models [6, 7].

The first step for adoptive transfer is to obtain lymphoid organs (e.g., lymph nodes (LNs) and spleens) from transgenic donor mice (Fig. 1). LNs and spleens are selected because they have higher frequency of CD4 T-cells and are easier starting material for cell isolations compared to other organs. Next, isolation of CD4 T-cells from cell suspension of LNs and spleens is performed by magnetic cell separation. Once purified CD4 T-cells are obtained, it can be transferred to congenic recipients followed by fungal infection. After the fungal infection, those fungal-specific CD4 T-cells can then be identified by congenic markers and multiple functional parameters analyzed using flow cytometry.

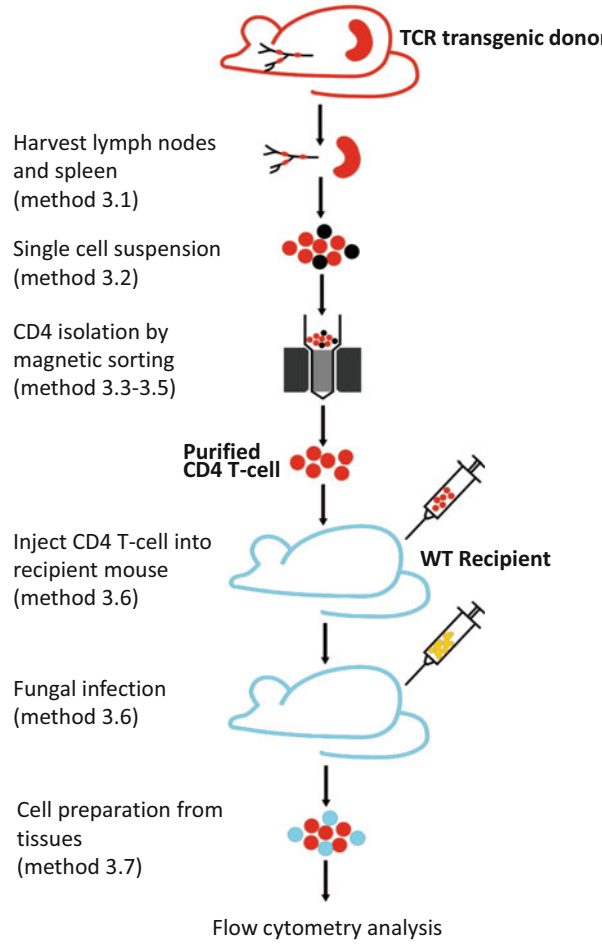

Fig. 1 Overview of experimental steps. First, lymphoid organs such as lymph nodes and spleen are isolated from donor mice with TCR-transgenic CD4 T-cells. Single cell suspension is then prepared from the tissues. After that, CD4 T-cells are isolated from cell suspensions using magnetic cell separation method. Purified CD4 T-cells from donor are then injected into WT recipient mice. At least 1 day after, recipients can be infected with fungi, and the responses of fungal-specific CD4 T-cells (e.g., cell proliferation or cell activation) from desired organs can be analyzed by flow cytometry

2 Materials

2.1 Animals

1. Donor mice (*see* **Notes 1** and **2**).
2. Recipient mice (*see* **Notes 1** and **2**).

2.2 Tissue Preparation (see Note 3)

1. 70% ethanol.
2. 2 mM EDTA in PBS. Store at room temperature.
3. Complete RPMI: RPMI supplemented with 10% FBS, 1% penicillin-streptomycin.
4. Digest buffer: RPMI supplemented with 10% FBS, 1% penicillin-streptomycin, 1 mg/mL collagenase, 1 mg/mL dispase, and 40 μg/mL DNAse. Use fresh or store aliquots at −20 °C.
5. Red blood cell lysing solution (BD Pharm Lyse): Prepare 1× solution according to manufacturer's instructions. Store at 4 °C.
6. FACS buffer: PBS supplemented with 1% BSA and 2 mM EDTA. Store at 4 °C.
7. 100% Percoll (1.130 g/mL density): 9 parts of Percoll from the bottle and 1 part of 10× PBS. Adding PBS is to create an isotonic Percoll solution.
8. 70% Percoll: 7 parts of 100% Percoll (see above) with 3 parts of 1× PBS.
9. Dissection instruments including forceps and scissors.
10. 25G needles (for perfusion) and 21G needles (for preparation of lung).
11. 1 mL syringe (for mashing LNs and spleens) and 20 mL syringe (for mashing brain).
12. 40 μM, 70 μM, and 100 μM strainers.

2.3 CD4 Isolation

1. CD4+ T-cell Isolation Kit, mouse (we recommend and use the MACS Miltenyi Kit).
2. LS column (MACS Miltenyi).
3. MACS Separator (MACS Miltenyi).
4. Separation buffer: 0.5% bovine serum albumin (BSA) and 2 mM EDTA in PBS pH 7.2.
5. Trypan blue solution for cell counting.
6. Hemocytometer.
7. CFSE (or similar) proliferation dye (*see* **Note 4**).
8. PBS supplemented with 10% BSA.

2.4 Infection

1. Animal restrainer for intravenous injections.
2. Heat lamp.
3. 25G needles and 1 mL syringe.
4. Fungal inoculum.

3 Methods

3.1 Isolation of Lymph Nodes and Spleens from Donor Mice

The lymphoid organs which have high frequency of CD4 T-cells are harvested from donor mice. In order to keep the organs sterilized, all the procedures are performed in a tissue culture hood. Mice dissection tools and incision area are sterilized with 70% ethanol. Organs should be kept on ice or refrigerated at all times.

1. Humanely euthanize donor animals using procedures approved in the animal license and by the institutional ethic committee.
2. Turn the mouse to ventral side and stabilize their limbs with pins to the dissection board. Spray 70% ethanol on the fur of mouse.
3. Cut the skin with scissors from urethral opening up to chin area. Avoid cutting into the lining of the peritoneal wall.
4. Pull back the skin and pin it on the dissection broad to allow access lymph nodes.
5. Remove all major lymph nodes (LNs; inguinal, auxiliary, brachial, mesenteric, and cervical) and spleens.
   (a) Remove two inguinal lymph nodes at the conjunction of the three blood vessels under the skin near the hip region.
   (b) Remove two brachial lymph nodes at the connective tissues near axilla.
   (c) Remove two axillary lymph nodes behind the pectoral muscles near axilla.
   (d) Remove six cervical lymph nodes at the neck.
   (e) For dissection of the mesenteric LN (mLN), cut open the lining of the peritoneal wall and take out the intestines. A string of 4–8 nodes can be found at the connective tissue that holds the intestines together.
   (f) Remove the spleen behind the stomach and intestines.
6. Pool all the LNs together and place them in 10 mL ice-cold RPMI. Pool and store spleens in same way but keep separate from LNs.

3.2 Preparation of Single Cell Suspension from Donor Lymphoid Organs

All the following procedures are performed in a tissue culture hood. Cells are kept on ice/cold wherever possible.

1. Place LNs onto a 70 μM filter sitting in a well of 6-well plate. Using the end of a plunger from a sterile syringe, gently smash the organs through the filter. Wash the filter with 5 mL complete RPMI. Discard filter.
2. Repeat **step 1** with spleens using a fresh filter.

3. Place a clean 40 μM filter over a 50 mL centrifuge tube. Pass the cell suspensions through the filter. Place the suspension on ice.
4. Centrifuge suspensions at 400 × g for 5 min at 4 °C.
5. For LNs, discard supernatants and resuspend cell pellet in 5–10 mL complete RPMI.
6. For spleen, treat with lysing solution (BD Pharm Lyse) to lyse red blood cells.
   (a) Add 1 mL of 1× lysing solution.
   (b) Gently shake immediately after adding the lysing solution.
   (c) Incubate at room temperature for 2 min.
   (d) Add 5 mL of 2 mM EDTA/PBS.
   (e) Centrifuge suspensions at 400 × g for 5 min at 4 °C.
   (f) Discard supernatants and resuspend cell pellet in 5–10 mL complete RPMI.
   (g) Pass suspensions through a 70 μM filter.
7. Count cells in 1:20 dilution using trypan blue exclusion and a hemocytometer.
8. Centrifuge suspensions at 400 × g for 5 min at 4 °C.

3.3 CD4 T-cell Isolation

CD4 T-cells are isolated from single cell suspension using magnetic-based separation method with a cocktail of biotin-conjugated antibodies against non-CD4 T-cells, anti-biotin magnetic beads, and magnet. The magnetically labeled non-CD4 T-cells are depleted by retaining them on column in the magnetic field while unlabeled CD4 T-cells pass through the column.

1. Resuspend cell pellet in 40 μL of separation buffer per 10×10^6 cells.
2. Add 10 μL of Biotin-Antibody Cocktail per 10×10^6 cells.
3. Mix well and incubate for 5 min at 4 °C.
4. Add 30 μL of buffer per 10×10^6 cells.
5. Add 20 μL of Anti-Biotin MicroBeads per 10×10^6 cells.
6. Mix well and incubate for 10 min at 4 °C.
7. Place LS column in the magnetic field of a suitable MACS Separator.
8. Prepare column by rinsing with 3 mL of buffer.
9. Apply cell suspension onto the column. Collect flow through containing unlabeled cells, representing the enriched CD4 T-cells.
10. Wash column with 3 mL of buffer. Collect unlabeled cells that pass through, representing the enriched CD4 T-cells, and combine with the effluent from **step 9**.

11. Count cells in 1:20 dilution using trypan blue exclusion and a hemocytometer (*see* **Note 5**).
12. If both LNs and spleen suspensions have purified well, combine both suspensions and centrifuge suspensions at 400 × g for 5 min at 4 °C.
13. Wash the cells twice in PBS using twice the volume of your suspension.
14. Resuspend the cells at 10–50 × 10^6 cells/mL in PBS.

3.4 Proliferation Dye Staining

Purified cells can be stained with a proliferation dye (e.g., CFSE) prior to the cell transfer for analyzing their cell division in recipient animal. We have provided the protocol for CFSE here, but other dyes may be used (e.g., CellTrace).

1. Add equal volume of PBS containing 10 μM CFSE or other proliferation dyes and leave cells on rotation at room temperature for 5–8 min.
2. Immediately add the equal volume of 1× PBS/10% FCS to quench the reaction.
3. Leave to rest for 1 min at room temperature.
4. Centrifuge the cells at 400 × g for 5 min at 4 °C.
5. Wash cells twice in 1×PBS/10% FCS to quench reaction and remove unreacted proliferation dye.
6. Following washing, resuspend cells in 1–2 mL PBS.
7. Count cells in 1:20 dilution using trypan blue exclusion and a hemocytometer.
8. Adjust the concentration of cells to 5 × 10^7 cells/mL in PBS.

3.5 Check of the Purity of CD4 T-Cells and the Staining of Proliferation Dye

1. Take 2 μL of the purified cells and add to a FACS tube. Add 200 μL PBS.
2. For control, add 5 μL of unlabeled, impurified suspension. Add 200 μL PBS.
3. Add 1 μL fluorophore-conjugated CD4 antibody to each tube.
4. Acquire samples on a multicolor flow cytometer.
5. Use unlabeled cells to set the gating for excluding out the cell debris in the plot of FSC and SSC.
6. Set a gate over CD4+ and positive for proliferation dye.
7. Acquire a few thousand events for each sample.
8. Determine approximate percentage (*see* **Note 6**).

3.6 Transfer and Infection

1. Warm the cells to room temperature.
2. Inject 100 μL of cells (5×10^6 cells) to each recipient mice intraperitoneally using a large gauge needle (minimum 25G).
3. Place the animal back into its cage and monitor for any complications for 5–10 min after the injection.
4. Infect mice with fungal species of interest approximately 24 h after adoptive transfer according to infection route and dose needed for the experiment (*see* **Note 7**).

3.7 Tissue Preparation: Analysis

At the chosen time point for analysis, recipient animals are euthanized and organs of interest are processed to analyze the transferred T-cells by flow cytometry. Here we give protocols to isolate leukocytes from lung and brain. Leukocytes can be isolated from spleen and LNs using protocol outlined in Subheadings 3.1 and 3.2.

3.7.1 Digestion and Preparation of Brain

1. Humanely euthanize donor animals using procedures approved in the animal license and your institutions' ethics committee.
2. Perfuse animal with PBS to remove peripheral blood. Open up the abdomen of the animal and cut the iliac blood vessel at the right. Cut the diaphragm cut open to expose the chest walls. Open thorax by a midline incision to expose the heart. Inject 5 mL PBS into heart using 25G needle slowly.
3. To remove the brain, spray head of animal with 70% ethanol and cut scalp away to expose the skull. Cut the head off by steady the head with forceps on griping the animal snout and cut where the spine joins. Cut the skull opened along the longitudinal fissure and between the eyes. Expose the brain by gently peeling the skull. Place the brain by using forceps into 1 mL PBS on ice.
4. Place the brain with PBS onto a sterile petri dish. Use the end of a 20 mL syringe plunger (the flat plastic end) to gently mash the brain into a paste.
5. Transfer the brain paste to a 15 mL centrifuge tube containing 6 mL FACS buffer (cut the end of a 1 mL tip to make it easier to pipette up the brain paste).
6. Add 3 mL of 100% Percoll to the brain suspension. Gently invert the tube 2–3 times to mix (the brain suspension is now in 30% Percoll).
7. Underlay the 30% Percoll/brain solution with 1.5 mL 70% Percoll using transfer pipette.
   (a) Pipette 2 mL of 70% Percoll with a transfer pipette and drop it to the bottom of the centrifuge tube. Gently

release the 70% Percoll. Two layers with top 30% Percoll/brain suspension and bottom clear 70% Percoll can be seen. Continue until the clear 70% Percoll reaches the 1.5 mL mark.

8. Centrifuge the Percoll gradients at 1100 × g for 30 min, at 4 °C with the brake off.
9. After centrifugation is completed, remove the cells (as white band) at the 70/30 interphase with a transfer pipette by sucking from top to bottom within the interphase and add to 5 mL FACS buffer in 15 mL tube.
10. Centrifuge the tubes at 400 × g for 5 min, at 4 °C.
11. Remove supernatants and resuspend cells in 200 μl PBS.
12. Pass the samples through a 100 μM cell strainer to FACS tubes for staining.

3.7.2 Digestion and Preparation of Lung

1. Euthanize animals and perfuse as above.
2. Surgically remove all the lobes of lung from the chest using forceps and scissors.
3. Mince the lobes with scalpel.
4. Place minced lobes in 4 mL digest buffer in 15 mL tube. Mix by shaking the tube.
5. Incubate the samples at 37 °C with continues shaking or shaking every 10 min for 30–60 min until there are no more large chunks of tissue remaining.
6. Pour the sample to a 20 mL syringe with needle and pass the sample through the 21G needle.
7. Pass the samples through a 100 μM cell strainer to 50 mL centrifuge tube.
8. Wash the cell strainer with 4 mL FACS buffer.
9. Centrifuge at 400 × g for 5 min at 4 °C.
10. Discard supernatant.
11. Add 1 mL of 1× BD Pharm Lyse.
12. Mix by invert the tubes several times.
13. Incubate RT for 2 min.
14. Add 5 mL of 2 mM EDTA in PBS.
15. Centrifuge the sample at 400 × g for 5 min at 4 °C.
16. Wash 5 mL PBS.
17. Centrifuge the sample at 400 × g for 5 min at 4 °C.
18. Remove supernatant and resuspend cells in 200 μL PBS.
19. Pass the samples through a 100 μM cell strainer to FACS tubes for staining.

3.8 Flow Cytometry Analysis

1. Add live/dead viability dye to each sample. Incubate and stain as per manufacturer's instructions.
2. Perform blockade of Fc receptors using anti-mouse CD16/32 (Fc-Block) in FACS buffer. Add Fc-Block to a final concentration of 5 μg/mL to samples and incubate for 15 min on ice.
3. Make up a fluorophore-conjugated antibody cocktail containing anti-CD45, anti-CD45.1 or anti-CD45.2 (congenic marker to identify donor cells), anti-CD4, anti-CD44 and/or anti-CD69 (activation makers), anti-CD62L, and anti CD127 (memory cell markers to identify naïve, effector, and memory T-cell subsets). Intracellular staining for cytokines and transcription factors can be additionally completed if information on T-cell differentiation and functional phenotype is required.
4. Add antibody cocktail to your samples and incubate for 15 min to 2 h on ice.
5. Wash samples by adding 1 mL FACS buffer to each sample and centrifuging at 400 × g for 5 min at 4 °C.
6. Acquire samples on a multicolor flow cytometer.
7. Gate out the cell debris, doublets and CD45- cells (*see* **Note 2**, Figs. 2 and 3).

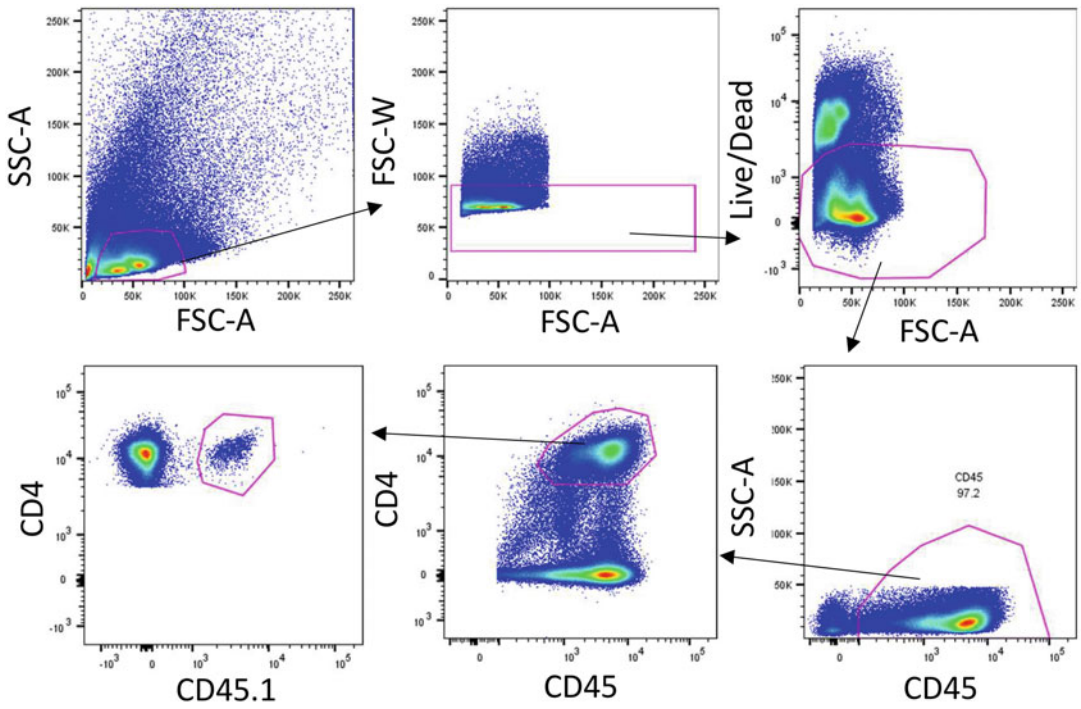

Fig. 2 Gating strategy for fungal specific CD4 T-cells from donor. Example shown is a spleen from a *Cryptococcus neoformans* infected WT animal transferred with 5×10^6 CnT. II T-cells at day 7 post-IV infection

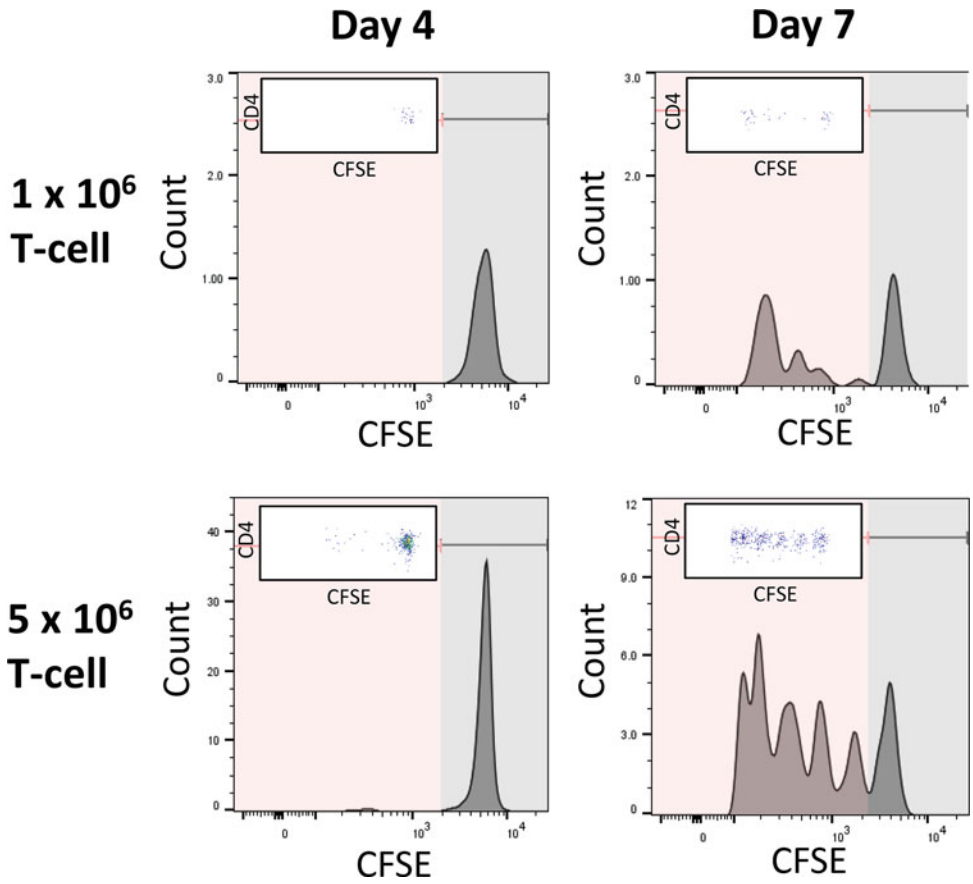

Fig. 3 Results of a test on transferring different doses of CD4 T-cells at 4- and 7-days post-IV infection. Plots shown are the proliferation of the fungal specific CD4 T-cells (follow gating strategy in Fig. 2). The discrete peaks represent successive generations (indicated in pink area). The undivided cell populations are indicated in grey area

4 Notes

1. *Donor and recipient animals.* This experiment requires animals that act as "donors" and "recipients." It is best to use only one sex and matched genetic background to avoid potential problems caused by immune reactivity. However, in order to distinguish the adoptive transferred cells from those of the recipients, congenic mice should be used. For example, CD45.1 and CD45.2 C57BL/6, which obtain allelic variants of the pan-hematopoietic cell marker CD45, are commonly used for adoptive transfer (and used in this protocol). The variant of donor mouse line can be checked by staining with CD45.1 or CD45.2 antibody, then recipients with opposing marker but same genetic background can be used.

2. *Optimal number of T-cell for adoptive transfer.* The numbers of donors used are based on the numbers of recipients used in the experiment. One donor normally will provide approximately 30–60 × 10^6 CD4 T-cells. In this protocol, the number of T-cell for transferring to the recipient mice is 5 × 10^6 cells in a volume of 100 μL. Therefore, one donor should be enough for injecting T-cells into four to eight recipients. Transferring lower numbers of donor T-cells may be tried. However, we have tested that injection of 1 × 10^6 T-cells might be too low to give enough tested T-cell for further analysis (at least during systemic cryptococcal infection model) while injection of 5 × 10^6 T-cells gives a better resolution (Fig. 3). Therefore, testing the dose of T-cell for adoptive transfer is important for each new infection model and experimental time point that is to be tested.
3. *Maintaining high yields of donor T-cells.* To have a high yield of T-cell for adoptive transfer, maintaining the viability of the cells is crucial. Storage conditions and chemical or biological treatments can affect the cell viability. Organs and cells should be stored on ice or refrigerator all the time. Single cell preparation should be prepared as soon as the lymphoid organs are isolated from mice. High speed centrifugation should be avoided. Incubating the sample with red blood cell lysing solution should not be longer than 5 min on ice or 2 min at room temperature. Otherwise, the lysing solution may have negative impact on other cells and affect their viability.
4. *Proliferation dye staining.* Staining cell with proliferation dye can be performed depending on research aim to monitor in vivo T-cell division. However, most of the proliferation dyes are toxic, so the incubation time and concentration have to be carefully titrated. For example, the timing of the CFSE staining should be 5–8 min, and the concentration of CFSE should not be above 10 μM. Extended incubation periods and/or exceeding the recommended maximum concentration of the dye will inhibit the proliferation or reduce viability. However, low concentration of proliferation dyes will give lower resolution because of the low signal-to-noise ratio. Therefore, we recommend to test the optimal concentration with specific flow cytometer setup. In addition to the points mentioned above, the fluorescent proliferation dyes are light sensitive, so the samples should be kept in dark during and after staining.
5. *Expected T-cell number isolated from spleen and LN.* Approximately 100 × 10^6 cells should be expected from spleen (per animal) and 50–100 × 10^6 cells should be expected from LNs (per animal), depending on age/sex. In general, 20–30 × 10^6 CD4 T-cells can be isolated from 100 × 10^6 lymphocytes. The

frequency of CD4 T-cells is normally much higher in the LNs than it is in the spleen, so it is better to try and obtain majority of your CD4 T-cells from LN suspension and supplement with those from spleen. Therefore, it is recommended to purify CD4 T-cells from the suspensions of LNs and spleen separately and pool them together following the isolation.

6. *Magnetic cell separation*. Sorting out the CD4 T-cells can be done by other techniques e.g. fluorescence-activated cell sorting (FACS), but its high-pressure flow could induce cellular stress and affect cell viability, and this method is generally more expensive and time-consuming. The method of magnetic cell separation is less time-consuming and also yields pure population of viable cells.

   There are two main strategies of magnetic cell separation: positive and negative cell selection. Negative selection is the strategy we used in this protocol, while positive selection can be achieved by labeling the desired cells directly with magnetic bead conjugated antibodies. We suggest negative selection for this protocol because the binding of cell surface antigen could potentially cause unwanted intracellular signaling and thus could change cell behavior.

   We describe the method using the separation kits available from Miltenyi, but other kits are also available. In all cases, trouble-shooting may be required to optimize the kit used to gain the maximum number of CD4 T-cells from donor tissues.

   The percentage of CD4+ cells should be around 20–30% before isolation, while it should be around 85–95% after isolation.

7. *Infection*. Infection dose, infection routes, and time points are depended on the fungal strains, desired endpoint, and observation. Pilot experimentation is recommended. Infection doses can be adjusted for the virulence of the strains. High infection dose may cause rapid death of mice while adaptive immune response may not be activated at the early stage of infection, but low-dose inoculum may be easily cleared by innate immune response. Infection routes are considered according to the routes of transmission in human, surgery requirement, and the desired experimental outcomes. Three common routes are intratracheal, intranasal, and intravenous infection. Intratracheal infection involves anesthesia so intranasal infection is a popular alternative procedure. Intravenous route allows rapid dissemination of the infectious fungi to the brain by bypassing the lung immune response, so it is well accepted route for studying brain immune response during *C. neoformans* infection. In overall, intravenous infection tends to give higher fungal burdens and antigen levels, whereas intranasal infection will concentrate antigen into the lung. Time points for tissue

harvest are affected by infection doses and infection routes. For studying adaptive immune response, mice will be better to harvest in the later stage of the infection. In our example, few CD4 T-cells undergo cell proliferation at day 4, but this increases by day 7 (Fig. 3).

References

1. Bongomin F et al (2017) Global and multinational prevalence of fungal diseases-estimate precision. J Fungi (Basel) 3(4)
2. Lionakis MS, Iliev ID, Hohl TM (2017) Immunity against fungi. JCI Insight 2:11
3. Sato K et al (2020) Production of IL-17A at innate immune phase leads to decreased Th1 immune response and attenuated host defense against infection with Cryptococcus deneoformans. J Immunol 205(3):686–698
4. Rivera A et al (2006) Innate immune activation and CD4+ T cell priming during respiratory fungal infection. Immunity 25(4):665–675
5. Trautwein-Weidner K et al (2015) Antigen-specific Th17 cells are primed by distinct and complementary dendritic cell subsets in oropharyngeal candidiasis. PLoS Pathog 11(10): e1005164
6. Drummond RA et al (2014) Cutting edge: failure of antigen-specific CD4+ T cell recruitment to the kidney during systemic candidiasis. J Immunol 193(11):5381–5385
7. Igyarto BZ et al (2011) Skin-resident murine dendritic cell subsets promote distinct and opposing antigen-specific T helper cell responses. Immunity 35(2):260–272

Chapter 8

Meningeal Whole Mounts for Imaging CNS Fungal Infection

Sofia Hain and Rebecca A. Drummond

Abstract

Invasive fungal infections may involve the brain and central nervous system (CNS), leading to often fatal meningitis in immunocompromised individuals. Recent technological advances have allowed us to move beyond studying the brain parenchyma to understanding the immune mechanisms of the meninges, the protective layer that surrounds the brain and spinal cord. Specifically, advanced microscopy techniques have enabled researchers to begin to visualize the anatomy of the meninges and the cellular mediators of meningeal inflammation. In this chapter, we describe how to make meningeal tissue mounts for imaging by confocal microscopy.

Key words Meninges, Microscopy, Fungi, Cryptococcus, Immunofluorescence, Neuroimmunology

1 Introduction

Imaging is a powerful tool for understanding neuroimmune mechanisms. This has been explored in disease models such as EAE and Alzheimer's; however, there are less data for fungal infections. Invasive fungal infections that result in meningitis include those caused by *Cryptococcus*, *Candida*, and *Histoplasma* species. Cryptococcal meningitis is the most predominant, causing over 100,000 deaths per year [1]. As fungal meningitis mostly affects immunocompromised individuals, the increased use of immunosuppressive therapies is partly driving the rising incidence of this disease [2]. While there are antifungals available, it is important that we understand the inflammatory response as this is thought to drive the disease morbidity and mortality.

Despite their anatomical relevance, the meninges are less well studied than the brain parenchyma in the context of fungal meningitis. The meninges are the protective outer layer that covers the brain and spinal cord. The cerebral meninges are composed of three layers: the pia mater, the subarachnoid space, and the dura mater [3, 4] (Fig. 1). The dura is the outermost layer of the meninges closest to the skull. This complex layer of connective tissue is highly

Rebecca A. Drummond (ed.), *Antifungal Immunity: Methods and Protocols*, Methods in Molecular Biology, vol. 2667,
https://doi.org/10.1007/978-1-0716-3199-7_8,

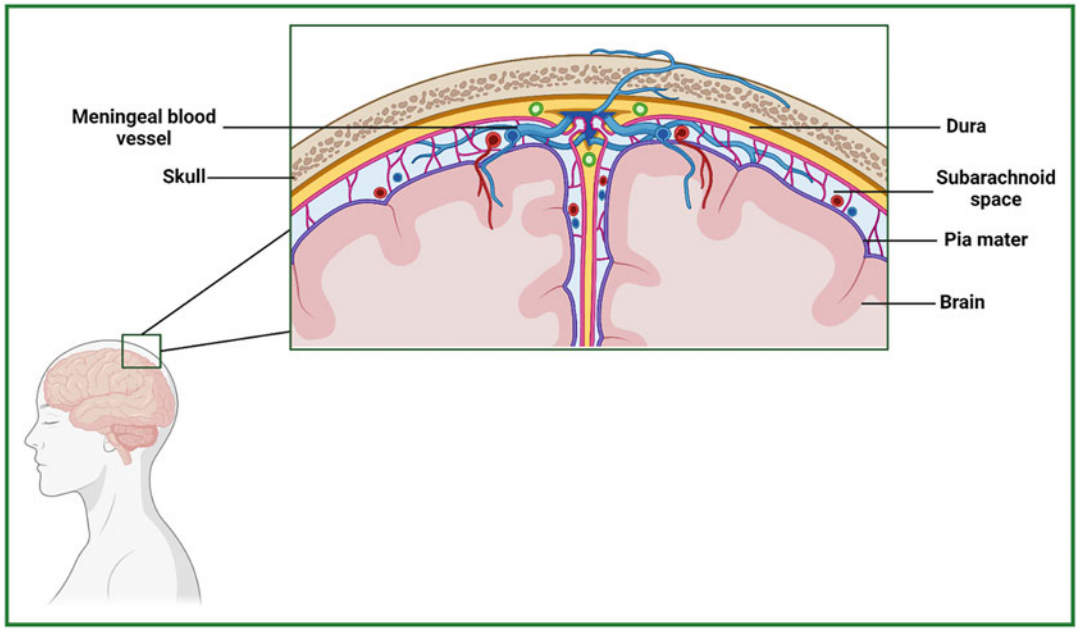

Fig. 1 Anatomy of the cerebral meninges. The cerebral meninges are the protective tissue that sits between the brain and the skull. The meninges are composed of three layers: the outer dural layer, the subarachnoid space, and the innermost layer, the pia matter. The meninges are a complex tissue containing nerves, blood vessels, CSF and lymphatic vessels

vascularized and innervated and contains the meningeal lymphatic vessels [3–5]. The dura has more recently been shown to have channels that allow bi-directional flow of cerebrospinal fluid (CSF) from the subarachnoid space into the skull bone marrow [6]. The subarachnoid space is the middle layer of the meninges through which the CSF flows, while the pia is the thin innermost layer closely associated with the brain surface [4]. The pia contains a dense network of blood vessels that go down into the brain parenchyma, enabling circulation from the meninges into the brain and vice versa [3, 4]. The meninges are therefore a highly specialized tissue that can be thought of as the immune highway of the CNS. The exact anatomy of the meninges is however not fully agreed upon; thus, further research may reveal additional complexities.

While the arguments for studying the anti-fungal immune mechanisms of the meninges are clear, the complexities of working with this delicate tissue in the lab have likely impeded research in this area. In recent years, however, the field has begun to take off, enabled by the development and increased availability of advanced imaging tools. In this protocol, we outline a method for creating meninges whole mounts for immunofluorescence analysis of anti-fungal immunity in vivo.

2 Materials

2.1 Dissection

1. Tissue collection buffer: 2% paraformaldehyde (PFA). In a 15 mL Falcon tube, prepare the desired volume of buffer by diluting 4% PFA by half using sterile 1× PBS (*see* **Note 1**). 5 mL of this solution can be aliquoted into a 15 mL Falcon tube for each sample to be collected. Store at 4 °C.
2. 70% ethanol: prepare a 70% ethanol solution using ethanol absolute and dH_2O.
3. Dissection kit: This should include sharp scissors, curved forceps, fine forceps, and ultra-fine forceps (watchmaker forceps).
4. Mouse cadavers (*see* **Note 2**).
5. Wash buffer: PBS plus 10 mM EDTA (*see* **Note 1**). Store at 4 °C.
6. 90 mM Petri dishes.

2.2 Immunostaining

1. Blocking buffer: 10% FCS (fetal calf serum) and 1% BSA (Bovine Serum Albumin) in 1× PBS. For example, if making up 100 mL, add 10 mL of FCS to 90 mL of PBS, then dissolve 1 g of BSA in this solution (*see* **Note 3**). Store at 4 °C.
2. Primary antibodies: Purchase anti-mouse antibodies for the antigen(s) of interest. These can be conjugated or unconjugated (*see* **Note 4**). For the latter, secondary antibodies will be needed to bind the primary antibody and produce the fluorescent signal.
3. Nuclear stain, for example, DAPI (*optional*).
4. 1× PBS, nonsterile.
5. 24-well flat bottom cell culture plates.
6. SuperFrost™ microscopy slides, 26 × 17 mM.
7. 50 mM coverslips.
8. Mountant: ProLongGold™ Anti-fade mountant or similar that will allow long-term storage at −20 °C.
9. Kimwipes™ or similar tissues that won't leave residue.
10. Aluminum foil.
11. Microscope slide storage box.

3 Methods

When working with meninges, it is very important to remember to treat it carefully so as not to damage or disturb the tissue, which could lead to difficulty in interpreting results.

3.1 Tissue Collection

1. Place 5 mL aliquots of the tissue collection buffer on ice.
2. Sacrifice mice at the appropriate endpoint (*see* **Notes 5** and **6**).
3. Disinfect the mouse head with 70% ethanol prior to making an incision in the skin above the middle of the skull. Pull the skin and ears forward so the entire top of the skull and the back of the cranium are exposed. Use scissors to cut through the top of the spine, releasing the back of the skull. The skull should then be cut on either side of the head at the level of the ear sockets. Using curved forceps, hold the nose of the mouse and cut the front of the skull at the base of the frontal bone. The calvaria (skull cap) should then be removed, leaving the brain and the base of the skull/jaw behind.
4. The skull cap should be briefly cleaned up using the dissection tools to remove any remaining scalp, hair, etc., and then placed in tissue collection medium on ice.

3.2 Dissecting the Meninges

1. Once the tissue has been in the tissue collection buffer for approximately 1 h (*see* **Note 7**), the skull cap should be placed in ice-cold wash buffer for 2 × 5 min to remove any fixative.
2. Place the skull cap in a receptacle (e.g., a Petri dish) containing enough ice-cold wash buffer/PBS to cover the skull cap. Orientate the skull cap so that the inside of the skull is facing up.
3. To remove the meninges from the skull (*see* **Note 8**), trim the around the entire edge of the skull cap using sharp dissection scissors; this will enable the edges of the meninges to be released from the skull.
4. The skull cap can be held in place using fine forceps, and ultrafine forceps used to peel the meninges. The large blood vessels of the meninges, the dural venous sinuses, form a clear "Y" shape which can be used as a guide for removing the meninges (Fig. 2). Begin detaching the meninges at the base of the frontal bone where the olfactory bulb would be located by lifting the bottom of the superior sagittal sinus (see Fig. 3). Next, detach the ends of the transverse sinus from the left and right edge of the skull, and the outer edge of the smaller middle meningeal arteries. Use these as a starting point to slide the forceps around the edge of the skull to gently detach the entire outer edge of the meninges, pushing the tissue towards the middle of the skull. Once the outer edge of the meninges has been detached from the skull cap, use the ultrafine forceps to peel the meninges upwards from the frontal bone towards the back of the skull, removing the entire intact tissue (*see* **Note 9**).
5. Place the tissue in the well of a 24-well plate containing 500 μL of wash buffer, allowing the tissue to flatten (*see* **Note 10**).

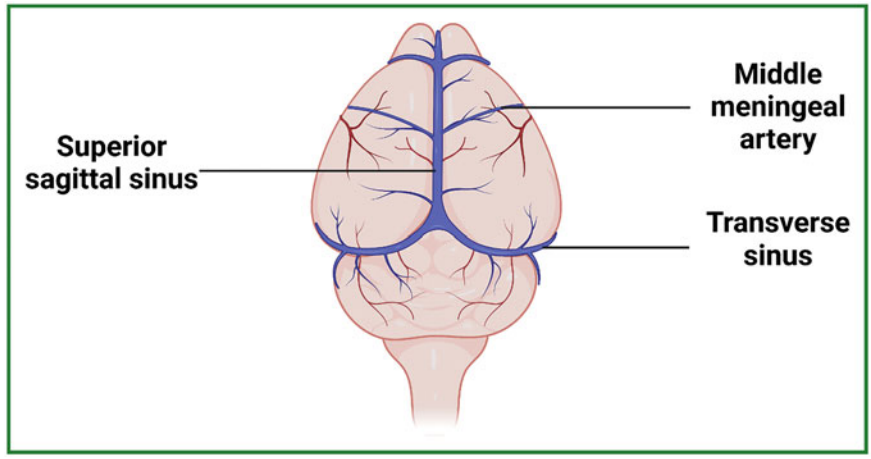

Fig. 2 Meningeal vasculature. The major blood vessels of the meninges and where they sit relative to the brain are illustrated. The dural venous sinuses are composed of the superior sagittal sinus that is positioned between the brain hemispheres, and the transverse sinuses which are positioned at the back of the brain. The middle meningeal artery is also shown, which is the largest artery in the meninges and can be seen clearly in meningeal whole mounts

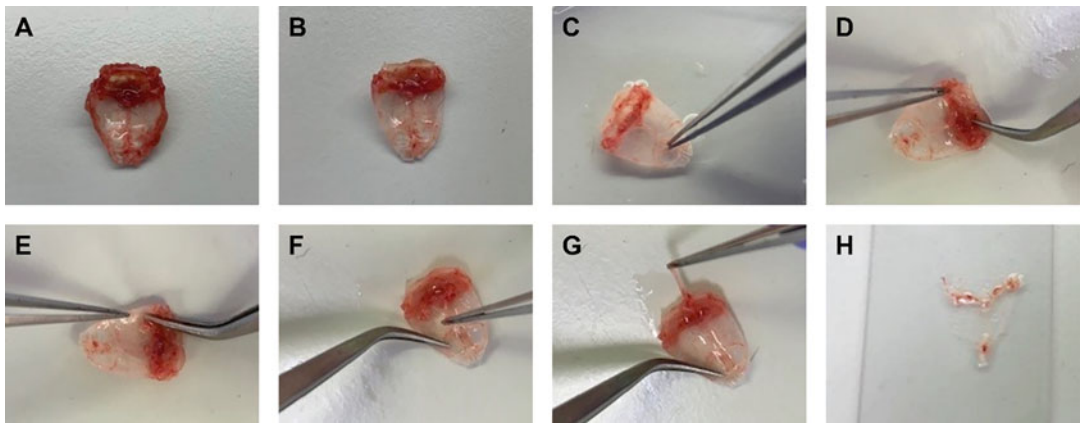

Fig. 3 Dissection of the meninges from the skull cap. (**a**) The skull cap of a mouse. (**b**) The skull cap after trimming the outer edge. (**c**) The meninges are first detached at the base of the superior sagittal sinus. (**d**) The fleshy outer ends of the transverse sinuses are next detached. (**e**) The ultrafine forceps can then be slid under the entire outer edge of the meninges. (**f**) To peel the meninges, we begin where we started by holding the end of the superior sagittal sinus and pulling it towards the back of the skull. (**g**) As the meninges is peeled it will roll up. The final step is to gently detach it from the very back of the skull. (**h**) The meninges can then be flattened on a slide

3.3 Immunostaining

1. Primary antibodies should be diluted to the desired concentration in blocking buffer. A minimum volume of 300 μL should be used in a 24-well plate (*see* **Note 11**). Place the meninges in the antibody staining solution and stain overnight in the dark (by covering the plate with foil) at 4 °C (*see* **Note 12**).

2. Wash the samples in ice cold wash buffer × 3 for 5 min (*see* **Note 13**).
3. If required, incubate with secondary antibodies for 45 min–1 h at room temperature (RT) (*see* **Note 4**), before repeating the washing step.
4. If using nuclear staining such as DAPI, this can then be performed in PBS for 5 min at RT, then washed × 2 for 5 min.

3.4 Mounting

1. Gently lift the meninges from the well and place on a SuperFrost slide. Pipette up to 200 μL of PBS onto the tissue.
2. Use the ultrafine forceps to guide the tissue so it is flattened on the slide, using the dural venous sinuses as a guide. Remove excess the liquid using a tissue (*see* **Note 14**).
3. Apply mounting medium to the slide before placing the cover slip over the sample. Cure if required (*see* **Note 15**) then the meningeal whole mount is ready for imaging via fluorescence/confocal microscopy. Alternatively, slides can be stored in a slide box at −20 °C (*see* **Note 16**).

4 Notes

1. As the meninges is a delicate tissue, the use of strong fixatives is not recommended. If the cell population of interest includes red blood cells (RBCs) such as platelets, add 10 mM EDTA to the tissue collection buffer to prevent activation of these cells by the buffer itself. Adding EDTA to any of the buffers used in this protocol will also keep the tissue samples sterile. Alternatively, the meninges can be collected into PBS for immunostaining without prior fixation. This is required if fixation interferes with antibody epitope binding (*see* **Note 12**). If RBCs are not of interest, perfusion can be performed using 2% PFA or PBS, again dependent on if fixation prior to immunostaining is appropriate. The removal of blood through perfusion will ensure RBCs to not interfere with staining for other cells; however, it is important to consider that once blood is removed from the meninges it can reduce the visibility of the dural venous sinuses which are a helpful guide for dissection.
2. For fungal infections, the appropriate conditions for the fungal species should be used, along with uninfected controls.
3. The exact recipe for the blocking buffer will depend on the species of antibodies being used. Here we have given a generic recipe; however, the addition of donkey or goat serum will proudly protect against nonspecific binding. Mouse on mouse staining should be avoided to prevent background

fluorescence. However, if required then it is recommended that the tissue is incubated in blocking buffer for 30 minutes prior to staining and that the blocking buffer contains both mouse serum and a CD16/32 Fc block.

4. We find conjugated antibodies give a stronger signal than nonconjugated antibodies. They also work best for short protocol required for live staining (*see* **Note 12**), so if nonconjugated antibodies are essential, it is recommended that the tissue is fixed first.
5. As mentioned in **Note 2**, appropriate experimental conditions should be used, including a humane endpoint. A severe CNS fungal infection can result in brain swelling and/or bleeding, which may affect the structural integrity of the meninges; thus, dissection should be performed with extreme care.
6. Similar to collecting brain tissue, when sacrificing mice to collect meninges, the method of culling used needs to be carefully considered in order to avoid damaging the skull and CNS tissue. However, it is also important to ensure that the tissue is not allowed to completely die due to the time required for the culling process. We therefore recommend anesthesia or cervical dislocation.
7. Fixation helps to stiffen the meninges, thus making it easier to peel from the skull cap. As previously mentioned, gentle fixation is required, so there needs to be a balance between ensuring the tissue is stiffened, ensuring the tissue is fixed properly to analyze the cells of interest, and not damaging the tissue. We find 1 h is sufficient to meet these criteria. If not fixing the tissue prior to immunostaining, skip this step. Please note that this will make the meninges more difficult to peel; however, an experienced user with ultrasharp forceps should be able to do so successfully.
8. There are protocols available for meninges whole mounts that recommend using the skull cap as a "well" for antibody staining and to remove the meninges from the skull just prior to mounting. However, this can result in uneven staining due to the curvature of the skull. We have found that peeling as early as possible in the protocol helps to ensure the meninges are intact, the staining is even, and that they can be flattened properly when mounted.
9. Due to how fragile the meninges are, there is risk of ripping and holes forming in tissue during the peeling process. To mitigate this, confirm the tissue is lifted all around the edge of the skull to ensure a clean peel. This will require practice, yet even experienced users may experience ripping of the tissue. It is therefore important to carefully consider the n numbers for each experiment. Nevertheless, depending on the area of interest, the meninges may not need to be entirely intact.

10. As the meninges is removed from the skull, it will roll up. Once in contact with the wash buffer in the well (or the tissue can first be placed in the liquid in the petri dish being used for dissection), the tissue should unroll. Forceps can be used to help this process if necessary but take care not to damage the tissue.
11. For the tissue to remain flat and not dry out during staining, a minimum volume of 300 μL is required. This must be balanced with the volume of antibody required, as they are often expensive. While a smaller plate would require a lower volume, it would not allow enough space for the flattened meninges to fit; therefore, a 24-well plate is the smallest size that can be used.
12. If fixation prior to immunostaining will alter antibody epitopes resulting in unsuccessful antibody binding, the meninges tissue must be live for staining. After collecting and carefully peeling the tissue (*see* **Note 7**), place in the blocking buffer containing the diluted antibodies for 1 h at RT in the dark. Unless otherwise stated (*see* **Note 3**), a blocking step before immunostaining should not be required. Wash the sample before fixing overnight at 4 °C in fixation buffer.
13. A plate rocker is the recommended instrument for gently agitating the tissue during the washing steps.
14. Removal of the meninges from the well plate will result in it rolling up. When placed on the slide, applying a small volume of PBS onto the tissue will encourage the tissue to re-flatten. Use the ultrafine forceps very carefully to complete the flattening process, removing some of the PBS, if necessary, as a smaller volume can make spreading the tissue out. As the tissue has already been allowed to flatten out in the well, it should be easier to flatten again on the slide. Once the tissue is as desired, remove the excess PBS using a tissue. This is important as excess PBS on the tissue can cause it to roll up once the coverslip is applied. This must be done carefully to ensure the meninges is not disturbed; the slide can be briefly left in the dark at RT to assist in drying excess liquid.
15. Follow the manufacturer's instructions to determine if curing is required for the mounting media to set. For example, it is recommended that ProLong Gold Antifade mountant is cured overnight at RT, which we have found works well and does not result in any reduction in fluorescence signal. A small amount of clear nail polish can be applied around the edge of the coverslip for extra security.
16. Slides can be stored long term at −20 °C. When removing slides from the freezer for imaging, allow 30 min for defrosting.

References

1. Rajasingham R, Meya DB, Boulware DR, Rajasingham R, Govender NP, Jordan A, Loyse A, Shroufi A, Denning DW, Meya DB et al (2022) The global burden of HIV-associated cryptococcal infection in adults in 2020: a modelling analysis. Lancet Infect Dis. https://doi.org/10.1016/S1473-3099(22)00499-6
2. Clark C, Drummond R (2019) The hidden cost of modern medical interventions: how medical advances have shaped the prevalence of human fungal disease. Pathogens 8:45. https://doi.org/10.3390/pathogens8020045
3. Derk J, Jones HE, Como C, Pawlikowski B, Siegenthaler JA (2021) Living on the edge of the CNS: meninges cell diversity in health and disease. Front Cell Neurosci 15:245. https://doi.org/10.3389/FNCEL.2021.703944/BIBTEX
4. Coles JA, Myburgh E, Brewer JM, McMenamin PG (2017) Where are we? The anatomy of the murine cortical meninges revisited for intravital imaging, immunology, and clearance of waste from the brain. Prog Neurobiol 156:107–148. https://doi.org/10.1016/J.PNEUROBIO.2017.05.002
5. das Neves SP, Delivanoglou N, Da Mesquita S (2021) CNS-draining meningeal lymphatic vasculature: roles, conundrums and future challenges. Front Pharmacol 12:964. https://doi.org/10.3389/FPHAR.2021.655052/BIBTEX
6. Lin CP, Moskowitz MA, Nahrendorf M. Cerebrospinal fluid can exit into the skull bone marrow and instruct cranial hematopoiesis in mice with bacterial meningitis. https://doi.org/10.1038/s41593-022-01060-2

Chapter 9

An Antibiotic-Free Model of *Candida albicans* Colonization of the Murine Gastrointestinal Tract

Simon Vautier

Abstract

The human gastrointestinal (GI) tract is home to trillions of commensal organisms. Some of these microbes have the capacity to become pathogenic following changes in the microenvironment and/or host physiology. *Candida albicans* is one such organism, usually inhabiting the GI tract as a harmless commensal in most individuals but with the potential to cause serious infection. Risk factors for *C. albicans* GI infections include the use of antibiotics, neutropenia, and abdominal surgery. Understanding how commensal organisms can transform into life-threatening pathogens is an important area of research. Mouse models of fungal GI colonization provide an essential platform to study the mechanisms involved in the transition of *C. albicans* from benign commensal to dangerous pathogen. This chapter presents a novel method of stable, long-term colonization of the murine GI tract with *Candida albicans.*

Key words *Candida albicans*, Colonization, Gastrointestinal tract, Antibiotic-free, Fructose

1 Introduction

The mammalian gastrointestinal (GI) tract is colonized by a diverse microbiota predominantly consisting of bacteria but with notable contributions from fungi and other eukaryotic organisms. The myriad interactions between the host and microbiota result in the microbiota performing a significant role in shaping host physiology, including immune responses. In humans, *Candida albicans* is a common commensal of the GI tract, where carriage is typically asymptomatic in healthy humans. However, antibiotic use and host immunosuppression can lead to otherwise harmless commensal fungi breaching mucosal barriers and disseminating, causing systemic infections [1].

Mouse models used to study *C. albicans* in the GI tract are hindered by *C. albicans* inability to colonize the adult murine GI

Rebecca A. Drummond (ed.), *Antifungal Immunity: Methods and Protocols*, Methods in Molecular Biology, vol. 2667,
https://doi.org/10.1007/978-1-0716-3199-7_9,

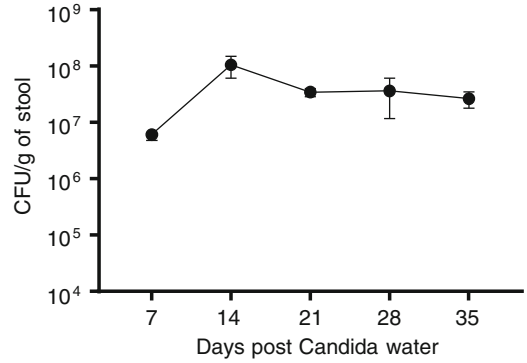

Fig. 1 Fructose supplemented drinking water enables murine gastrointestinal colonization. Stool fungal burdens are shown for C57 BL/6 mice (n = 5) following oral colonization with *C. albicans* SC5314. Bars represent mean values with SD

tract without continual antibiotic treatment [2, 3]. Although antibiotics facilitate the colonization of the murine GI tract, antibiotic usage disrupts the normal microbiota and impacts the host immune response allowing dissemination of gut bacteria [4, 5].

Here, we demonstrate an antibiotic-free model to establish long-term and stable colonization of the murine GI tract efficiently by *C. albicans*. We utilize fructose in the drinking water to facilitate *C. albicans* colonization. With this protocol, colonization levels in the region of ~10^7 CFU/g stool are possible (Fig. 1), which is similar in level to previously published models utilizing antibiotics to enable colonization [2, 3].

2 Materials

2.1 Preparation of Fructose Water

1. Sterile drinking water: Autoclave your usual facility water for 15 min at 121 °C. One liter will provide sufficient water for four average Individually Ventilated Cages (IVCs) water bottles with 5 mice per cage.
2. Fructose water: To make 1 liter of 15% Fructose water add 150 mL of high fructose corn syrup to 850 mL of autoclaved water (*see* **Notes 1** and **2**).

2.2 Growth of Candida albicans

1. YPD broth: Suspend 50 g/L of YPD broth powder in water (composition Bacteriological peptone, 20 g/L Glucose, 20 g/L Yeast extract, 10 g/L). Autoclave for 15 min at 121 °C.
2. YPD agar plates: Dissolve 70 g/L of YPD agar powder in water (composition agar 20 g/L, dextrose 20 g/L, bacteriological peptone 20 g/L, yeast extract 10 g/L). Autoclave for 15 min at

121 °C. Allow to cool until comfortable to handle, then add 10 ml/L Penicillin-Streptomycin (10,000 U/mL) and mix. Add 20–25 mL to individual petri dishes (**Note 3**). Store in fridge.

2.3 Stool Collection and Processing

1. Autoclaved water: Autoclave 500 mL of water for 15 min at 121 °C.

3 Methods

3.1 Candida albicans *Culture*

1. From your frozen stock of *Candida albicans*, streak out colonies onto an agar plate and incubate at 30 °C overnight.
2. The next day, select a colony and inoculate into ~20 mL YPD broth (*see* **Note 4**).
3. Incubate overnight at 30 °C with shaking.
4. The next day, centrifuge the overnight culture for 4 min at 400 g.
5. Pour off supernatant and resuspend in 10 mL of sterile media (either water or 1×PBS).
6. Count yeast cells using a hemocytometer.
7. Adjust your culture to 1×10^7 CFU/mL in 15% Fructose water (*see* **Note 5**).

3.2 Candida albicans *Colonization*

1. Provide mice with 15% fructose water supplemented with 1×10^7 CFU/mL *Candida albicans* for 5 days. Each IVC cage will require approximately 250 mL of water.
2. Gently shake each bottle every day to maintain the *Candida* in suspension.
3. Maintain the mice on 15% fructose water supplemented with *Candida* for 5 days.
4. Replace Candida water with water with 15% fructose water only (no *Candida*).
5. Change the water twice a week to maintain a fresh water supply.

3.3 Monitoring of Candida albicans *Colonization Levels*

1. Label and weigh an individual 1.5 mL Eppendorf tube containing 1 mL of sterile water for each mouse stool is to be collected from.
2. Collect stool from individual mice prior to exposure to *Candida* water to ensure mice are culture free from fungi (*see* **Note 6**). Using sterile tweezers place 1–2 stools in the appropriate Eppendorf tube and re-weigh tube. Store tube on ice while collecting other stool samples.

3. Vortex vigorously to homogenize sample (*see* **Note 7**). If the sample is resistant to homogenization, you can use a sterile pipette tip to manually break up the stool before continuing to vortex.
4. Using a multichannel pipette add 180 μL of sterile water to each well of a 96-well plate.
5. Add 20 μL of stool sample to the first column of the 96-well plate.
6. Mix well and transfer 20 μL to the well in the next column and repeat. Four serial dilutions should be sufficient to enable colony counting.
7. After completing serial dilutions, remove 20 μL from each well and spot on to an agar plate (*see* **Note 8**).
8. Incubate overnight at 37 °C and count the colony forming units (CFU). Use the dilution that allows you to count in the range 1–10 CFU (*see* **Notes 9** and **10**).

4 Notes

1. Adding corn syrup while the water is still warm aids dissolution.
2. Mice will readily drink fructose water so you may need to prepare top-up/change water bottles more regularly than the usual twice a week. Mice on sugar water initially put on more weight than mice on plain drinking water (around 10% heavier), but this evens out after 7–8 weeks.
3. Placing bottle in water will cool agar quicker. Be careful to mix regularly to prevent setting of agar at the bottom of the bottle. Cool until bottle can be handled comfortably ~50 °C. Pour quickly to prevent heat inactivation of the antibiotics. Place plates individually on a bench/flow cabinet to allow quick cooling.
4. If you find one colony is insufficient after overnight culture to produce enough yeast cells, scrape off more colonies for your next culture. You may also want to culture more than one 50 mL Falcon tube depending on volume of culture required. If you are not experienced in culturing *Candida*, you may wish to practice culturing sufficient volume ahead of your experiment.
5. If culturing more than 1 × 50 mL falcon tube for use in more than one cage, be sure to mix *Candida* from separate cultures first before distributing to individual drinking bottles. This will enable *Candida* to be evenly distributed between bottles and avoid cages receiving different concentrations of *Candida* in the drinking water.

6. In our experience, mice produce more stool in the morning than the afternoon so this is best performed first thing in the morning. Do not collect stool from the cage floor as you will not know how long it has been there and will not be able to account for *Candida* growth/death post excretion.
7. If available, you can use a bead-beater with appropriate tubes. This is a labor-saving option but not strictly necessary as stools will break up easily with the use of a pipette tip.
8. Take plates out of the fridge a day or two before use to allow the surface to dry a little. If plates are too wet when used the spots will run. With practice you should be able to plate 4 rows of 4 × 20 μL spots per agar plate.
9. Culturing at 37° will cause the *Candida albicans* to form hyphae which will result in colonies with a crinkled appearance. This can aid in the confirmation of the cultured colonies being *Candida albicans.*
10. The use of a GFP-expressing (or other fluorescent protein) strain can aid in the visualization of *Candida albicans* for microscopy.

References

1. Alonso-Monge R, Gresnigt MS, Roman E, Hube B, Pla J (2021) Candida albicans colonization of the gastrointestinal tract: a double-edged sword. PLoS Pathog 17(7):e1009710. https://doi.org/10.1371/journal.ppat.1009710
2. Koh AY, Kohler JR, Coggshall KT, Van Rooijen N, Pier GB (2008) Mucosal damage and neutropenia are required for Candida albicans dissemination. PLoS Pathog 4:e35. https://doi.org/10.1371/journal.ppat.0040035
3. Vautier S, Drummond RA, Redelinghuys P, Murray GI, MacCallum DM, Brown GD (2012) Dectin-1 is not required for controlling Candida albicans colonization of the gastrointestinal tract. Infect Immun 80:4216–4222
4. Goto Y, Panea C, Nakato G, Cebula A, Lee C, Diez MG, Laufer TM, Ignatowicz L, Ivanov II (2014) Segmented filamentous bacteria antigens presented by intestinal dendritic cells drive mucosal Th17 cell differentiation. Immunity 40(4):10.1016/j.immuni.2014.03.005
5. Drummond RA, Desai JV, Ricotta EE, Swamydas M, Deming C, Conlan S, Quinones M, Matei-Rascu V, Sherif L, Lecky D, Lee CC, Green NM, Collins N, Zelazny A, Prevots R, Bending D, Withers D, Belkaid Y, Segre J, Lionakis M (2022) Long-term antibiotic exposure promotes mortality after systemic fungal infection by driving lymphocyte dysfunction and systemic escape of commensal bacteria. Cell Host Microbe. https://doi.org/10.1016/j.chom.2022.04.013

Chapter 10

An Experimental Model of Chromoblastomycosis Caused by *Fonsecaea* sp. Species

Anamelia L. Bocca and Isaque Medeiros Siqueira

Abstract

The experimental rodent models for the fungal disease are a handy tool for understanding host–fungus interactions. To *Fonsecaea* sp., one of the causative agents of chromoblastomycosis, there is an extra challenge because the animals preferably used show a spontaneous cure; so until now, there is no model to reproduce the long-term disease similar to human chronic disease. In this chapter, we described an experimental model using rats and mice with a subcutaneous route, with the checkpoints of acute-like and chronic-like lesion analysis comparable with human lesions, the fungal burden, and the lymphocytes investigation.

Key words *Fonsecaea* sp., Chromoblastomycosis, Murine model, Fungal burden, Granuloma

1 Introduction

The genus of human pathogenic black fungi *Fonsecaea* sp. is considered the most common agent of chromoblastomycosis (CBM), a chronic cutaneous and subcutaneous mycosis. Even though CBM occurs worldwide, it is observed most frequently in tropical and subtropical regions of Africa and Latin America [1]. CBM infection initiates with the traumatic implantation of propagules into the skin by thorns [1, 2]. The disease is characterized by the slow development of polymorphic skin lesions, such as nodules, warts, tumors, plaques, and scars [3]. The treatment is challenging due to long-term antifungal chemotherapy and surgical treatment to remove the infected tissue [2, 4].

Although *Fonsecaea* sp. is classified as dimorphic, its life cycle includes distinct morphological stages comprising the conidia, hypha (infective forms), and sclerotic cells (pathogenic form, also called muriform cells) [5–9].

Rebecca A. Drummond (ed.), *Antifungal Immunity: Methods and Protocols*, Methods in Molecular Biology, vol. 2667,
https://doi.org/10.1007/978-1-0716-3199-7_10,

In the host tissue, *Fonsecaea* sp. infective forms convert to sclerotic cells or muriform cells (MC), which are more resistant to phagocytosis and destruction by immunological action, associated with the persistence inside the mammalian host and development of chronic disease [3, 7, 10, 11]. Transition into sclerotic cells is essential in fungal virulence [11]; however, this process is not understood.

The granulomatous reaction in CBM is associated with macrophages, different degrees of maturation and activation, and high levels of neutrophils [12]. The phagocytes destroy fungal cells by producing reactive oxygen intermediates (ROI) and myeloperoxidase production. Activated macrophages have shown only fungicidal activity against *F. pedrosoi*, and there is evidence that some fungal structures, such as melanin, may negatively modulate certain microbicidal activities in macrophages [13].

The *Fonsecaea* sp. virulence and pathogenicity are not well understood and consequently, the host immune response, in part by the absence of an experimental model *in vivo* that perfectly mimics the disease's chronic phase [5, 14, 15]. The development of animal models is a challenge because all animals tested showed a "nonprogressive" disease, with granuloma inflammatory reaction, with abscesses and viable fungi into the lesion, but with spontaneous cure after a specific postinfection time [16]. The development of the experimental disease changes according to the inoculation route, as the intratesticular and subcutaneous route produce localized lesions with granuloma and MC cells; nevertheless, the intraperitoneal inoculation does not develop the same lesions. The murine model shows a 30-day spontaneous cure of the disease, while the model using rats shows a more prolonged disease; the lesion outcome is also a spontaneous cure [17–19]. The authors used the athymic mice to increase the time of infections, which showed a systemic disease or a very long-term lesion (around 90 days postinfection) in the footpad [20, 21]. However, the nude model is unsuitable for studying the cellular host immune response. Considering these limitations of a progressive and chronic experimental CBM, it is possible to carry out experiments for defined points like acute or chronic inflammatory reactions to study immune cell infiltrations, cytokine production, and fungal burden.

In this chapter, we described an experimental model using the subcutaneous route to mimic the skin lesion of CBM.

2 Materials

2.1 Preparation of Fungal Solution

1. Human pathogenic *Fonsecaea* sp.
2. Sabouraud Dextrose Agar.
3. Chloramphenicol.
4. Potato Dextrose Medium (PD).

5. Sterile fiberglass.
6. 40 μM cell strainers.
7. 70 μM cell strainers.
8. Phosphate-buffered saline (PBS).
9. 14 μM filter paper.
10. DL-propranolol.
11. Chemically defined medium.
12. Rotary shaker with temperature control.
13. 0.1% (w/v) yeast extract solution.

2.2 Suspension of Infection

1. *Trypan blue dye.*
2. Hemocytometer.
3. Phosphate-buffered saline (PBS).
4. 15 mL conic tubes.
5. 200–1000 μL pipettes.
6. 20–200 μL pipettes.

2.3 Animals and Experimental Design

1. Wistar rats (*Rattus norvegicus albinus)*, 7–9 weeks old.
2. 1 mL syringes.
3. C57BL/6 or Balb/c mice, 6–8 weeks old.

2.4 Morphometry

1. Sterically surgical material, such as scissors and tweezers (one per group).
2. Caliper.
3. Petri dishes.
4. Phosphate-buffered saline (PBS).

2.5 Fungal Burden

1. Phosphate-buffered saline (PBS).
2. Sabouraud Dextrose Agar.
3. Chloramphenicol.
4. Petri dishes (90 × 15 mM).
5. Stove at 37 °C.

2.6 Histopathology

1. Buffered formalin 10% solution.
2. Paraffin.
3. Hematoxylin solution.
4. Eosin solution.
5. Lamina.
6. Coverslip.
7. Alcohol (absolute, 95% and 80%).
8. Xylol.

2.7 Lymphocytes Isolation from Draining Lymph Node (dLN) and Footpad

1. 15 mL conic tubes.
2. 40 μM cell strainers.
3. RPMI 1640.
4. Centrifuge.
5. Serum fetal bovine.
6. Collagenase D solution (0.5–2,5 mg/mL—working solution).
7. Collagenase buffer.

   HEPES (2.39 g/L).

   Potassium chloride (KCL 0.37 g/L).

   Magnesium chloride (MgCl2 0.2 g/L).

   Calcium Chloride (CaCl2 0.2 g/L).

   Sodium Chloride (14.09 g/L).
8. Petri dishes.
9. 70 μM cell strainers.
10. EDTA (50 mM).
11. Neubauer chamber.
12. Trypan blue solution.

3 Methods

3.1 Preparation of Fungal Solution

3.1.1 Fungal Propagules

1. Maintain the human pathogenic *Fonsecaea* sp. in Sabouraud Dextrose Agar medium (SDA) supplemented with 100 mg/mL chloramphenicol at 37 °C [9].
2. Culture the *Fonsecaea* sp. cells in potato dextrose medium (PD) in a rotary shaker (180 rpm) at 37 °C for 7–14 days.
3. Filter the culture suspensions (containing conidia and hyphal fragments) in sterile fiberglass (to remove large hyphae clumps).
4. Perform sequential filtrations on 70 μM and after 40 μM cell strainers with the filtrate.
5. Resuspend the hyphae after being retained in a 40 μM cell strainer in phosphate-buffered saline (PBS) (measuring 40–70 μM).
6. Centrifuge the hyphae suspension twice at 1000 g (98% purified hyphae).
7. Filter the filtrate from the 40 μM cell strainer (containing conidia and small hyphal fragments) using a 14 μM filter paper.
8. Centrifuge the filtrate twice at 3000 g (98% purified conidia).
9. Prepare the fungal propagules adding the purified hyphae and conidia at a 1:3 rate.

3.1.2 Muriform Cells

1. Culture the mycelium fragments from PD cultures into an unacidified CDM supplemented with 0.1% (w/v) yeast extract (pH 6.5) for 7 days at 37 °C and 120 rpm.
2. Add an aliquot of the supernatant from the previous step into the acid CDM (1%, v/v) for another 40 days and 120 rpm.
3. Filter the suspension containing *F. pedrosoi* muriform cells through a 40 μM cell strainer (90% purified muriform cells).

3.2 Suspension of Infection

1. Count of live and purified fungal cells, trypan blue dye, within a hemocytometer.
2. Prepare the final suspension at 2×10^7 live fungal cells per mL to be inoculated into an experimental animal footpad.

3.3 Animals and Experimental Design

3.3.1 Rat Infection Model

1. Use the male Wistar rats (*Rattus norvegicus albinus*), 7–9 weeks old.
2. Infect five animals per day of analysis, in the plantar cushion, with 100 μL of the fungal solution containing 2×10^6 fungal cells (Fig. 1) (including fragments of hyphae and conidia of *Fonsecaea* sp.) at the right or left hind footpad.
3. Maintain the animals under appropriate conditions by the Institution Animal Care Committee following the Care and Use of Laboratory Animals issued guidelines.

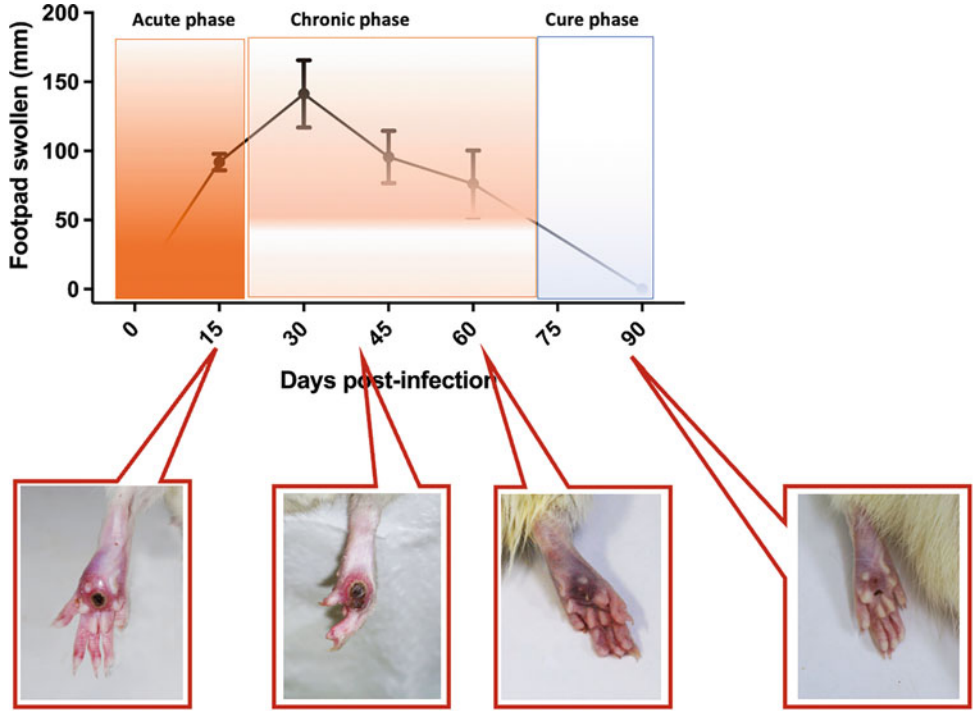

Fig. 1 Rat morphometry of lesion. The plantar cushion was measured every 15 days postinfection with a caliper and photographed to follow the lesion development

3.3.2 Mouse Infection Model

1. Use C57BL/6 (Fig. 2) or Balb/c (Fig. 3) mice, 6- to 8-week-old males.
2. Infect five animals per day of analysis and infected in the plantar cushion with 50 μL of the fungal propagules, containing 1×10^6 fungal cells. (including fragments of hyphae and conidia of *Fonsecaea* sp.) at the right or left hind footpad.
3. Maintain the animals under appropriate conditions by the Institution Animal Care Committee following the Care and Use of Laboratory Animals issued guidelines.

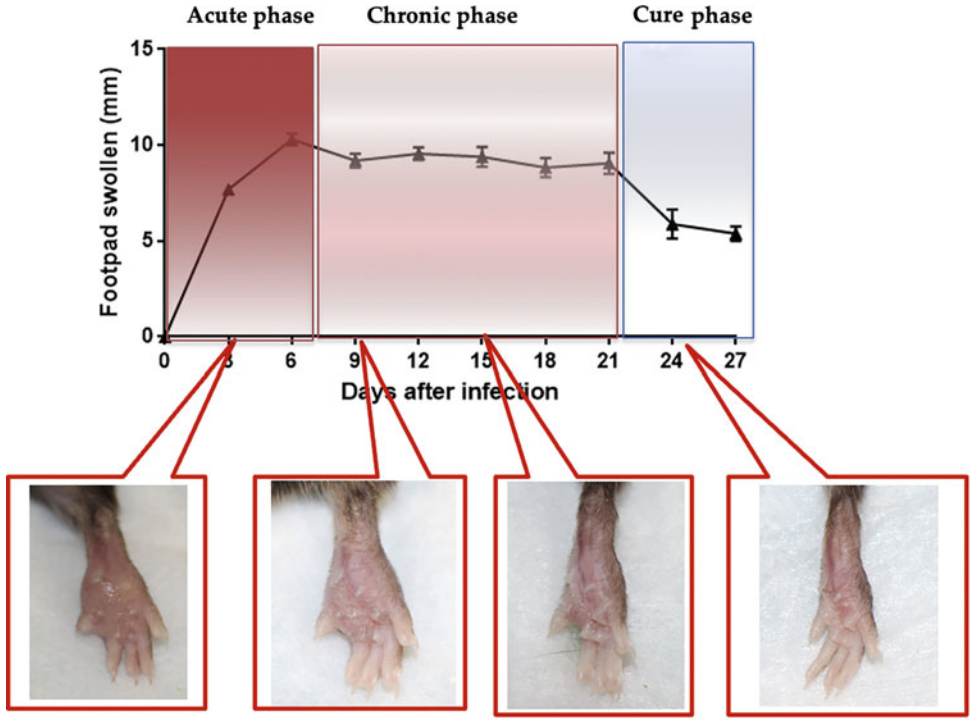

Fig. 2 C57Bl/6 morphometry of lesion. The plantar cushion was measured every 3 days postinfection with a caliper and photographed to follow the lesion development

Fig. 3 Balb/c lesion of plantar cushion—Photograph of footpad lesion after (**a**) 15, (**b**) 30, and (**c**) 45 days postinfection with *F. pedrosoi*

3.4 Analysis Checkpoints

1. Euthanize the rats at 15-, 30-, 45-, 60-, and 90-day postinfection (DPI), miming the acute and chronic phases (Fig. 1).
2. Euthanize the mice at 07-, 14-, 21-, and 28-DPI, mimicking the acute and chronic phases (Fig. 2).

3.5 Morphometry

1. Measure the area with a caliper every 3 days.
2. Euthanize the animals on each specific day postinfection (Figs. 1 and 2), according to the Care and Use of Laboratory Animals guidelines.
3. After euthanizing, remove the plantar cushion and popliteal lymph node by surgical excision.
4. Maintain the host tissue in Petri plate with sterile PBS after being removed from the animals.

3.6 Fungal Burden

1. Homogenize part of the plantar cushion tissue from each experimental animal in PBS (pH 7.2) and then plate it onto SDA medium in Petri dishes, supplemented with 100 mg/mL of chloramphenicol, and cultivated at 37 °C for 7 days.
2. Measure the fungal burden through CFU of *Fonsecaea* sp. Results are expressed as the number of CFU ± standard mean error (SEM).

3.7 Histopathology

1. Fix the small fragments of infected tissue in buffered formalin until processing.
2. Dehydrate the fragments with alcohols (85%, 90%, and absolute) and xylol.
3. Use paraffin to embed the tissue.
4. Perform serial sections of 5 μM and stain with hematoxylin and eosin (HE).
5. Analyze the granuloma organization, fungal presence, and fibrosis formation in light microscopy (Fig. 4).

3.8 Lymphocytes Isolation from Draining Lymph Node (dLN) and Footpad

3.8.1 Lymph Node

1. Collect the popliteal lymph node and homogenize it in a 40 μM cell strainer with a syringe plunger.
2. Wash the cells with 5 mL of simple RPMI and centrifuge at 300 g for 5 min.
3. Resuspend the cells in 1 mL of RPMI supplemented with 10% FBS.
4. Filter the cells in a 40 μM cell strainer.
5. Quantify the cells with trypan blue to discriminate the viable cells in a Neubauer chamber.

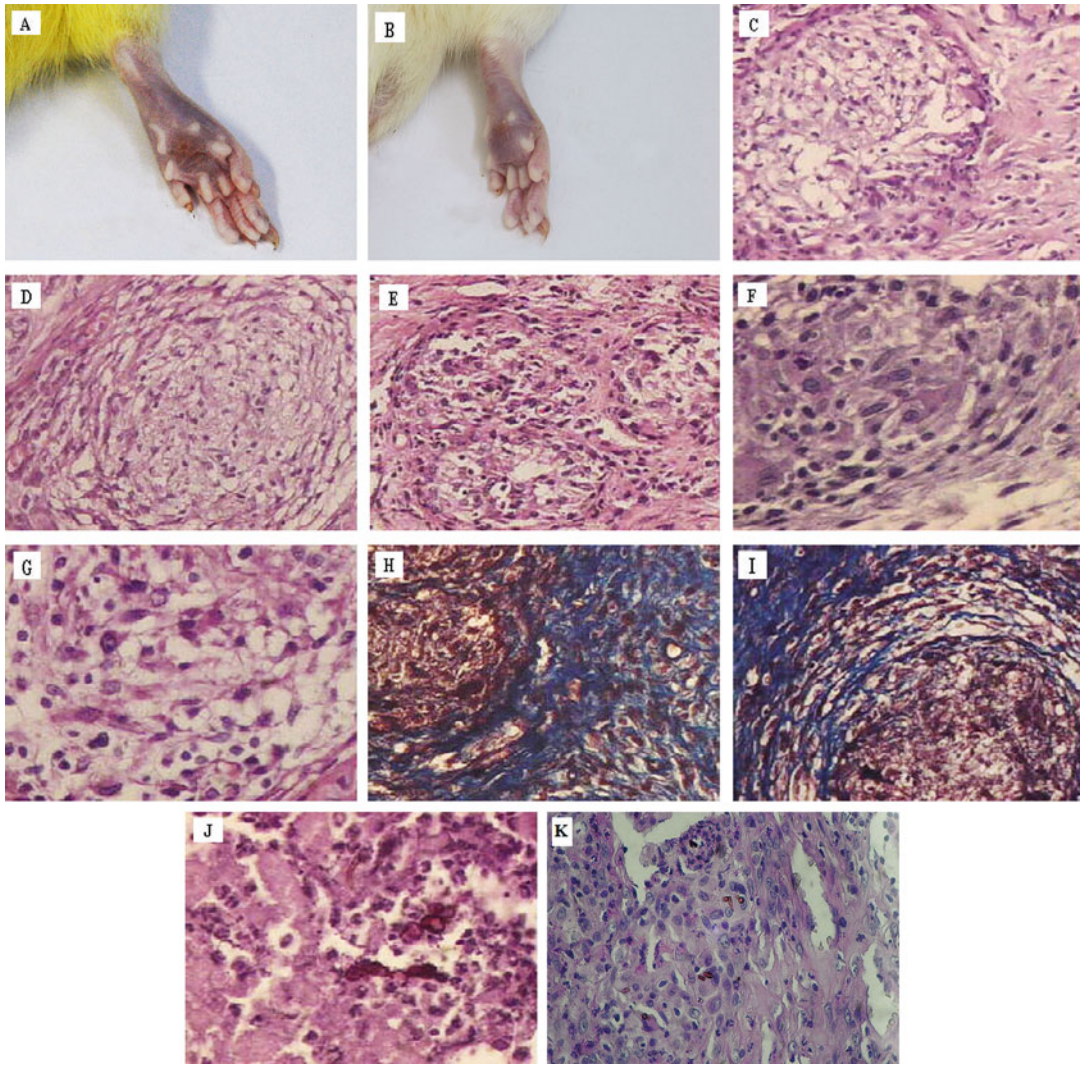

Fig. 4 Lesion area analysis. The analysis of infection chronic (**a**, **b**) Photograph of footpad infection; (**c**, **d**, **e**) Histopathology of tissue, showing granuloma formation, HE (20×); (**f**, **g**) Histopathology of tissue, showing cellular infiltration patter, HE (40×); (**h**, **i**) Histopathology of tissue, showing the collagen deposition in a blue area, PAS (20×); (**j**, **k**) Histopathology of tissue, showing the fungal presence in a brown area, HE (40×)

3.8.2 Footpad Tissue

1. Cut the removed tissue from the mice footpad into small pieces.
2. Submit the tissue to 5 mL of collagenase D solution at 1 mg per mL of collagenase buffer (described in Subheading 2.7–**item 7**) for 1 h of incubation at 37 °C in Petri dishes.
3. Homogenize the tissue fragments in a 70 μM cell strainer and wash with 5 mL of RPMI.
4. Stop the collagenase activity by adding 1 mL EDTA at 50 mM and centrifuging at 300 g for 5 min.

5. Resuspend the pellet in 5 mL of RPMI, filter in a 70 μM cell strainer, and then centrifuge.
6. Resuspend the cells in 1 mL of supplemented RPMI.
7. Quantify the cells with trypan blue to discriminate the viable cells in a Neubauer chamber.

4 Notes

1. Some experimental models have developed; however, none form a long-term lesion because of the rodent immune system adaptation to the fungal stimuli. However, the models described below can mimic, in part, human lesions.
2. The footpad increases its size and can occur skin pigmentation and ulcerative lesions like those in humans.
3. There are some differences in lesion aspects between C57Bl/6 and Balb/c mice (Figs. 2 and 3), with pigmentation lesions on the skin in Balb/c mice and a higher inflammatory response in C57Bl/6.
4. The tissue histopathology shows ulceration of exudative areas, necrotic material, and multifocal lymphocytic infiltrate outlining the granuloma, like that observed in humans with the disease.
5. There are in the tissue muriform and hyphae fungal cells, in a small amount than in other fungal-infected tissue.
6. The cells from LN or foot pad tissue can be used in different immune response analyses such as cytokines production, T and B cell phenotypes, microbicidal mechanisms, and others.

References

1. Santos LS, Palmeira VF, Rozental S, Kneipp LF, Nimrichter L (2007) Biology and pathogenesis of Fonsecaea pedrosoi, the major etiologic agent of chromoblastomycosis. FEMS Microbiol Rev 31:570–591. https://doi.org/10.1111/j.1574-6976.2007.00077.x
2. Salgado CG, da Silva JP, Diniz JAP, da Silva MB, da Costa PF, Teixeira C, Salgado UI (2004) Isolation of Fonsecaea pedrosoi from thorns of Mimosa pudica, a probable natural source of chromoblastomycosis. Revista Do Instituto de Medicina Tropical de Sao Paulo 46(1):33–36. Retrieved from https://www.ncbi.nlm.nih.gov/pubmed/15057332
3. Queiroz-Telles F, Esterre P, Perez-Blanco M, Vitale RG, Salgado CG, Bonifaz A (2009) Chromoblastomycosis: an overview of clinical manifestations, diagnosis, and treatment. Med Mycol 47(1):3–15. https://doi.org/10.1080/13693780802538001
4. Brandt ME, Warnock DW (2003) Epidemiology, clinical manifestations, and therapy of infections caused by dematiaceous fungi. J Chemother 15(Suppl 2):36–47. https://doi.org/10.1179/joc.2003.15.Supplement-2.36
5. Alviano DS, Kneipp LF, Lopes AH, Travassos LR, Meyer-Fernandes JR, Rodrigues ML, Alviano CS (2003) Differentiation of Fonsecaea pedrosoi mycelial forms into sclerotic cells is induced by platelet-activating factor. Res Microbiol 154:689–695. https://doi.org/10.1016/j.resmic.2003.09.002
6. Florencio CS, Brandão FAS, de Teixeira M, Bocca AL, Felipe MSS, Vicente VA, Fernandes L (2018) Genetic manipulation of Fonsecaea

pedrosoi using particles bombardment and agrobacterium mediated transformation. Microbiol Res 207:269–279. https://doi.org/10.1016/j.micres.2018.01.001

7. Machado AP, Silva MRR, Fischman O (2011) Local phagocytic responses after murine infection with different forms of Fonsecaea pedrosoi and sclerotic bodies originating from an inoculum of conidiogenous cells. Mycoses 54:202–211. https://doi.org/10.1111/j.1439-0507.2009.01792.x
8. Siqueira IM, de Castro RJA, de Miranda Leonhardt LC, Jerônimo MS, Soares AC, Raiol T et al (2017) Modulation of the immune response by Fonsecaea pedrosoi morphotypes in the course of experimental chromoblastomycosis and their role on inflammatory response chronicity. PLoS Negl Trop Dis 11(3): e0005461
9. Alviano CS, Farbiarz SR, Travassos LR, Angluster J, de Souza W (1992) Effect of environmental factors on Fonsecaea pedrosoi morphogenesis with emphasis on sclerotic cells induced by propranolol. Mycopathologia [Internet] 19(1):17–23. [Cited 2013 Oct 28]. Available from: http://www.ncbi.nlm.nih.gov/pubmed/1406903
10. Esterre P, Queiroz-Telles F (2006) Management of chromoblastomycosis: novel perspectives. Curr Opin Infect Dis 19(2):148–152. https://doi.org/10.1097/01.qco.0000216625.28692.67
11. de Hoog GS, Queiroz-Telles F, Haase G, Fernandez-Zeppenfeldt G, Attili Angelis D et al (2000) Black fungi: clinical and pathogenic approaches. Med Mycol 38:243–250. https://doi.org/10.1080/mmy.38.1.243.250
12. Minotto R, Albano Edelweiss MI, Scroferneker ML (2017) Study on the organization of cellular elements in the granulomatous lesion caused by chromoblastomycosis. J Cutan Pathol 44(11):915–918. https://doi.org/10.1111/cup.13014
13. Bocca AL, Brito PP, Figueiredo F, Tosta CE (2006) Inhibition of nitric oxide production by macrophages in chromoblastomycosis: a role for Fonsecaea pedrosoi melanin. Mycopathologia 161(4):195–203. https://doi.org/10.1007/s11046-005-0228-6
14. Mendoza L, Karuppayil SM, Szaniszlo PJ (1993) Calcium regulates in vitro dimorphism in chromoblastomycotic fungi: calcium reguliert in vitro den Dimorphismus von Chromoblastomykose-Erregern. Mycoses 36(5–6):157–164. Retrieved from https://onlinelibrary.wiley.com/doi/abs/10.1111/j.1439-0507.1993.tb00744.x
15. de Soares RMA, Angluster J, de Souza W, Alviano CS (1995) Carbohydrate and lipid components of hyphae and conidia of human pathogenFonsecaea pedrosoi. Mycopathologia 132:71–77. https://doi.org/10.1007/bf01103778
16. Salgado CG (2010) Fungal x host interactions in Chromoblastomycosis: what we have learned from animal models and what is yet to be solved. Virulence 1(1):3–5. https://doi.org/10.4161/viru.1.1.10169. PMID: 21178406
17. Xie Z, Zhang J, Xi L, Li X, Wang L, Lu C, Sun (2010) A chronic chromoblastomycosis model by Fonsecaea monophora in Wistar rat. J Med Mycol 48(1):201–206. https://doi.org/10.3109/13693780902785320. PMID: 19255903
18. Siqueira IM, Ribeiro AM, Nóbrega YK, Simon KS, Souza AC, Jerônimo MS, Cavalcante Neto FF, Silva CL, Felipe MS, Bocca AL (2013) DNA-hsp65 vaccine as therapeutic strategy to treat experimental chromoblastomycosis caused by Fonsecaea pedrosoi. Mycopathologia 175(5–6):463–475. https://doi.org/10.1007/s11046-012-9599-7
19. Cardona-Castro N, Agudelo-Flórez P (1999) Development of a chronic chromoblastomycosis model in immunocompetent mice. Med Mycol 37(2):81–83
20. Calvo E, Pastor FJ, Mayayo E, Hernández P, Guarro. (2011) Antifungal therapy in an athymic murine model of chromoblastomycosis by Fonsecaea pedrosoi. J Antimicrob Agents Chemother 55(8):3709–3713. https://doi.org/10.1128/AAC.01662-10
21. Dong B, Liu W, Li R, Chen Y, Tong Z, Zhang X, Chen L, Li (2020 Aug) Muriform cells can reproduce by dividing in an athymic murine model of chromoblastomycosis due to fonsecaea pedrosoi. Am J Trop Med Hyg 103(2):704–712. https://doi.org/10.4269/ajtmh.19-0465

Chapter 11

Modeling Chronic Coccidioidomycosis in Mice

Lisa F. Shubitz, Christine D. Butkiewicz, and Hien T. Trinh

Abstract

Coccidioidomycosis, caused by the dimorphic pathogens *Coccidioides posadasii* and *C. immitis*, is a fungal disease endemic to the southwestern United States, Mexico, and some regions of Central and South America. The mouse is the primary model for studying pathology and immunology of disease. Mice in general are extremely susceptible to *Coccidioides* spp., which creates challenges in studying the adaptive immune responses that are required for host control of coccidioidomycosis. Here, we describe how to infect mice to model asymptomatic infection with controlled, chronic granulomas and a slowly progressive but ultimately fatal infection that has kinetics more similar to the human disease.

Key words Mice, *Coccidioides*, Intranasal, Quiescent, Survival, Immunology, Histopathology, Cp1038

1 Introduction

Humans almost always acquire coccidioidomycosis by inhaling tiny, barrel-shaped arthroconidia (spores) of *Coccidioides posadasii* or *C. immitis* from the air deep into the respiratory tract. This infection is usually limited to the thorax (lungs, thoracic lymph nodes), but in 1–5% of cases, it disseminates to other sites, the most common of which are skin, lymph nodes, bone, and central nervous system [1, 2]. Uncomplicated lung infections may be asymptomatic, cause a weeks-long but self-limiting illness with cough, chest pain, fevers, and fatigue, or manifest as severe respiratory disease which requires drug therapy [2]. Disseminated disease may involve one or multiple sites, making patients very ill and always requires protracted treatment with antifungal drugs. Average annual coccidioidomycosis-associated deaths in the USA are approximately 200 (https://www.cdc.gov/fungal/diseases/coccidioidomycosis/statistics.html).

Mice are the primary model utilized to research disease processes and therapeutic interventions for coccidioidomycosis. In mice, intranasal infection with *Coccidioides* spp., including the

Rebecca A. Drummond (ed.), *Antifungal Immunity: Methods and Protocols*, Methods in Molecular Biology, vol. 2667,
https://doi.org/10.1007/978-1-0716-3199-7_11,

most widely utilized laboratory fungal strains (Silveira, C735, and RS), causes severe pyogranulomatous pneumonia with rapid dissemination to spleen and liver. Death ensues within 2–3 weeks following introduction of 30–50 spores into the lungs through intranasal insufflation [3, 4]. The time to death can be shortened by increasing the dose, and it can be lengthened by a few weeks or less with lower doses. However, with reduced infecting doses, the likelihood of uninfected mice for technical reasons increases, resulting in studies that are difficult to interpret. Fate of intranasally administered spores may include entrapment in upper airways and nasal passages with removal by normal bronchial and tracheal mechanisms and swallowing part of the inoculum as it passes through the nasopharynx. As few as 10% of the spores may reach the distal airways and infect the lung tissue [5, 6].

Infected people seldom experience the rapid rate of disease expansion that mice exhibit, leaving room for improvement in the model to more closely approximate the kind of progression seen clinically. Even people who have poor outcomes seldom acutely die within three weeks of infection. Additionally, the majority of people experience asymptomatic or self-limited disease, in which a dense nodule may be discovered years later on a routine lung x-ray [7]. These lesions often contain quiescent organisms, which may be recovered upon culture, or result in recurrent disseminated disease if the patient becomes immunosuppressed [8–10]. With a model of chronic progressive or asymptomatic controlled disease in mice, researchers can differentiate and define mechanisms that lead to control vs. progression of disease, explore adaptive immune mechanisms that do not have time to fully develop in rapidly progressive models of infection, and elucidate host–pathogen interactions of controlled disease, the most common outcome of human infection.

Chronic coccidioidomycosis is induced in mice using *C. posadasii* strain 1038 (Cp1038), which was originally isolated from a patient in Arizona (USA) and subsequently shown to have reduced virulence in BALB/c mice [3, 11]. We have developed two models which have potentially different applications. The first is a slowly progressive but ultimately fatal infection (median survival time ~ 70 days, usually all dead between 12 and 16 weeks) in susceptible C57BL/6 (B6) mice. B6 mice are extensively used in vaccine and immunology studies, and there are a large number of genetically modified mice available on this strain background for studying mechanisms of innate and adaptive immunity. The slowly progressive B6 model allows more time to study adaptive responses and can also better define mutations that worsen disease outcomes but are difficult to study in mice that die in 2–3 weeks [12].

The second model is a chronically infected but indefinitely asymptomatic mouse model that more closely approximates the typical condition of host control exhibited by humans. Resistant

C57BL/6 × DBA/2 (B6D2F1) mice infected intranasally with 50 spores of Cp1038 remain healthy and gain weight over time. Lung fungal burdens stabilize in the vicinity of 1×10^4 colony-forming units (cfu) by 4 weeks postinfection and remain static through 16 weeks [11]. Spleen fungal dissemination remains low and most spleen fungal burdens are between 0 and 200 cfu. In mice monitored for 9 months, the lung fungal burden reduced almost another log without clearance of disease while spleen dissemination remained minimal. This chronic model allows for study of adaptive immunity and host–pathogen interactions under the conditions of host control. Further, host immunity can be disrupted experimentally to determine what happens at the cellular and molecular level when control breaks down. A chronic coccidioidomycosis model in mice provides for more diverse studies on adaptive immunity, host–pathogen interactions in the state of disease control, and cellular and molecular mechanisms associated with either genetic or induced immuno-incompetence.

The following methods include anesthesia and intranasal infection of mice with Cp1038 spore suspension, monitoring of infected mice, and selected tissue collections for analysis.

2 Materials

Personal protective equipment (PPE), certified biosafety cabinets (BSC), and certified Biosafety Level 3 and Animal Biosafety Level 3 (BSL3, ABSL3) laboratories are required for preparation and administration of spore suspensions and for handling and procedures of infected mice.

2.1 Intranasal Infection

1. Concentrated suspension of Cp1038 spores with current viability count ($>1 \times 10^6$/ml). See References [11, 13, 14] for details on growth, harvesting, and enumeration of *Coccidioides* spp. for animal inoculation. Perform a viable count of the suspension to be used for mouse infections the week prior according to reference [14] (*see* **Note 1**).
2. 1000 μL and 200 μL micropipettors with sterile barrier tips.
3. Sterile 10 mL polypropylene screw cap tubes: 6–8.
4. Saline.
5. Alcohol-resistant marking pen.
6. Small rodent anesthesia chamber.
7. Isoflurane.
8. Small Kimwipes® or similar laboratory tissues.
9. Autoclave bags.
10. Portable scale to weigh mice to 0.1 g accuracy.

11. Ketamine/xylazine anesthesia 80/8 mg/kg; using a 1 mL syringe and a needle of ≤20G, draw up 1.52 mL sterile isotonic USP saline (saline), 0.32 mL ketamine (100 mg/mL), and 0.16 mL xylazine (20 mg/mL) to make 2 mL anesthesia at a concentration of 16 mg/mL ketamine and 1.6 mg/mL xylazine. (*see* **Note 2**) Dispense into a sterile tube or vial with a septum and rock tube to mix or triturate with syringe. Label contents and date. (*see* **Note 2**).
12. 1 mL syringe and 27 G needles.
13. Absorbent paper towels and/or underpad for work surface.
14. 70% ethanol in a spray bottle.
15. 3–4 GYE plates;1% glucose, 0.5% yeast extract, 1.5% Bacto agar, 50 μg/mL cycloheximide, 50 μg/mL chloramphenicol, 50 μg/mL streptomycin. Antibiotic stock solutions; dissolve 2 g cycloheximide in 40 mL of 75% ethanol; dissolve 2 g chloramphenicol in 40 mL of 75% ethanol; dissolve 2 g streptomycin in 40 mL sterile water, or filter sterilize after it dissolves in deionized water. GYE agar; add to a > 500 mL bottle or Erlenmeyer flask 7.5 g Bacto agar, 5 g glucose, 2.5 g yeast extract and 500 mL deionized water. Tighten lid on flask/bottle completely, then loosen it by a quarter turn. Autoclave this on a liquid cycle (30 minutes at 121 °C and 15 psi); cool in a 55 °C water bath for 1 hour after autoclaving. Place bottle on a stir plate and while stirring aseptically add 0.5 mL each of cycloheximide, chloramphenicol, and streptomycin stock solutions. Wipe benchtop with disinfectant to clean and remove dust. Place 10 cm × 1 cm Petri dishes on the benchtop right side up in a monolayer. Open lid and pour approximately 20–25 mL into each dish and close the lid. Allow 20 minutes to set. (Makes about 20 plates) (*see* **Note 3**).
16. Sterile cell spreader.
17. ¾" wide time tape for plate edges.

2.2 Terminal Exsanguination

1. Ketamine/xylazine anesthesia 100/10; using a 1 mL or 3 mL syringe and a needle of ≤20G, draw up 1.45 mL sterile isotonic USP saline (saline), 0.35 mL ketamine (100 mg/mL), and 0.18 mL xylazine (20 mg/mL) to make 2 mL anesthesia at a concentration of 17.5 mg/mL ketamine and 1.8 mg/mL xylazine. (*see* **Note 2**) Dispense into a sterile tube or vial with a septum and rock tube to mix or triturate with syringe. Label contents and date. (*see* **Notes 1** and **4**).
2. Small, sharp scissors.
3. Disposable plastic transfer pipets that hold more than 1 mL.
4. Tubes/cryovials in which to dispense blood.

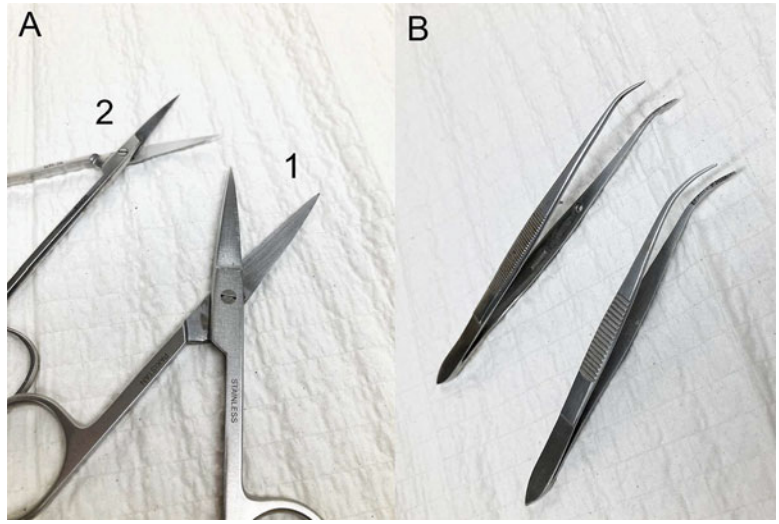

Fig. 1 (**a**) Small scissors 4–5 inches long and with sharp tips are most suitable for mouse dissections. Sturdy 5″ scissors (1) are good for incising skin and bone and removing organs for fungal culture or general histopathology. Very fine, sharp-tipped 4″ iris scissors (for eye surgery) (2) are used for the fine dissections of soft tissue, in particular the throat and trachea for lung fixation with formalin. (**b**) 4″–4.5″ fine tipped forceps with serrated tips for gripping make it easy to grip small parts and are essential for the light, nonslip grip of the trachea for lung inflation with formalin

5. Absorbent paper towels.
6. Small rodent anesthesia chamber and isoflurane.

2.3 Organ Collection

1. Small, sharp scissors (Fig. 1a #1).
2. Small, fine forceps (Fig. 1b).
3. Sterilizer for instruments that will fit in BSC, for example, bead sterilizer, small gas flame system with tap-on mechanism.
4. Nasco Whirlpak bags (1 oz).
5. Portable scale that weighs to 0.01 g accuracy.
6. Autoclave bag(s).
7. Disposable plastic-backed underpads.
8. Absorbent paper towels.
9. Sterile screw cap tubes with 4–5 mL cell culture medium (if needed).
10. Small rodent anesthesia chamber and isoflurane for euthanasia.

2.4 Preparation of Lungs for Histopathology

1. 4% paraformaldehyde (PFA); fill 50 mL conical tube with 26 mL of sterile water, 4 mL of 10X PBS, and 10 mL (1 ampule) of 16% methanol-free PFA. (Stable in refrigerator [4°-8 °C] for 1 month).

2. 18 G × 1″ or 1.25″ peripheral intravenous catheters.
3. 3 mL luer lock syringes.
4. Iris scissors (Fig. 1a #2) (*see* **Note 5**).
5. Fine forceps, 4″ with serrated tips for grip (Fig. 1b) (*see* **Note 5**).
6. Sharps container.
7. 4% paraformaldehyde – 1 tube of 3 mL for each mouse plus extra bulk tube containing ~1–1.2 mL per mouse.
8. Screw cap vials containing 4–5 mL 70% ethanol – 1 per mouse or tissue collected.

3 Methods

All Cp1038 spore suspensions, spore plates, and infected organs for culture must be handled in Biosafety Level 3 (BSL3) laboratories. All mouse infections must be performed and animals housed in Animal BLS3 (ABSL3) laboratories. Wear appropriate PPE and respiratory protection with primary barriers or PAPR (Power Air-Purifying Respirator). Perform all manipulation of suspensions and infected animals and tissues within approved and certified biosafety cabinets (BSC). Where possible, such as tubes, plates, and Whirlpak bags for collection of tissues, prelabel collection materials. Preload tubes with solutions that can be refrigerated or kept at room temperature. All wastes from procedures involving infectious spores, live, or dead animals must be autoclaved to decontaminate prior to disposal.

3.1 Preparation of Infecting Suspension

1. Label tubes in ten-fold dilutions and final dilution to achieve a concentration of 50 spores per 30 μL (1667 spores/mL). (*see* **Notes 6** and **7**).
2. Dispense 900 μL saline into ten-fold serial dilution tubes. Calculate needed volume and final dilution and add saline to the final tube.
3. Vortex concentrated spore suspension for ~30 seconds to mix well, then pipet 100 μL into 1:10 dilution. Vortex well and transfer to next tube until final dilution is prepared.

3.2 Intranasal Infection

1. Individually identify animals and weigh them. Permanently record weights for monitoring.
2. Anesthetize with ketamine/xylazine anesthetic cocktail (80/8). Give 0.1 mL for 18–21 g mouse intraperitoneally with a 1 mL syringe and 27G × 1/2” needle. For every 2–3 g increase in weight, give an extra 0.025 mL (*see* **Note 8**).

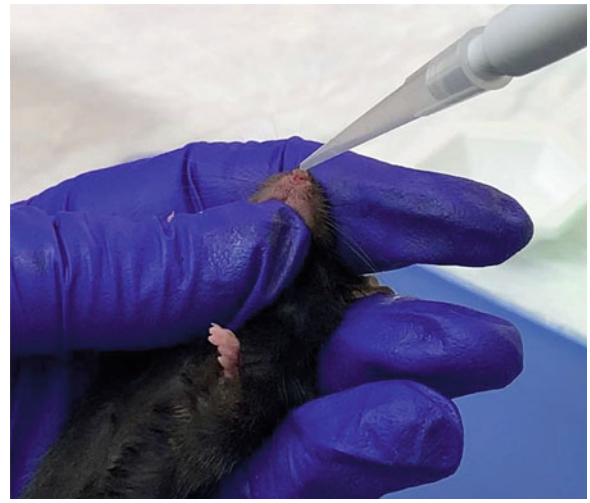

Fig. 2 Intranasal infection. Mouse is gripped gently between closed fingers of the hand and thumb is softly holding the mouth closed to ensure nasal breathing. Nose angle is about 70% of vertical. Droplets of spore suspension are delivered onto the nares with micropipettor

3. When mice are asleep, about 10 minutes, place cage in BSC. Remove all the mice from the cage and place them on an absorbent paper towel.
4. Pick the mouse up so its back is against your hand. Grip the mouse gently between thumb and open palm with closed fingers and use the thumb to gently close the mouth. Hold the mouse with nose at about 70% of vertical. Use care to avoid pressure on the throat (Fig. 2).
5. Aspirate 30 μL of vortexed infecting suspension with 200 μL pipettor with a barrier tip attached. Slowly drop onto the nares and wait for the liquid to be inhaled up the nose, then add another droplet until the entire 30 μL is administered. (*see* **Notes 9** and **10**).
6. If there any droplets on face/nares/whiskers, wipe the face gently with a Kimwipe wetted with 70% ethanol. (*see* **Note 11**).
7. Place the infected mouse in the home cage in lateral recumbency and make sure it continues to breathe. Repeat infection procedure for each mouse and place them close together for warmth. (*see* **Notes 12** and **13**).
8. Close cage. CLOSE suspension tube. (*see* **Note 11**) Spray all cage sides generously with 70% ethanol to decontaminate and replace in the housing area.
9. Vortex suspension between every 2 cages and continue until all mice in the experiment are infected. Check mice regularly while working to make sure all are waking up and are breathing.

3.3 Postinfection Verification of Infectious Dose

1. Place 3 or 4 10-cm GYE plates into BSC along with plate spreader.
2. Vortex the vial with the infecting suspension in it. Dispense 30 μL of the infecting suspension on each of the plates. Add 100 μL of saline and spread with a plate spreader. Dispose of plate spreader in autoclave bag. (*see* **Note 14**).
3. Replace lid and wrap time tape around the entire circumference of each plate so the lid and bottom remain together and spores will not easily disperse from the plate.
4. Incubate for 3–4 days at 37 °C and count colonies; take average to determine infecting dose.

3.4 Monitoring Mice

1. Check all mice following infection to make sure animals are breathing and regaining ambulation. The next day make sure all animals are alert and active in the cage. They do not normally suffer ill effects of the infection procedure, but rarely a mouse will be found dead the following day. After 24-hour check, monitor the activity of the animals 1–2 times weekly and weigh and record weights once weekly.
2. When mice start to lose weight or look sick, increase frequency of monitoring to daily. Euthanize moribund animals as needed. Signs of illness include weight loss, hunched posture, reduced activity, tachypnea, weakness and dullness, and ruffled fur. Most signs are detected by observing the animals in the opened cage. Weakness is easily felt when you pick them up to weigh them. Criteria for moribundity include dehydration ≥10% based on skin turgor test, isolation from cagemates, weakness and dullness, weight loss ≥25% from weight at the time of infection (mice may gain weight early on and have more weight to lose before they appear ill), difficulty eating, drinking, or ambulating, any CNS signs (paresis, paralysis, seizures, head tilt, circling, obtundation, coma). (*see* **Note 15**) Check with your animal welfare committee to determine if your criteria for moribundity differ from these.
3. Chronic infection model studies are frequently carried out for 10 weeks or more. Resistant B6D2F1 mice remain asymptomatic for at least 9 months. (*see* **Note 16**).

3.5 Collection of Tissue for Quantitative Fungal Culture or Flow Cytometry

1. When mice are moribund (*see* Subheadings 3.4) or at the scheduled termination date, euthanize the animals inside the biosafety cabinet in the ABSL3 laboratory. Record terminal weights.
2. Have your Nasco Whirlpak bags and GYE plates prelabeled for the organ and mouse. Place the portable scale accurate to 0.01 g in the BSC. To weigh lungs and spleens, place Whirlpak bag on the scale and zero it before placing the tissue in the bag. (*see* **Note 17**).

3. Place a beaker with 1/2–3/4″ of 70% to 100% ethanol in the biosafety cabinet. Place your instruments, functional end down, in the beaker.
4. Place 2–4 mice together on an absorbent towel. Snip approximately ¼” of skin laterally across the midline for each mouse just above the level of the groin. Place your instruments back in the ethanol. Firmly grasp the skin you have snipped and pull the tag toward the head and over the head so the mouse is “peeled” in a single motion. (*see* **Note 18**) This helps to reduce hair and contamination of the abdominal and thoracic wall.
5. Sterilize your instruments with the sterilization tool available in your BSC. (*see* **Note 19**).
6. Make a cut from mid-abdomen to the bottom of the sternum keeping your scissors shallow and tenting the abdominal wall with your forceps so you do not cut gut. Cutting the gut will contaminate your cultures with bacteria. Make a second cut along the left side of the body wall to expose the left side abdominal organs. Push the body wall out of the way. Expose spleen from behind the stomach and intestines on the left side of the mouse. Grasp the spleen with your forceps, exteriorize it from the abdomen, and sharply dissect it from the ligament that holds it in place. (Fig. 3) (*see* **Note 20**).

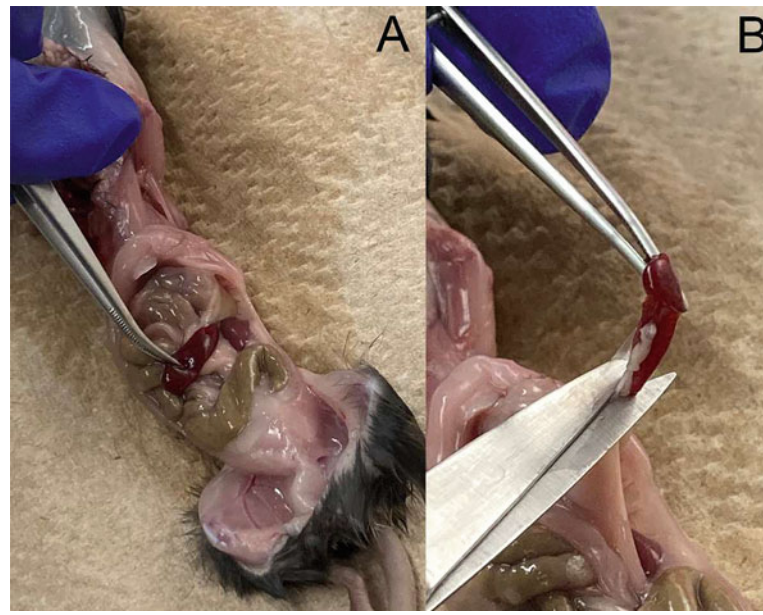

Fig. 3 (**a**) Spleen has been exteriorized from its position on the left side of the abdomen under the stomach and cranial to the left kidney. (**b**) Cut the ligament away on the underside to release the spleen

Fig. 4 Early fungal growth on a spleen plated whole on GYE agar to determine dissemination if organs are not being cultured for fungal burden

7. For quantitative culture, place spleen in a Whirlpak bag and fold down the top and secure the ends. (*see* **Note 21**) **For Flow Cytometry,** place spleen in prelabeled tube with 3–4 mL of cell culture medium. **For nonquantitative culture** to check the presence of dissemination, place the spleen on a prelabeled GYE plate. Seal the plate around its circumference with ¾" wide time tape and incubate at 35–37 °C for up to 7 days or until fuzzy white growth is observed on the spleen. (Fig. 4) (*see* **Notes 22** and **23**).
8. To open the thorax, snip the ribs and diaphragm to release vacuum in the thorax. The lungs will pull away. Cut along the edge of the diaphragm and both sides of the ribcage and push it up over the mouse's head, or snip it off.
9. Before grasping the lungs with forceps and cutting blood vessels in the thorax, gently move lungs around to note extent and number of lesions in the lungs. Pinching the lung tissue with forceps creates marks that may be mistaken for coccidioidal granulomas or hemorrhage, so tissue handling should be kept to a minimum. Lungs may have few, small lesions of 1–2 mm diameter (Fig. 5a), or the lungs could be 50–90% abnormal tissue with many granulomas or consolidated lobes and very enlarged lymph nodes (Fig. 5b). Collect lungs by cutting at the base under the heart.
10. Place lungs in Whirlpak bag and weigh. (*see* **Note 24**) **For flow cytometry,** place the lungs into a prelabeled tube with 3–4 mL of cell culture medium. (*see* **Note 25**).

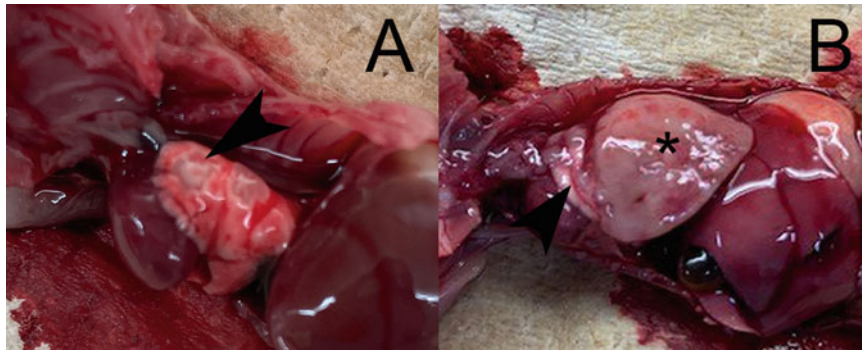

Fig. 5 Chronically infected lungs at dissection may have small, well-defined granulomas as in (**a**) (arrowhead), multiple coalescing granulomas, or one or more consolidated lung lobes (**b**). In (**b**), the asterisk marks an extremely enlarged consolidated lung lobe, while the arrowhead points out a small amount of normal lung tissue visible in the cranial thorax. In both images, the mouse's head is to the left and the ribcage has been cut away

3.6 Terminal Exsanguination (see Note 26)

1. Anesthetize mice with the 100/10 ketamine/xylazine mixture IP for surgical plane of anesthesia and deep pain relief. (*see* **Note 4**) Wait until toe pinch reflexes are gone. If anesthesia is not adequate, briefly expose mice to isoflurane in a rodent anesthesia chamber.
2. Place mouse in dorsal recumbency on absorbent towels. Have a plastic transfer pipet and receptacle for blood at close hand. Moisten the axillary area with ethanol.
3. Retract the forelimb away from the body and dissect the skin only for about 8–10 mm in the axillary region.
4. In one definitive cut, sever the axillary vessels deeply between the body wall and the scapula. The blood will flow very fast. Collect the blood with the transfer pipet to reduce the blood on the animal, which gets in the way of visualizing the tracheal dissection. Suction blood until bleeding stops.
5. If the mouse is not deceased from the blood loss, place it in isoflurane in a small rodent anesthesia chamber until breathing stops or use other approved method of euthanasia.

3.7 Collection of Lungs for Histopathology

1. Perform terminal exsanguination (3.6 or other approved method and *see* **Note 26**) and make sure mice are deceased before dissection. (*see* **Note 27**).
2. Remove the skin as described above (*see* Subheading 3.5 #4). After collecting any abdominal organs required for study per Subheading 3.5, dissect the axillary areas and pull the forelegs over the head as well, exposing the throat with a sharp dissection of the subcutaneous tissues to above the level of the larynx. You should see the jaw when you have dissected far enough toward the nose (Fig. 6a).

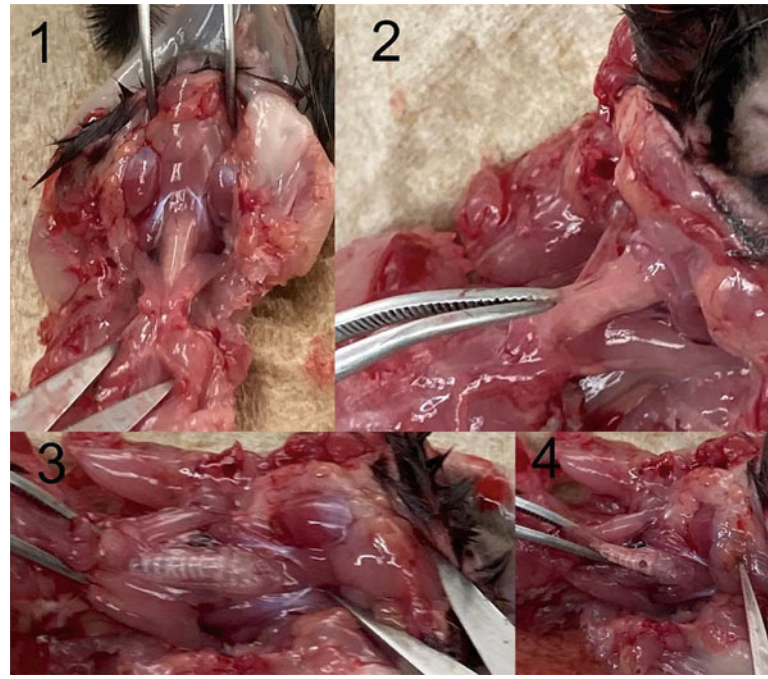

Fig. 6 Dissection of trachea to infuse lungs with paraformaldehyde. (**1**) Dissection of throat showing forelegs and soft tissue cut away on sides and skin pulled far up along the jaw. (**2**) Grasp the thin layer of tissue overlying the trachea with fine forceps and cut it away. (**3**) Dissected trachea showing tracheal rings. (**4**) Initial nick in trachea with iris scissors. Hole can be carefully enlarged just enough to work catheter tip in

3. Carefully snip a hole in the thorax at the bottom of ribcage where it meets the diaphragm to allow the lungs to pull away; take care not to cut the lungs. Cut across the diaphragm and up both sides of the ribcage, avoiding the lung tissue. Turn the mouse 180 degrees so your dominant hand is closest to the head of the mouse.
4. Open an 18G catheter and remove the metal stylet and discard in a sharps container. Attach the catheter hub to a 3 mL luer lock syringe. Draw up 0.8–1 mL of 4% paraformaldehyde.
5. Using fine-tipped iris scissors, sever the throat muscles carefully and push them aside. Grasp the tissue overlying the trachea (Fig. 6b) with your fine forceps and dissect it carefully out of the way, exposing the tracheal rings and larynx (Fig. 6c). Nick the trachea between cartilage rings 1–3 rings below the larynx. Cut the trachea about 1/3–1/2 way through its diameter (Fig. 6d) (*see* **Note 28**).

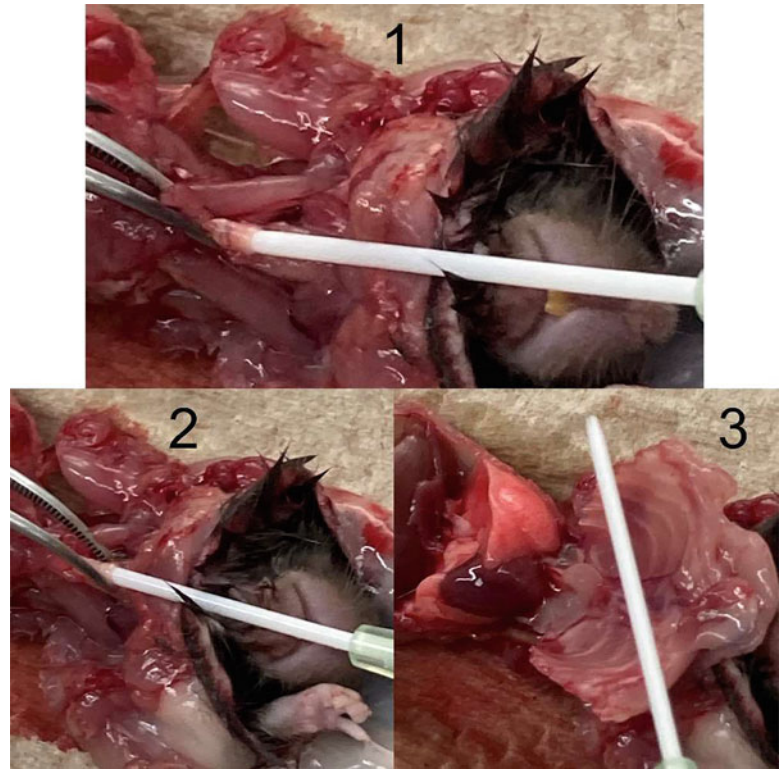

Fig. 7 Perfusion of lungs with paraformaldehyde. (**1**) Hold trachea lightly with forceps to work the tip of the catheter into the hole. (**2**) Feed the catheter into the trachea until it is within the thorax and feels firmly seated, maybe 5–7 mm. (**3**) Lungs properly inflated with paraformaldehyde

6. Gently work the tip of the catheter attached to the syringe into the trachea, holding the trachea gently with fine forceps in your other hand (Fig. 7a). Feed the catheter beyond the thoracic inlet toward the bifurcation, maintaining a light grip with the forceps (Fig. 7b). Fill the lungs with the fixative by gently depressing the syringe. You will see them inflate with the fluid (Fig. 7c).
7. Withdraw the catheter and clamp the trachea closed for 10–-15 seconds with the forceps, then release. (*see* **Note 29**).
8. Dissect lungs and place in 4–5 mL of 4% PFA in a prelabeled screw-cap tube.
9. Fix for ~24 hours in PFA, then transfer to tubes with the same volume of 70% ethanol. (*see* **Note 30**).

4 Notes

1. Detailed instructions for growth and harvesting of *Coccidioides* species cultures to produce arthroconidia are outside the scope of this article and it is thoroughly presented in reference [14]. All procedures must be performed at Biosafety Level 3. Briefly, we grow mycelial cultures of Cp1038 on 2X GYE plates for 8 weeks at 30 °C in an ambient air incubator to allow for maximal production of arthroconidia. Arthroconidia are harvested using the spin bar method in water [13], centrifuged at 4000 g for 25–30 minutes, and filtered through Pellon® to remove remaining mycelial fragments. Spores are centrifuged again and resuspended in 1–5 ml of sterile water. To count the spores, ten-fold dilutions are made until the spores can be counted on a hemocytometer. Anticipate about 10^7 spores per plate harvested and store them at around 10^7/ml. Using the hemocytometer count, make ten-fold serial dilutions and plate 100 μL on 3–4 GYE plates. Spread with a plate spreader. Incubate at 35–37 °C for 72–96 hours and count cfu. Calculate viable concentration.
2. Draw up saline first so as not to contaminate the saline bottle with anesthetic. Dispense 1 mL into the sterile empty vial/tube. Draw up the rest of the saline, then the ketamine and xylazine to fill the syringe the second time to 2 mL. This minimizes "insensible losses" of the ketamine in a needle hub for controlled substance record-keeping purposes as well; 2 mL will anesthetize about 18 18–20 g mice. Ketamine/xylazine cocktail is stable at room temperature or 4 °C for up to 3 months [15] but check with your institution for its specific guidelines for storage. We calculate what we need and make it fresh for each experiment. It is also useful to create a table with quantities of ketamine, xylazine, and saline for quick reference to make larger volumes of ketamine/xylazine cocktail.
3. If there are concerns regarding contamination while pouring plates on the benchtop, plates can be poured inside a BSC. If space is limited, plates can be stacked 4–5 high to set. However, this will increase the amount of time needed to set the plates. There is no need to measure the volume inside the plate. If you get 20–25 plates per bottle, then the plates are suitable for cultures of *Coccidioides* spp. If plates are too thin (<15 mL), the agar is not as strong and the plates may dry out during incubation. If plates are too thick, counting the colonies becomes difficult.
4. See **Note 2**. Use 0.15 ml per 25 g mouse. This mixture provides a surgical plane of anesthesia with better immobility, relaxation, and pain relief. It is appropriate for anesthetizing

mice for performing painful procedures such as terminal exsanguination. For smaller mice and strains sensitive to anesthesia, reduce the volume to 0.1 or 0.125 mL. Many mice in the chronic disease model that have survived 12–16 weeks will be well over 25 g in body weight and this anesthesia is appropriate to bleed them out.

5. It is very important that these be very fine, sharp scissors for dissection of throat. Approximately 4″ iris scissors are the best for this (Fig. 1a #2). We preserve these scissors for fine soft-tissue dissections and use a more rugged 5″ pair (Fig. 1a #1) for cutting skin and bone and routine organ collections. Fine forceps with serrations – so the tissue does not slip – are appropriate for all dissections but are necessary for the tracheal dissection. We use 4″ iris forceps (Fig. 1b).
6. Concentrated spore suspensions are typically around 1×10^7/mL. Concentrated suspensions store better and maintain viability longer under refrigeration. Reference [14] states spores can be stored up to 6 months before making new suspensions. Our experience with Cp1038 is that it will retain acceptable viability in this concentrated suspension for at least 3 months at 4 °C. Reduction in viability, which we assess before each infection, triggers the harvest of fresh spores. We prepare fresh diluted suspensions from concentrated suspensions for every infection and discard all diluted materials.
7. Multiple tubes of ten-fold serial dilutions allow you to move a larger volume of the starting suspension to the next tube, reducing the effects of having an error in a very tiny volume of spores. However, other dilution schemes can be used if desired.
8. Our BSC holds two cages at a time and we anesthetize four cages initially, then anesthetize another two cages in between each set of two cages placed in the BSC for infection. This minimizes the amount of time spent waiting for animals to become asleep enough for infection. This is an efficient process if there are two people working on it. A single person might adopt a slightly different work flow.
9. If bubbles form or the droplet comes back out of the nose, aspirate suspension back into the pipet, release the mouth and allow the mouse to take a breath or swallow. Drop suspension onto the nares again. If mouse is holding its breath, try pinching the rear foot; this may stimulate the mouse to take a breath and then you can continue the infection procedure.
10. If the mouse is not sufficiently asleep as evidenced by stiff extension of neck and forelimbs, crawling on the paper towel before infection, or unwillingness to inhale suspension placed on nares, briefly expose the animal to isoflurane in a small

rodent anesthesia chamber until voluntary motion ceases and quickly infect it. If left too long in isoflurane, the combination of anesthetics will cause permanent respiratory arrest. You only need relaxation to the point where dropping the fluid on the nose causes a reflexive sniffing. If most mice require immersion in isoflurane to infect, increase the dose of injectable anesthetic or change the ketamine/xylazine concentration to the 100/10 cocktail. This may be mouse strain dependent. B6D2F1 mice seem to be less sensitive to anesthesia than C57BL/6 or BALB/c mice and may need the higher concentration.

11. Take extreme care and cover your suspension with a cap when spraying 70% ethanol in the BSC or near your suspension. It is easily killed by ethanol [16].
12. If mouse does not breathe after infection, place it in lateral recumbency in your hand and begin gentle but vigorous rubbing of the thorax, or tapping of the thorax for a few seconds at a time, then see if it has started breathing; repeat if not yet breathing or breaths look agonal and infrequent.
13. If the mice are slow to wake from your anesthesia (not sternal and moving in ~15–20 minutes), place chemically activated, disposable handwarmer packs in the cage under a thick paper towel and place the mice on or near the warming pack (half on, half off works well). Monitor the mice and remove the pack and paper towel soon after all the mice are moving around. You can reuse it in another cage of mice until infection is completed, then discard in autoclave bag. Be sure to move your cages back into the BSC before adding or taking out the warming packs.
14. To kill the suspensions after you have done your final plating, spray 70% ethanol in the tube, then close it again and discard in autoclave bag. This reduces risk of aerosols for personnel.
15. Susceptible C57BL/6 mice will begin to lose weight around 6 weeks postinfection. Mice infected with Cp1038 typically decline more slowly than those infected with a virulent strain and may survive several days or a few weeks after they start to look unthrifty. This model is useful for studying genetic mutations and exogenous treatment that worsen disease. In a 2-week infection model, it is difficult to determine the effects of factors that make coccidioidomycosis worse, while this slower model will separate them. Genetically immunodeficient or immunosuppressed mice may die 2–3 weeks earlier than normal mice and should be monitored accordingly.
16. Resistant mouse strains, such as B6D2F1, Swiss-Webster, and DBA/2, are asymptomatic. After a brief initial loss of weight during the first week following infection, they gain weight throughout the observation period, 10–16 weeks for most studies. One group of B6D2F1 mice maintained for 9 months

postinfection doubled their infection weight, had low lung fungal burdens, and minimal or no dissemination. During the 9 months, some mice would lose 1–2 g of body weight over a couple of days, but this was always followed by a spell of continued growth. DBA/2 mice were reported many years ago to be resistant compared to other inbred mice tested with the virulent *C. immitis* strain RS [17]. With Cp1038, DBA/2 mice survive at least 16 weeks, but they differ histopathologically from the B6D2F1 mice, which have very controlled, mature granulomas.

17. The organs most commonly quantitated following intranasal infection are the lungs and the spleen. The spleen fungal burden is a good marker of the extent of dissemination. In immunodeficient strains of mice, such as TNFα knockouts, dissemination may be more severe and some mice may develop CNS signs. Quantitative fungal burdens of other organs, such as brain, may be applicable for your specific studies.
18. If you have not done this before, it takes some practice and you may need to cut some skin on the back of the mouse that does not separate. If you prefer not to use the peeling motion, you can dissect the skin sharply with scissors up the midline from groin to throat, then across at the bottom and top, and lay the haired skin back. This takes more time and dulls scissors rapidly.
19. The two primary methods available to prevent contamination between organs/animals are sterilization in a hot bead sterilizer or dipping in 100% ethanol and flaming the instruments with a tap-on gas flame (e.g., Touch-O-Matic Bunsen burner). The instruments are hot from either of these methods of sterilization. Allow them to cool before grasping or cutting tissue so it does not sear it or stick. Another method is a series of ethanol dips and rinse. Fill and label 50 mL conical tubes in a rack with 100% and 70% ethanol and a final tube with sterile saline or sterile water. Dip the instruments sequentially in 100% ethanol, 70% ethanol, then the rinse. The dips should be refreshed every other day if mice are sacrificed over several days. If the dips look very contaminated after sacrificing a lot of animals in one day, discard and make fresh solutions for the next day. While the ethanol effectively kills any cocci, we have found the alcohol dip method leads to more contamination by extraneous fungal colonies on the culture plates and we prefer a tap-on flame for this procedure.
20. Enlarged spleens are usually very friable (fragile) and easily crushed from the pressure of forceps and tear from pulling. Grasp and pull them gently.
21. If you want a spleen weight, place the Whirlpak bag on the scale and zero it before placing the spleen in the bag. A normal

spleen weighs about 0.08–0.1 g. Chronic, progressive infection and dissemination can increase them several fold.

22. Grossly infected spleens have whitish-grey to whitish-tan granulomas visible on the surface. These spleens should be checked daily if incubating them whole on GYE plates and discarded by autoclaving as soon as fuzzy mold growth is observed (Fig. 4). In spleens with grossly visible granulomas, mold growth may be observed by 48 hrs. Autoclaving as soon as observed minimizes the risk of spore formation, which is an aerosol risk to personnel. Spleens without obvious granulomas may need to be incubated for up to 7 days to assure they are negative for fungal growth.
23. If you are interested in the presence/absence of fungal growth in any other organs, these can be added to the GYE spleen plate. Organs that might be of interest in determining extent of dissemination include, but are not limited to, liver, kidney, and brain. Unless using high virulence models designed to create CNS disease [18–20], identifiable neurological signs are uncommon in mice that die in 2–3 weeks. In developing and using the chronic disease model of Cp1038, we have found that mice with immunodeficiencies may develop seizures, head tilt, circling, or paresis. In surveying B6 mice with spleen dissemination, we have also discovered there is fungal growth from the brain in many mice without overt neurological signs.
24. Normal mouse lungs weigh ~0.2–0.25 g. Lung weights correlate well with fungal burden [21] and, along with gross disease assessment, can help determine the number of ten-fold serial dilutions for quantitation. If lungs are estimated to consist of ≥50% grossly abnormal lung tissue or they weigh more than 0.35 g, ten-fold dilutions between 10^2 and 10^5 will need to be plated for counting until you determine the relationship between lung weight and lung fungal burdens for the strains of mice and time points you are assessing. Plates that have between 25 and 100 colonies are the best dilutions to count. For the B6D2F1 mice lungs weighing ≥0.35 g, serial dilutions through 10^4 will yield countable plates. For lungs with 1–2 lesions and mainly normal tissue, or no gross disease, undiluted homogenates will need to be plated in addition to the 1:10 and 1:100 serial dilutions.
25. If a lung weight is needed, zero the scale with the cell culture medium tube before adding the lung, or weigh lungs on a sterile weighing dish, then transfer to the tube.
26. Various methods exist for exsanguination. Obtain the assistance of your laboratory animal department to determine what protocols are recommended for terminal bleeding. You need a method of terminal bleeding that does not involve any

organs inside the thorax. If you don't have a method that you use routinely, this one leaves the lungs intact for the best histopathological specimens.

27. Bleeding the mice out greatly improves the quality of lung histopathology sections.
28. Do not cut trachea all the way through because it will retract into the thoracic cavity and is very difficult or impossible to locate and grasp for catheter insertion.
29. Filling the lungs with fixative expands the collapsed alveoli and makes the histopathological sections easier to evaluate. This is highly recommended if you want publication quality photomicrographs. Excess fixative will flow out of the trachea when you release the forceps and this is normal.
30. Discard all formaldehyde waste per your institution's chemical hygiene protocols.

References

1. Drutz DJ, Catanzaro A (1978) Coccidioidomycosis. Am Rev Resp Dis 117(559–585): 727–771
2. Galgiani JN, Blair JE, Ampel NM et al (2019) Treatment for early, uncomplicated coccidioidomycosis: what is success? Clin Infect Dis 70: 2008–2012. https://doi.org/10.1093/cid/ciz933
3. Cox RA, Magee DM (2004) Coccidioidomycosis: Host response and vaccine development. Clin Microbiol Rev 17:804–839
4. Shubitz LF, Peng T, Perrill R et al (2002) Protection of mice against *Coccidioides immitis* intranasal infection by vaccination with recombinant antigen 2/PRA. Infect Immun 70: 3287–3289. https://doi.org/10.1128/iai.70.6.3287-3289.2002
5. Shubitz LF, Perrill R, Lewis ML, et al (2011) Early post-infection detection of *Coccidioides* in intranasally infected mice. Proceedings 55th annual Coccidioidomycosis study group. University of California, Davis:40
6. Roberts LM, Tuladhar S, Steele SP et al (2014) Identification of early interactions between *Francisella* and the host. Infect Immun 82: 2504–2510. https://doi.org/10.1128/IAI.01654-13
7. Galgiani JN, Ampel NM, Blair JE et al (2016) Infectious Diseases Society of America (IDSA) clinical practice guideline for the treatment of coccidioidomycosis. Clin Infect Dis 63:e112–e146. https://doi.org/10.1093/cid/ciw360
8. Brewer JH, Parrott CL, Rimland D (1982) Disseminated coccidioidomycosis in a heart transplant recipient. Sabouraudia 20:261–265. https://doi.org/10.1080/00362178285380381
9. Keckich DW, Blair JE, Vikram HR et al (2011) Reactivation of coccidioidomycosis despite antifungal prophylaxis in solid organ transplant recipients. Transplantation 92:88–93
10. Jones JL, Fleming PL, Ciesielski CA et al (1995) Coccidioidomycosis among persons with AIDS in the United States. J Infect Dis 171:961–964. https://doi.org/10.1093/infdis/171.4.961
11. Shubitz LF, Powell DA, Butkiewicz CD et al (2021) A chronic murine disease model of coccidioidomycosis using *Coccidioides posadasii*, strain 1038. J Infect Dis 223:166–173. https://doi.org/10.1093/infdis/jiaa419
12. Shubitz LF, Robb EJ, Powell DA et al (2021) Δcps1 vaccine protects dogs against experimentally induced coccidioidomycosis. Vaccine 39:6894–6901. https://doi.org/10.1016/j.vaccine.2021.10.029
13. Huppert M, Sun SH, Gross AJ (1972) Evaluation of an experimental animal model for testing antifungal substances. Antimicrob Agents Chemother 1:367–372
14. Mead HL, Van Dyke MCC, Barker BM (2020) Proper care and feeding of *Coccidioides*: A laboratorian's guide to cultivating the dimorphic stages of *C. immitis* and *C. posadasii*. Curr Protoc Microbiol 58:e113. https://doi.org/10.1002/cpmc.113
15. Dodelet-Devillers A, Zullian C, Vachon P et al (2016) Assessment of stability of ketamine-

xylazine preparations with or without acepromazine using high performance liquid chromatography-mass spectrometry. Can J Vet Res 80:86–89

16. Vogler AJ, Nottingham R, Parise KL et al (2015) Effective disinfectants for *Coccidioides immitis* and *C. posadasii*. Appl Biosafety 20: 154–158. https://doi.org/10.1177/153567601502000306
17. Kirkland TN, Fierer J (1983) Inbred mouse strains differ in resistance to lethal *Coccidioides immitis* infection. Infect Immun 40:912–916. https://doi.org/10.1128/IAI.40.3.912-916.1983
18. Kamberi P, Sobel RA, Clemons KV et al (2003) A murine model of coccidioidal meningitis. J Infect Dis 187:453–460
19. Wiederhold NP, Shubitz LF, Najvar LK et al (2018) The novel fungal Cyp51 inhibitor VT-1598 is efficacious in experimental models of central nervous system coccidioidomycosis caused by *Coccidioides posadasii* and *Coccidioides immitis*. Antimicrob Agents Chemother 62:e02258
20. Shubitz LF, Trinh HT, Galgiani JN et al (2015) Evaluation of VT-1161 for treatment of coccidioidomycosis in murine infection models. Antimicrob Agents Chemother 59: 7249–7254. https://doi.org/10.1128/AAC.00593-15
21. Huppert M, Sun SH, Gleason-Jordan I et al (1976) Lung weight parallels disease severity in experimental coccidioidomycosis. Infect Immun 14:1356–1368

Chapter 12

Mouse Models of Phaeohyphomycosis

Yi Zhang and Ruoyu Li

Abstract

Infections by dematiaceous fungi especially phaeohyphomycosis are an emerging group of infectious diseases worldwide with a variety of clinical presentations. The mouse model is a useful tool for studying phaeohyphomycosis, which can mimic dematiaceous fungal infections in humans. Our laboratory has successfully constructed a mouse model of subcutaneous phaeohyphomycosis and found significant phenotypic differences between *Card9* knockout and wild-type mice, mirroring the increased susceptibility to this infection observed in CARD9-deficient humans. Here we describe construction of the mouse model of subcutaneous phaeohyphomycosis and related experiments. We hope that this chapter can be beneficial for the study of phaeohyphomycosis and facilitate the development of new diagnostic and therapeutic approaches.

Key words Phaeohyphomycosis, Dematiaceous fungi, Mouse models, Subcutaneous infection, Immunity

1 Introduction

Phaeohyphomycosis refers to infections caused by a large group of heterogenous organisms called "dematiaceous" or "melanized" fungi [1]. It includes a broad spectrum of diseases, which usually include keratitis, superficial cutaneous or subcutaneous disease, deep local infections, pulmonary infections, central nervous system (CNS) infections, as well as disseminated disease [2]. Dematiaceous fungi comprise a group of polyextremotolerant fungi, mainly belonging to the order Chaetothyriales, which are capable of colonizing a wide range of extreme environments [2]. Most clinically relevant species are located in the genera such as *Exophiala*, *Cladophialophora*, *Coniosporium*, *Cyphellophora*, *Fonsecaea*, *Phialophora*, and *Rhinocladiella* [3].

Although phaeohyphomycosis is rare, it is significant because of its occurrence in otherwise healthy individuals and the emergence within immunocompromised populations [4]. Recently, some of the highly recalcitrant, disseminated dematiaceous fungal infections

Rebecca A. Drummond (ed.), *Antifungal Immunity: Methods and Protocols*, Methods in Molecular Biology, vol. 2667,
https://doi.org/10.1007/978-1-0716-3199-7_12,

associated with *CARD9* mutations were reported [5–12]. At the same time, a *Card9* knockout (*Card9*$^{-/-}$) mouse model was created to study CARD9 immunity [13]. So phaeohyphomycosis was modeled by the subcutaneous injection of live *P. verrucosa* or *E. spinifera* conidia into the footpads of *Card9*$^{-/-}$ mice [14, 15].

Here, we describe the materials, methods, and notes for constructing mouse models of phaeohyphomycosis in detail. These steps include conidia suspension preparation, establishment of subcutaneous phaeohyphomycosis mouse model, footpad swelling rate assay, fungal burdens measurement in the infected footpads, survival rates assay, histopathological analysis, and local immune responses study. We hope that this chapter could be helpful to benefit the study of phaeohyphomycosis and facilitate the development of new diagnostic and therapeutic approaches.

2 Materials

2.1 Subcutaneous Phaeohyphomycosis Mouse Model

1. Mice: Six- to 8-week-old C57BL/6 mice should be maintained in specific pathogen-free facilities. WT and knockout mice should be matched for sex and age. Animal studies needed to be approved by the Institutional Ethics Committee of your affiliation and performed in the Biosafety Level II Laboratory (*see* **Note 1**).
2. Fungal isolates: *P. verrucose*, *F. pedrosoi*, *C. carrionii*, *E. spinifera*, and other black yeast isolates (*see* **Note 2**).
3. Potato dextrose agar (PDA) medium: prepare PDA powder and distilled water and autoclave PDA medium (3.9% in water), then pour into 75 cm^2 culture flask to make PDA slants.
4. Oatmeal agar (OA) medium: prepare OA powder and distilled water and autoclave OA medium (7.25% in water), then pour into 75 cm^2 culture flask to make OA slants.
5. Sterile saline.
6. PBS.
7. Pipette.
8. Gauze.
9. Hemocytometer (*see* **Note 3**).
10. Microscope.
11. 0.5% sodium pentobarbital.
12. 1 mL sterile syringe.
13. Mouse fixator.

2.2 Footpad Swelling Rate Assay

1. Micrometric caliper.
2. Camera (*see* **Note 4**).

2.3 Fungal Burdens Measurement

1. Sterile scissors and tweezers.
2. Tissue homogenizer (*see* **Note 5**).
3. Sterile saline.
4. 75% alcohol.
5. Sabouraud dextrose agar (SDA) medium: prepare SDA powder and distilled water and autoclave SDA medium (6.5% in water), then pour into culture dish.

2.4 Histopathological Analysis

1. Sterile scissors and tweezers.
2. 75% alcohol.
3. 4% formalin solution.
4. Hematoxylin and eosin (HE) staining buffer: hematoxylin staining solution, eosin staining solution.
5. Periodic acid–Schiff (PAS) staining buffer: periodic acid solution, Schiff reagent, hematoxylin staining solution.

2.5 Local Immune Responses Study

1. Sterile scissors and tweezers.
2. 75% alcohol.
3. RNA later (*see* **Note 6**).
4. Electric homogenizer.
5. Trizol.
6. Chloroform (*see* **Note 7**).
7. Isopropanol.
8. DEPC solution.
9. Takara reverse transcriptase.
10. Power SYBR® Green PCR Master Mix.
11. Primer (*see* **Note 8**).
12. RNase-free water.
13. Tissue homogenizer.
14. Mouse cytometric bead array (CBA) Th1/Th2/Th17 kit, Mouse CXCL1 duo-set ELISA kit, Mouse CXCL2 duo-set ELISA kit, Mouse IL-22 duo-set ELISA kit, ELISA solution buffer.
15. Liberase, DNAse I.
16. Fluorescent conjugated antibodies (*see* **Note 9**).
17. 7-amino-actinomycin D (7-AAD).
18. Staining buffer.

3 Methods

Carry out all procedures with attention to aseptic operation.

3.1 Conidia Suspension Preparation

1. Culture *P. verrucose*, *F. pedrosoi,* and *C. carrionii* isolates on oatmeal agar for 14–21 days at 28 °C, and *E. spinifera* isolate should be cultured on potato dextrose agar for 14–21 days at 28 °C (*see* **Note 10**).
2. Rinse the agar slants with sterile saline and collect the conidia suspension with the sterile pipette.
3. The suspensions of *P. verrucose*, *F. pedrosoi*, *C. carrionii,* and *E. spinifera* were filtered through 8 layers of sterile gauze to remove hyphae and medium components (*see* **Note 11**).
4. Wash the conidia suspensions twice with sterile PBS buffer and centrifuge at 1000 g for 8 min. Then resuspend sediment with sterile saline, and adjust the concentration of conidia suspensions to 1×10^9 CFU/mL.

3.2 Establishment of Subcutaneous Phaeohyphomycosis Mouse Model

1. Before inoculation, each mouse was restrained and injected intraperitoneally with 0.5% sodium pentobarbital at 10 μL/g (*see* **Note 12**).
2. Using a 1 mL sterile syringe, subcutaneously inject 100 μL of the viable conidia suspensions of different dematiaceous fungi into the two hind footpads of the mouse. The injection concentrations of the viable conidia suspensions were: *P. verrucose* 1×10^8 CFU/mL, *F. pedrosoi* 1×10^9 CFU/mL, *C. carrionii* 1×10^9 CFU/mL, and *E. spinifera* 5×10^8 CFU/mL (*see* **Note 13**).

3.3 Footpad Swelling Rate Assay

1. Using micrometric caliper to measure the thickness of mouse hind footpads before inoculation and every week after inoculation and calculate the footpad swelling rate;

   Footpad swelling rate (%) = {footpad thickness after inoculation (mm) − footpad thickness before inoculation (mm)}/ footpad thickness before inoculation (mm) × 100% (*see* **Note 14**).

3.4 Fungal Burdens Measurement in the Infected Footpads

1. The footpad skin lesions were excised under aseptic operation, weighed, and recorded.
2. Transfer the excised tissue to a tissue homogenizer, add 1 mL of sterile saline, and grind it to prepare the tissue homogenate (*see* **Note 15**).
3. The tissue homogenate was serially diluted with sterile saline, and the dilutions were 1:1, 1:10, 1:100, and 1:1000, respectively. Add 100 μL of the tissue homogenate of different

dilutions on the SDA medium, and evenly spread. Do two replicates for each dilution.

4. Count the colony forming unit (CFU) after culturing at 28 °C for 1 week, and the fungal burdens ($Log_{10}CFU/g$) were calculated. $Log_{10}CFU/g = Log_{10}$ {CFU/ tissue weight(g)}.

3.5 Survival Rates Assay

Observe mice over 12 weeks and record mice that were found moribund as deaths for survival analysis. The amount of mice kept to observe the survival rate is 10–12, and the death due to improper operation was recorded as data lost (*see* **Note 16**).

3.5.1 Expected Results

In our experience, the death of *Card9* KO mice often occurs 4–6 weeks after infection with 1×10^7 CFU *P. verrucose*, 1×10^8 CFU *F. pedrosoi*, 1×10^8 CFU *C. carrionii*, and 5×10^7 CFU *E. spinifera*, respectively. Generally, there was no mortality in WT mice.

3.6 Histopathological Analysis

1. At week 6–10 post-infection, two mice from each group infected with dematiaceous fungi were euthanized, immersed in 75% alcohol for 10 min.
2. Use sterile scissors and tweezers to cut the footpad skin lesions and visceral tissues, including brain, lung, liver, spleen, kidney, inguinal lymph node tissue, in a benchtop. Then place them in formaldehyde (10%), and fix at room temperature for 24 hours (*see* **Note 17**).
3. The tissues were washed with water and dehydrated with 70%, 80%, 90%, 95%, and 100% ethanol gradient for 30 min.
4. We used xylene to transparent, then dipped wax, embedded in paraffin, and cut into slices.
5. The slices were about 2 μm in thickness and stained with hematoxylin–eosin (HE) and periodic acid–Schiff stain (PAS) separately.
6. Histopathological characteristics were observed under light microscope. HE staining showed chronic granulomatous changes with intense lymphocytes, histocytes, neutrophils and other inflammatory cells infiltrating throughout the dermis. Dematiaceous yeast and hyphae were noted with HE staining and were obvious with PAS staining (Fig. 1).

3.7 Local Immune Responses Study

3.7.1 qRT-PCR Analysis for Relative Cytokine and Chemokine Gene Expression in Footpad Skin Tissue

1. At day 3 and 7 post-infection, three mice from each group were euthanized and immersed in 75% alcohol for 10 min. The relative mRNA expression levels of proinflammatory cytokines (IL-1β, TNF-α, and IL-6) and neutrophils attracting chemokines (CXCL1, CXCL2, and CXCL5) were determined in day 3 samples, and those of adaptive cytokine (IFN-γ, IL-17A, and IL-22) were assessed in day 7 samples.

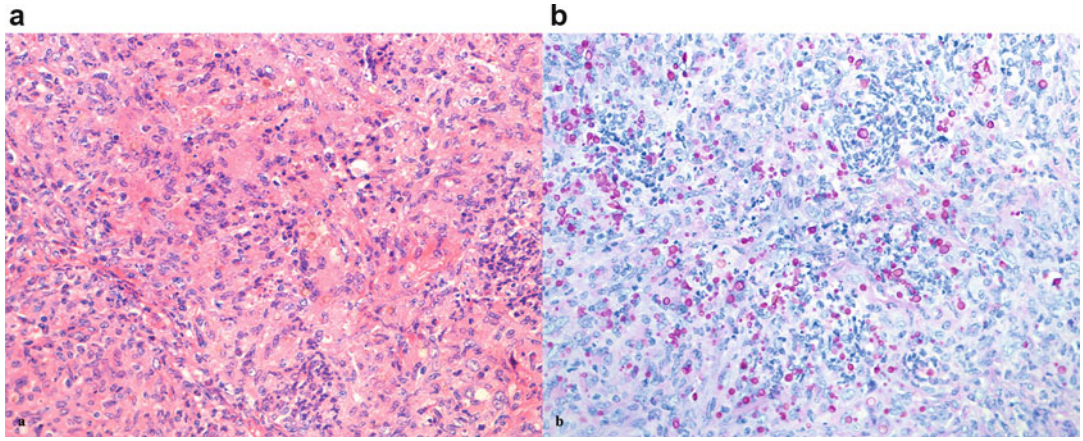

Fig. 1 Histopathology of HE-stained (**a**) or PAS-stained (**b**) footpad from infected *Card9* KO mice at 8 weeks after *E. spinifera* infection. HE staining showed intense lymphocytes, histocytes, neutrophils, and other inflammatory cells infiltrating throughout the dermis. Dematiaceous yeast and hyphae were red with PAS staining

2. Use sterile scissors and tweezers to cut the footpad skin lesions in a benchtop, and put them into sterile EP tube containing RNA later.
3. Total RNA extracts from tissues were prepared with TRIzol reagent, and the subsequent reverse transcription was carried out using Takara reverse transcriptase according to the protocol supplied by the manufacturer's instructions (*see* **Note 18**).
4. Power SYBR® Green PCR Master Mix-based quantitative real-time polymerase chain reaction was performed by real-time PCR with the ViiATM 7 system (*see* **Note 19**).
5. Relative gene expression of each target gene was determined after normalization with transcript levels of GAPDH using the $2^{-\Delta\Delta Ct}$ method.

3.7.2 Measurement for Proteins of Cytokine and Chemokine in Footpad Homogenates

1. At day 3 and 7 post-infection, three mice from each group were euthanized and immersed in 75% alcohol for 10 min.
2. Use sterile scissors and tweezers to cut the footpad skin lesions in a benchtop, put them into the pre-weighed sterile EP tube, and use a balance to measure the weight of the skin tissue.
3. Transfer the skin tissue to an autoclaved tissue grinder, add pre-cooled sterile saline at the rate of 10 μL of pre-cooled sterile saline to 1 mg of tissue, and grind it on ice to prepare tissue homogenate. Then centrifuge at 4 °C, 1000 g for 10 min, aspirate the supernatant, aliquot them, and store in −70 °C refrigerator (*see* **Note 20**).
4. The protein levels of cytokines TNF-α, IL-1β, IL-6, IFN-γ, IL-17A in the skin tissue homogenate were detected using the

Cytometric Bead Array (CBA) Mouse TH1/TH2/TH17 Cytokine kit (BD Biosciences) according to the manufacturer's instructions. The protein levels of proinflammatory cytokines (TNF-α, IL-1β, IL-6) were determined in day 3 samples, and those of adaptive cytokine (IFN-γ, IL-17A) were assessed in day 7 samples (*see* **Note 21**).

5. Use R&D duo-set ELISA kit to detect the protein levels of cytokine IL-22 and chemokines CXCL1 and CXCL2 in skin tissue homogenate as the manufacturer's instructions (*see* **Note 22**). The protein levels of chemokines CXCL1 and CXCL2 were determined in day 3 samples, and those of cytokine IL-22 were assessed in day 7 samples.

3.7.3 Local Neutrophils Infiltration by FACS Analysis

1. Prepare the dissociation solution. Add 0.025 mg/mL Liberase and 50 mg/mL DNAse I to PBS, and store at 4 °C (*see* **Note 23**).
2. Use sterile scissors and tweezers to cut the footpad skin lesions under sterile conditions, and transfer them to a 6-well culture plate containing dissociation solution.
3. Mince the tissue with sterile scissors and incubate them at 37 °C and 5% CO_2 condition for 30 minutes.
4. Transfer the above digested tissue to a 70 mm cell strainer above the 50 mL centrifuge tube, and mildly grind the tissue with the plunger of a 5 mL syringe.
5. Use ice-cold PBS to wash the remaining tissue on the strainer, centrifuge the single-cell suspension at 400 g for 5 min, and discard the supernatant.
6. Wash the digested cells with ice-cold PBS, resuspend them in staining buffer, and adjust the cell concentration to 1×10^6/mL.
7. Transfer 1 mL of single-cell suspension into a flow cytometry tube, adjust the total volume to 100ul, add up to 0.25 μg Alexa Fluor 488 anti-mouse CD11b antibody, phycoerythrin anti-mouse Ly-6G antibody and the corresponding isotype antibody, and incubate at 4 °C for 30 minutes according to the manufacturer's instructions.
8. Wash stained cells with ice-cold PBS, centrifuge them at 400 g for 6 min, and discard the supernatant.
9. Resuspend the cells in 300 μL staining buffer, add 5 μL 7-amino-actinomycin D (7-AAD) to each tube, and incubate for 5 minutes (*see* **Note 24**).
10. The proportion of 7-AAD$^-$CD11b$^+$Ly-6G$^+$ neutrophils was assessed by flow cytometry.

4 Notes

1. During the experiment, the number of mice in each group needed to be designed in advance according to the project to be carried out. For example, at least 10–12 mice were required for the observation of survival rate. C57BL/6 mice were relatively ferocious, so operators should wear thick gloves to grasp the mice when they established the subcutaneous phaeohyphomycosis mouse model.
2. According to the experimental purpose, select clinical strains or environmental strains. The strains needed to be recovered first and then passaged at least 2 times after recovery.
3. There will be artificial error in conidia counting, so it should be counted at least 3 times and the average value should be taken.
4. When taking photos of footpads, you should pay attention to the focus, so as to ensure the clarity of the photos. In addition, abnormal signs such as extremity mutilation, local or distant skin masses or ulcers, and central nervous system involvement should be recorded.
5. The tissue homogenizer should be autoclaved and then placed in an oven to dry before use.
6. If the tissue RNA could not be extracted immediately, the tissue could be stored for at least 2 months by immersing in RNA later and placing in −30 °C or − 70 °C.
7. TRIzol, chloroform, isopropanol, and DEPC solutions were toxic and harmful, so you needed to wear masks and gloves during the experiments.
8. The quantitative real-time PCR reaction system included 50 ng cDNA, 10 μL SYBR Green Mix, 1 μL sense primer, 1 μL antisense primer, RNase-free ddH_2O adding to make up the total volume to 20 μL.
9. The recommended antibodies were Alexa Fluor 488 anti-mouse CD11b antibody and isotype antibody, phycoerythrin anti-mouse Ly-6G antibody, and isotype antibody. The concentration of antibodies should be tested before starting.
10. *P. verrucose, F. pedrosoi, and C. carrionii* had difficulty producing spores so nutrient-rich oatmeal agar medium was required. *E. spinifera* was a black yeast that could be cultured on potato dextrose agar. Pay attention to prevent contamination during incubation.
11. The filter was made by cutting off the end of a 15 mL centrifuge tube and placing the 8-layer gauze in it, and then autoclaving.
12. Expose the hind footpads of the mouse using a specialized mouse fixator.

13. The injection concentrations of the viable conidia suspensions were obtained according to the preliminary experimental conditions such as the conidia production and growth rate.
14. Footpad swelling rate was entered into GraphPad software and graphed to observe trends. Then you can compare differences between different groups.
15. Grind the tissue as finely as possible while allowing the liquid from the pestle to drain into the grinding fluid after grinding.
16. When mice were died, it was necessary to determine the cause of death and perform an autopsy. Dissect the viscera, observe the gross appearance and histopathology of the viscera, and determine whether there was the dissemination of dematiaceous fungi. When the dissemination of dematiaceous fungi occurred, black spots were occasionally observed on the surface of the organ, and pigmented hyphae, pseudohyphae, and conidia positive for PAS staining could be seen in tissue sections like lung and brain [7, 14, 15].
17. Pathological skin tissue collection should pay attention to protect the integrity of epidermis and dermis.
18. Take care to extract RNA in an RNase-free environment to prevent RNA degradation.
19. Add Power SYBR® Green PCR Master Mix in dark conditions.
20. The entire procedure should be performed on ice to prevent protein degradation.
21. The catalogue number of CBA Mouse TH1/TH2/TH17 Cytokine kit (BD Biosciences) is 560,485. This is what we recommend, but other kits may be suitable for your experiment.
22. The catalogue number of R&D Mouse IL-22 duo-set ELISA kit is DY582.
23. Dissociation solution should be prepared immediately before use.
24. Neutrophils had a short lifespan and were prone to death, so 7-amino-actinomycin D (7-AAD) was used to exclude dead cells.

References

1. Arcobello JT, Revankar SG (2020) Phaeohyphomycosis. Semin Respir Crit Care Med 41: 131–140
2. Moreno LF, Vicente VA, de Hoog S (2018) Black yeasts in the omics era: achievements and challenges. Med Mycol 56:32–41
3. Seyedmousavi S, Netea MG, Mouton JW et al (2014) Black yeasts and their filamentous relatives: principles of pathogenesis and host defense. Clin Microbiol Rev 27:527–542
4. Chowdhary A, Perfect J, de Hoog GS (2014) Black molds and Melanized yeasts pathogenic to humans. Cold Spring Harb Perspect Med 5: a019570
5. Wang X, Wang W, Lin Z et al (2014) *CARD9* mutations linked to subcutaneous

phaeohyphomycosis and TH17 cell deficiencies. J Allergy Clin Immunol 133:905–908

6. Lanternier F, Barbati E, Meinzer U et al (2015) Inherited CARD9 deficiency in 2 unrelated patients with invasive Exophiala infection. J Infect Dis 211:1241–1250
7. Wang X, Zhang R, Wu W et al (2018) Impaired specific antifungal immunity in CARD9-deficient patients with Phaeohyphomycosis. J Investig Dermatol 138:607–617
8. Huang C, Zhang Y, Song Y et al (2019) Phaeohyphomycosis caused by *Phialophora Americana* with *CARD9* mutation and 20-year literature review in China. Mycoses 62:908–919
9. Arango-Franco CA, Moncada-Velez M, Beltran CP et al (2018) Early-onset invasive infection due to *Corynespora cassiicola* associated with compound heterozygous *CARD9* mutations in a Colombian patient. J Clin Immunol 38:794–803
10. Wang C, Xing H, Jiang X et al (2019) Cerebral Phaeohyphomycosis caused by *Exophiala dermatitidis* in a Chinese CARD9-deficient patient: a case report and literature review. Front Neurol 10:938
11. Guo Y, Zhu Z, Gao J et al (2019) The Phytopathogenic fungus *Pallidocercospora crystallina*-caused localized subcutaneous Phaeohyphomycosis in a patient with a homozygous missense *CARD9* mutation. J Clin Immunol 39:713–725
12. Perez L, Messina F, Negroni R et al (2020) Inherited CARD9 deficiency in a patient with both *Exophiala spinifera* and *aspergillus nomius* severe infections. J Clin Immunol 40:359–366
13. Hsu YM, Zhang Y, You Y et al (2007) The adaptor protein CARD9 is required for innate immune responses to intracellular pathogens. Nat Immunol 8:198–205
14. Wu W, Zhang R, Wang X et al (2016) Impairment of immune response against dematiaceous fungi in *Card9* knockout mice. Mycopathologia 181:631–642
15. Wu W, Zhang R, Wang X et al (2018) Subcutaneous infection with dematiaceous fungi in *Card9* knockout mice reveals association of impair neutrophils and Th cell response. J Dermatol Sci 92:215–218

Chapter 13

Genetic Mouse Models of Pneumocystis Pneumonia

J. Claire Hoving, Ferris T. Munyonho, and Jay K. Kolls

Abstract

Pneumocystis jirovecii causes pneumonia in immunocompromised patients. A major challenge in drug susceptibility testing and in understanding host/pathogen interactions is that *Pneumocystis* spp. are not viable in vitro. Continuous culture of the organism is not currently available, and therefore, developing new drug targets is very limited. Due to this limitation, mouse models of Pneumocystis pneumonia have proven to be an invaluable resource to researchers. In this chapter, we provide an overview of selected methods used in mouse models of infection including, in vivo *Pneumocystis murina* propagation, routes of transmission, genetic mouse models available, a *P. murina* life form-specific model, a mouse model of PCP immune reconstitution inflammatory syndrome (IRIS), and the experimental parameters associated with these models.

Key words *Pneumocystis murina*, Immunocompromised, Rag1-deficient, Lung fungal infection, Immune response

1 Introduction

Despite the challenges faced in studying Pneumocystis pneumonia (PCP), there have been major accomplishments in this field. For example, the development of a PCR-based diagnostic assay, which has improved noninvasive diagnosis, and the genome analysis of three *Pneumocystis* spp., which identifies key players in metabolic functions and pathways [1]. This analysis has provided invaluable insight into the genetic composition of *Pneumocystis* spp. and has clearly demonstrated the very many genes that have been lost, resulting in obligate biotrophy. This unusual pathogen composition also challenges current anti-fungal treatment strategies. For example, *Pneumocystis* spp. contain cholesterol rather than ergosterol within the cell wall, which is the target for Azoles and Amphotericin B. Also, only the cell wall of the cyst and not the trophs contain beta-glucan, which limits the efficacy of Echinocandins. Therefore, current treatment strategies make use of antibiotics that target folate biosynthesis in microorganisms.

Rebecca A. Drummond (ed.), *Antifungal Immunity: Methods and Protocols*, Methods in Molecular Biology, vol. 2667,
https://doi.org/10.1007/978-1-0716-3199-7_13,

Not only has the development of various mouse models significantly advanced our understanding of the host–organism interactions and host defense mechanisms, but these models also allow for the propagation of *Pneumocystis murina*. Numerous attempts to culture this pathogen outside of murine hosts have been made with limited success, which are elegantly reviewed by Cushion and colleagues [2]. Therefore, immunocompromised mice play an important role in maintaining *P. murina* stock for infection studies. Initially, athymic mice (nu/nu) were used to propagate *P. murina* [3]. However, additional genetically modified, immunocompromised mice have been included in this protocol due to their inability to clear infection. There are various methods used to infect mice with *P. murina*. Early experiments demonstrate that *Pneumocystis* spp. is naturally acquired by horizontal transmission as an airborne organism because animals co-housed with infected mice develop disease [4–8]. While this infection model replicates natural transmission, due to the lack of reproducibility, and control of the infection timeline, other modes of infection are favored. For a more reproducible and reliable infection model, the organisms can be deposited directly into the respiratory tract. A limitation of this approach is that animals are typically infected with a combination of asci and trophs, which does not model natural transmission. However, this inoculation model has been useful to define cellular immune requirements for fungal clearance. This is done with either intranasal, oropharyngeal, or intratracheal instillation or the more invasive transtracheal deposition [3, 8].

While the cyst is thought to be transmitted from one host to another, it is the trophic form that is associated with tight adherence to the type I pneumocyte and replication within the host. Indeed, the trophic form has also been shown to manipulate host immunity, potentially allowing the cyst to evade detection by the host immune response [9]. Models that can differentiate the host immune response to individual life-stage forms during infection are invaluable. By taking advantage of the fact that cysts and trophs vary in structure in that β-1,3-D glucan, the target of echinocandins, is absent in trophic forms but abundant in the cyst wall, the mouse model for depleting cysts is described in this chapter [10]. Cushion et al. demonstrate that while echinocandin treated mice still have trophs present, these trophs are unable to transmit infection [10]. Since *Pneumocystis* spp. takes advantage of a weakened immune system, there is usually an underlying predisposing factor which promotes infection and leads to disease. Most patients affected by PCP have HIV. PCP develops in advanced HIV disease where CD4 T cell counts have been significantly depleted. As there is a weakened immune response, *Pneumocystis* spp. may go undetected until the CD4 T cell number increases because of antiretroviral therapy (ART). The recovery of T cell-mediated immunity can lead to a rapid and exaggerated immune response to previously

"hidden" pathogens. This is immune reconstitution inflammatory syndrome (IRIS) and pulmonary IRIS, is associated with *P. jirovecii* in humans, and has a high morbidity and mortality rate [11–14]. In this chapter, we additionally include a description of the PCP-IRIS mouse model. Lastly, we also describe key experimental parameters used to evaluate and analyze the mouse models of infection, including microscopy, qPCR, β-D-glucan measurement, and plethysmography, for lung function analysis.

2 Materials

2.1 Pneumocystis Murina *Propagation In Vivo*

1. Sterile PBS.
2. 70 μm sieve attached to a 4 mL syringe.
3. Giemsa stain.
4. Fisher brand slides of known circumference.

2.2 Pneumocystis Murina *Infections*

1. Anesthetic (e.g., isofluorane).
2. Suture wire.
3. Forceps, pipettor, and tips.
4. 18-gauge blunt needle.
5. Polyethylene catheter.

2.3 *Tissue Collection and Analysis*

1. 10% formalin.
2. PBS (containing 0.5 mM EDTA).
3. 20-gauge cannula.
4. 3–10 cc syringe.
5. Giemsa stain.
6. Trizol or Qiagen RLT+.
7. RNA isolation kit.
8. cDNA synthesis kit.
9. *Pneumocystis murina*-specific mitochondrial small subunit (mtSSU) rRNA primers or/and mitochondrial large subunit (mtLSU) primers MouseOx or other murine pulse oximeter.

3 Methods

3.1 Pneumocystis Murina *Propagation In Vivo*

1. *Pneumocystis murina* is propagated and passaged in immunocompromised mice [3, 9, 15, 16] (*see* **Note 1**).
2. Prepare a single cell suspension from the whole lung of an infected mouse, stored at −80 °C in 1 mL PBS. Thaw the

lung suspension and strain through a 70 μm cell strainer in 4 mL PBS.

3. Wash the suspension by centrifugation at 2000 rpm for 10 minutes at 4 °C and resuspend the pellet in 1 mL PBS.
4. Quantify the inoculum with a 1:10 dilution (5 μL) on fisher brand microscope slides with a known diameter and stain with Giemsa stain, which stains both cysts and trophs.
5. Count the number of cysts with a light microscope x 100 oil immersion lens and adjust the inoculum concentration to 2 x 10^6 cysts/mL in PBS (*see* **Note 2**).
6. Infect mice with the freshly prepared inoculum at 2x10^6 cysts/mL via oropharyngeal instillation in 100 μL (or 2 x 10^5 cysts per mouse).

3.2 Route of Experimental Infection

Host-to-host transmission of *Pneumocystis* spp. is established in rodent models and is highly suggested in humans. In mice:

3.2.1 Natural Transmission/Co-Housing Model

1. Place two immunocompromised /immunosuppressed seed mice (previously infected with *P. murina* for 4 weeks), with 10 to 15 recipient mice and cohabitate for up to 4 weeks (*see* **Note 3**).
2. After the seeding period, sacrificed mice to confirm *P. murina* infection with microscopy or qPCR.

3.2.2 Intranasal Instillation

1. Administer 50 μL (4 × 10^6 cysts/mL) of the inoculum to anesthetized mice as droplets at the nares using a pipettor.
2. Observe the inhalation of inoculum and allow mice to recover from anesthesia.

3.2.3 Oropharyngeal Instillation

1. Suspended anesthetized mice by their front incisors, gently extending tongue with forceps (*see* **Note 4**). Administer 100 μL of the inoculum (2 × 10^6 cysts/mL) via the trachea with a pipettor.
2. Observe the inhalation of inoculum, release the tongue, and allow mice to recover from anesthesia.

3.2.4 Transtracheal Injection

1. This procedure requires the surgical exposure of the anterior trachea in anesthetized mice.
2. Place mice supine with the head slightly elevated at 45 degrees. Make a superficial midline incision in the anterior neck to expose the trachea.
3. Pass an 18-gauge blunt needle through the mouth into the trachea and verify the position visually.
4. Thread a polyethylene catheter through the needle so that the catheter tip extends just beyond the needle in the mid-trachea.

Laboratory tape can be applied to the catheter to prevent advancement of the catheter into a distal mainstem bronchus.

5. Inject the inoculum (100 μL of 2×10^6 cysts/mL) through the catheter into the lungs and follow immediately with 0.25 mL air.
6. Remove the needle and catheter suture the incision and allow mice to recover from anesthesia [3].

In addition to the route of infection, genetic mouse models play a key role in understanding host response to infection. These models are summarized in Table 1 and **Note 5**.

Furthermore, there are infection models used to target specific life forms, such as the specific depletion of cysts using echinocandins (*see* **Note 6**).

3.3 IRIS Mouse Model

A mouse model of PCP IRIS has been established to determine the underlying factors which contribute to the immune mechanism of this pathological response [11, 13, 14]. There are slight variations to this model but essentially include the following:

1. Infect female SCID mice with *P. murina* by either direct intranasal inoculation (1×10^5 cysts) or co-housing.
2. For co-housing experiments, house mice with heavily infected SCID mice for 6 weeks prior to immune reconstitution.
3. After 17–21 days, reconstitute mice with 5×10^7 splenocytes from naive C57BL/6 J donor females or congenic spleen cells from normal C.B-17 mice via intraperitoneal injection.
4. Following reconstitution mice develop IRIS and clear *P. murina* infection within 3 weeks.
5. Depleting $CD4^+$ T cells, protects mice from the acute pathophysiology of IRIS, but these mice are unable to clear infection [11].
6. The depletion of regulatory T cells from the splenocytes accelerates IRIS [17].

3.4 Experimental Parameters

Euthanize mice with slow rising halothane (5% in air) or other AALAC approved methods followed by cardiac puncture for blood collection.

3.4.1 BAL Fluid Collection for P. Murina Detection

1. Collect BAL fluid from infected mice by inserting a cannula in the trachea of terminally anesthetized mice (BAL is also used for β-1,3-D-Glucan detection, *see* **Note 7**).
2. Lavage three times with 1 mL, warmed PBS (containing 0.5 mM EDTA) instilled into the bronchioles.
3. Gently retract the fluid to maximize BAL fluid retrieval and to minimize shearing.
4. Stain BAL fluid with Giemsa to enumerate *P. murina* cysts.

Table 1
Summary of the susceptible genetic mouse models and laboratory strategies used to induce Pneumocystis pneumonia

Genetic mouse models	Susceptibility	Inoculation strategy
Rag1$^{-/-}$	Lack B cells and T cells	By co-housing with Pneumocystis infected RAG-1 mice [15]
Rag2$^{-/-}$	Lack B cells and T cells	By injecting the PCP inoculum intratracheally [23, 24]
CB-17 SCID	These mice are on a Balb/c background and are useful for genetic studies on that background	Passively by co-housing with Pneumocystis infected SCID mice [25]. Passively without co-housing; by nonaxenically housing untreated SCID mice [26]
Cd40$^{-/-}$	CD40 is required for B cell proliferation and immunoglobulin class switch recombination	Injecting the PCP inoculum intratracheally [27]
Cd40lg$^{-/-}$	CD40L is expressed on activated T cells and both mice and humans with CD40L mutations develop hyper-IgM syndrome	By co-housing with PCP-infected mice [28]
B6.129S2-Ighmtm1Cgn/J	uMT mice lack B cells, which have been shown to be critical antigen presenting cells to prime *Pneumocystis* spp. specific CD4+ T response in the lung AID/μS$^{-/-}$ mice lack surface B cell receptors as well as secreted immunoglobulins	By injecting the PCP inoculum intratracheally [27]
Cd4-Stat3$^{-/-}$	CD4+ T cells are essential for fungal clearance and deletion of STAT3 in T cells greatly perturbs fungal clearance in mice	By injecting the PCP inoculum intratracheally [3]
Il21R$^{-/-}$	Il21r−/− as well as Il21−/− mice fail to clear *P. murina* infection	By oropharyngeal aspiration using the tongue-pull technique [18]
Sftpa1$^{-/-}$	These mice also support a higher fungal burden compared to control mice	By co-housing with PCP infected mice [29]

3.4.2 Lung Histopathology

5. Remove the right lobe by first tying off the right mainstem bronchus with suture.
6. Cannulate the trachea with a polyethylene cannula attached to 3–10 cc syringe filled with 10% formalin solution in PBS.
7. Inflate the left lung with 0.5–1 mL formalin and tie the trachea with suture to keep the lung inflated.
8. Place the left lung in 10% formalin solution in PBS for histological processing (embedded in paraffin and stained with GMS or hematoxylin-eosin stains).

3.4.3 RNA Isolation and Quantitative PCR for P. Murina

Total RNA is isolated from the lung tissue of infected mice using the Trizol or Qiagen RLT+ method as per the manufacturer's instructions [18–21]. Below is the Trizol protocol:

1. Remove two right lobes and homogenize in 800 μL Trizol.
2. Isolate RNA and synthesize cDNA as per the manufacturer instructions (using 1 μg of total RNA per 20 μL reaction).
3. Quantify *P. murina* burden using SsoAdvanced quantitative RT-PCR (qRT-PCR) universal probe super mix, with the following *P. murina*-specific **mitochondrial small subunit (mtSSU) rRNA primers**:

   Forward: 5′-CATTCCGAGAACGAACGCAATCCT;

   Reverse: 5′-TCGGACTTGGATCTTTGCTTCCCA;

   FAM probe: 5′-TCATGACCCTTATGGAGTGGGCTACA.
4. Alternatively, the *P. murina*-specific **mitochondrial large subunit (mtLSU) rRNA** can be quantified using one-step TaqMan RT-PCR reagents and the following primers [19]:

   Forward: 5′-ATG AGG TGA AAA GTC GAA AGG G-3′.

   Reverse: 5′-TGA TTG TCT CAG ATG AAA AAC CTC TT-3′.

   FAM probe: 5′-6FAM- AACAGCCCAGAATAATGAA TAAAGTTCCTCAATTGTTAC-TAMRA.

3.4.4 Plethysmography (for IRIS)

To measure the effect of PCP IRIS on lung function, the physiological assessment of live and ventilated mice can be determined [13, 14]. For this procedure, dynamic pulmonary compliance and resistance is measured.

1. Anesthetize mice by intraperitoneal injection of 0.13 mg pentobarbital sodium/gram body weight.
2. If desired pulse oximetry can be performed at this stage using a MouseOx or other murine pulse oximeter.
3. Perform a tracheostomy and insert a 20-gauge cannula 3 mm into an anterior nick in the exposed trachea.
4. Open the thorax to equalize airway and transpulmonary pressure.

5. To assure mice tolerate the procedure, examine them for spontaneous respirations before proceeding further.
6. Place mice in the plethysmograph immediately and connect to a Harvard rodent ventilator.
7. The data collected is analyzed as described by Bhagwat et al. (2006) [13].
8. Lung compliance and resistance is calculated and normalized for peak body weight.
9. As an alternative to Plethysmography (for IRIS), investigators can measure parameters of lung injury in BAL fluid including LDH and total protein as measures of lung injury.

4 Notes

1. *Pneumocystis murina* is incapable of being continuously cultivated in ex vivo culture systems. Therefore, immunocompromised mice can be used to propagate organisms. These include recombinant activating gene (Rag)1-deficient mice (B6.129S7-*Rag1*^{tm1Mom}/J) [15], Rag2-deficient mice (B6-Rag2tm1Fw) [9], and *Rag2*$^{-/-}$*Il2rg*$^{-/-}$ (B10; B6-*Rag2*^{tm1Fwa} *Il2rg*^{tm1Wjl}) double deficient mice [16].
2. To enumerate the number of cysts, the slide has a circle of known area. The number of cysts is counted per diameter and πr2 used to calculate the number of cysts for the known area where π =3.14 and r = number of cysts/2. Alternatively, an aliquot of the inoculum can be used for RNA extraction followed by RT-PCR to assess the mtLSU or other gene target to quantify the inoculum.
3. Depending on local animal husbandry requirements, the ratio of infected mice to naïve mice can be as low as 1:4 per cage. Unseeded immunocompromised/immunosuppressed control mice are housed separately to prevent exposure to seeded mice.
4. It is important to be gentle in the tongue pull procedure to not bruise the tongue that can result in swelling which can compromise food and water intake. Pulling the tongue forward creates mild pressure on the upper esophagus which allows the inoculum to be deposited in the trachea.
5. Failure to successfully propagate *Pneumocystis* spp. in vitro has been a major impediment to studying the biology of this pathogen. This has necessitated the development of various in vivo animal models of Pneumocystis pneumonia to study the pathogenesis, virulence, elicited immune responses, diagnosis, and treatment strategies for this opportunistic fungal pathogen [8]. Genetically modified mouse models represent a keystone

for the in vivo studies of Pneumocystis pneumonia and have been widely used for their well-characterized physiology along with their genetic and biochemical similarities with human [8, 22]. These models can be broadly categorized into two groups: (I) models that are generally immunocompromised, such as the SCID (severe combined immunodeficiency disease), Rag-$1^{-/-}$ and Rag-$2^{-/-}$ mice which do not have functional B- or T-cells; and (II) models with a specific target gene involved in the host response [8], for example, the CD40, CD40L, B cells, IL-21R, and SP-A-knockout mice. Table 1 summarizes susceptible mouse strains and the various strategies used to induce *P. murina* to these models. Lastly, resistant mouse strains can be used to determine immune mechanisms in human disease. These include wild-type BALB/c mice, C57Bl/6 mice, as well Il17Ra$^{-/-}$ or Rorc$^{-/-}$ mice (on a C57Bl/6 mouse background). These mice develop productive *P. murina* infection up to 2 weeks but then eradicate the fungus by 4–6 weeks postinoculation.

6. To directly study the role the trophic form plays in the host, the cysts can be depleted using echinocandins. Cushion and colleagues describe a mouse model for selectively depleting cysts but not trophs using anidulafungin, an echinocandin [10]. Immunosuppressed mice are treated with echinocandins and exposed to *P. murina* infected mice using the natural exposure route. Anidulafungin modulates the *P. murina* life cycle and depletes almost all cysts from the mouse.
7. β-1,3-D-Glucan is a high-molecular-weight polymer consisting of β-(1,3)-linked glucose residues present in the cyst but not trophic form of Pneumocystis species. Detection in the blood or BAL fluid has been used as a diagnostic marker for PCP in patients [30, 31]. β-1,3-D-Glucan is therefore detected in the mouse model of infection to complement qPCR fungal burden data and a commercial assay is used, Glucatell assay kit [32]. The Glucatell assay kit is an enzymatic reaction specific for β-1,3-D-Glucan. This is achieved by the ability of samples containing beta glucan in their cell walls to activate Factor G (serine protease zymogen) of the horseshoe crab coagulation cascade. This pro-clotting enzyme cleaves p-nitroaniline from the substrate, creating a chromophore that absorbs at 405 nm (alternatively, the pNA is diazotized to form a compound that absorbs at 540–550 nm). This assay is nonresponsive to endotoxin due to the removal of Factor C (an endotoxin-activated serine protease zymogen of the horseshoe crab cascade). Importantly, all laboratory materials (pipette tips, syringes, tubes, etc.) should be certified free of contaminating glucan [33].

References

1. Ma L, Chen Z, Huang D et al (2016) Genome analysis of three Pneumocystis species reveals adaptation mechanisms to life exclusively in mammalian hosts. Nat Commun 7:10740
2. Cushion MT, Tisdale-Macioce N, Sayson SG et al (2021) The persistent challenge of *Pneumocystis* growth outside the mammalian lung: Past and future approaches. Front Microbiol 12:681474
3. Shellito J, Suzara VV, Blumenfeld W et al (1990) A new model of *Pneumocystis carinii* infection in mice selectively depleted of helper T lymphocytes. J Clin Invest 85:16861693
4. Hughes WT (1982) Natural mode of acquisition for de novo infection with *Pneumocystis carinii*. J Infect Dis 145:842–848
5. Powles MA, McFadden DC, Pittarelli LA et al (1992) Mouse model for *Pneumocystis carinii* pneumonia that uses natural transmission to initiate infection. Infect Immun 4:1397–1400
6. Wolff L, Horch S, Gemsa D (1993) The development of Pneumocystis Carinii Pneumonia in germ-free rats requires immunosuppression and exposure to the *Pneumocystis carinii* organism. Comp Immunol Microbiol Infect Dis 16:73–76
7. An CL, Gigliotti F, Harmsen AG (2003) Exposure of immunocompetent Adult Mice to *Pneumocystis carinii* f. Sp. Muris by Cohousing: Growth of P. Carinii f. Sp. Muris and Host immune response. Infect Immun 71:2065–2070
8. Chesnay A, Paget C, Heuzé-Vourc'h N et al (2022) Pneumocystis Pneumonia: pitfalls and hindrances to establishing a reliable animal model. J Fungi (Basel) 8:129
9. Evans HM, Garvy BA (2018) The trophic life cycle stage of *Pneumocystis species* induces protective adaptive responses without inflammation-mediated progression to pneumonia. Med Mycol 56:994–1005
10. Cushion MT, Linke MJ, Ashbaugh A et al (2010) Echinocandin treatment of pneumocystis pneumonia in rodent models depletes cysts leaving trophic burdens that cannot transmit the infection. PLoS One 5:e8524
11. Wright TW, Gigliotti F, Finkelstein JN et al (1999) Immune-mediated inflammation directly impairs pulmonary function, contributing to the pathogenesis of *Pneumocystis carinii* pneumonia. J Clin Invest 104:1307–1317
12. Barry SM, Lipman MC, Deery AR et al (2002) Immune reconstitution pneumonitis following Pneumocystis carinii pneumonia in HIV infected subjects. HIV Med 3:207–211
13. Bhagwat SP, Gigliotti F, Xu H et al (2006) Contribution of T cell subsets to the pathophysiology of Pneumocystis-related immunorestitution disease. Am J Physiol Lung Cell Mol Physiol 291:L1256–L1266
14. Wang J, Gigliotti F, Bhagwat SP et al (2010) Immune modulation with sulfasalazine attenuates immunopathogenesis but enhances macrophage-mediated fungal clearance during Pneumocystis pneumonia. PLoS Pathog 19: e1001058
15. Hanano R, Reifenberg K, Kaufmann SH (1996) Naturally acquired pneumocystis carinii pneumonia in gene disruption mutant mice: roles of distinct T-cell populations in infection. Infect Immun 64:3201–3209
16. Zheng M, Cai Y, Eddens T et al (2014) Novel pneumocystis antigen discovery using fungal surface proteomics. Infect Immun 82:2417–2423
17. McKinley L, Logar AJ, McAllister F et al (2006) Regulatory T cells dampen pulmonary inflammation and lung injury in an animal model of pneumocystis pneumonia. J Immunol 177:6215–6226
18. Elsegeiny W, Zheng M, Eddens T et al (2018) Murine models of pneumocystis infection recapitulate human primary immune disorders. JCI Insight 21:e91894
19. Zheng M, Shellito JE, Marrero L et al (2001) CD4+ T cell-independent vaccination against *Pneumocystis carinii* in mice. J Clin Invest 108: 1469–1474
20. Ricks DM, Chen K, Zheng M et al (2013) Dectin immunoadhesins and pneumocystis pneumonia. Infect Immun 81:3451–3462
21. Eddens T, Elsegeiny W, Nelson MP et al (2015) Eosinophils contribute to early clearance of *Pneumocystis murina* infection. J Immunol 195:185–193
22. Nature (2002) Initial sequencing and comparative analysis of the mouse genome. Nature 420:520–562
23. Kelly MN, Zheng M, Ruan S et al (2013) Memory CD4+T cells are required for optimal NK cell effector functions against the opportunistic fungal pathogen *Pneumocystis murina*. J Immunol 190:285–295
24. Opata MM, Hollifield ML, Lund FE et al (2015) B lymphocytes are required during the early priming of CD4+ T cells for clearance of Pneumocystis infection in mice. J Immunol 195:611–620
25. Wright TW, Johnston CJ, Harmsen AG et al (1999) Chemokine gene expression during

Pneumocystis carinii-driven pulmonary inflammation. Infect Immun 67:3452–3460

26. Roths JB, Marshall JD, Allen RD (1990) Spontaneous Pneumocystis carinii pneumonia in immunodeficient mutant scid mice. Natural history and pathobiology. Am J Pathol 136: 1173
27. Lund FE, Schuer K, Hollifield ML et al (2003) Clearance of *pneumocystis carinii* in mice is dependent on B cells but not on P. carinii-specific antibody. J Immunol 171:1423–1430
28. Wiley J, Harmsen A (1995) CD40 ligand is required for resolution of Pneumocystis carinii pneumonia in mice. J Immunol 155:3525–3529
29. Linke MJ, Ashbaugh AD, Demland JA et al (2009) *Pneumocystis murina* colonization in immunocompetent surfactant protein a deficient mice following environmental exposure. Respir Res 10:1–15
30. Tasaka S, Hasegawa N, Kobayashi S et al (2007) Serum indicators for the diagnosis of pneumocystis pneumonia. Chest 131:1173–1180
31. Linke MJ, Ashbaugh A, Collins MS et al (2013) Characterization of a distinct host response profile to *Pneumocystis murina* asci during clearance of pneumocystis pneumonia. Infect Immun 81:984–995
32. Cushion MT, Collins MS, Linke MJ (2009) Biofilm formation by *Pneumocystis spp*. Eukaryot Cell 8:197–206
33. Odabasi Z, Paetznick VL, Rodriguez JR et al (2006) Differences in beta-glucan levels in culture supernatants of a variety of fungi. Med Mycol 44:267–272

Chapter 14

Mouse Models of Mucormycosis

Ilse D. Jacobsen

Abstract

Animal models have been crucial in understanding the pathogenesis and developing novel therapeutic approaches for fungal infections in general. This is especially true for mucormycosis, which has a low incidence but is often fatal or debilitating. Mucormycoses are caused by different species, via different routes of infections, and in patients differing in their underlying diseases and risk factors. Consequently, clinically relevant animal models use different types of immunosuppression and infection routes.

This chapter describes how to induce different types of immunosuppression (high dose corticosteroids and induction of leukopenia, respectively) or diabetic ketoacidosis as underlying risk factors for mucormycosis. Furthermore, it provides details on how to perform intranasal application to establish pulmonary infection. Finally, some clinical parameters that can be used for developing scoring systems and define humane endpoints in mice are discussed.

Key words Rhizopus, Lichtheimia, Mucor, Immunosuppression, Ketoacidosis, Intranasal application, Intratracheal application, Dissemination

1 Introduction

Mucormycosis is a term used to describe rare but severe fungal infections caused by members of the *Mucoromycotina*, most commonly caused by *Rhizopus*, *Mucor*, *Lichtheimia*, and *Cunninghamella* species [1–5]. Infections occur commonly in the upper or lower the respiratory tract if inhaled conidia are not cleared by the innate immune system, resulting in rhinocerebral mucormycosis or pulmonary mucormycosis [2]. Cutaneous infections can develop after direct inoculation of spores into the tissue, for example, after trauma [6–10], or as a manifestation of disseminated infection [2]. Gastrointestinal mucormycosis is rare and likely results from ingested spores [2, 11, 12]. A typical feature of mucormycoses is angioinvasion, leading to hemorrhage, thrombosis, and tissue necrosis and facilitating dissemination [13–16]. Similar to other invasive fungal infections, immunosuppression is an important risk factor for mucormycosis (Ref). Affected patients often have

Rebecca A. Drummond (ed.), *Antifungal Immunity: Methods and Protocols*, Methods in Molecular Biology, vol. 2667,
https://doi.org/10.1007/978-1-0716-3199-7_14,

prolonged, severe neutropenia, malignant hematological disease with or without stem cell transplantation, or used corticosteroids long term for other diseases [1, 2, 17]. More specific risk factors are poorly controlled diabetes mellitus with or without diabetic ketoacidosis, iron overload, and therapy with the iron chelator deferoxamine [1, 2, 17]. In previously healthy individuals, mucormycosis is usually associated with trauma (Ref).

Rhinocerebral, pulmonary, and disseminated mucormycoses are typically rapidly progressing infections (Ref) with high mortality rates [18]. Together with the low incidence rate (approx. 0.1–0.2 per 100,000 [5]), and the variety of pathogens and risk factors involved, this poses a significant challenge for the design of clinical trials in humans. Consequently, animal models are essential to study pathogenesis of and therapeutic approaches to mucormycosis. Pathogenesis is significantly affected by the route of infection and underlying risk factors (Ref). For example, fungal spores initially interact with lung epithelial cells during the establishment of pulmonary mucormycosis, whereas the lung is not a primary target after intravenous infection [19]. Diabetic ketoacidosis leads to elevated extracellular iron levels and increased expression of host cell proteins that are used by *Mucorales* for invasion [20], whereas immunosuppression increases susceptibility by reducing fungal clearance. Within immunocompromised patients and animals, pathogenesis differs between those receiving leukoablative therapy and corticosteroids, respectively. Leukopenia, and especially neutropenia, directly impairs the host's ability to respond to invading pathogens by pathogen clearance, resulting in insufficiently restricted microbial growth [21] and pathogen-driven tissue damage. In contrast, corticosteroids impair antifungal activity of neutrophils [22], leading to overt neutrophil influx which contributes to pathogenesis by immunopathology [21].

Consequently, diverse animal models have been used to study specific types and aspects of mucormycosis (see [23]). Some approaches are technically straightforward, such as inducing disseminated infection by intravenous injection of spores. Others, like induction of pulmonary infection, require less commonly used application techniques. Both can be combined with different types of immunosuppression or diabetic ketoacidosis as underlying risk factors. Here, I describe methods to induce (i) immunosuppression by corticosteroids, (ii) induction of leukopenia using cyclophosphamide, (iii) induction of diabetic ketoacidosis (DKA), and (iv) intranasal application for induction of pulmonary infection. Parameters useful for monitoring infection progression and establishing humane endpoints are also discussed. Protocol variations are mentioned in the Notes.

2 Materials

2.1 Immunosuppression by Corticosteroids

1. Cortisone 21-acetate (*see* **Note 1**).
2. Sterile microcentrifuge or conical tubes (volume depending on the number of animals).
3. Sterile endotoxin-free Dulbecco's phosphate-buffered saline (DPBS).
4. Sterile glass beads (diameter approx. 2 mm).
5. Ultrasonic water bath.
6. 1 mL Leur-Lok syringes.
7. 23-G syringe needles.

2.2 Induction of Leukopenia Using Cyclophosphamide

1. Cyclophosphamide (*see* **Note 2**).
2. Cortisone 21-acetate (cortisone acetate; purity ≥99%).
3. Weighing balance for mice.
4. Sterile microcentrifuge or conical tubes (volume depending on the number of animals).
5. Sterile physiological saline.
6. Sterile DPBS.
7. Sterile glass beads (diameter approx. 2 mm).
8. 1 mL Leur-Lok syringes.
9. 27-G and 23-G syringe needles.

2.3 Induction of Diabetic Ketoacidosis (DKA)

1. Streptozocin (streptozotocin; Sigma-Aldrich; purity ≥98%; *see* **Note 3**).
2. Fresh citrate buffer: Combine 20 mL of 0.1 M sodium citrate with 30 mL of 0.1 M citrate acid to produce 0.1 M citrate buffer. Adjust the pH to 4.0 by using 1 N NaOH. Filter-sterilize the citrate buffer and store it in a sterile conical tube on ice.
3. Sucrose-supplemented drinking water: Add 10% w/v white sugar (*see* **Note 4**) to autoclaved water, 200 mL/bottle, and cage.
4. Blood glucose meter and test strips (2 strips per mouse).
5. pH meter.
6. Biosafety hood.
7. Weighing balance for mice.
8. Sterile microcentrifuge or conical tubes (volume depending on the number of animals).
9. Sterile syringe filters.
10. 1 mL Leur-Lok syringes.
11. 27-G syringe needles.

2.4 Intranasal Infection

1. Sporulated cultures of your fungi of interest (*see* **Note 5**).
2. Sterile DPBS.
3. Anesthetics for use in mice (*see* **Note 6**).
4. Heating pad (or similar device) to keep mice warm during anesthesia (*see* **Note 7**).
5. Neubauer hemocytometer.
6. Sterile microcentrifuge or conical tubes (volume depending on the number of animals).
7. 1 mL Leur-Lok syringes.
8. 27-G syringe needles.
9. 100 or 200 μL micropipette and fitting pipette tips.

2.5 Clinical Monitoring and Humane Endpoints

1. Weighing balance for mice.
2. Optional: Contactless infrared thermometer (range 25–40 °C; measuring accuracy ±0.1 °C; *see* **Note 8**).

3 Methods

3.1 Experimental Planning and Acclimatization of Animals

As outlined in the Introduction, mucormycoses are diverse infections and differ in the type of pathogen, underlying risk factors, and localization. Thus, the first planning step is to decide which model best reflects the scientific question to be answered.

For experiments involving mice, permission by specific regulatory bodies is usually required. Depending on local regulations, the application process might require submission of experimental details and attention to the 3R principle (replacement, reduction, and refinement). Furthermore, publishers increasingly support adherence to the ARRIVE guidelines (Animal Research: Reporting of In Vivo Experiments) to ensure that studies report sufficient details. Based on this, an experimental plan should be prepared that includes at minimum the following:

1. Calculation of the group size (number of animals per experimental group). This depends on the level of variation within a group and the expected difference between groups. To ensure reproducibility of results, it is usually preferable to perform two independent experiments with a minimal group size over one experiment with larger group size. If variability within groups and effect size are unknown, pilot experiments with a small number of mice (e.g., $n = 3$ mice) might be necessary. This is often the case if no previous experience with the fungal strain exists (to determine the optimal infectious dose); it might also be helpful if personnel is not yet familiar with technical details. Also *see* **Note 9**.

2. Choice of mouse strain, sex, and age. Different inbred and outbred strains have been used to study mucormycosis, and the methods presented here are suitable for BALB/c, C57Bl/6, and CD1 mice. However, infection kinetics and outcome might differ between strains [24, 25]. Both male and female mice can be used, but the course of infection might differ (as recently shown for infection with *Mucor circinelloides* in DKA mice [26]). If necessary, pilot experiments should be performed to ensure that the course of infection with the used dose is compatible with the study aim. Young adult mice (6–12 weeks of age) are usually used, and the methods presented here were evaluated for this age group. Aged animals might differ in their response to medication and drugs (pilot experiments are recommended).
3. List of experimental procedures, humane endpoints (*see* Subheading 3.6), and samples to be taken postmortem. It is recommended to consult the ARRIVE guidelines for planning additional aspects, such as inclusion/exclusion criteria, randomization, blinding.
4. Based on the experimental plan, randomly allocate mice into the groups at least 7 days before the first procedure to allow them to get used to the new group structure. Mark the individual mice to allow easy identification within the groups. Record the individual weights and compare the weights across groups to ensure equal distribution.
5. Weigh mice daily starting latest on the day before the first procedure.

3.2 Immunosuppression by Corticosteroids

Corticosteroids impair antifungal activity of neutrophils, but do not negatively affect neutrophil recruitment. Cortison derivatives (such as prednisolone and dexamethasone) are widely used in (veterinary) medicine, but have not been established for immunosuppression in fungal infection models. These are based on application on cortisone acetate, which is adsorbed slowly after intraperitoneal application, creating a depot effect. It is applied on days −3 and day 0, with day 0 being the day of infection (Fig. 1).

1. Weigh a sterile tube of sufficient volume (approx. 300 μL/dose) and add the required amount of cortisone acetate (25 mg/mouse) aseptically. Prepare 1 mL more than needed to cover volume lost in needles/syringes.
2. Add sterile DPBS at the appropriate volume (200 μL/25 mg) and sterile glass beads.
3. Shake vigorously and place in an ultrasonic water bath for 30 min. A homogenous slurry should be obtained; repeat incubation in ultrasonic water bath if necessary (*see* **Note 1**).

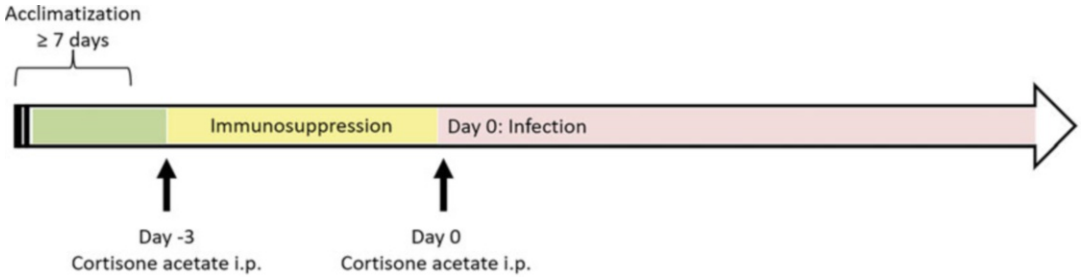

Fig. 1 Timing of interventions in the cortisone acetate model. Day 0 is defined as the day of infection; all other days are designated in reference to day 0. Green: Acclimatization period before the first intervention; yellow: period of immunosuppression; pink: period of immunosuppression and infection. i.p. intraperitoneal application

4. Mix the suspension by inversion prior to loading into 1 mL syringes; remove all air bubbles from the syringe.
5. Inject 200 µL intraperitoneally using a 23-G syringe needle (*see* **Note 10**).
6. Check the animals 1 h and 3–4 h after injection (*see* **Note 11**).

3.3 Induction of Leukopenia Using Cyclophosphamide

Cyclophosphamide (*see* **Note 12**) is metabolized to the active alkylating agent phosphoramide mustard, which causes irreversible DNA and RNA crosslinking and thereby induces programmed cell death [27]. It is used in cancer therapy and, in high dose, for myeloablative conditioning chemotherapy [28]. The protocol described here, consisting of repeated application of cyclophosphamide and a single injection of cortisone acetate (to impair function of resident tissue macrophages), leads to sustained leukopenia (including neutropenia). Successful immunosuppression can be easily confirmed by the determination of leukocyte numbers in blood smears or by using hematology counters (*see* **Note 13**).

1. The first application is given on day −4, with day 0 being the day of infection (Fig. 2). Weigh each mouse.
2. Dissolve the cyclophosphamide powder with sterile physiological saline to obtain a solution of 14 mg/mL (*see* **Note 14**). The dose to be applied is 140 mg/kg, equivalent to 10 µL/g body weight.
3. Load 1 mL syringes with the appropriate volume (10 µL/g body weight); remove all air bubbles from the syringe.
4. Inject the appropriate volume intraperitoneally using a 27-G syringe needle.
5. Check the animals 1 h and 3–4 h after injection (*see* **Note 11**).
6. Repeat **steps 1–5** every third day (day −1, day 2, day 5, and so forth) until the end of the experiment (Fig. 2).

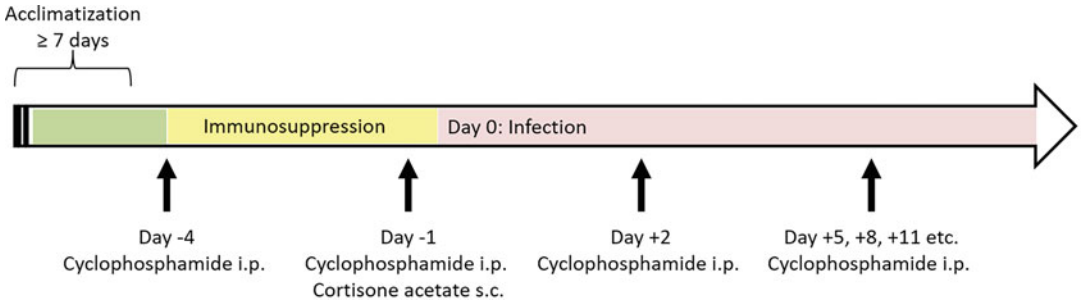

Fig 2 Timing of interventions in the leukopenic (cyclophosphamide) model. Day 0 is defined as the day of infection; all other days are designated in reference to day 0. Green: Acclimatization period before the first intervention; yellow: period of immunosuppression; pink: period of immunosuppression and infection. i.p. intraperitoneal application, s.c. subcutaneous application

7. On day −1, prepare a 40 mg/mL cortisone acetate solution as described in Subheading 3.2, **steps 1–4**. Cortisone acetate can be applied immediately after cyclophosphamide injection.
8. Inject 100 μL (4 mg) per mouse subcutaneously using a 23-G syringe needle. Check the animals 1 h after injection (*see* **Note 11**).

3.4 Induction of Diabetic Ketoacidosis (DKA) Using Streptozotocin

DKA is a risk factor for various infections but especially prominent in mucormycosis. Although various mouse models to study type 1 and type 2 diabetes have been developed, chemical ablation of insulin producing beta cells by the application of streptozotocin or alloxan is most commonly used model to study DKA in the context of infectious diseases, including mucormycosis. One advantage is that this model can be employed independent of the genetic background and age of the animals.

1. On day −14 (day 0 being the day of infection; Fig. 3), collect a drop of blood from each mouse (e.g., by pricking the tail vein with a 27-G syringe needle) and determine blood glucose levels using a blood glucose meter and test strips according to the manufacturer's instruction (*see* **Note 15**) to establish baseline blood glucose levels.
2. In the morning of day −10, weigh each mouse and remove the food from the cage at least 4 h before streptozotocin injection (*see* **Note 16**).
3. Prepare drinking water supplemented with 10% sucrose (1 bottle/cage).
4. Calculate the amount of streptozotocin needed: 2 mg/10 g bodyweight plus extra to cover volume lost in needles/syringes. Prepare the streptozotocin aliquot in a sterile conical tube in a biosafety hood (*see* **Note 3**). Calculate the corresponding buffer volume to be added to your aliquot to reach a concentration of 19 mg/mL.

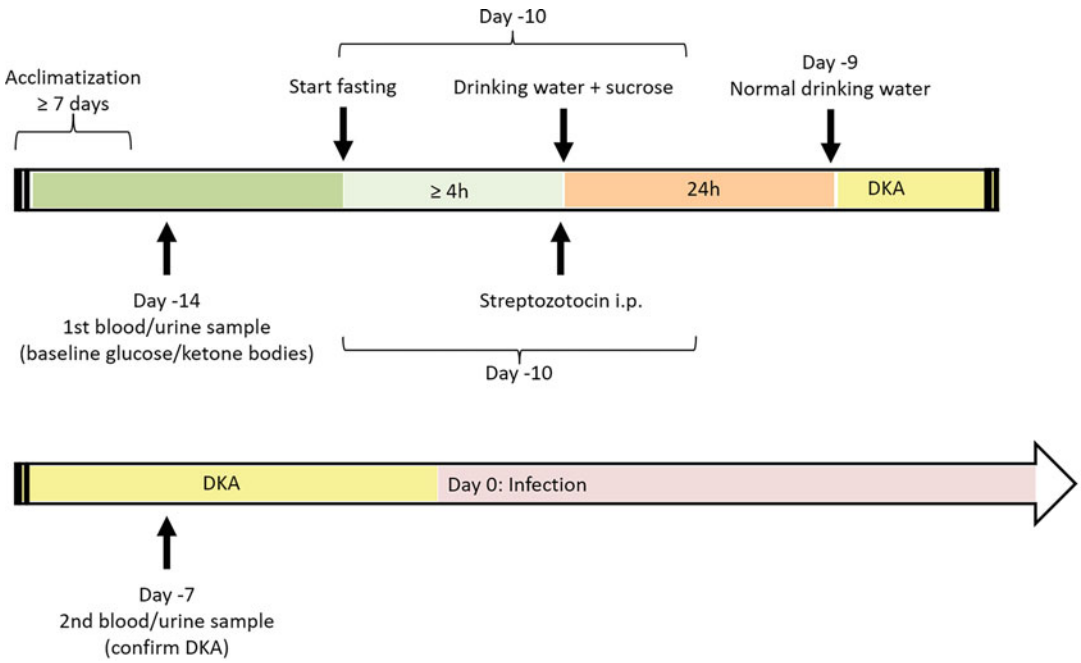

Fig 3 Timing of interventions in the leukopenic (cyclophosphamide) model. Day 0 is defined as the day of infection; all other days are designated in reference to day 0. Green: Acclimatization period before the first intervention; light green: fasting period; orange: sucrose supplementation; yellow: period of diabetic ketoacidosis (DKA); pink: period of ketoacidosis and infection. i.p. intraperitoneal application

5. Prepare fresh citrate buffer and store it in a sterile conical tube on ice.
6. Right before use, add fresh citrate buffer to the streptozotocin (1 mL/19 mg) in a biosafety hood. Vortex. Avoid storage, keep on ice if necessary.
7. Load 1 mL syringes; remove all air bubbles from the syringe.
8. Inject 100 µL/10 g body weight intraperitoneally using a 27-G syringe needle. Citrate buffer without streptozotocin can be used for control animals, if applicable.
9. Swap the normal drinking bottle with drinking water supplemented with 10% sucrose (*see* **Note 16**); supply normal food.
10. After 24 hours, replace the sucrose-supplemented drinking water with normal water.
11. Monitor the weight by weighing mice daily.
12. On day −7, repeat blood collection (**step 1**) and determine blood glucose levels. Successful induction of DKA results in blood glucose levels ≥200 mg/dl (*see* **Note 15**).

3.5 Intranasal Infection

Both intranasal and intratracheal applications have been used to successfully induce pulmonary mucormycosis. As a method for nonsurgical oropharyngeal intratracheal administration has been described in detail elsewhere [29], I'll describe intranasal application only. For either method, the effective spore concentration reaching the lung can be determined in pilot experiments by sacrificing two to three mice immediately after the infection, dissecting and homogenizing the lungs, and quantitative culture.

1. Harvest spores from agar plate cultures (*see* **Note 5**) using sterile DPBS. Centrifuge, remove the supernatant, and resuspend in sterile DPBS; repeat this step. Determine the spore concentration by counting using a Neubauer hemocytometer and adjust to the desired concentration (*see* **Note 5**) with sterile DPBS (the volume used for infection is 20 μL).
2. Prepare a heating pad or similar device to keep the animals warm during anesthesia.
3. Inject the first group of mice with anesthetics (*see* **Note 6**). Place mice which have lost the righting reflex on the warming pad. Monitor mice for loss of pinna and/or pedal reflex.
4. Once the reflex is absent, hold the mouse with the nondominant hand in loose restraining grip in an angled supine position (the skin fold of the neck fixed between the thumb and the index finger, the back supported by your palm). The head should be in vertical position.
5. Using a 100 or 200 μL micropipette with your other hand, slowly apply 20 μL of the spore solution as small drops onto both nostrils. The drops should be inhaled without any coughing, breathing should continue normally (*see* **Note 16**). Hold the mouse in this position for 30–60 sec after the last drop was applied and monitor breathing.
6. Place the mouse back onto the heating pad. If antagonizable anesthesia is used, inject the antidote. Keep mice on the heating pad until they regained consciousness, then place them back in their cage. Depending on the type of anesthesia, repeated monitoring during the recovery phase might be indicated (*see* **Note 6**).

3.6 Clinical Monitoring and Humane Endpoints

Frequent monitoring of the health status and definition of humane endpoints is an integral part of the 3R concept. Furthermore, frequent clinical monitoring facilitates collection of data to describe the course of disease (onset, type, and severity of symptoms) and thus provides information beyond mere survival time. Humane endpoints are defined as one or more predetermined physiological or behavioral signs that define a level of welfare impairment that requires action from the researcher. In some cases, this could be

medication to reduce pain, but more commonly the animal will be euthanized. Euthanizing severely ill mice not only reduces the amount and time of suffering for the animal, but also allows to collect fresh samples for further analyses (e.g., determination of fungal burden, analysis of immune responses, tissue samples for histopathology). Humane endpoints must be scientifically justified and applied consistently; often a clinical score based on several parameters is used, and the animal is euthanized if a threshold is reached in the cumulative score and/or if single parameters reach a critical stage. The parameters to be monitored, the scoring system, and the humane endpoints are usually part of the permission procedure for animal experiments and should be reported in detail in publications. The following points are suggestions based on experience and literature and should be discussed with the attending veterinarian or responsible committees before or during the experimental planning. For qualitative parameter (such as behavior), the scoring categories must be defined clearly and personnel trained accordingly.

1. Mice should be checked daily before the first procedure to establish the baseline of the parameters to be monitored. This is especially important if an unfamiliar mouse strain is used, as strains can differ significantly in their activity. After infection, check mice at least twice per day, ideally at the start and end of the light cycle. Monitoring frequency should be increased if rapid progression of disease can be expected and for animals that score close to the humane endpoints.
2. Weigh mice once per day, at roughly the same time. Body weight has the advantage of being a quantitative parameter and is therefore often used to define humane endpoints, for example, euthanasia if 20% of the original body weight have been lost. This works well for rapid weight loss, as it is a clear indicator of disease progression, and is usually accompanied with other symptoms. Judging slow weight loss over several days can be more challenging, especially in the absence of other disease symptoms. For such cases, humane endpoints based on the body condition score [30], rather than percentage weight loss, might be more appropriate.
3. In healthy, young mice, the fur is shiny and the coat is flat. "Ruffled fur" (piloerection) is a common unspecific symptom of impaired health, which initially becomes evident in the face.
4. Behavior can be easily monitored by observing spontaneous activity (exploration, resting, climbing, grooming, foraging, etc.), and the response to stimuli can be tested by touching the mouse. Moderate to severe lethargy is a clear indication of severe disease and commonly used to define humane endpoints.

5. Similarly, body posture and movement can be assessed easily by watching the mice. Sitting or walking with a hunched back is a common symptom of pain or respiratory disease. A tilted head (torticollis) occurs if infection involves the middle and/or inner ear or central nervous system; it may progress to the inability to walk straight and affect the ability of the mouse to reach food or water (which is a reason for euthanasia). Thrombosis of distal veins after dissemination of infection from the lung can lead to paralysis of limbs.
6. Breathing is a specific parameter that changes in pulmonary infections. Counting the breathing rate (80–230 in healthy mice) is difficult in mobile mice, but with some training increased breathing rates indicating early pulmonary mucormycosis can be qualitatively assessed. Progressing pneumonia leads to labored breathing (dyspnea), characterized by reduced breathing rate and increased thoracic/abdominal movement. Open-mouthed breathing is a sign of severe dyspnea and associated with severe suffering warranting euthanasia.
7. Mice that survive acute pulmonary mucormycosis might develop disseminated disease that can target various organ systems (e.g., liver or kidney). Consequently, various symptoms can develop, for example, excretion of large amounts of colorless urine as an indication of impaired kidney function. Thus, any unusual observation should be documented and discussed with experienced personnel, if necessary.
8. Measuring body temperature allows you to detect fever, but more importantly for humane endpoints, reduced body temperature is a common sign in severe infections indicating that essential physiological functions can no longer be maintained. It is a clear indicator of imminent death, usually associated with moderate to severe lethargy. Rectal probes give very accurate readings of the core temperature but cause stress to the animals and can cause injuries. For daily measurements, we therefore use contactless infrared thermometers: The mouse is gently restrained and the surface temperature is measured at the cardiac region. Reduction of body surface temperature by 2–3 °C (depending on the mouse strain) is used as humane endpoint (*see* **Note 8**).
9. Even if no organ samples are to be collected from euthanized animals, a full dissection is useful to (i) record the type and extent of visible organ alterations induced by the infection and (ii) to exclude conditions unrelated to the infection as the cause of symptoms.

4 Notes

1. Due to the lack of solubility, working with cortisone acetate can be tricky. It is essential to obtain a homogenous slurry without clumps that can be injected without blocking the syringe needle. I recommend to prepare a test slurry before the injection day to have time to optimize the protocol (duration and strength of ultrasound, size of glass beads, use of a bead beater). Make sure that the mixture does not heat up beyond 40 °C during the preparation process; include cooling periods if necessary. A possible alternative is the use of other corticosteroids with immunosuppressive function that are available as ready-to-use licensed drug formulations and have been used in bacterial infection or transplantation models (prednisolone 50 mg/kg intraperitoneally [31] or dexamethasone 5 mg/kg of body weight intraperitoneally [32]). These protocols have not been tested in murine mucormycosis models, and a pilot experiment to determine if sufficient immunosuppression can be achieved would be necessary.
2. Cyclophosphamide is available both as licensed drug and chemical. Use of research-grade chemicals instead of licensed drug formulations in animal experiments is legally restricted in some countries (e.g., Germany). Check with the vivarium staff and/or attending veterinarian to discuss options available to you.
3. Streptozotocin is highly toxic for pancreatic beta cells. Thus, adequate personal protection equipment must be used and the substance must be handled in a biosafety hood. Aliquots of streptozotocin powder can be stored at −20 °C in tubes that are sealed well with cap and parafilm. The solution should be used as soon as possible after preparation.
4. Both sucrose purchased for laboratory use and plain white sugar for human consumption can be used.
5. The optimal media, incubation time, and temperature depend on the fungal species and might vary from lab to lab. Similarly, the optimal infectious dose will depend on the fungal species, strain, and aim of the study (targeted survival rate in the infected control group). Use information in published studies for guidance and perform pilot experiments if necessary.
6. In principle, all types of anesthesia can be used; a disadvantage of inhalation anesthesia, however, is the limited time available for the intranasal application between stopping inhalation of the anesthetic and awakening of the mouse. This can be challenging in the beginning. We use a combination of fentanyl (0.05 mg/kg), medetomidine (0.5 mg/kg), and midazolam (5 mg/kg) injected intraperitoneally, with naloxone (1.2 mg/

kg), atipamezole (2.5 mg/kg), and flumazenil (0.5 mg/kg) as specific antidotes injected subcutaneously after intranasal infection. The advantage is that the anesthesia can be antagonized, thereby reducing anesthesia duration to the necessary minimum. However, fentanyl is a regulated opioid and might not be available in all facilities. A combination of ketamine and xylazine can also be used, but this type of anesthesia cannot be antagonized and, thus, results in longer immobility of mice. Discuss the options available to you with the attending veterinarian, who can also provide detailed guidance on how to best monitor the recovery period.

7. It is important that the temperature of the heating device can be controlled to avoid overheating of the mice.
8. We use standard contactless infrared thermometers designed to measure forehead temperature of humans. As the body surface temperature of healthy mice is usually between 30.5 °C and 33 °C, it is important to choose a model that is accurate in the range of 25–35 °C.
9. If changes of immunological or other physiological parameters caused by infection are to be measured, a group mock-infected with DPBS should be included. Such a control group can also be used to assess the impact of immunosuppression/DKA and other procedures on animal welfare (recommended to refine methods during establishment of the protocol) and as sentinel animals to detect other infections caused by facultative pathogens or a breach in hygiene. The latter is essential if non-SPF mice are used, or if no sufficient physical hygiene barriers are available (use of IVCs for keeping the mice and opening cages in a clean bench only are recommended), as both immunosuppressive regimens and DKA render the mice more susceptible to various types of opportunistic infections.
10. A 23-G syringe needle is recommended as smaller diameter needles are more prone to be blocked by particles in the suspension. Use a fresh needle for each animal; repeated use of the same needle increases the risk of blocking.
11. Mice may temporarily show signs of abdominal pain after intraperitoneal injection (either due to the trauma caused by the injection itself or as a reaction to the injected substance). If this occurs, it is usually evident 1 h after injection by separation from the group and reluctance to move out of a sitting position. In that case, check mice again 3–4 h later—the mouse should behave normal again. If symptoms persist, continue to monitor the animal and contact your attending veterinarian for specific advice. A possibility for refinement is (besides optimizing the injection technique) the use of suitable analgesics. Subcutaneous injections are usually tolerated very well, but mice should be checked 1 h after injection.

12. Cyclophosphamide can be teratogenic and therefore should not be handled during pregnancy. For disposal, collect unused solutions in a container for cytotoxic waste.
13. Depending on the fungal species, strain, and infection dose, cyclophosphamide alone might induce sufficient immunosuppression, without the need of the additional cortisone acetate application. This can be tested in a pilot experiment. As a quality control, I recommend to always confirm cyclophosphamide-induced leukopenia by comparing blood taken before treatment and at euthanasia by counting leukocytes in a blood smear or flow cytometry.
14. Dissolved cyclophosphamide is stable for 24 h in the fridge and should not be used after 24 h.
15. We use a standard blood glucose meter and test strips designed for use by human diabetic patients. Such devices and test strips are inexpensive, easy to use, and require only a single drop of blood which can be easily obtained by pricking the lateral tail vein with a 27-G syringe needle. Streptozotocin treatment is a reliable way to induce DKA, but not necessarily successful in all mice (80 to ≥90% of mice develop DKA). It is therefore essential to repeat the blood glucose measurement approx. one week after treatment to be able to exclude animals without DKA from the study. As an alternative to blood glucose, ketones and glucose can be quantified in urine.
16. Fasting the mice before streptozotocin treatment and providing sugar with the drinking water is crucial to prevent lethal hypoglycemia.
17. Both the volume and the speed of application are crucial: Excess volume or too rapid application can induce suffocation and death. Allow for a few breaths between drops. If a mouse stops breathing during/after application, gently compress the thorax to push air out of the lungs and into the airways. Repeat as necessary. Spontaneous breathing usually resumes after a few compressions.

References

1. Binder U, Maurer E, Lass-Flörl C (2014) Mucormycosis--from the pathogens to the disease. Clin Microbiol Infect 20(Suppl 6):60–66. https://doi.org/10.1111/1469-0691.12566
2. Petrikkos G, Skiada A, Lortholary O, Roilides E, Walsh TJ, Kontoyiannis DP (2012) Epidemiology and clinical manifestations of mucormycosis. Clin Infect Dis 54 (Suppl 1):S23–S34. https://doi.org/10.1093/cid/cir866
3. Gomes MZ, Lewis RE, Kontoyiannis DP (2011) Mucormycosis caused by unusual mucormycetes, non-*Rhizopus*, –*Mucor*, and -*Lichtheimia* species. Clin Microbiol Rev 24(2): 411–445. https://doi.org/10.1128/CMR.00056-10
4. Lewis RE, Kontoyiannis DP (2013) Epidemiology and treatment of mucormycosis. Future Microbiol 8(9):1163–1175. https://doi.org/10.2217/fmb.13.78

5. Hassan MIA, Voigt K (2019) Pathogenicity patterns of mucormycosis: epidemiology, interaction with immune cells and virulence factors. Med Mycol 57(Supplement_2):S245–S256. https://doi.org/10.1093/mmy/myz011
6. Kronen R, Liang SY, Bochicchio G, Bochicchio K, Powderly WG, Spec A (2017) Invasive fungal infections secondary to traumatic injury. Int J Infect Dis 62:102–111. https://doi.org/10.1016/j.ijid.2017.07.002
7. Garcia-Hermoso D, Criscuolo A, Lee SC, Legrand M, Chaouat M, Denis B, Lafaurie M, Rouveau M, Soler C, Schaal JV, Mimoun M, Mebazaa A, Heitman J, Dromer F, Brisse S, Bretagne S, Alanio A (2018) Outbreak of invasive wound Mucormycosis in a burn unit due to multiple strains of *Mucor circinelloides f. circinelloides* resolved by whole-genome sequencing. mBio 9(2). https://doi.org/10.1128/mBio.00573-18
8. Kyriopoulos EJ, Kyriakopoulos A, Karonidis A, Gravvanis A, Gamatsi I, Tsironis C, Tsoutsos D (2015) Burn injuries and soft tissue traumas complicated by mucormycosis infection: a report of six cases and review of the literature. Ann Burns Fire Disasters 28(4):280–287
9. Struck MF, Gille J (2013) Fungal infections in burns: a comprehensive review. Ann Burns Fire Disasters 26(3):147–153
10. Lelievre L, Garcia-Hermoso D, Abdoul H, Hivelin M, Chouaki T, Toubas D, Mamez AC, Lantieri L, Lortholary O, Lanternier F (2014) Posttraumatic mucormycosis: a nationwide study in France and review of the literature. Medicine 93(24):395–404. https://doi.org/10.1097/md.0000000000000221
11. Kaur H, Ghosh A, Rudramurthy SM, Chakrabarti A (2018) Gastrointestinal mucormycosis in apparently immunocompetent hosts-A review. Mycoses 61(12):898–908. https://doi.org/10.1111/myc.12798
12. Mitchell SJ, Gray J, Morgan ME, Hocking MD, Durbin GM (1996) Nosocomial infection with *Rhizopus microsporus* in preterm infants: association with wooden tongue depressors. Lancet 348(9025):441–443
13. Pana ZD, Seidel D, Skiada A, Groll AH, Petrikkos G, Cornely OA, Roilides E (2016) Invasive mucormycosis in children: an epidemiologic study in European and non-European countries based on two registries. BMC Infect Dis 16(1):667. https://doi.org/10.1186/s12879-016-2005-1
14. Corzo-Leon DE, Chora-Hernandez LD, Rodriguez-Zulueta AP, Walsh TJ (2018) Diabetes mellitus as the major risk factor for mucormycosis in Mexico: epidemiology, diagnosis, and outcomes of reported cases. Med Mycol 56(1):29–43. https://doi.org/10.1093/mmy/myx017
15. Spellberg B, Edwards J Jr, Ibrahim A (2005) Novel perspectives on mucormycosis: pathophysiology, presentation, and management. Clin Microbiol Rev 18(3):556–569. https://doi.org/10.1128/CMR.18.3.556-569.2005
16. Jeong W, Keighley C, Wolfe R, Lee WL, Slavin MA, Kong DCM, Chen SC (2019) The epidemiology and clinical manifestations of mucormycosis: a systematic review and meta-analysis of case reports. Clin Microbiol Infect 25(1):26–34. https://doi.org/10.1016/j.cmi.2018.07.011
17. Skiada A, Pagano L, Groll A, Zimmerli S, Dupont B, Lagrou K, Lass-Florl C, Bouza E, Klimko N, Gaustad P, Richardson M, Hamal P, Akova M, Meis JF, Rodriguez-Tudela JL, Roilides E, Mitrousia-Ziouva A, Petrikkos G (2011) Zygomycosis in Europe: analysis of 230 cases accrued by the registry of the European Confederation of Medical Mycology (ECMM) Working Group on Zygomycosis between 2005 and 2007. Clin Microbiol Infect 17:1859. https://doi.org/10.1111/j.1469-0691.2010.03456.x
18. Roden MM, Zaoutis TE, Buchanan WL, Knudsen TA, Sarkisova TA, Schaufele RL, Sein M, Sein T, Chiou CC, Chu JH, Kontoyiannis DP, Walsh TJ (2005) Epidemiology and outcome of zygomycosis: a review of 929 reported cases. Clin Infect Dis 5:634–653. CID36019 [pii]. https://doi.org/10.1086/432579
19. Van Cutsem J, Fransen J, Janssen PA (1988) Experimental zygomycosis due to Rhizopus spp. infection by various routes in Guinea-pigs, rats and mice. Mycoses 31(11):563–578
20. Ibrahim AS (2014) Host-iron assimilation: pathogenesis and novel therapies of mucormycosis. Mycoses 57(Suppl 3):13–17. https://doi.org/10.1111/myc.12232
21. Balloy V, Huerre M, Latge JP, Chignard M (2005) Differences in patterns of infection and inflammation for corticosteroid treatment and chemotherapy in experimental invasive pulmonary aspergillosis. Infect Immun 73(1):494–503
22. Philippe B, Ibrahim-Granet O, Prevost MC, Gougerot-Pocidalo MA, Sanchez Perez M, Van der Meeren A, Latge JP (2003) Killing of *aspergillus fumigatus* by alveolar macrophages is mediated by reactive oxidant intermediates. Infect Immun 71(6):3034–3042
23. Jacobsen ID (2019) Animal models to study Mucormycosis. J Fungi (Basel) 5(2):27. https://doi.org/10.3390/jof5020027

24. Dos Santos AR, Fraga-Silva TF, de Fátima A-DD, Dos Santos RF, Finato AC, Soares CT, Lara VS, Almeida NLM, Andrade MI, de Arruda OS, de Arruda MSP, Venturini J (2022) IFN-γ mediated signaling improves fungal clearance in experimental pulmonary Mucormycosis. Mycopathologia 187(1):15–30. https://doi.org/10.1007/s11046-021-00598-2
25. Dos Santos AR, Fraga-Silva TF, Almeida DF, Dos Santos RF, Finato AC, Amorim BC, Andrade MI, Soares CT, Lara VS, Almeida NL, de Arruda OS, de Arruda MS, Venturini J (2020) *Rhizopus*-host interplay of disseminated mucormycosis in immunocompetent mice. Future Microbiol 15:739–752. https://doi.org/10.2217/fmb-2019-0246
26. Gebremariam T, Alkhazraji S, Alqarihi A, Wiederhold NP, Najvar LK, Patterson TF, Filler SG, Ibrahim AS (2021) Evaluation of sex differences in murine diabetic ketoacidosis and neutropenic models of invasive mucormycosis. J Fungi (Basel) 7 (4):313. doi:10.3390/jof7040313
27. Ogino MH, Tadi P (2022) Cyclophosphamide. In: StatPearls (ed) StatPearls Publishing Copyright © 2022. StatPearls Publishing LLC, Treasure Island (FL)
28. Ahlmann M, Hempel G (2016) The effect of cyclophosphamide on the immune system: implications for clinical cancer therapy. Cancer Chemother Pharmacol 78(4):661–671. https://doi.org/10.1007/s00280-016-3152-1
29. Allen IC (2014) The utilization of oropharyngeal intratracheal PAMP administration and bronchoalveolar lavage to evaluate the host immune response in mice. J Vis Exp 86: 51391. https://doi.org/10.3791/51391
30. Ullman-Culleré MH, Foltz CJ (1999) Body condition scoring: a rapid and accurate method for assessing health status in mice. Lab Anim Sci 49(3):319–323
31. Diehl R, Ferrara F, Müller C, Dreyer AY, McLeod DD, Fricke S, Boltze J (2017) Immunosuppression for in vivo research: state-of-the-art protocols and experimental approaches. Cell Mol Immunol 14(2):146–179. https://doi.org/10.1038/cmi.2016.39
32. Martins TG, Gama JB, Fraga AG, Saraiva M, Silva MT, Castro AG, Pedrosa J (2012) Local and regional re-establishment of cellular immunity during curative antibiotherapy of murine *Mycobacterium ulcerans* infection. PLoS One 7(2):e32740. https://doi.org/10.1371/journal.pone.0032740

Chapter 15

Bioluminescence Imaging, a Powerful Tool to Assess Fungal Burden in Live Mouse Models of Infection

Agustin Resendiz-Sharpe, Eliane Vanhoffelen, and Greetje Vande Velde

Abstract

Aspergillus fumigatus and *Cryptococcus neoformans* species infections are two of the most common life-threatening fungal infections in the immunocompromised population. Acute invasive pulmonary aspergillosis (IPA) and meningeal cryptococcosis are the most severe forms affecting patients with elevated associated mortality rates despite current treatments. As many unanswered questions remain concerning these fungal infections, additional research is greatly needed not only in clinical scenarios but also under controlled preclinical experimental settings to increase our understanding concerning their virulence, host–pathogen interactions, infection development, and treatments. Preclinical animal models are powerful tools to gain more insight into some of these needs. However, assessment of disease severity and fungal burden in mouse models of infection are often limited to less sensitive, single-time, invasive, and variability-prone techniques such as colony-forming unit counting. These issues can be overcome by in vivo bioluminescence imaging (BLI). BLI is a noninvasive tool that provides longitudinal dynamic visual and quantitative information on the fungal burden from the onset of infection and potential dissemination to different organs throughout the development of disease in individual animals. Hereby, we describe an entire experimental pipeline from mouse infection to BLI acquisition and quantification, readily available to researchers to provide a noninvasive, longitudinal readout of fungal burden and dissemination throughout the course of infection development, which can be applied for preclinical studies into pathophysiology and treatment of IPA and cryptococcosis in vivo.

Key words *Aspergillus fumigatus*, *Cryptococcus neoformans*, Bioluminescence imaging, Mouse model, Preclinical research

1 Introduction

Compared to diseases caused by other microorganisms such as parasites, bacteria, and viruses, fungal infections have been erroneously considered to be rare with little impact on patient's health [1, 2]. This has serious consequences as resources and methodologies to study these neglected diseases are scarce, limiting our understanding on the development of fungal infections and their treatments [2]. Usually, most fungi are opportunistic pathogens

Rebecca A. Drummond (ed.), *Antifungal Immunity: Methods and Protocols*, Methods in Molecular Biology, vol. 2667,
https://doi.org/10.1007/978-1-0716-3199-7_15,

and do not cause infection except in immunocompromised patients [3]. However, as the number of patients receiving immunosuppressive therapies is on the rise, the number of patients at risk for fungal infections is constantly increasing. *Aspergillus* (mold) and *Cryptococcus* (yeast) spp. infections are two of the most common life-threatening fungal infections in the immunocompromised population.

Amongst *Aspergillus* spp., the *Aspergillus fumigatus* complex is the most frequent infecting species causing disease worldwide. The clinical spectrum of this fungus is diverse, ranging from allergic and chronic infections to acute invasive pulmonary aspergillosis (IPA), the most severe form of aspergillosis [4]. High prevalence rates of IPA have been reported in specific patient populations like hematological and solid organ transplant patients, chronic pulmonary infections, and recently, in association with severe influenza and COVID-19 pneumonia [4–6]. Each year, it is estimated that more than a million patients develop IPA globally, with high mortality rates ranging between 30% and 50% despite treatment [4, 7, 8]. Moreover, an increasing number of reports of resistance to the recommended first line therapy of triazole antifungals are of grave concern due to its increased associated mortality in patients [8–11].

Cryptococcus spp., particularly *Cryptococcus neoformans* and *Cryptococcus gattii*, are likewise important pathogens affecting immunocompromised patients, particularly in HIV-positive individuals [12, 13]. Cryptococcosis is a pulmonary or disseminated infection acquired by inhalation of encapsulated cryptococcus cells in the environment [13]. *Cryptococcus neoformans* causes most infections, while *C. gattii* apparently also causes disease in immunocompetent patients. After a pulmonary infection, a disseminated infection can develop with a predilection to the brain, with annual global burden of cryptococcal meningitis of approximately 500,000 cases and mortality rates of 100% if untreated [12]. Despite these alarming statistics, treatment options for cryptococcosis remain limited, with only three major classes of drugs approved for clinical use hampered by host toxicity and pathogen resistance [14, 15].

Many unanswered questions remain concerning these fungal infections. Therefore, additional research is greatly needed not only in clinical context but also under controlled preclinical scenarios to increase our understanding concerning their virulence, host–pathogen interactions, infection development, and effective treatment.

Preclinical animal models are powerful tools to address these needs. Rodent models are currently the gold standard to study these fungal infections in vivo as they present several similarities to humans on disease infection development and immune responses [16]. However, in most study models, assessment of disease severity and fungal burden is performed exclusively by invasive and variability-prone techniques such as colony-forming

unit (CFU) counting or histopathology. These methodologies capture only a single snapshot of the disease development limiting our readouts and longitudinal assessment. Moreover, the statistical power of these methods is low, particularly of CFU counts that suffer from reproducibility issues and require to be addressed by increasing the number of animals needed per timepoint [17, 18]. These concerns can be overcome by implementing in vivo real-time imaging techniques such as bioluminescence imaging (BLI). The technique is based on the sensitive detection of light emission (photons) generated by genetically engineered luciferase-expressing microorganisms secondary to the oxidation of the substrate luciferin [19]. BLI is a noninvasive tool that provides longitudinal dynamic visual and quantitative information on fungal burden and fungal dissemination to different infection sites in individual infected animals as of the onset of disease, decreasing inter-animal variability and number of animals needed per experiment [20, 21].

To facilitate the study of fungal infections in vivo, BLI-compatible fungal strains and infection models are recently emerging, based on codon-optimized luciferases engineered for expression by the specific fungus [19–34]. For the study of cryptococcosis and aspergillosis, our research group recently developed and validated a novel *C. neoformans* (KN99α-CnFLuc) and three *A. fumigatus* red-shifted luciferase expressing strains, one susceptible and two triazole antifungals resistant strains harboring the most commonly reported resistance mechanisms in *A. fumigatus* (-Af_luc$_{OPT}$_red_TR34 and Af_luc$_{OPT}$_red_TR46) [20, 35]. Compared to other luciferases, light emitted by red-shifted luciferases (600–700 nm) is less absorbed by hemoglobin and has reduced tissue scattering [20, 30, 35]. These features successfully increased the sensitivity of detection of BLI signal from low fungal burdens, particularly at earlier stages of infection, and provided powerful dynamic longitudinal infection readouts of these deep-seated fungal infections to be used for several applications such as antifungal therapy efficacy studies in mouse fungal infection studies [20, 35, 36].

Here, we describe an entire experimental pipeline from mouse infection to bioluminescence imaging acquisition and data processing in a neutropenic mouse model of IPA and a mouse model of pulmonary cryptococcosis, readily applicable to monitor fungal burden progression from early disease onset throughout infection development and dissemination.

2 Materials

2.1 Fungal Strains

1. *Aspergillus fumigatus* isogenic strains expressing a red-shifted thermostable firefly luciferase (derivatives of *A. fumigatus* reference strain CBS144.89) [35]: Our laboratory has available one triazole antifungal susceptible (wild type) strain (-Af_luc$_{OPT_red}$_WT) and two triazole antifungal resistant strains harboring either the TR$_{34}$/L98H (Af_luc$_{OPT_red}$_TR34) or the TR$_{46}$/Y121F/T289A (Af_luc$_{OPT_red}$_TR46) *cyp51A* gene mutations.
2. *Cryptococcus neoformans* red-shifted thermostable firefly luciferase-expressing strain (KN99α-CnFLuc) [20].

2.2 Fungal Culture and Harvesting

1. Incubator at 37 °C (*A. fumigatus*), 30 °C (*C. neoformans*).
2. Sabouraud dextrose agar plates with chloramphenicol: 42.5 grams of medium in one liter of purified/distilled water (pH 5.6 ± 0.2; agar 12 grams (g), dextrose 40 g, peptones 10 g, chloramphenicol 0.05 g).
3. Liquid Sabouraud medium.
4. Sterile distilled water with 0.1% Tween 80.
5. Dulbecco's phosphate-buffered saline solution (PBS).
6. Disposable loops.
7. Syringe filter holder (25 mm).
8. 11 μm nylon net filter.
9. Vortex mixer.
10. Disposable sterile plastic tube of 15 mL for fungal suspension containment.
11. Microscope.
12. Neubauer hemocytometer with top lid for spore counting (0.100 mm depth–0.0025 mm^3) (*see* **Note 1**).

2.3 Animals and Housing

1. 8- to 10-week-old BALB/c mice (*see* **Note 2**).
2. 10% oral solution broad-spectrum antibiotic (Enrofloxacin).
3. Individually ventilated cages in biosafety level 2 environment.
4. Water and standard food ad libitum.

2.4 Immunosuppression to Allow for invasive *A. fumigatus* Infection

1. Cyclophosphamide monohydrate powder (≥98%).
2. Sterile distilled water for reconstitution.
3. 0.5 mL disposable insulin syringes for intraperitoneal administration.

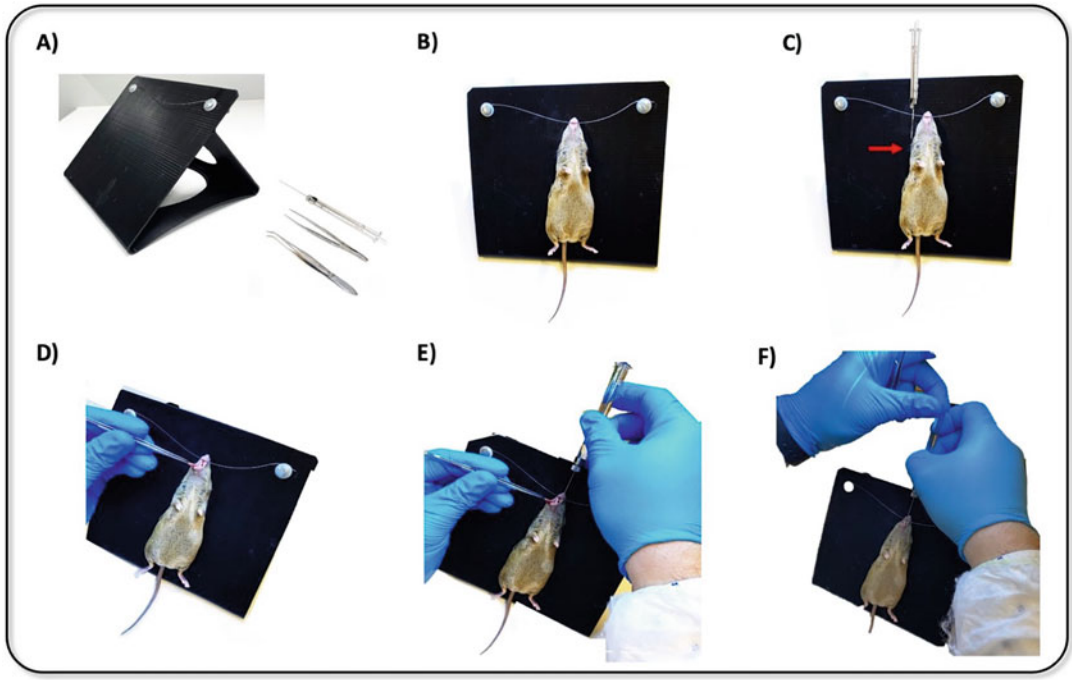

Fig. 1 Orotracheal inoculation. For mouse inoculation, prepare the (**a**) vertical support, the Hamilton syringe fitted with a sterile bent gavage needle with the desired inoculum concentration and small forceps. (**b**) Once a mouse is anesthetized (typically achieved in an induction box with 1.5–2% isoflurane in 100% oxygen), suspend the mouse on vertical support through its upper incisors. (**c**) Determine cannula insertion depth (upper third of the chest; red arrow maximum depth). (**d**) Open the inoculation path by pulling out the animal's tongue with surgical tweezers and holding it to the side and next, (**e**) gently introduce the cannula needle through the oropharynx until the predetermined depth, and (**f**) push plunger to release the inoculum

2.5 Orotracheal Inoculation

1. Hamilton® GASTIGHT syringe, 1700 series, removable needle (1705RN), volume 50 µL (Nevada, USA, Fig. 1a).
2. Hamilton ® SUPELCO Needle 19,139-U blunt tip. Needle size 22 s ga, L 51 mm (2 in.), stainless steel (Fig. 1a).
3. Backboard vertical mouse support (*see* **Note 3,** Fig. 1a).

2.6 Anesthesia

1. Isoflurane vaporizer (Piramal critical care; Pennsylvania, USA) with an anesthesia scavenging system (e.g., via charcoal filter or active evacuation) to provide gas anesthesia mixture of 2–3% isoflurane (Abbott Laboratories; Queensborough, UK) in 100% oxygen with controlled flow. The vaporizer should be tubed and connected to an anesthesia induction box and the BLI scanner.

2.7 BLI

1. BLI camera, such as IVIS Spectrum (Perkin Elmer, USA).
2. Living Image software (version 2.50.1 and 4.7.3 for PC) provided by the manufacturer.

3. D-luciferin solution: 50 mg/mL D-luciferin sodium in 0.9% sterile saline (luciferin-EF, Promega, Wisconsin, USA) (*see* **Note 4**).
4. 0.3 or 0.5 mL disposable insulin syringes for luciferin administration.

2.8 Tissue Isolation at Endpoint

1. General microsurgery kit for organ harvesting.
2. Labeled organ recipient containers (e.g., 2 mL, 15 mL or 50 mL tubes or sample containers) prefilled with storage solution (PBS, saline solution, fixative, etc.) depending on further sample processing steps.

3 Methods

3.1 Immunosuppression for Neutropenic Model of IPA

1. Render mice neutropenic by intraperitoneal (i.p.) injections of cyclophosphamide (reconstituted in 0.9% saline-solution) at a dose of 150 mg/kg on day −4 and − 1 with a booster (additional dose) of 150 mg/kg dose on day 2; day 0 is considered as the day of infection (fungal inoculation).
2. At the initiation of immunosuppressive therapy, add Enrofloxacin 10% oral solution antibiotic (50 mg/kg/day) to the drinking water of the mice to reduce the possibility of bacterial infections [37].
3. Control the Immunosuppressive status on day 0 and day 2 by drawing blood by cardiac puncture from two mice per timepoint with insulin syringes precoated with 3.8% trisodium citrate (1 unit per 9 parts of blood) to avoid coagulation. Measure blood cell counts using a hematology system (Advia 2120i, Siemens Healthcare GmbH, Erlanger, Germany). Mice are considered immunosuppressed (severe neutropenia) when <100 neutrophils/μL blood are counted.

3.2 Fungal Culture and Spore Harvesting

1. *A. fumigatus*
   1.1. Defrost collection tube of designated fungal strain.
   1.2. With a cotton swab, gently touch the spore suspension and plate in a Sabouraud agar plate and incubate for 48 hours at 37 °C.
   1.3. Perform a subculture from previous culture and incubate for 72 hours at 37 °C (minimum 3 plates to assure adequate number of spores).
   1.4. Add 5 mL of saline 0.1% tween-80 solution to each culture agar plate to facilitate spore removal, dispersion and to reduce clumping.

1.5. Gently scrape the surface of each plate to detach the spores with a disposable loop.

1.6. Collect the suspension with a 5 mL syringe and place in a 15 mL tube.

1.7. Vortex vigorously for approximately 1 minute.

1.8. Filter the suspension using a syringe filter holder with the 11 μm nylon net filter to restrict the passage to single spores only and to remove hyphae, clumps, and agar and place the filtrate into a new labeled sterile 15 mL tube.

2. *C. neoformans*

2.1. Defrost collection tube of designated strain.

2.2. With a cotton swab gently touch the cell suspension, inoculate a Sabouraud agar plate and incubate for 48 hours at 30 °C.

2.3. Transfer cells to liquid Sabouraud medium and incubate for 2 days at 30 °C.

2.4. Harvest fungal cells by centrifugation.

2.5. Remove supernatant and perform two washing steps with PBS.

3. *Inoculum preparation*

3.1. Using a Neubauer Hemacytometer count the number of fungal cells in suspensions.

3.2. Calculate total spore amount per milliliter and prepare suspension to desired concentration.

3.3 Inducing Mouse Model of Infection by Orotracheal Inoculation

1. For inoculation, load the Hamilton syringe fitted with a sterile bent gavage needle with 20 μL air followed by the desired inoculum concentration (should not exceed a volume of 30 μL; Fig. 1a). The air pocket behind the inoculum is used to ensure that all the fluid is instilled into the lung (*see* **Notes 5** and **6**).
2. Anesthetize a mouse using 1.5–2% isoflurane in 100% oxygen. Animals should remain in the anesthesia isoflurane induction box until fully anesthetized; 3–5 minutes approximately (*see* **Notes 7** and **8**).
3. Place the anesthetized mouse on the vertical support, suspended by its upper incisors (best visualization with the ventral side of the mouse facing researcher; Fig. 1b).
4. Determine visually and note the desired insertion depth of the Hamilton syringe and needle (upper third of the chest region, before trachea bifurcation) by placing the syringe next to the suspended mouse (Fig. 1c).

5. Gently pull out the animal tongue with surgical tweezers and hold it to the side. Straighten the orotracheal inoculation path (Fig. 1d); if required, the angle of the head should be adjusted with the little finger behind the neck.
6. With your other hand, take the loaded syringe containing the inoculum and push the needle through the visualized oropharynx (orotracheal opening, *see* **Note 9**). When inserted, carefully advance the cannula further until the previously determined depth (upper third of the chest cavity; Fig. 1e). No resistance should be encountered during the cannula introduction, which is usually associated with erroneous insertion into the esophagus.
7. Push the plunger evenly to deliver the inoculum (including prefilled air; Fig. 1f).
8. Hold the mouse upright for a few seconds to allow inoculum to be inhaled into the lungs.
9. Monitor the mice daily for general appearance, weight loss, and survival.

3.4 BLI Acquisition and Quantification

1. Acquire BL images daily (IPA model) or weekly (cryptococcosis model) using the IVIS Spectrum system (*see* **Notes 10, 11,** and **12**). Consider acquiring baseline scan prior to infection or longitudinal scans of control animals for analysis.
2. For BLI scanning, inject the mouse intraperitoneally with D-luciferin (dose range 126–500 mg/kg body weight, the later giving the highest sensitivity of detection in the lung region [35]). To improve the imaging sensitivity of detection for cryptococcal brain infection, we recommend administering the D-luciferin intravenously via the tail vein of the mouse (dose of 126 mg/kg body weight).
3. Subsequently, place the mouse in anesthesia induction box and anesthetize with gas-anesthesia.
4. Once anesthetized, transfer the mouse to the IVIS system chamber on the heated platform in supine position for image acquisition (*see* **Note 13**). Acquire consecutive frames (10–15 frames of 60 seconds each, f/stop 1, medium binning, height 1.5 cm) for a period of 20 min to allow maximum signal intensity detection (reached after approximately 15 sequences).
5. Measure the intensity of the BLI signals (photon-flux per second) through a rectangular region of interest (ROI) of pre-established dimensions containing the lung or brain regions (Fig. 2) in accordance with experimental setting using the Living Image software. Representative BLI scans and mouse peak signals (highest measured total flux expressed in p/s) are used for analysis and reporting (Fig. 3).

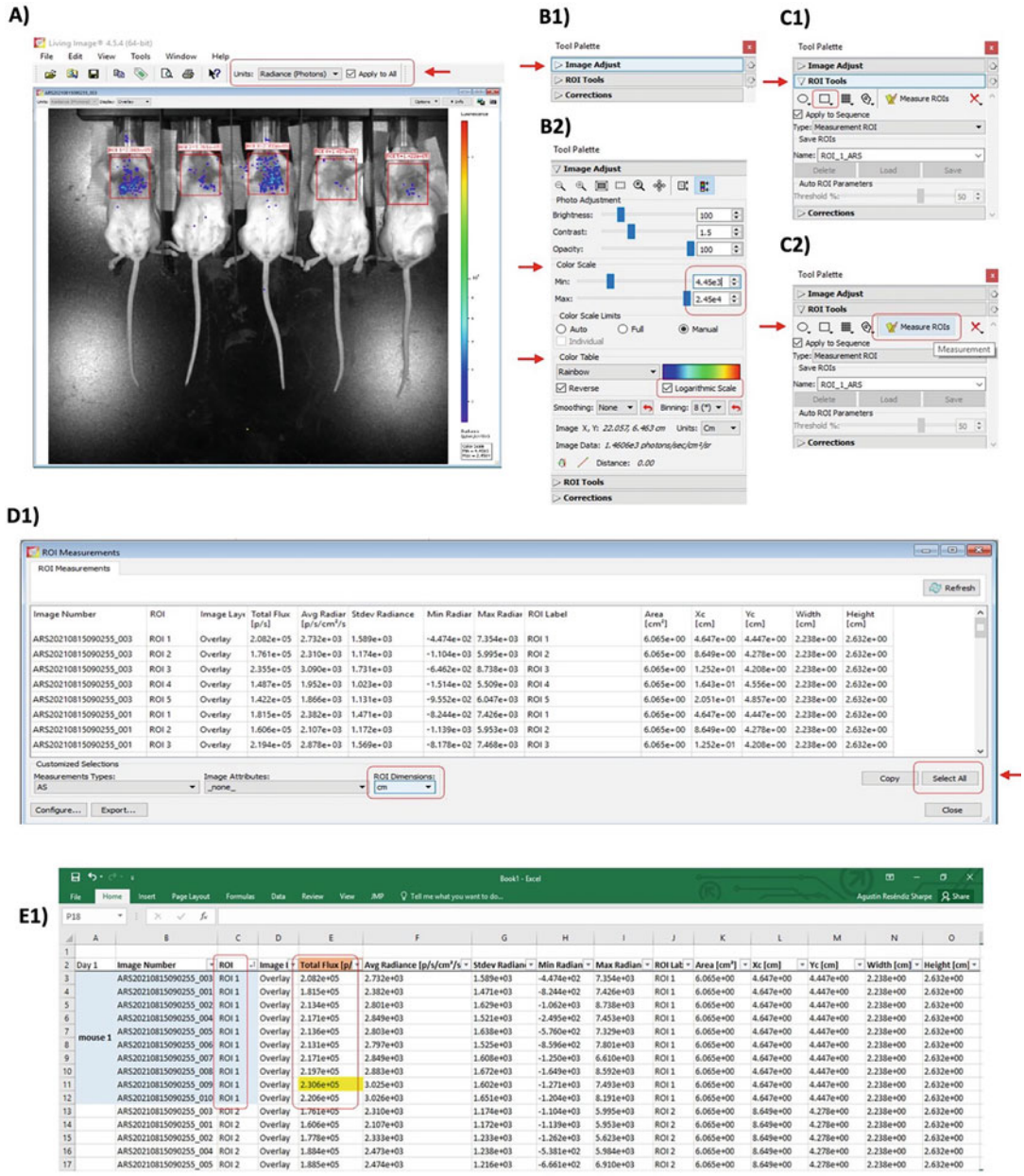

Fig. 2 Quantification of BLI signal from a region of interest. In Living Image, to begin with, select on the representative BLI image scan window (**a**) the readout "radiance" in units of photons and apply to all (red arrow). Adjust the color scale display of the image (**b1**) by selecting "logarithmic scale" on the color table section (**b2**; red arrow). Adjust color scale manually to same minimum and maximum values for representative image comparison within the same experiment (B2; red arrow). Subsequently, open ROI tools palette (**c1**) and select the desired shape of the ROI to be quantified (e.g., square, circle), in this case a rectangle covering the lung area. Locate and adjust the size of the ROI to designated area of interest (**a**, lung region). Repeat the process based on the number of required regions to be analyzed (**a**; ROIs in the lung region of 5 mice). Use the tab "Measure ROIs" (**c2**; red arrow) to quantify BLI signals. ROIs measurements will appear in a new window (**d1**). Choose the option "cm" in ROI dimensions tab (red square) followed by "select all" (red arrow) and "copy" data. Paste copied data into a spreadsheet file (**e1**) and select from each ROI the highest (peak) total flux (red square) for further analysis and reporting

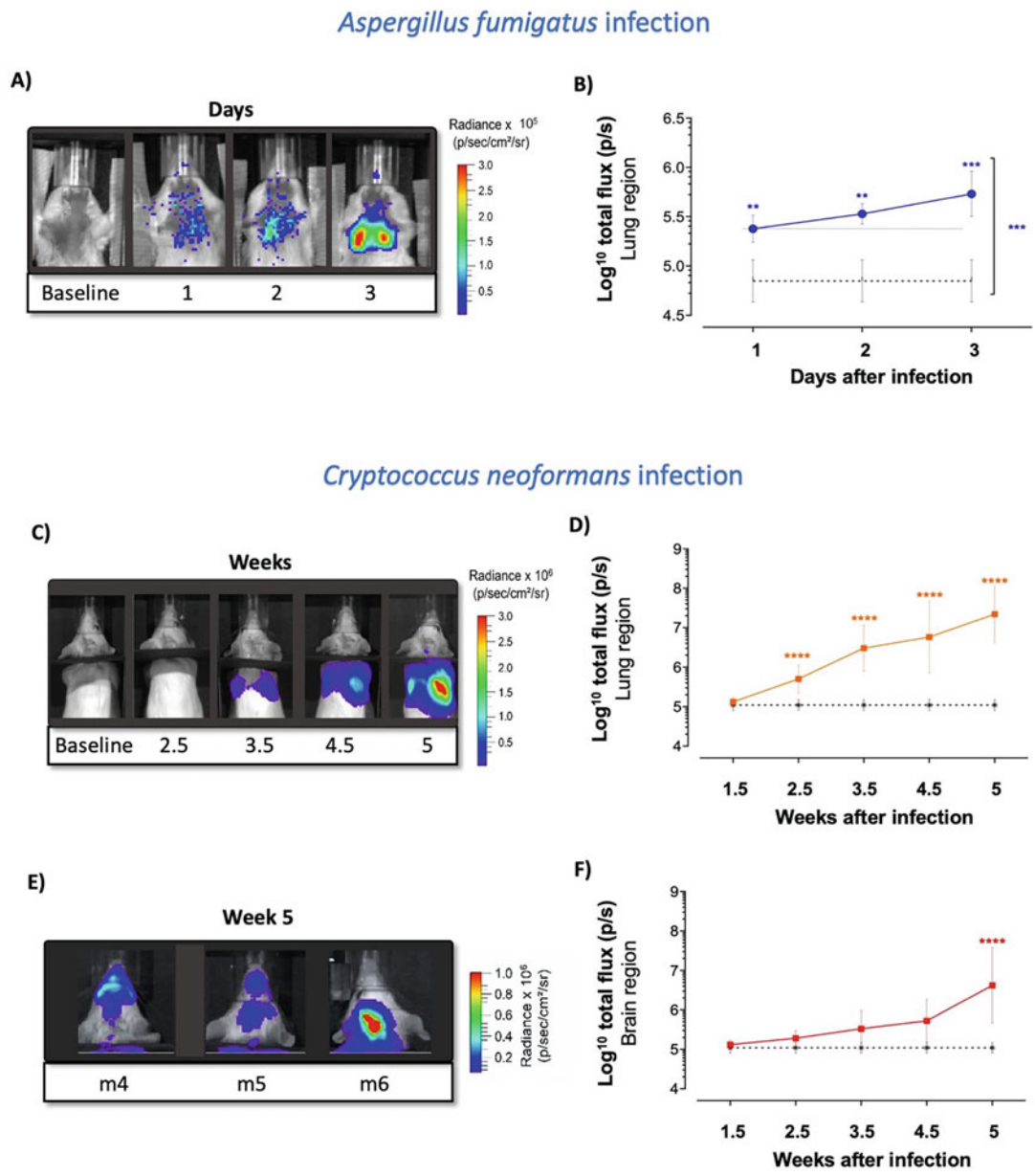

Fig. 3 BLI to longitudinally monitor fungal burden and infection dissemination in IPA and cryptococcosis mouse models. (**a**) Longitudinal BLI images of a representative mouse orotracheally inoculated with the red-shifted luciferase-expressing *A. fumigatus* strain (Af_lucOPT_red_WT; 5X10 [5] spores) after infection ($n = 5$). (**b**) Quantified BLI signals ($\log_{10}$ total flux) from pulmonary ROI of infected mouse compared to baseline scans over time. (**c**) Longitudinal representative BLI images of a mouse infected with the red-shifted luciferase-expressing *C. neoformans* strain (KN99α-CnFLuc; 1X10 [4] spores orotracheally) of the lung region and (**e**) of selected mice (3 mice) at week 5 of the brain region. Mice total peak fluxes quantification over time of the (**d**) lung and (**f**) brain regions ($n = 12$); cryptococcosis data adapted from Vanherp L. et al. [20] Data are mean + s.d. $P = * \leq 0.05, ** \leq 0.005, *** \leq 0.0005$ to baseline per day (above) and overall (lateral); two-way repeated measures ANOVA (multiple comparison analysis, Tukey's correction. ***Abbreviations***: ns (not significant), BLI (bioluminescence imaging), ROI (region of interest)

3.5 Experiment Termination

1. After the last imaging time point or when humane endpoint is reached (*see* **Note 14**), euthanize animals by intraperitoneal (i.p.) administration of 100 µL of 200 mg/mL sodium pentobarbital.
2. Remove aseptically and weigh relevant organs, such as the lungs or brain, for analysis (*see* **Note 15**).
3. Organ samples can be removed and stored for several purposes such as CFU counting, ex vivo BLI, histology, and molecular analysis.
4. For lung CFU counts determination, homogenize desired organ (according to experimental setting) in 600 µL of saline solution. Prepare dilution series (e.g., ten-fold dilution) from homogenized suspension and plate 100 µL of selected dilutions on Sabouraud agar plates (e.g., undiluted, 1/10, 1/100 and 1/1000 dilutions) (*see* **Note 16**). Incubate plates at 37 °C and count CFU at 24, 48, and 72 hours ($\log_{10}$ CFU counts per gram of weighted lung tissue).

4 Notes

1. Neubauer chamber's counting grid should contain 9 square subdivisions (1 × 1 mm) comprising 25 medium sized squares (0.2 × 0.2 mm) with 16 small squares each (0.05 × 0.05 mm); the later used for spore counting (0.00025 µL content in a small square).
2. All animal experiments should be conducted in accordance with international and national regulations and approved by the animal ethics committee from the research institution.
3. The vertical support equipment was manufactured in-house using a 3D printer (E3D NANO 3D printer, Karsten International; North Holland, The Netherlands) and commercially available 75 mm PLA-filaments. The used dimensions fit the following measurements: 6 mm thick, 42 cm in length, 22 cm in width, and bent to a 45° angle. Two holes were drilled on each side of the backboard 2 cm from the top and side edge. Galvanized metal-style screws, nuts, and washers were used to secure a stainless-steel wire strung from one screw to the other from which a mouse could be hung by its incisors.
4. Luciferin is light sensitive and should always be kept in the dark during reconstitution, aliquoting, and experiments. Aluminum foil can be used to cover working materials containing luciferin.
5. The following inoculum doses have been validated in our models: *C. neoformans* 500 to 50,000 fungal cells, *A. fumigatus* 500,000 spores. We recommend to always plate dilutions of the inoculum for CFU counts confirmation.

6. A pipette tip near the tracheal entrance can be used for orotracheal inoculation as an alternative to the Hamilton syringe fitted with a sterile bent gavage needle.
7. Animal inoculation could be performed likewise through intraperitoneal systemic anesthesia (i.p.) with a mixture of ketamine (45–60 mg/kg, Nimatek®; Bladel, The Netherlands) and medetomidine (0.6–0.8 mg/kg, Domitor®; Espoo, Finland) and reversed by i.p. injection of atipamezole hydrochloride (0.5 mg/kg, Antisedan®, Espoo, Finland). Yet, anesthesia induced by i.p. injection has been associated with increased weight loss compared to gas anesthesia-induced mice[35].
8. A mouse is considered fully anesthetized in the presence of slowed down breathing and not responsiveness when stimulated.
9. The terminology of oropharynx inoculation is commonly interchanged with orotracheal inoculation in research reports. Indeed, the orotracheal route of inoculation requires a laryngoscope and direct visualization of the vocal cords. Nonetheless, delivery of an inoculum to the lower respiratory tract (oropharynx, trachea, and bronchia) by orotracheal introduction of a syringe (canula) can be successfully achieved through the oropharynx with the above mentioned methodology.
10. To improve BLI signal detection, hair from the thoracic region should be removed in advance using a commercially available hair-removal cream (e.g., Nair). Spread evenly a small amount of hair-removal cream on the mouse chest. Wait for 2 minutes and remove gently the cream and hair with a soft tissue paper.
11. Fur on the top of the head can be clipped to optimize the detection of BLI signals originating from the brain.
12. A black partition over the neck of the animal can be placed to separate the bioluminescence of the lung region from the bioluminescence of the brain region (disseminated cryptococcosis).
13. When doing *D*-luciferin i.p injection, up to 5 mice can be imaged in one field of view.
14. Humane endpoint sacrifice was done when any of the following symptoms was observed: >20% weight loss, lethargy impending feeding, and drinking or respiratory distress.
15. Ex vivo BLI can be also performed after sacrifice (within one hour of previous D-luciferin administration). Place organs in a 6-well plate inside the IVIS Spectrum system and acquire images using an F/stop of 1 and medium binning, with exposure times depending on the magnitude of the signal (range 4–60 s).
16. For CFUs counting, Sabouraud agar with chloramphenicol should be used to select for fungal pathogens and to reduce the presence of bacteria.

Acknowledgements

This work was supported by the Flemish Research Foundation (Fonds Wetenschappelijk Onderzoek, FWO, grants 1506114 N and G057721N). E.V. acknowledges support by an aspirant mandate from the FWO (ISF2222N).

References

1. Rodrigues ML, Nosanchuk JD (2020) Fungal diseases as neglected pathogens: a wake-up call to public health officials. PLoS Negl Trop Dis 14(2):e07964. https://doi.org/10.1371/JOURNAL.PNTD.0007964
2. Nature Microbiology Editorial (2017) Stop neglecting fungi. Nat Microbiol 2(8):1–2. https://doi.org/10.1038/nmicrobiol.2017.120
3. The Fungal Infection Trust (GAFFI, Global action fund for fungal infections) (2017) How common are fungal diseases?. http://www.gaffi.org/media/fact-. Accessed 25 Mar 2022
4. Latgé JP, Chamilos G (2020) *Aspergillus fumigatus* and aspergillosis in 2019. Clin Microbiol Rev 33(1):e00140. https://doi.org/10.1128/CMR.00140-18
5. Verweij PE, Gangneux J-P, Bassetti M et al (2020) Diagnosing COVID-19-associated pulmonary aspergillosis. The Lancet Microbe. https://doi.org/10.1016/s2666-5247(20)30027-6
6. Vanderbeke L, Spriet I, Breynaert C et al (2018) Invasive pulmonary aspergillosis complicating severe influenza: epidemiology, diagnosis and treatment. Curr Opin Infect Dis 31(6):471–480. https://doi.org/10.1097/QCO.0000000000000504
7. GAFFI (2020) Fungal disease frequency – Gaffi | Gaffi – Global action fund for fungal infections. Global Action Fund for Fungal Infection. https://gaffi.org/why/fungal-disease-frequency/. Published 2020. Accessed 25 Mar 2022
8. Resendiz-Sharpe A, Lagrou K et al (2018) Triazole resistance surveillance in *Aspergillus fumigatus*. Med Mycol 56(suppl_1):S83–S92. https://doi.org/10.1093/mmy/myx144
9. Nywening AV, Rybak JM, Rogers PD et al (2020) Mechanisms of triazole resistance in aspergillus fumigatus. Environ Microbiol 22(12):4934–4952. https://doi.org/10.1111/1462-2920.15274
10. Resendiz-Sharpe A, Mercier T, Lestrade PPA et al (2019) Prevalence of voriconazole-resistant invasive aspergillosis and its impact on mortality in haematology patients. J Antimicrob Chemother 74(9):2759–2766. https://doi.org/10.1093/jac/dkz258
11. Lestrade PP, Bentvelsen RG, Schauwvlieghe AFAD et al (2019) Voriconazole-resistant Aspergillosis Voriconazole resistance and mortality in invasive aspergillosis: a multicenter retrospective cohort study. Clin Infect Dis CID 68(9):1463–1471. https://doi.org/10.1093/cid/ciy859
12. Iyer KR, Revie NM, Fu C et al (2021) Treatment strategies for cryptococcal infection: challenges, advances and future outlook. Nat Rev Microbiol 19(7):454–466. https://doi.org/10.1038/S41579-021-00511-0
13. Lin X, Heitman J (2006) The biology of the *Cryptococcus neoformans* species complex. Annu Rev Microbiol 60:69–105. https://doi.org/10.1146/annurev.micro.60.080805.142102
14. Perfect JR, Dismukes WE, Dromer F et al (2010) Clinical practice guidelines for the management of Cryptococcal disease: 2010 update by the Infectious Diseases Society of America. Clin Infect Dis 50(3):291–322. https://doi.org/10.1086/649858
15. Spec A, Mejia-Chew C, Powderly WG et al (2018) EQUAL Cryptococcus score 2018: a European Confederation of Medical Mycology score derived from current guidelines to measure quality of clinical cryptococcosis management. Open Forum Infect Dis 5(11):ofy299. https://doi.org/10.1093/OFID/OFY299
16. Desoubeaux G, Cray C (2017) Rodent models of invasive aspergillosis due to *aspergillus fumigatus*: still a long path toward standardization. Front Microbiol 8:841. https://doi.org/10.3389/fmicb.2017.00841
17. Cundell T (2015) The limitations of the colony-forming unit in microbiology. Eur Pharm Rev 20(6):11–13
18. Olsen RA, Bakken LR (1987) Viability of soil bacteria: optimization of plate-counting technique and comparison between total counts and plate counts within different size groups. Microb Ecol 13(1):59–74. https://doi.org/10.1007/BF02014963

19. Papon N, Courdavault V, Lanoue A et al (2014) Illuminating fungal infections with bioluminescence. PLoS Pathog 10(7):1–4. https://doi.org/10.1371/journal.ppat.1004179
20. Vanherp L, Ristani A, Poelmans J et al (2019) Sensitive bioluminescence imaging of fungal dissemination to the brain in mouse models of cryptococcosis. DMM Dis Model Mech 12(6): dmm039123. https://doi.org/10.1242/dmm.039123
21. Poelmans J, Himmelreich U, Vanherp L et al (2018) A multimodal imaging approach enables *in vivo* assessment of antifungal treatment in a mouse model of invasive pulmonary aspergillosis. Antimicrob Agents Chemother 62(7):e00240. https://doi.org/10.1128/AAC.00240-18
22. Defosse TA, Courdavault V, Coste AT et al (2018) A standardized toolkit for genetic engineering of CTG clade yeasts. J Microbiol Methods 144:152–156. https://doi.org/10.1016/J.MIMET.2017.11.015
23. Vande Velde G, Kucharíková S, Van Dijck P et al (2014) Bioluminescence imaging of fungal biofilm development in live animals. Meth Mol Biol 1098:153–167. https://doi.org/10.1007/978-1-62703-718-1_13
24. Van Dyck K, Van Dijck P, Vande VG (2020) Bioluminescence imaging to study mature biofilm formation by *Candida spp.* and antifungal activity *in vitro* and *in vivo*. In: Ripp S (ed) Bioluminescent imaging: methods and protocols, pp 127–143. https://doi.org/10.1007/978-1-4939-9940-8_9
25. Brock M (2012) Application of bioluminescence imaging for *in vivo* monitoring of fungal infections. Int J Microbiol 2012:956794. https://doi.org/10.1155/2012/956794
26. Seldeslachts L, Jacobs C, Tielemans B et al (2021) Overcome double trouble: Baloxavir Marboxil suppresses influenza thereby mitigating secondary invasive pulmonary Aspergillosis. J Fungi (Basel, Switzerland) 8(1):1. https://doi.org/10.3390/JOF8010001
27. Vande Velde G, Kucharíková S, Van Dijck P, Himmelreich U (2018) Bioluminescence imaging increases *in vivo* screening efficiency for antifungal activity against device-associated *Candida albicans* biofilms. Int J Antimicrob Agents 52(1):42–51. https://doi.org/10.1016/J.IJANTIMICAG.2018.03.007
28. Jacobsen ID, Lüttich A, Kurzai O et al (2014) *In vivo* imaging of disseminated murine *Candida albicans* infection reveals unexpected host sites of fungal persistence during antifungal therapy. J Antimicrob Chemother 69(10): 2785–2796. https://doi.org/10.1093/jac/dku198
29. Galiger C, Brock M, Jouvion G et al (2013) Assessment of efficacy of antifungals against *aspergillus fumigatus*: value of real-time bioluminescence imaging. Antimicrob Agents Chemother 57(7):3046–3059. https://doi.org/10.1128/AAC.01660-12
30. Dorsaz S, Coste AT, Sanglard D (2017) Red-shifted firefly luciferase optimized for *Candida albicans in vivo* bioluminescence imaging. Front Microbiol 8:01478. https://doi.org/10.3389/fmicb.2017.01478
31. Binder U, Navarro-Mendoza MI, Naschberger V et al (2018) Generation of a *Mucor circinelloides* reporter strain—a promising new tool to study antifungal drug efficacy and Mucormycosis. Genes (Basel) 9(12):613. https://doi.org/10.3390/genes9120613
32. Vande Velde G, Kucharíková S, Schrevens S et al (2014) Towards non-invasive monitoring of pathogen-host interactions during *Candida albicans* biofilm formation using *in vivo* bioluminescence. Cell Microbiol 16(1):115–130. https://doi.org/10.1111/cmi.12184
33. Avci P, Karimi M, Sadasivam M et al (2018) *In-vivo* monitoring of infectious diseases in living animals using bioluminescence imaging. Virulence 9:28. https://doi.org/10.1080/21505594.2017.1371897
34. Vecchiarelli A, d'Enfert C (2012) Shedding natural light on fungal infections. Virulence 3(1):15–17. https://doi.org/10.4161/viru.3.1.19247
35. Reséndiz Sharpe A, Peres Ds Silva R, Geib E et al (2022) Longitudinal multimodal imaging-compatible mouse model of triazole sensitive and resistant invasive pulmonary aspergillosis. Dis Model Mech 15:dmm049165
36. Seldeslachts L, Vanderbeke L, Fremau A et al (2021) Early oseltamivir reduces risk for influenza-associated aspergillosis in a double-hit murine model. Virulence 12(1): 2493–2508. https://doi.org/10.1080/21505594.2021.1974327
37. Marx JO, Vudathala D, Murphy L et al (2014) Antibiotic administration in the drinking water of mice. J Am Assoc Lab Anim Sci 53(3): 301–306. PMID: 24827573 PMCID: PMC4128569

Chapter 16

Microcomputed Tomography to Visualize and Quantify Fungal Infection Burden and Inflammation in the Mouse Lung Over Time

Eliane Vanhoffelen, Agustin Resendiz-Sharpe, and Greetje Vande Velde

Abstract

Pulmonary mycoses are an important threat for immunocompromised patients, and although current treatments are effective, they suffer from multiple limitations and fail to further reduce mortality. With the increasing immunocompromised population and increased antifungal resistance, fungal infection research is more relevant than ever. In preclinical respiratory fungal infection research, animal models are indispensable. However, too often researchers still rely on endpoint measurements to assess fungal burden while the dynamics of disease progression are left undiscovered. To open up this "black box", microcomputed tomography (μCT) can be implemented to longitudinally visualize lung pathology in a noninvasive way and to quantify μCT-image derived biomarkers. That way, disease onset, progression, and responsiveness to treatment can be followed up with high resolution spatially and temporally in individual mice, increasing statistical power. Here, we describe a general method for the use of low-dose high-resolution μCT to longitudinally visualize and quantify lung pathology in mouse models of respiratory fungal infections, applied to mouse models of aspergillosis and cryptococcosis.

Key words Microcomputed tomography (μCT), μCT-derived biomarkers, Respiratory fungal infection, Aspergillosis, Cryptococcosis, Mouse model

1 Introduction

Pulmonary mycoses are a major cause of morbidity and mortality, especially in the growing immunocompromised population. Early diagnosis and effective therapy are key factors for a successful outcome, but nonspecific and late symptoms, together with a plateauing effectiveness of our current antifungal treatments, often complicate disease management and keep mortality high [1, 2]. Increased efforts are therefore being made to improve our understanding of pathogenesis, identify novel treatment targets and diagnostic biomarkers, decrease off-target toxicity and resistance development of antifungals, develop vaccines, etc., in which preclinical animal models are indispensable [2].

Rebecca A. Drummond (ed.), *Antifungal Immunity: Methods and Protocols*, Methods in Molecular Biology, vol. 2667,
https://doi.org/10.1007/978-1-0716-3199-7_16,

Preclinical animal research of pulmonary infections typically relies on endpoint techniques such as survival analysis, lung tissue histology, bronchoalveolar lavage, serum analysis, and colony-forming unit (CFU) counts. These measures deliver intrinsically snapshots of a dynamic disease process. Particularly in the typically highly variable context of infection and inflammation, endpoint techniques suffer inherently from low statistical power and are prone to sampling errors. Adding sacrifice timepoints to gain longitudinal insights into disease and to overcome interanimal variability requires a high number of animals and large investments in terms of time, labor, and funds [3]. In the clinic, on the other hand, diagnosis and therapeutic monitoring of fungal respiratory diseases are commonly performed using computed tomography (CT) because of its ability to repeatedly visualize typical fungal lesions in the lung [4]. A preclinical alternative for CT, microcomputed tomography (μCT), is increasingly embraced as a novel state-of-the-art tool in preclinical disease evaluation, but implementation in fungal infection research lags behind despite its advantages.

In vivo μCT provides instant longitudinal and three-dimensional anatomical information on lung pathology, such as fungal lesions and host response, because of the clear endogenous air-tissue contrast [5–13]. It enables spatial and temporal follow-up of disease onset, progression, and recovery upon treatment in the complete lung region of free-breathing individual animals [5, 14, 15]. This does not only reduce multifold the number of animals needed but also overcomes sampling bias as present in histopathological readouts. By following the same animal over time, statistical power is increased and inter-animal variability in disease progression and treatment efficacy can be picked up allowing for correct interpretation of the corresponding endpoint measurements, thus improving preclinical treatment study efficacy and translation of results towards clinical study design [3, 16].

In addition to qualitative assessment of μCT images, different quantitative biomarkers can be derived by separating hyperdense voxels from voxels with lower density by thresholding within the volume of interest, that is, the entire lung: aerated lung volume, nonaerated lung volume, total lung volume (sum of aerated and nonaerated volumes), and mean lung density [16]. Fungal lesions or other pulmonary (inflammatory) infiltrates will typically appear as hyperdense patterns such as ground glass opacities and different types of nodular lesions, thereby increasing the nonaerated lung volume and lung density. Hyperinflation or emphysema, on the other hand, will present as hyperlucent areas, decreasing lung density [4]. Aerated lung volume is also considered a biomarker of lung function since it correlates with inspiratory capacity [3], and efforts are being made to extract more detailed lung function parameters from μCT scans.

Longitudinal μCT of lung infection and inflammation has already proven useful in multiple animal models [7, 10, 11, 14, 15, 17], including two mouse models of major pulmonary mycoses, namely, invasive pulmonary aspergillosis (IPA) and pulmonary cryptococcosis [5, 6]. The mouse model of IPA is a rapidly progressing model (timespan of 4 days) upon orotracheal infection with *Aspergillus fumigatus*, while the cryptococcosis mouse model develops more slowly (timespan of 6 weeks) after physiological pulmonary infection with *Cryptococcus neoformans*. μCT can visualize lung pathology and consequent affected lung volume changes caused by these fungal pathogens long before typical symptoms of distress and weight loss appear, thereby opening up the "black box" in these mouse models. μCT images are particularly relevant to follow lung pathology in the slowly developing cryptococcosis mouse model, because despite progressing infection, mice remain asymptomatic and stay apparently healthy until several weeks after infection, thereby blinding researchers for infection severity and key events in pathogenesis such as infection dissemination. μCT overcomes this issue by delivering sensitive and insightful quantitative information on fungal burden and infection progression long before symptom onset, thereby obviating the need to let mice suffer and succumb from infection [6, 16]. Moreover, by applying μCT in the cryptococcosis mouse model, it was discovered that total lung volume increased over time as a compensatory mechanism for the increased nonaerated lung volume, that is, the fungal lesions, causing the aerated lung volume to stay more or less constant over time and explaining the long-lasting healthy appearance of the mice. This underscores the importance of adding μCT as a readout of pulmonary changes, which would otherwise be missed or interpreted incorrectly [3, 16]. Furthermore, the early confirmation of infection by μCT is especially relevant in treatment experiments, to prevent false positive treatment conclusions [5, 14–16].

Due to its very short handling time (<5 min per animal), μCT of fungal lung infection can be easily implemented as part of a multimodal imaging approach, for instance, in combination with magnetic resonance imaging (MRI) to establish fungal dissemination to the brain [6] and/or with bioluminescence imaging (BLI) for fungal load quantification when using luciferase-transgenic fungal strains for infection [5, 6] (*cfr chapter 15*).

Here, we describe a general method for longitudinal μCT acquisition, visualization, and quantification of fungal lung pathology in individual, free-breathing mice with respiratory fungal infections, applied on a mouse model of invasive pulmonary aspergillosis [5] and cryptococcosis [6]. The protocol is readily applicable to evaluate pulmonary pathology progression and antifungal drug efficacy in virtually any mouse model of pulmonary infection or inflammation [7, 14, 15].

2 Materials

2.1 Animal Models

2.1.1 Mouse model of IPA [5]

(a) 8- to 10-week-old BALB/c mice **(Note 1).**

(b) Cyclophosphamide (0.9% in saline) dosed 150 mg/kg to render the mice neutropenic via intraperitoneal (i.p.) injection on day 4 and 1 before infection and on day 2 post-infection.

(c) Broad-spectrum antibiotic (Enrofloxacin; Baytril, Bayer), 10% oral solution (50 mg/kg/day) in the drinking water.

(d) 20 μl of 5×10^5 spores of *Aspergillus fumigatus* (red-shifted firefly luciferase-expressing derivatives of *A. fumigatus* reference strain CBS144.89 [5]) in PBS to induce pulmonary infection via orotracheal instillation (see Subheading 2.2) (**Note 2**).

2.1.2 Mouse model of Pulmonary cryptococcosis [6]

(e) 9- to 10-week-old BALB/c mice (**Note 2**).

(f) 40 μL of 500 spores of *Cryptococcus neoformans* (red-shifted firefly luciferase-expressing KN99α-CnFLuc [6]) in PBS to induce pulmonary infection via orotracheal instillation (see Subheading 2.2) (**Notes 3** and **4).**

2.2 Orotracheal Inoculation

1. Hamilton® GASTIGHT® syringe (1700 series) equipped with a removable needle with blunt tip (1705RN), with a total volume of 50 μL.
2. Vertical mouse support (**Note 5**).
3. Fungal suspension in desired concentration (max. Volume of 40 μL).

2.3 Anesthesia

Isoflurane vaporizer to provide gas anesthesia mixture of 2–3% isoflurane in 100% oxygen with adjustable flow to an anesthesia induction box (for inoculation, scanning) and to the animal bed of the μCT scanner. Anesthesia scavenging can be obtained via, for example, charcoal filter or active evacuation.

2.4 Microcomputed Tomography (μCT)

1. SkyScan 1278 (Bruker, Kontich, Belgium) in vivo μCT system: (https://www.bruker.com/products/microtomography/in-vivo-micro/skyscan-1278). The required system components are: a low-dose, high-resolution SkyScan 1278 scanner with sensitive flat-panel detector; 4 filter options, spatial beam shaper; integrated physiological monitoring with breathing sensor, ECG (optional, not essential for lung imaging), temperature stabilization and body movement detection; oxygen regulator (**Note 6).**
2. Windows workstation with data output in format of choice (tiff, bmp, dicom, among others).

2.5 Software

Software for data acquisition, animal monitoring, image reconstruction, and quantification is provided by the manufacturer: https://www.bruker.com/products/microtomography/micro-ct-software/3dsuite.html. Visualization of reconstructed μCT data can be done with DataViewer (version 1.5.6.2) and data processing by CTAnalyser (CTAn) (version 1.17.7.2).

3 Methods

3.1 Experimental Fungal Infection (Orotracheal Instillation)

1. Anesthetize each animal in an induction box using a gas mixture of 2–3% isoflurane in 100% oxygen until breathing is slowed down and the mouse is irresponsive to touch (**Note 7**).
2. Fill the Hamilton syringe with 20 μL of the inoculum, leaving 20 μL of air behind the inoculum to ensure that the complete volume of inoculum is instilled into the lungs (**Note 8**).
3. Swiftly transfer the anesthetized mouse to the vertical support, suspended by its upper incisors with the ventral side facing the researcher.
4. Using surgical tweezers, gently pull out the tongue and hold it to the side with one hand.
5. With the other hand, take the loaded syringe and gently move down against the ventral side of the oral cavity, until pushing it through the vocal cords into the trachea. When inserted, advance the cannula ≈ 5 mm further (depending on size of the mouse) without moving into the bronchi.
6. Push the plunger evenly to deliver the inoculum. After successful delivery into the lungs, the mouse may make a rattling, bubbling, or clicking sound for a short time.
7. Keep the mouse in upright position for a few more seconds to ensure inhalation of the inoculum into the lungs, before placing it back into the cage.

3.2 μCT Acquisition for Skyscan 1278

1. Turn on the scanner and initialize it using the acquisition software.
2. After initialization, set acquisition parameters optimized for high-resolution, low-dose longitudinal lung imaging as follows:
   (a) Source voltage: 50 kV.
   (b) Source current: 350 μA.
   (c) Image pixel size: 51.62 μM.
   (d) Exposure time: 150 ms.
   (e) Rotation step: step-and-shoot with increment of 0.9° over a total angle of 220°.

(f) Filter: X-ray filter of 1 mm aluminum.

(g) Field of view covering lung area: 54.1 mm.

(h) Partial width: 50% (to reduce file size).

(i) Frame averaging: 3.

(j) Camera pixel: 1944 × 1536 resulting in isotropic voxel size of ≈ 50 μm.

3. Acquire flatfield correction for marked modes without the animal bed in place. After verifying adequate flatfield correction, proceed to place the animal bed in the scanner.
4. Anesthetize each animal in the induction box using a gas mixture of 2–3% isoflurane in 100% oxygen and a flow of 1 L/min. When breathing is slowed down and the animal is irresponsive to touch, transfer it in supine position into the animal bed in the scanner, making sure that the nose is inserted in the nose cone providing gas anesthesia.
5. Align the animal as straight as possible and use tape to stick the front paws away from the lungs next to the head for optimal lung region exposure. Stretch out the back paws (Fig. 1a).
6. Set the temperature inside the scanner at 32–33 °C and monitor the respiration rate via the physiological monitoring

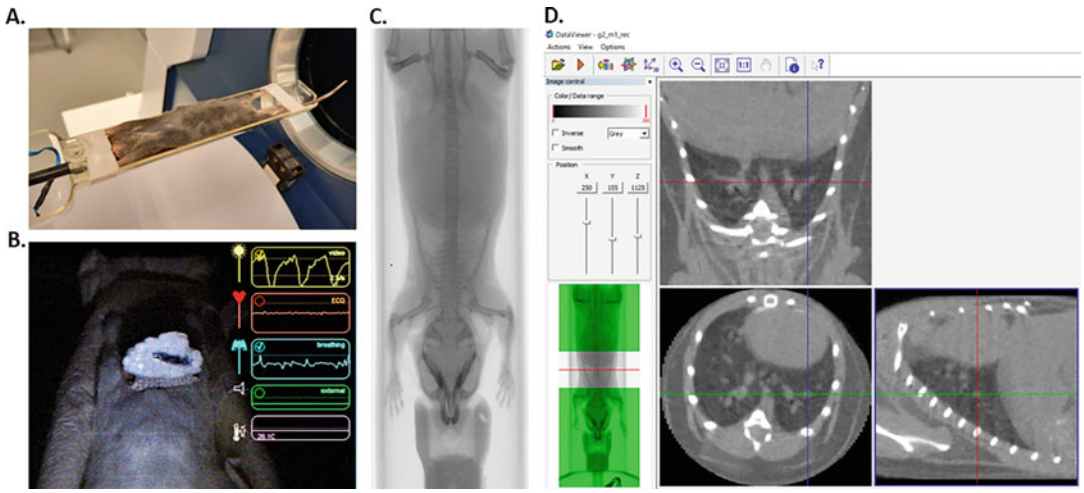

Fig. 1 μCT acquisition and visualization. (**a**) Supine positioning of a mouse in the animal bed of a dedicated small animal μCT scanner (SkyScan1278), stretched out with both front paws taped away from the lung area. (**b**) Via a camera and physiological monitoring system, the animal's breathing and temperature inside the scanner is monitored throughout the scan. In this case, the breathing frequency and depth is tracked by a visual camera sensitively recording movement of the abdomen translated to a marked piece of polystyrene foam. (**c**) Whole-body μCT projection image of a mouse. Note how the paws are positioned away from the lungs, and the spine and neck are straight for optimal lung imaging. (**d**) Tomographic visualization of a reconstructed μCT scan using DataViewer, showing a healthy mouse lung in coronal (up), transverse (middle), and sagittal (right) cross-sections

application (Fig. 1b). For adequate lung imaging, respiration rate should be as constant as it can be with breathing cycles of around 1 s length.

7. Start the scan to acquire projection images of the free-breathing anesthetized mouse (Fig. 1c). Each scan will take approximately 2 min 45 s. Make sure to store the acquired data in a separate folder for each mouse.
8. Before removing the mouse, reconstruct at least one image section as quality control (see Subheading 3.3, μCT scan reconstruction).
9. Repeat **steps 4–8** to scan the next mice.
10. After the last animal scan, start batch reconstruction (see Subheading 3.3). Meanwhile, remove and clean the animal bed from the scanner, clean induction box and other used surfaces, and turn down the scanner (**Note 9**).

3.3 μCT Scan Reconstruction

1. Open the acquired μCT data using the NRecon software and adapt the field of interest to the lung area.
2. Choose a section for preview and apply the following settings:
   (a) Smoothing (Gaussian): 2.
   (b) Beam hardening correction: 10%.
   (c) Optimize lung visualization using a window with lower limit at 0.00 and upper limit at 0.012.
   (d) Region of interest (ROI): Ellipse. Place the ellipse around the complete animal section, excluding the animal bed.
3. Finetune the image for improved reconstruction quality:
   (a) Postalignment: set parameter step at 0.5 px and choose the best alignment, that is, avoid the appearance of "shadows" behind bones into the lungs.
   (b) Ring artefact reduction (only if needed) (**Note 10**): set parameter step at 1.0 and choose image with the least ring artefacts.
4. Change image output as preferred. We recommend 8-bit BMP file format for reducing file size towards storage and subsequent data processing.
5. Add reconstruction to batch.
6. Repeat reconstruction **steps 1–5** for each animal. After the last animal is scanned, reconstruct the batch of scans.

3.4 μCT Data Visualization

The reconstructed μCT data can be visualized using different commercial and noncommercial software tools such as DataViewer or 3D Slicer. We use DataViewer to load the three orthogonal planes and get an idea of the 3D image (Fig. 1d). This can be used for

visual inspection of the lungs and semi-quantitative scoring (see Subheading 3.5).

3.5 μCT Data Quantification

3.5.1 Semi-quantitative Scoring of μCT Scans Based on Visual Observation

1. Load the reconstructed lung μCT data in a visualization software (e.g., DataViewer) and open the 3D viewing option.
2. Choose four predefined transverse or coronal cross-sections at different reproducible trans-axial positions in the lung, covering the complete lung (Fig. 2) (**Note 11**).
3. Assign an initial score of zero to baseline scans. Compare the lung slices of the same animal acquired on the first imaging time point after infection to the corresponding lung slices at baseline. Assign a value of −0.25, 0, or + 0.25 depending on a respective worsening, stabilization, or improvement of the pulmonary damage based on the observable changes in each lung

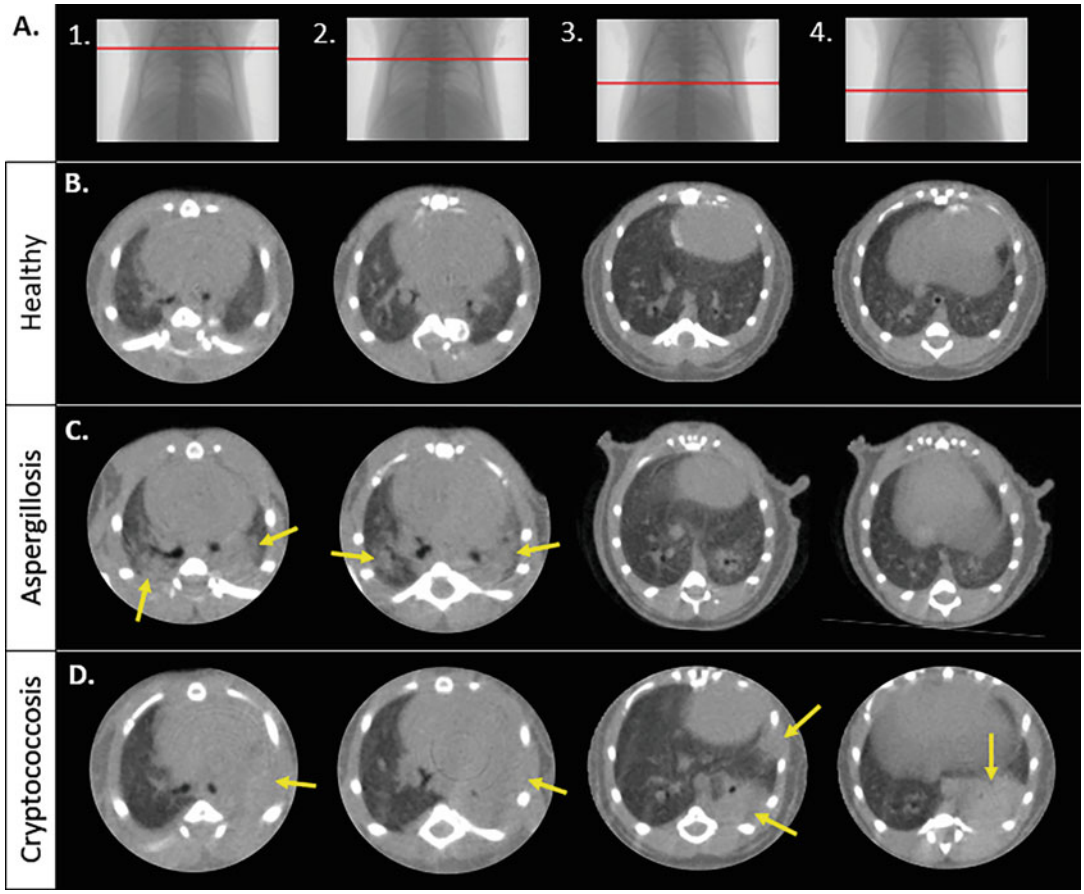

Fig. 2 Visualization of fungal lung infection by μCT. (**a**) Image plane selection along trans-axial orientation for semi-quantitative visual scoring (red lines). **b**, **c,** and **d** show transversal cross-sections at four different trans-axial positions in the lung (according to positions illustrated in (**a**)), illustrating (**c**) healthy lungs, (**d**) *Aspergillus fumigatus* infected lungs, and (**e**) *Cryptococcus neoformans* infected lungs**.** Yellow arrows indicate lung pathology

slice. Based on the same principle, compare and score the image slices of every next imaging time point to those of the previous time point. Add the obtained values for a final cumulative score (Fig. 4a).

3.5.2 Quantification of μCT-Derived Biomarkers

1. Load the reconstructed transverse image μCT data in CTAn software.
2. Manually determine top and bottom of the lungs and delineate the lung as an interpolated region of interest (ROI) on as many sections as necessary for correct interpolation by the software. Stay on the inside of the ribs and avoid the heart and diaphragm (Fig. 3a, b) (**Note 12**). This will result in a volume of interest (VOI) covering the entire lung.

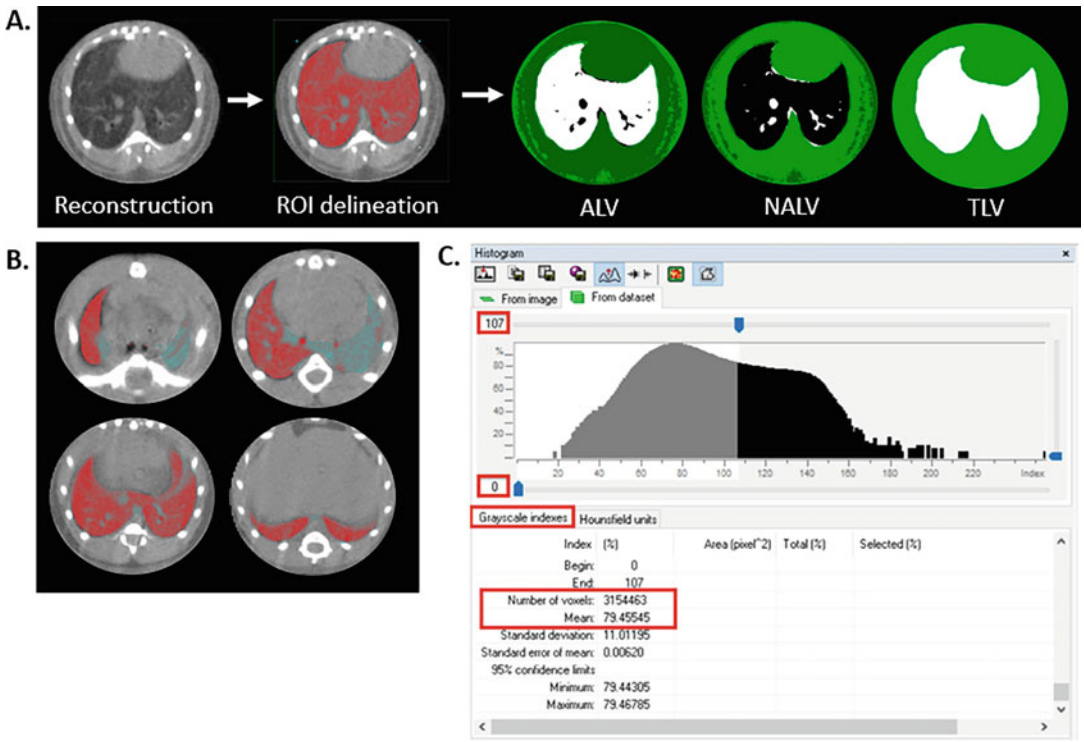

Fig. 3 Quantification of μCT-derived biomarkers of lung infection and host response. (**a**) Manual delineation of ROI on the reconstructed transverse μCT images of a healthy lung, with the resulting binary selection of those voxels with lower densities belonging to the aerated lung volume (ALV), higher density voxels making up the nonaerated lung volume (NALV), and the sum of both giving the total lung volume (TLV) in CTAn software. (**b**) Illustrational ROI delineation on different transverse cross-sections through the lung of a mouse with pulmonary cryptococcosis. (**c**) Density histogram in 8-bit grey values of the segmented volume of interest covering the total lung from the μCT dataset, showing the thresholding of grey values from 0 to 107 to select the ALV. This segmentation step by thresholding returns the number of voxels and the mean density of the ALV in grey value, which can be converted to report the ALV in mm^3 and its density in Hounsfield units (HU)

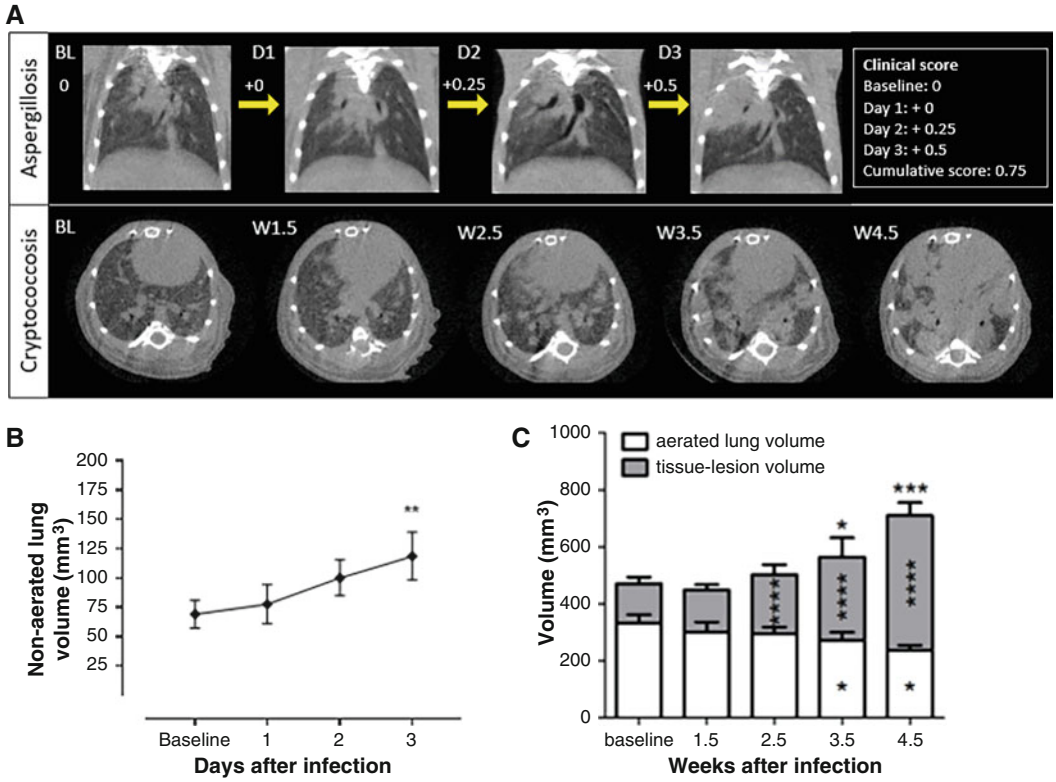

Fig. 4 (Semi)-quantification of μCT-derived biomarkers over time. (**a**, *upper panel*) Visual overview of progressing lung pathology over time in the aspergillosis mouse model (coronal cross-sections) and cumulative ("clinical") score assessment (yellow arrow; right panel). (**a**, *lower panel*) Longitudinal visual lung pathology development in the cryptococcosis mouse model (transverse cross-sections). (**b**) Longitudinal quantification of nonaerated lung volume in an aspergillosis mouse model upon *A. fumigatus* infection, showing an increase in lung lesion volume over time. Two-way repeated measures ANOVA with Tukey's multiple comparison test. $^{**}P \leq 0.005$ compared to baseline. (**c**) Longitudinal quantification of aerated, nonaerated, and total lung volume in a cryptococcosis mouse model, showing an increase in lung lesion volume, a decrease in aerated volume, and a compensatory increase in total lung volume over time. Two-way repeated measures ANOVA with Bonferroni post-test. $^{*}P < 0.05$; $^{****}P < 0.0001$ compared to baseline. Adapted from [6] and [5]

3. Based on the resulting VOI, relevant image-derived biomarkers can be determined and gathered in a spreadsheet (Fig. 3a): aerated lung volume (ALV), nonaerated lung volume (NALV), total lung volume (TLV) and all corresponding mean densities. To distinguish air and tissue in the mouse lung, manually set the following thresholds on the 8-bit grey-scale histogram "from dataset" in CTAn and keep them constant for all data sets (Fig. 3c):
   (a) ALV: 0–107 grey value.
   (b) NALV: 108–255 grey value.
   (c) TLV: 0–255 grey value.

4. For reporting volume and density measurements, convert from voxels to mm^3 and from grey values to Hounsfield units (HU), respectively, in the spreadsheet. For HU calibration, scan a phantom such as a 50 mL tube filled with water, containing an air-filled 1.5 mL microcentrifuge tube, using the same scanning settings as in mice (see Subheading 3.2). Set greyscale index of water to 0 HU and air to −1000 HU.
5. Backup your data and report (**Notes 13** and **14**). Examples of quantification of ALV, NALV, and TLV over time in mouse models of aspergillosis and cryptococcosis are shown in Fig. 4 (**Note 15**).

4 Notes

1. Isogenic strains expressing a red-shifted thermostable firefly luciferase (derivatives of *A. fumigatus* reference strain CBS144.89): our laboratory has available one triazole antifungal susceptible (wild type) strain ($Af_luc_{OPT_red}$_WT) and two triazole antifungal resistant strains harboring either the TR_{34}/L98H (Af_lucOPT_red_TR34) or the TR_{46}/Y121F/T289A ($Af_luc_{OPT_red}$_TR46) *cyp51A* gene mutations [5].
2. We used BALB/c mice because it is one of the most widely used inbred mouse strains, especially used in infectious diseases research. However, the described aspergillosis model was also successfully developed in C57BL/6NTac mice to study influenza-associated aspergillosis (IAPA) [14, 15], showing the possibility to use other mouse strains depending on your specific research interest.
3. Both *C. neoformans* and *A. fumigatus* are classified as biosafety level 2 agents and should be handled according to the corresponding safety regulations.
4. All animal experiments should be approved by the institutional ethical committee and should comply with national and international regulations.
5. The angled vertical support was manufactured in-house using a 3D printer and 75 mm PLA-filaments (Zhuhai Sunlu Industry Co., Ltd., Xiangshan District, China). The support is 6 mm thick, 42 cm long, 22 cm wide and bent to a 45° acute angle. On each side of the backboard, 2 cm from the top and side edge, 2 holes were drilled and galvanized metal-style screws, nuts, and washers were used to secure a stainless-steel wire strung from one screw to the other, enabling to hang a mouse by its incisors.
6. Before installing the μCT system, make sure to comply with the manufacturer's installation requirements, that is, a table that

can hold the scanners' weight, a correct power source (230 V AC, 50–60 Hz), and adequate room temperature and humidity (18–22 °C with <70% humidity at 25 °C).

7. Orotracheal inoculation can also be performed under systemic anesthesia by i.p. injecting a mixture of ketamine (45–60 mg/kg, Nimatek®, Bladel, The Netherlands) and medetomidine (0.6–0.8 mg/kg, Domitor®, Espoo, Finland). I.p. injection of atipamezole hydrochloride (0.5 mg/kg, Antisedan®, Espoo, Finland) reverses anesthesia [6]. However, it was shown that i.p. administered anesthesia is associated with more weight-loss in mice when compared to gas anesthesia [5].
8. As an alternative for the orotracheal inoculation using the Hamilton syringe, a regular pipet tip can be placed in the oropharynx near the trachea for oropharyngeal inoculation.
9. Scanning frequency depends on the rate infection progresses in the model of interest, as well as on the research question. In the IPA mouse model, mice develop serious infection as fast as 4 days post-infection, so daily scanning is essential to study longitudinal differences in lung pathology. In the cryptococcosis mouse model, infection progresses relatively slowly over a time span of 5 weeks, so weekly or 2-weekly scanning is sufficient.
10. Ring artefacts appear as concentric rings on the transversal image that influence the local grey values and thus prohibit accurate quantitative analysis. If present, reducing these artefacts is necessary to increase the reconstructed image quality.
11. Depending on the type of pathology and/or preference of the researcher, image scoring can be done either on coronal [5, 11] or on trans-axial cross-sections [15, 17] and different scoring methods can be used, as long as the scoring method is consistently applied and reported.
12. By not excluding the large blood vessels in the lung ROI, we assume no effect of disease on blood vessel volume. Alternatively, the large blood vessels can be excluded from the ROI during lung delineation. However, some fungal lesions tend to develop close to blood vessels and distinguishing both may increase bias in ROI delineation.
13. To statistically compare lung volumes longitudinally, a two-way ANOVA repeated measures with Tukey's multiple comparison post hoc test can be performed.
14. Data size will be around 3–4 GB per dataset, so provide sufficient storage space.
15. Usually, typical symptoms of lung disease such as weight loss and breathing difficulties inversely correlate with the remaining ALV. However, disease symptoms do not necessarily correlate

with the NALV, since the increasing NALV can be paralleled by a compensatory increase in total lung volume, thereby preventing the ALV from declining and (temporarily) saving the animal from severe breathing difficulties. This phenomenon has been observed in mouse models of cryptococcosis (Fig. 4), lung metastasis, and lung fibrosis [6, 7, 16, 18].

Acknowledgements

The authors acknowledge funding by the Flemish Research Foundation (FWO) (grants 1506114 N and G057721N). E.V. was supported by an aspirant mandate from FWO (1SF2222N).

References

1. Yao Z, Liao W (2006) Fungal respiratory disease. Curr Opin Pulm Med 12(3):222–227
2. Perfect JR (2017) The antifungal pipeline: a reality check. Nat Rev Drug Discov 16(9): 603–616
3. Tielemans B, Dekoster K, Verleden SE, Sawall S, Leszczyński B, Laperre K et al (2020) From mouse to man and back: closing the correlation gap between imaging and histopathology for lung diseases. Diagn Basel Switz 10(9)
4. Christe A, Lin MC, Yen AC, Hallett RL, Roychoudhury K, Schmitzberger F et al (2012) CT patterns of fungal pulmonary infections of the lung: comparison of standard-dose and simulated low-dose CT. Eur J Radiol 81(10):2860–2866
5. Resendiz-Sharpe A, da Silva RP, Geib E, Vanderbeke L, Seldeslachts L, Hupko C et al (2022) Longitudinal multimodal imaging-compatible mouse model of triazole-sensitive and -resistant invasive pulmonary aspergillosis. Dis Model Mech 15(3):dmm049165
6. Vanherp L, Ristani A, Poelmans J, Hillen A, Lagrou K, Janbon G et al (2019) Sensitive bioluminescence imaging of fungal dissemination to the brain in mouse models of cryptococcosis. Dis Model Mech 12(6):dmm039123
7. Dekoster K, Decaesteker T, Berghen N, Van den Broucke S, Jonckheere AC, Wouters J et al (2020) Longitudinal micro-computed tomography-derived biomarkers quantify non-resolving lung fibrosis in a silicosis mouse model. Sci Rep 10(1):16181
8. Tsui HC, Decaesteker T, Jonckheere AC, Vande Velde G, Cremer J, Verbeken E et al (2020) Cobalt exposure via skin alters lung immune cells and enhances pulmonary responses to cobalt in mice. Am J Physiol Lung Cell Mol Physiol 319(4):L641–L651
9. Berghen N, Dekoster K, Marien E, Dabin J, Hillen A, Wouters J et al (2019) Radiosafe micro-computed tomography for longitudinal evaluation of murine disease models. Sci Rep 9(1):17598
10. Van Den Broucke S, Pollaris L, Vande Velde G, Verbeken E, Nemery B, Vanoirbeek J et al (2018) Irritant-induced asthma to hypochlorite in mice due to impairment of the airway barrier. Arch Toxicol 92(4):1551–1561
11. Poelmans J, Hillen A, Vanherp L, Govaerts K, Maertens J, Dresselaers T et al (2016) Longitudinal, in vivo assessment of invasive pulmonary aspergillosis in mice by computed tomography and magnetic resonance imaging. Lab Investig 96(6):692–704
12. Vande Velde G, De Langhe E, Poelmans J, Bruyndonckx P, d'Agostino E, Verbeken E et al (2015) Longitudinal in vivo microcomputed tomography of mouse lungs: no evidence for radiotoxicity. Am J Physiol Lung Cell Mol Physiol 309(3):L271–L279
13. Vande Velde G, De Langhe E, Poelmans J, Dresselaers T, Lories RJ, Himmelreich U (2014) Magnetic resonance imaging for non-invasive assessment of lung fibrosis onset and progression: cross-validation and comparison of different magnetic resonance imaging protocols with micro-computed tomography and histology in the bleomycin-induced mouse model. Investig Radiol 49(11):691–698
14. Seldeslachts L, Jacobs C, Tielemans B, Vanhoffelen E, Van der Sloten L, Humblet-Baron S et al (2021) Overcome double trouble: baloxavir marboxil suppresses influenza

thereby mitigating secondary invasive pulmonary aspergillosis. J Fung 8(1):1

15. Seldeslachts L, Vanderbeke L, Fremau A, Reséndiz-Sharpe A, Jacobs C, Laeveren B et al (2021) Early oseltamivir reduces risk for influenza-associated aspergillosis in a double-hit murine model. Virulence 12(1):2493–2508
16. Vande Velde G, Poelmans J, De Langhe E, Hillen A, Vanoirbeek J, Himmelreich U et al (2016) Longitudinal micro-CT provides biomarkers of lung disease that can be used to assess the effect of therapy in preclinical mouse models, and reveal compensatory changes in lung volume. Dis Model Mech 9(1):91–98
17. Seldeslachts L, Cawthorne C, Kaptein SF, Boudewijns R, Thibaut HJ, Sanchez Felipe L et al (2022) Use of micro-computed tomography to visualize and quantify COVID-19 efficiency in free-breathing hamsters. In: Thomas S (ed) Vaccine design, vol. 2410. Methods in molecular biology [Internet]. Springer, New York, pp 177–192 [Cited 2022 Mar 30]. Available from: https://link.springer.com/10.1007/978-1-0716-1884-4_8
18. Marien E, Hillen A, Vanderhoydonc F, Swinnen JV, Vande VG (2017) Longitudinal micro-computed tomography-derived biomarkers for lung metastasis detection in a syngeneic mouse model: added value to bioluminescence imaging. Lab Investig 97(1):24–33

INDEX

Rebecca A. Drummond (ed.), *Antifungal Immunity: Methods and Protocols*, Methods in Molecular Biology, vol. 2667,
https://doi.org/10.1007/978-1-0716-3199-7,

L

M

N

P

Q

R

S

T

Y

Z